Universidade de Aveiro Departamento de Biologia
2010

Sandra Carla Fernandes Craveiro Mendes Calado

Ultrastrutura e filogenia de dinoflagelados peridinióides

Ultrastructure and phylogeny of peridinioid dinoflagellates

Universidade de Aveiro Departamento de Biologia
2010

Sandra Carla Fernandes Craveiro Mendes Calado

Ultrastrutura e filogenia de dinoflagelados peridinióides

Ultrastructure and phylogeny of peridinioid dinoflagellates

Dissertação apresentada à Universidade de Aveiro para cumprimento dos requisitos necessários à obtenção do grau de Doutor em Biologia, realizada sob a orientação científica da Professora Doutora Salomé Fernandes Pinheiro de Almeida, Professora Auxiliar do Departamento de Biologia da Universidade de Aveiro e do Professor Øjvind Moestrup, Professor do Departamento de Biologia da Universidade de Copenhaga

Sandra C. F. Craveiro Mendes Calado was supported by a PhD grant (SFRH/BD/16794/2004) from Fundação para a Ciência e Tecnologia, co-funded by the POPH/FSE programme

To my husband and daughters

o júri/ the jury

presidente/ president

Doutor Carlos Fernandes da Silva
Professor Catedrático da Universidade de Aveiro

vogais/ members

Doutora Marina Montresor
Investigadora Principal da Estação Zoológica Anton Dohrn, Nápoles, Itália

Doutora Lília Maria Antunes dos Santos
Professora Auxiliar da Universidade de Coimbra

Doutor Amadeu Mortágua Velho da Maia Soares
Professor Catedrático da Universidade de Aveiro

Doutor Jorge Manuel Estima de Almeida Rino
Professor Associado Aposentado da Universidade de Aveiro

Doutor Øjvind Moestrup (Co-orientador)
Professor Catedrático da Universidade de Copenhaga, Dinamarca

Doutora Salomé Fernandes Pinheiro de Almeida (Orientadora)
Professora Auxiliar da Universidade de Aveiro

agradecimentos/ acknowledgements

My sincere thanks:
To my supervisor Professor Øjvind Moestrup for providing all the facilities regarding the electron microscopy; for being always able to see some “light“ when everything looked “dark” and for being the most enthusiastic scientist I ever met, and probably will ever meet.
To my supervisor Professor Salomé Almeida for accepting this assignment and for her friendship of more than twenty years.
To Professor Niels Daugbjerg for teaching me all I know about work in the DNA laboratory.
To all the phycologists (students, technicians and professors) in the Department of Biology, University of Copenhagen that were so friendly and helpful during all my stays in Denmark. Thanks to Nina Lundholm, Marianne Ellegaard, Gert Hansen, Lisbeth Haukrogh, Karin Lindberg, Aase and Jørgen Kristiansen, Poul Møller Pedersen, Lene Christiansen, Mårten Flø Jørgensen, Sofia Ribeiro and others too numerous to mention by name, but not forgotten, for making me feel that I belonged there!
To all the colleagues that worked throughout these years in our small phycology laboratory at the University of Aveiro, for the friendship and for listening patiently to me when things were not so well.
To Professor José Alberto Duarte for allowing me to use the transmission electron microscope at the Faculty of Sports, University of Oporto.
To Ruth Nielsen, the most extraordinary person! Thanks for receiving me and António (and sometimes also our daughters, family and friends…) in her home, making everything so much easier and pleasant! Thanks also to Palle for putting up with our invasions!
Aos meus queridos pais e avó, por me terem apoiado incondicionalmente e desde sempre, em tudo o que necessitei. Nestes cinco anos, muitos foram os periodos, durante as nossas ausências, em que cuidaram das minhas filhas. Muito obrigada pela vossa eterna disponibilidade!
To my sister Marta, a fantastic one! For all her love, for being always present and caring about me. To Hugo, my brother-in-law, that was, with my sister, each time ready to take care of two more daughters (mine!).
To my husband, António Calado. He is my friend, my teacher, my supervisor, my colleague and the reason and force behind all this work! This project was his idea and without him, this would have never been possible. Thank you for being so patient with me!
Às minhas filhas, Beatriz e Leonor, por todo o amor e carinho!

palavras-chave

Dinoflagelados, Dinophyceae, filogenia molecular, *Palatinus apiculatus*, peridinióides, *Peridinium lomnickii*, *P. palatinum*, *Peridiniopsis berolinensis*, *Tyrannodinium berolinense*, *Sphaerodinium cracoviense*, taxonomia, ultrastrutura

resumo

Os dinoflagelados são um grupo muito diverso de protistas que possuem um conjunto de características pouco comuns. Os peridinióides são dinoflagelados com teca que é formada por seis séries latitudinais de placas, incluindo a série cingular e um anel incompleto de placas intercalares anteriores, embora as últimas estejam ausentes em algumas espécies de *Peridiniopsis*. São dinoflagelados com simetria bilateral em relação ao plano apical que contem o eixo dorso-ventral. Na série sulcal há apenas uma placa posterior que contacta com o limite ventral de duas grandes placas antapicais. Entre os peridinióides, a presença ou ausência de um poro apical e o número de placas no cíngulo são geralmente consideradas marcas filogenéticas importantes ao nível de género ou família. Actualmente, a definição de *Peridinium* Ehrenberg, o dinoflagelado mais comum de água doce, inclui organismos com combinações diferentes destas duas características. Trabalhos anteriores sobre a ultrastrutura e afinidade filogenética das espécies tipo de *Peridinium*, *P. cinctum*, e *Peridiniopsis* Lemmermann, *P. borgei* também sugerem a necessidade de reexaminar as relações taxonómicas dos peridinióides. Esta tese combina o estudo ultrastrutural de uma selecção de espécies com hipóteses filogenéticas baseadas nas sequências de LSU rDNA, para aumentar o nosso conhecimento das diferenças e afinidades dentro dos peridinióides. Tem como objectivo aumentar o nosso conhecimento das características individuais das células que possam levar a reconhecer sinapomorfias que possam ser usadas como marcadores dos peridinióides como um todo e dos seus subgrupos. As espécies escolhidas para exame pormenorizado foram: *Peridinium palatinum* Lauterborn, de um grupo com duas placas intercalares anteriores, seis placas cingulares e sem poro apical; *Peridinium lomnickii* Wołoszyńska, de um grupo com poro apical, três placas intercalares e seis cingulares; *Peridiniopsis berolinensis* (Lemmermann) Bourrelly, uma espécie heterotrófica com poro apical, sem placas intercalares e com seis placas cingulares; e *Sphaerodinium cracoviense* Wołoszyńska, um membro de um género de formas com teca com um tipo de tabulação marginalmente peridinióide, com um suposto poro apical e quatro placas intercalares anteriores.

Peridinium palatinum difere de *Peridinium* e *Peridiniopsis* típicos, quer em características da teca, quer internas. As diferenças estimadas entre as sequências parciais de LSU rDNA de *P. palatinum* e a espécie próxima *P. pseudolaeve*, relativamente a *P. cinctum* são comparativamente grandes e, juntamente com a topologia da árvore filogenética, apoiam a separação de *P. palatinum* e formas próximas ao nível de género. *Palatinus* nov. gen. foi, então, descrito com as novas combinações *Palatinus apiculatus* nov. comb. (espécie tipo; sin. *Peridinium palatinum*), *P. apiculatus* var. *laevis* nov. comb. e *P. pseudolaevis* nov. comb.. As características distintivas de *Palatinus* incluem

resumo (continuação)

uma superfície das placas lisa ou um tanto granulosa, mas não areolada, um grande pirenóide central penetrado por canais citoplasmáticos e de onde radiam lobos plastidiais, e a presença de uma fiada microtubular homóloga à de um pedúnculo. As células de *Palatinus* saem da teca pela zona antapical-pos-cingular.

Peridinium lomnickii apresenta tabulação semelhante às formas marinhas, produtoras de quistos calcários, do género *Scrippsiella* A.R. Loeblich. Para comparação, adicionámos novas observações ultrastruturais de *S. trochoidea*. *Peridinium lomnickii* tem uma combinação de características diferente de *Peridinium*, *Peridiniopsis* e *Scrippsiella*. As hipóteses filogenéticas baseadas em DNA colocam *P. lomnickii* no mesmo ramo que *Pfiesteria* Steidinger et Burkholder, *Tyrannodinium* e outras Pfiesteriaceae, com as quais partilha um 'microtubular basket' e uma ligação peculiar entre duas placas do sulco. As características distintivas do novo género proposto *Chimonodinium* gen. ined. incluem, além da tabulação, a ausência de pirenóides, a presença de um 'microtubular basket' com quatro ou cinco fiadas sobrepostas de microtúbulos associados a um pequeno pedúnculo, um sistema pusular com tubos pusulares bem definidos ligados aos canais flagelares, e a produção de quistos não calcários.

Peridiniopsis berolinensis partilha várias características significativas com *Pfiesteria* e afins, como um 'microtubular basket' com a capacidade de suportar um tubo de alimentação, quimiossensibilidade para encontrar presas apropriadas, o modo de natação junto às presas e a organização geral da célula. Hipóteses filogenéticas com base em LSU rDNA confirmam a afinidade entre *P. berolinensis* e *Pfiesteria* bem como a relação mais remota com a espécie tipo de *Peridiniopsis*, *P. borgei.* Estas razões justificam a proposta de *Tyrannodinium* gen. nov., uma nova Pfiesteriaceae que difere de outros membros do grupo por viver em água doce e nos pormenores da tabulação.

Sphaerodinium cracoviense revelou a tabulação típica do género *Sphaerodinium*, que apresenta um número de placas intercalares superiores e pos-cingulares maior que o que é típico em peridinióides: 4 e 6, respectivamente. Observações em SEM mostraram uma estrutura apical diferente da dos peridinióides, e um sulco apical numa das placas fazendo lembrar a área apical de alguns woloszynskióides. Os pormenores do aparelho flagelar e do sistema pusular ligam o *Sphaerodinium* aos woloszynskióides em geral e ao género *Baldinia* em particular, mas não aos peridinióides. O volumoso estigma de *S. cracoviense* revelou ser extraplastidial e de um modelo único, composto por elementos que se encontram em woloszynskióides, mas nunca encontrados anteriormente juntos. A análise filogenética baseada nas sequências parciais de LSU rDNA também sugerem uma maior proximidade de *S. cracoviense* com os woloszynskióides do que com os peridinióides.

Futuras análises pormenorizadas de dinoflagelados peridinióides, em especial entre os do numeroso grupo de espécies com poro apical, serão necessárias para clarificar as suas relações taxonómicas; e a produção de descrições melhoradas das características finas particulares das células serão um requisito para perceber a evolução dos caracteres dos peridinióides por forma a podermos identificar marcadores filogenéticos.

keywords

Dinoflagellates, Dinophyceae, molecular phylogeny, *Palatinus apiculatus*, peridinioids, *Peridinium lomnickii*, *P. palatinum*, *Peridiniopsis berolinensis*, *Tyrannodinium berolinense*, *Sphaerodinium cracoviense*, taxonomy, ultrastructure

abstract

Dinoflagellates are a diverse and widespread group of protists that combine a number of unusual features. Peridinioids are thecate dinoflagellates with six latitudinal series of plates, including the cingular series and the incomplete ring of anterior intercalary plates, although the latter is absent in some species currently classified as *Peridiniopsis*. They tend to be bilaterally symmetrical in relation to the apical plane containing the dorsiventral axis. In the sulcal series there is only one posterior plate, which contacts with the ventral edge of two large subequal antapical plates. Among peridinioids, the presence or absence of an apical thecal pore and the number of plates in the cingulum are often considered important phylogenetic markers at genus or family level. As currently delimited, *Peridinium* Ehrenberg, the most widely represented dinoflagellate genus in freshwater, includes organisms with different combinations of these features. Previous studies on the fine-structure and phylogenetic affinites of the type species of *Peridinium*, *P. cinctum*, and of *Peridiniopsis* Lemmermann, *P. borgei*, likewise suggested the need for reexamination of the taxonomical relationships of peridinioids. This thesis combines the ultrastructural examination of selected species with phylogenetic hypothesis based on partial LSU rDNA sequences to extend our knowledge of variation and affinities within the peridinioid group. It aims to advance our understanding of individual cell features that may lead to the recognition of synapomorphies that may be used as markers for the peridinioid group as a whole and for its subgroups. The species targetted for detailed examination were: *Peridinium palatinum* Lauterborn, representative of a group with two anterior intercalary plates, six cingular plates and no apical pore complex; *Peridinium lomnickii* Wołoszyńska, of a group with apical pore complex, three anterior intercalary and six cingular plates; *Peridiniopsis berolinensis* (Lemmermann) Bourrelly, an heterotrophic species with apical pore complex, zero anterior intercalary and six cingular plates; and *Sphaerodinium cracoviense* Wołoszyńska, a member of a genus of thecate forms with a marginally peridinioid type of tabulation, with a putative apical pore complex and four anterior intercalary plates.

Peridinium palatinum was found to differ from typical *Peridinium* and *Peridiniopsis* in both thecal and internal features. The relatively large estimated differences in the partial LSU rDNA sequences of *P. palatinum* and its close relative *P. pseudolaeve* compared to *P. cinctum*, together with the topology of the molecular tree, supported the separation of *P. palatinum* and related forms at the generic level. *Palatinus* nov. gen. was therefore described with the new combinations *Palatinus apiculatus* nov. comb. (type species; syn. *Peridinium palatinum*), *P. apiculatus* var. *laevis* nov. comb. and *P. pseudolaevis* nov. comb.. Distinctive characters for *Palatinus* include a smooth or slighty granulate, but not areolate, plate surface, a large central pyrenoid penetrated by cytoplasmic channels and radiating into chloroplast lobes, and the presence of a peduncle-homologous microtubular strand. *Palatinus* cells exit the theca through the antapical-postcingular area.

abstract (continuation)

Peridinium lomnickii has a similar tabulation to the mostly marine, calcareous cyst producers of the genus *Scrippsiella* A.R. Loeblich and fine-structural observations on *S. trochoidea* were added for comparison. *Peridinium lomnickii* showed a different combination of features from *Peridinium*, *Peridiniopsis* and *Scrippsiella*. Interestingly, the DNA-base phylogenetic hypothesis placed *P. lomnickii* in the same clade as *Pfiesteria* Steidinger et Burkholder, *Tyrannodinium* and other pfiesteriaceans, with which it shares a microtubular basket and a peculiar connection between two plates in the sulcus. Distinctive characters of the proposed new genus *Chimonodinium* gen. ined., include, in addition to the tabulation, the absence of pyrenoids, the presence of a microtubular basket with four or five overlapping rows of microtubules associated with a small peduncle, a pusular system with well-defined pusular tubes connected to the flagellar canals, and the production of non-calcareous cysts.

Peridiniopsis berolinensis shares a number of important features with *Pfiesteria* and its allies, including a microtubular basket with the capacity of driving and supporting a feeding tube, the ability to follow chemical clues to find suitable prey, the swimming behaviour near the prey and the general organization of the cell. Partial LSU rDNA-based phylogenetic hypotheses strongly confirm the close affinity between *P. berolinensis* and *Pfiesteria* and the more remote relationship with the type species of *Peridiniopsis*, *P. borgei.* These reasons justify the proposal of *Tyrannodinium* gen. nov., a new pfiesteriacean that differs from other genera in the group in being a freshwater form and in details of the plate arrangement.

Sphaerodinium cravoviense showed the tabulation typical of its genus, which extends beyond normal peridinioid tabulation numbers in the anterior intercalary and in the postcingular series, with 4 and 6 plates, respectively. SEM observations revealed that the apical structure differed from the typical arrangement seen in peridinioids and included a furrow with knob-like protuberances reminiscent of the apical area of the thinly thecate woloszynskioids, which usually possess larger numbers of amphiesmal vesicles. Details of the flagellar apparatus and associated pusular system link *Sphaerodinium* to the woloszynskioids in general and to *Baldinia anauniensis* in partidular, rather than to peridinioids. The prominent eyespot found in *S. cracoviense* was shown by TEM to be extraplastidial and of a unique type, made of two components, each known from some eyespot types found in woloszynskioids, but not previously found together. A closer relationship of *S. cracoviense* with woloszynskioids than with peridinioids was also suggested by a phylogenetic analysis based on LSU rDNA.

Further analyses of peridinioids, particularly within the sizeable group of species with an apical pore complex, is needed before general taxonomic relationships become clear; and improved descriptions of fine-structural features of cells are required to unravel the evolution of particular characters, allowing phenotypic phylogenetic markers to be identified.

This thesis is based on, and includes, the following articles:

Craveiro, S.C., Calado, A.J., Daugbjerg, N. & Moestrup, Ø. 2009. Ultrastructure and LSU rDNA-based revision of *Peridinium* group palatinum (Dinophyceae) with the description of *Palatinus* gen. nov. *Journal of Phycology* 45 (5): 1175-1194 — CHAPTER 2

Craveiro, S.C., Calado, A.J., Daugbjerg, N., Hansen, G. & Moestrup, Ø. (submitted to *Protist*). Ultrastructure and LSU rDNA-based Phylogeny of *Peridinium lomnickii* and Description of *Chimonodinium* gen. nov. (Dinophyceae). — CHAPTER 3 — *Inclusion in this thesis is not intended as effective publication of the new taxa proposed in the manuscript*

Calado, A.J., Craveiro, S.C., Daugbjerg, N. & Moestrup, Ø. 2009. Description of *Tyrannodinium* gen. nov., a freshwater dinoflagellate closely related to the marine *Pfiesteria*-like species. *Journal of Phycology* 45 (5): 1195-1205 — CHAPTER 4

Craveiro, S.C., Moestrup, Ø., Daugbjerg, N. & Calado, A.J. 2010. Ultrastructure and Large Subunit rDNA-based phylogeny of *Sphaerodinium cracoviense*, an unusual freshwater dinoflagellate with a novel type of eyespot. *The Journal of Eukaryotic Microbiology* 57 (6) — CHAPTER 5

The author of this thesis declares that she has done the greater part of the preparation and study of material that gave origin to the scientific information used in the articles. She was involved in all steps of interpretation of data, development and discussion of ideas, and led the preparation of the manuscripts.

TABLE OF CONTENTS

LIST OF ABBREVIATIONS

ab, accumulation body
apc, apical pore complex
as, anterior sulcal plate
b, bacterium
ALP, apical line of narrow plates
BA, Bayesian analysis
BBc, connective between basal bodies
Ch, chloroplast
cp, cover plate
d/D, dictyosome
e/E, eyespot
EAV, single elongate amphiesmal vesicle
EV, elongated vesicle
f, fibre
gv, granulose vesicles
LB, longitudinal basal body
LB-LMRc, connective between LB and LMR
LC, layered connective
LF, longitudinal flagellum
LFC, longitudinal flagellar canal
LM, light microscopy
LMR, longitudinal microtubular root
LSP, longitudinal sac pusule
LSU rDNA, nuclear DNA sequence that codes for large subunit ribosomal RNA
LSU rRNA, large subunit ribosomal RNA (the 28S strand)
ls, left sulcal plate
LSC, longitudinal striated collar
MB, microtubular basket
ML, maximum likelihood
MSP, microtubular strand of the peduncle
mt, mitochondria
N, nucleus
n, nucleolus
o/**O**, oil droplets
p, peduncle
P, pyrenoid
pc, peduncle cover plate
PEV, pair of elongate amphiesmal vesicles
pl, platelets
Po/pp, pore plate
PP, posterior probabilities
ps, posterior sulcal plate
PSC, peduncle striated collar
pt, pusular tube
rs/sd, right sulcal plate
s, starch
sa, anterior sulcal plate
SBc, striated basal body connective
SCc, striated collar connective
SEM, scanning electron microscopy
sm, medium sulcal plate
SMR, single-stranted microtubular root
SRC, striated root connective
sp, posterior sulcal plate
ss, left sulcal plate
SSU rDNA, nuclear DNA sequence that codes for small subunit ribosomal RNA
SSU rRNA, small subunit ribosomal RNA
T, trichocyst
TB, transverse basal body
TB-LMRc, connective between TB and LMR
TEM, transmission electron microscopy
TF/tf, transverse flagellum
TFC, transverse flagellar canal
TMR, transverse microtubular root
TMRE, transverse microtubular root extension
TSC, transverse striated collar
TSP, transverse sac pusule
TSR, transverse striated root
TSRM, transverse striated root microtubule
x, canal plate

LIST OF FIGURES

CHAPTER 1

CHAPTER 2

CHAPTER 3

CHAPTER 4

CHAPTER 5

LIST OF TABLES

CHAPTER 1

CHAPTER 2

CHAPTER 3

CHAPTER 4

CHAPTER 6

CHAPTER 1

GENERAL INTRODUCTION

GENERAL FEATURES AND THE TRADITIONAL CRITERIA FOR DINOFLAGELLATE CLASSIFICATION

General features. Dinoflagellates are a diverse, widespread group of protists that combine a number of unusual features. The majority of dinoflagellates is free-living in marine or freshwater habitats but they can also be parasitic (e.g., in copepods) or symbiotic (e.g., in corals). About half of the known dinoflagellate species have chloroplasts; the others lack chloroplasts and are exclusively heterotrophic. Some of the chloroplast-bearing species combine the photosynthetic capability with heterotrophy and may be termed mixotrophic. The latter term is often restricted to forms that complement a partial autotrophy with the ingestion of food particles (Hansen and Calado 1999).

The type of nucleus and flagella are two of the most characteristic features found in dinoflagellates. The nucleus, in the majority of taxa of the group, has permanently condensed chromosomes, visible throughout the mitotic cycle, including the non-dividing stage (interphase) (Fig. 1). Dinoflagellate DNA is not associated with histones and therefore lacks nucleosomes (with the possible exception of the Syndiniales and perhaps the Noctilucales; Saldarriaga et al. 2003, 2004). In typical motile cells there are two heteromorphic flagella: the transverse flagellum (TF) usually encircles the cell, undulating in a transverse groove (the cingulum) that divides the cell in an apical (episome or epicone) and an antapical part (hyposome or hypocone); and the longitudinal flagellum (LF) that trails posteriorly with its proximal end in a ventral-antapical groove (the sulcus) (Fig. 2, a and b). Alternatively, in the Prorocentrales, both flagella are inserted apically and there are no grooves (Fig. 3, a and b). In the transverse flagellum the helical axoneme is accompanied by a fibrous strand throughout its entire length, and both structures are bounded by a common membrane forming a ribbon-like structure. The fibrous strand is shorter and less sinuous than the axoneme and is located near the cell surface, outside the helical turns of the axoneme (Fig. 2a) (Gaines and Taylor 1985). Along the outer edge of the transverse flagellum there is a row of simple hairs. The longitudinal flagellum is cylindrical or, when paraxonemal rods are present, flattened, but never as broad as the transverse flagellum (Figs. 2a; 3b) (Fensome et al. 1993).

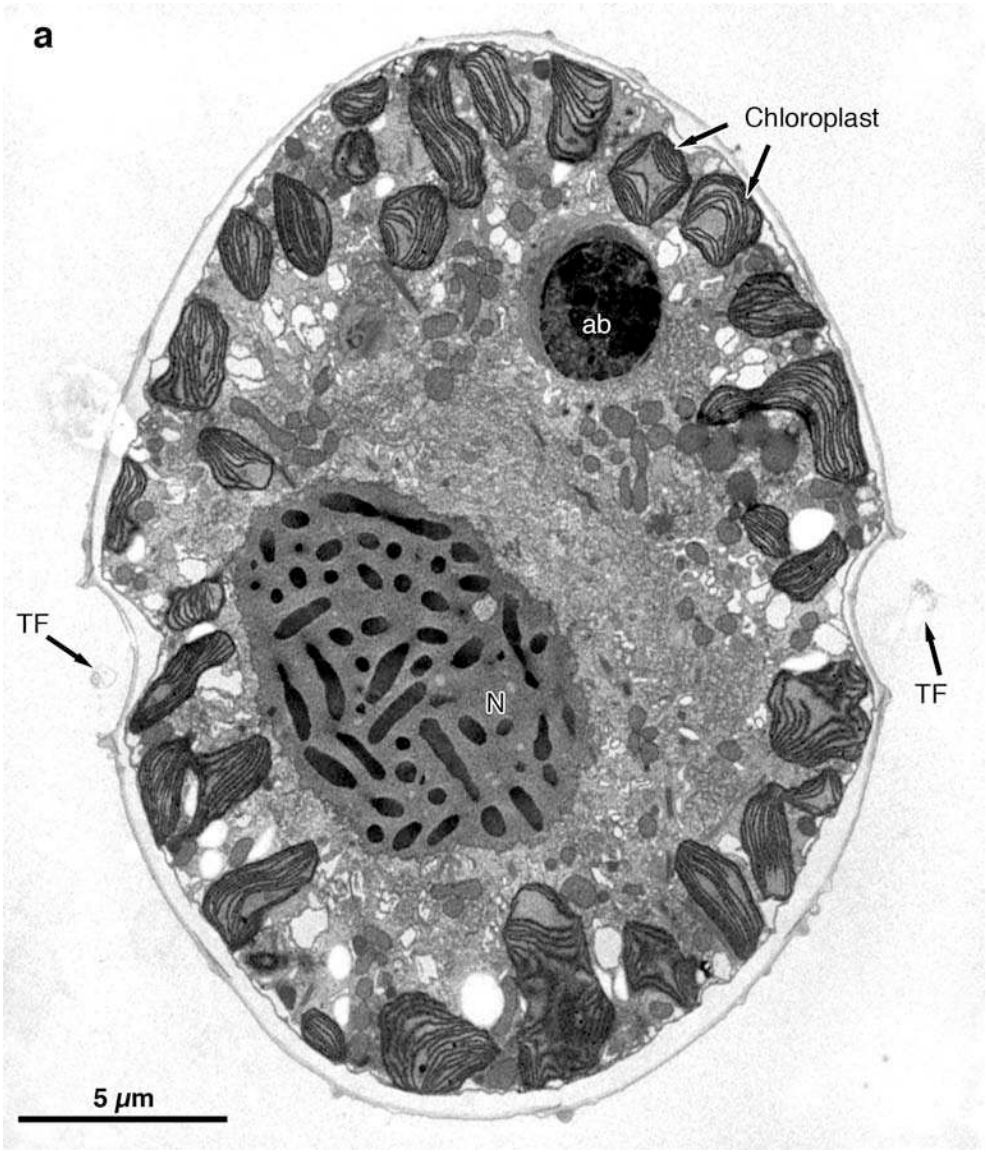

Fig. 1. General ultrastructure of *Chimonodinium lomnickii* (Wołoszyńska) comb. ined. (=*Peridinium lomnickii* Wołoszyńska; see Chapter 3), TEM. Longitudinal section showing the chloroplast lobes near the cell surface and the nucleus (N), typical of dinoflagellates, with condensed chromosomes. The transverse flagellum (TF) is visible in the cingulum. ab, accumulation body. (Original.)

Dinoflagellate cells are usually bounded by a complex outer region, the so-called amphiesma (Loeblich 1970). This region comprises a single layer of flat vesicles (amphiesmal vesicles) and the plasmalemma (cell membrane). The amphiesmal vesicles may enclose more or less thick cellulose-like plates, in the so-called thecate dinoflagellates (Fig. 2, b and d), or contain very thin or no plate-like material at all, in the so-called athecate or naked dinoflagellates (Fig. 2, a and c). Beneath the amphiesmal vesicles there are usually microtubules and numerous

peripheral vesicles (Dodge 1987). In thecate forms that may replace the whole theca, either following cell division or through ecdysis, many cells display partly broken up amphiesmal vesicles underlain by a layer of resistant material — this is usually called the pellicle (Loeblich 1970, Morrill and Loeblich 1981).

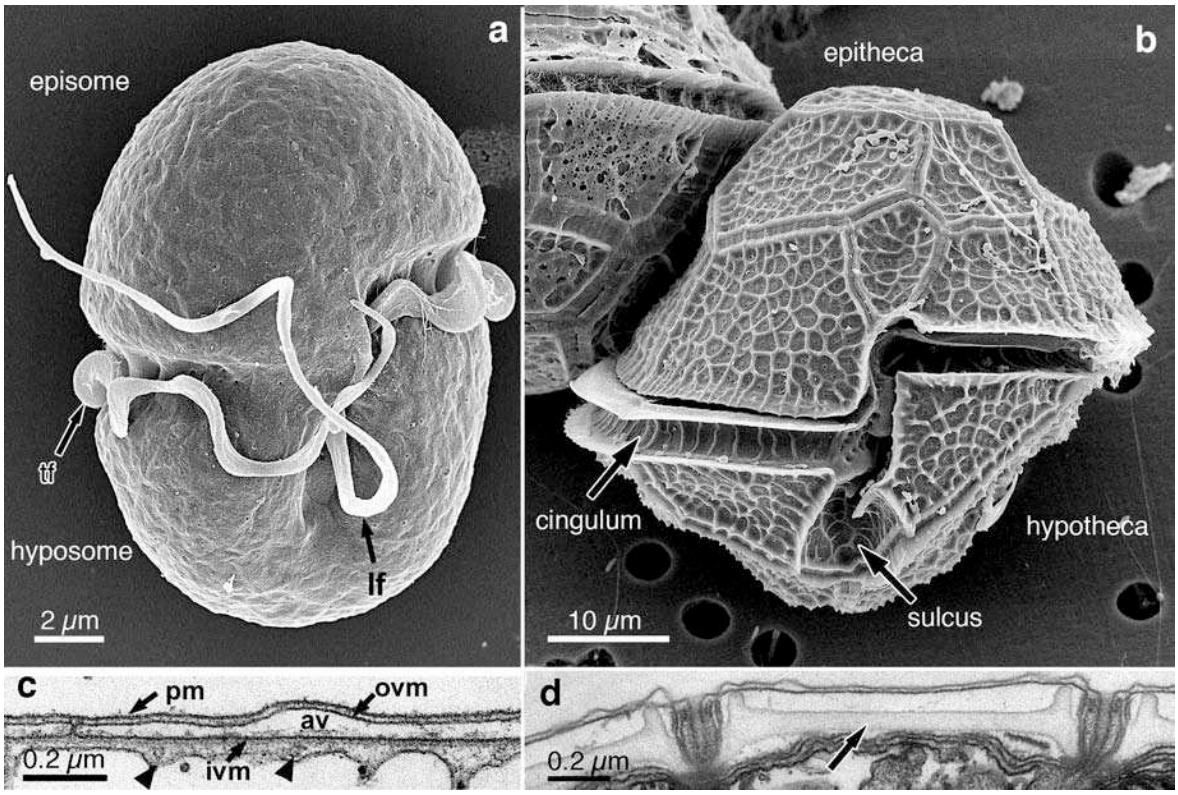

Fig. 2. Athecate and thecate dinoflagellates. (a) *Baldinia anauniensis*, SEM. Athecate dinoflagellate showing the ribbon-like transverse flagellum (tf) that encircles the cell. The longitudinal flagellum (lf) is visible emerging from the proximal part of the sulcus. (b) *Peridinium gatunense* Nygaard, SEM. Thecate dinoflagellate showing the cellulosic plates with reticulated ridges. The cingulum divides the theca into epi- and hypotheca. (c) The amphiesma of *Baldinia anauniensis*, TEM. Amphiesmal vesicle (av) with fuzzy electron-opaque material. ovm, outer amphiesmal vesicle membrane; ivm, inner amphiesmal vesicle membrane; pm, plasma membrane. Arrowheads point to cortical (subthecal) microtubules. (d) The amphiesma of *Palatinus apiculatus* (Ehrenberg) Craveiro, Calado, Daugbjerg et Moestrup, TEM. Thick cellulosic plates inside the amphiesmal vesicles (arrow). Two thecal pores are visible. (a) and (c) adapted from Hansen et al. 2007; (b) original; (d) adapted from Craveiro et al. 2009 (see Chapter 2).

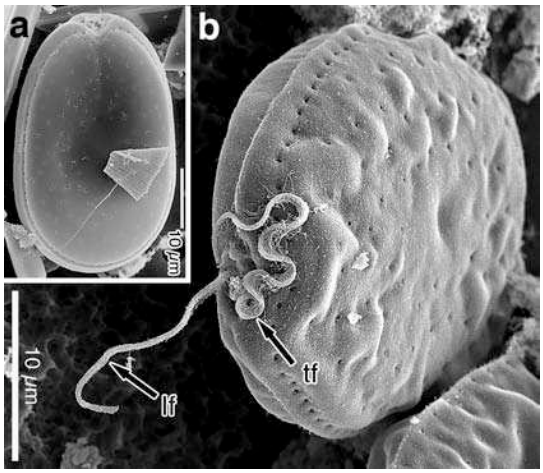

Fig. 3. SEM of *Prorocentrum lima*, a thecate dinoflagellate without cingulum or sulcus. (a) Longitudinal view of indented valve showing the platelets surrounding the flagellar opening. (b) Apical view showing the longitudinal (lf) and transverse (tf) flagella. (Original.)

Traditionally, the arrangement of thecal plates in an armoured cell has been called tabulation. However, since thecal plates are inside amphiesmal vesicles and there is a continuum between species with empty vesicles and those with plates, the term has been extended to mean arrangement of amphiesmal vesicles on the cell surface (Fensome et al. 1993). Out of several different systems that have been proposed for naming or numbering individual plates and their distribution in the theca, it was the system of Kofoid (1907, 1909) that eventually came into universal use. In this system, as applied to gonyaulacoids and peridinioids, the major plates are arranged in five latitudinal series, to which the cingular and sulcal plates may be added. From apex to antapex the series are called: apical (with individual plates denoted by a prime, ′, after the number of the individual plate), anterior intercalary (denoted by an a after the plate number) and precingular (double primed numbers, ″) series in the epitheca; cingular (with c after plate number) in the cingulum; postcingular (marked with ‴), posterior intercalary (marked with p) and antapical (marked with ⁗) series in the hypotheca. For example, the Kofoidian tabulation formula for *Peridinium cinctum* (O.F. Müller) Ehrenberg is 4′, 3a, 7″, 5c, 5s, 5‴, 2⁗. The plate arrangement of *Peridiniopsis borgei* Lemmermann labelled according to the system of Kofoid is represented in Fig. 4.

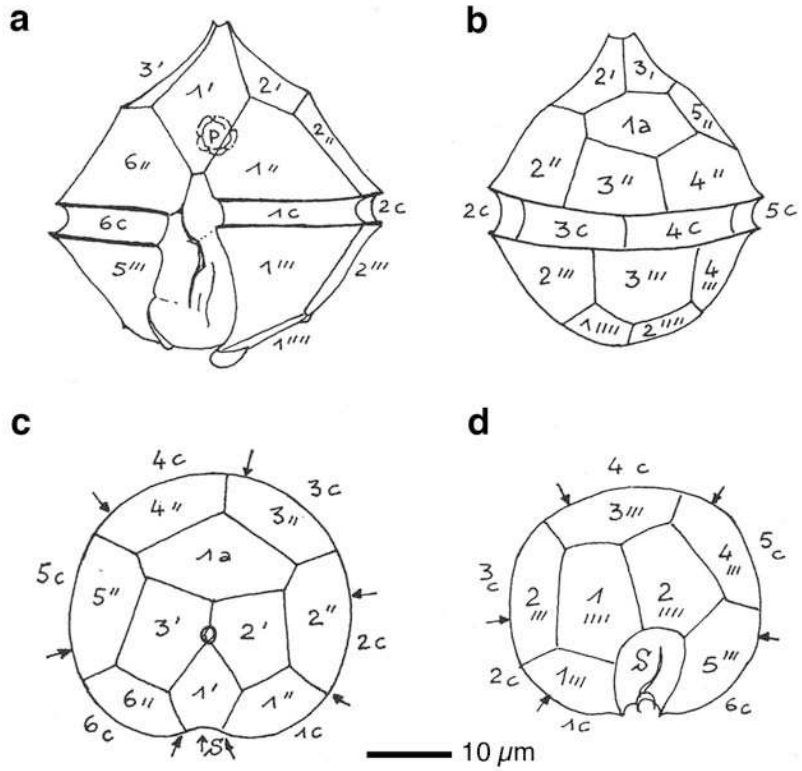

Fig. 4. Tabulation of *Peridiniopsis borgei* in the Kofoidian system. (a) Ventral view. P, pyrenoid. (b) Dorsal view. (c) Apical view. Note the apical pore surrounded by apical plates 1′–3′ and a single intercalary plate (1a). The arrows mark the position of the sutures between cingular plates, showing its relation to the precingular plates (1″–6″) (d) Antapical view. The arrows mark the position of the sutures between cingular plates, showing its relation to the postcingular plates (1‴–5‴). Adapted from Bourrelly (1970, pl. 12, p. 71).

Traditional classification. Appart from early reports of luminescent marine organisms in which *Noctiluca* Suriray may be recognized (e.g., Baker 1753), the first identifiable descriptions of dinoflagellates were published by the Dane Otto Friedrich Müller in the late 1700s (1773, 1786). Müller described several freshwater and marine species, which he treated as animals, assigning them to genera containing protists now classified in widely different groups (*Bursaria*, *Cercaria*, *Vorticella*; Müller 1773, 1776). The first generic name to be coined for a dinoflagellate and still in use today was *Ceratium*, created by Schrank (1793). The celebrated German microscopist and professor of natural sciences at the University of Berlin, Christian Gottfried Ehrenberg, starting from about 1828, produced a long series of works in which many of the common species of

dinoflagellates were described and several new genera proposed. In one of his earliest works he created the genus *Peridinium* Ehrenberg, which stands at the core of the present work (Ehrenberg 1830). In his classic work *Die Infusionsthierchen als vollkommende Organismen* (Infusion Animalcules as Complete Organisms) Ehrenberg (1838) grouped his 'Kranzthierchen', as he named most of the dinoflagellates, in the family Peridinaea. Out of the numerous contributions to the general knowledge of dinoflagellates produced during the nineteenth century (briefly reviewed in Taylor 1987), Stein (1883) stands out as the first to consistently use thecal plate arrangements as taxonomically useful features. Most of the taxonomic work on dinoflagellates published up to the 1930s was organized by Josef Schiller in his important contribution to the series *Kryptogamen-flora von Deutschland, Österreich und der Schweiz* (Schiller 1933, 1937), which is still useful for the identification of species, both freshwater and marine. During all this period the bulk of the genera were defined only on the basis of general cell morphology and the nature and arrangement of the parts composing the cell cover.

The latest species-level identification manual for freshwater dinoflagellates (Popovský and Pfiester 1990) again used the nature and constitution of the cell cover as a determinant feature. In thecate taxa the number, arrangement and shape of thecal plates was the main character used for identification. Following Lefèvre (1932) and subsequent monographers, Popovský and Pfiester (1990) subdivided into sections the genera *Peridinium* and *Peridiniopsis* Lemmermann, two of the most widely represented genera in freshwater, on the basis of the plate pattern formulae and the presence or absence of a pore in the apex of the theca. Popovský and Pfiester (1990) followed Bourrelly (1970) in incorporating in their taxonomic arrangement the genus *Woloszynskia* R.H. Thompson (Thompson 1951), introduced to separate species with a cell cover of numerous thin plates from the truly "naked" *Gymnodinium* species. However, the concepts used for most groups down to generic level were essentially the same as in previous monographs (e.g., Huber-Pestalozzi 1950, Kiselev 1954, Matvíïenko and Lytvynenko 1977).

The systematic arrangement of dinoflagellates in Fensome et al.'s (1993) *A Classification of Living and Fossil Dinoflagellates* is still based primarily on external morphology, and attempts to reconcile in a single system fossil and extant species. Six different types of tabulation (in a sense nearly equivalent to Netzel and Dürr's (1984) 'corticotypes'; Fensome et al. 1993, p. 12) were recognized. Within Dinophyceae sensu stricto, subdivision into subclasses followed differences in tabulation type combined with differences in general morphology of vegetative cells or cysts. The six tabulation types were defined as follows: 1) gymnodinioid, when the amphiesmal vesicles are numerous and arranged either randomly or in apparent latitudinal series, in the latter case with more than 10 series; dinoflagellates with this kind of tabulation are naked (i.e., without cellulose-like plate material) like *Gymnodinium* F. Stein; 2) suessioid, when the amphiesmal vesicles contain thecal plates and are arranged in more than six but less than eleven latitudinal series; this type of tabulation is present in, e.g., *Symbiodinium* Freudenthal; 3) gonyaulacoid-peridinioid, in the cases where there are thecal plates in the amphiesmal vesicles that are organized in five latitudinal series plus the cingular and longitudinal sulcal series; *Peridinium*, *Protoperidinium* Bergh and *Gonyaulax* Diesing are examples of genera with this type of tabulation; 4) dinophysioid when the theca is divisible in two lateral halves separated by a serrated sagittal suture, but a cingulum and a sulcus are still present; *Dinophysis* Ehrenberg and *Ornithocercus* F. Stein have this kind of tabulation; 5) prorocentroid, in the cases where there is neither cingulum nor sulcus and the cell is divided into two large plates with an apical insertion of the flagella; *Prorocentrum* Ehrenberg is the main taxon with this tabulation; 6) nannoceratopsioid, known only for a fossil genus that has a cingulum dividing the cell into a dinophysioid hypotheca and a gonyaulacoid-peridinioid epitheca.

MODERN TOOLS USED IN DINOFLAGELLATE CLASSIFICATION AND TAXONOMY

Molecular phylogeny. The great development of molecular techniques involved in the sequencing of genes have led, in the last 20 years, to a major use of molecular phylogenies in works on dinoflagellate classification, taxonomy, phylogeny and population genetics.

The sequences of nuclear DNA that code for ribosomal RNA subunits (hereafter designated rDNA) are the most commonly used for phylogenetic inference (Logares 2007). The four RNA strands involved in eukaryotic ribosome constitution are relatively conservative; the 18S (small subunit, SSU), the 28S (large subunit, LSU) and the 5.8S, together with two internal transcribed spacers (ITS1 and ITS2), are included in a single pre-rRNA transcription unit; the 5S fragment included in the large subunit of the ribosome is coded for in other regions of the genome. The ITS sequences are less conservative and may therefore be used for a different level of discrimination. The use of rDNA has the advantage that these genes are widespread in eukaryotes, since all have ribosomes, and exist in many copies in the genome, which means there is abundant template for genetic amplification; the different rates of evolution between the fragments (including the ITS regions) provides information at different levels. Mitochondrial genes, e.g., the mitochondrial cytochrome *b* (*cob*) and mitochondrial cytochrome *c* oxidase 1 (*cox1*) genes have also been used in several works (Zhang et al. 2005, 2007). Other genes have been used to a lesser extent, e.g., HSP90, actin, alpha- and beta-tubulin genes (see Saldarriaga et al. 2004, Leander and Keeling 2004).

Early molecular studies of dinoflagellates were largely concerned with the origin of the group relative to other protistan lines, rather than the relationships between the various dinoflagellate lineages. The first gene sequence of a dinoflagellate to appear was the 5S rDNA for *Crypthecodinium cohnii* (Seligo) Javornický (Hinnebusch et al. 1981) and it indicated that dinoflagellates were not the most primitive of the eukaryotes, in opposition to an idea current at the time (the Mesocaryota hypothesis, mainly fundamented on the lack of histones; Dodge 1966). In later phylogenetic studies, dinoflagellates consistently formed a monophyletic group together with the apicomplexans and the ciliates (Gajadhar et al. 1991, Van de Peer et al. 1996); the group was named Alveolata by Cavalier-Smith (1991). Within this group, dinoflagellates were found to be more closely related to the apicomplexans than to the ciliates (Van de Peer and De Wachter 1997, Fast et al. 2002).

The number of available sequences of both large and small subunit rDNA from different dinoflagellate taxa increased during the 1990s and were used in

several works about phylogenetic relationships within the group and in studies focused on closely related groups. Saunders et al. (1997) used about 40 complete or partial sequences of SSU rDNA, from 20 dinoflagellate genera, to suggest that *Noctiluca* was the earliest diverging dinoflagellate lineage, and that the Gonyaulacales formed a monophyletic group separate from a large group including Gymnodiniales, Peridiniales and Prorocentrales (the GPP clade).

Saldarriaga et al. (2004) produced phylogenetic trees based either on SSU or LSU rDNA and combined the data to produce a concatenated tree. Their results suggested that thecal plates had been lost repeatedly during evolution and that the Peridiniales were a paraphyletic group. Murray et al. (2005) also used the concatenated alignment of LSU and SSU rDNA of several dinoflagellates, which, however, did not provide better resolution than the phylogenetic trees based on the individual genes. Contrary to previous analyses, the Peridiniales, excluding the genus *Heterocapsa* F. Stein, appeared to be monophyletic, although with low statistical support (Murray et al. 2005).

Several recent works dealing with molecular phylogeny were focused on subgroups within dinoflagellates and led to the creation or redefinition of a number of genera. Some of the major changes at generic level involved atecathe dinoflagellates. Daugbjerg et al. (2000), using morphological features supported by a phylogenetic hypothesis based on LSU rDNA partial sequences, described three new genera (*Karenia* Gert Hansen et Moestrup, *Karlodinium* J. Larsen and *Akashiwo* Gert Hansen et Moestrup) and redefined the genus *Gymnodinium*. The genus *Amphidinium* Claparède et J. Lachmann was later redefined on the basis of a combination of morphological features and partial LSU rDNA-derived phylogenies (Flø Jørgensen et al. 2004). A group of thinly thecate dinoflagellates, the woloszynskioids, have been extensively revised on the basis of ultrastructure and LSU rDNA phylogenies and several new genera and two new families (Tovelliaceae and Borghiellaceae) have been described (Lindberg et al. 2005, Moestrup et al. 2008, 2009a, 2009b). Another assemblage of taxa that has been the subject of several studies in which molecular phylogeny had an important role is a group of essentially marine dinoflagellates that includes the very common genus *Scrippsiella* Balech ex A. R. Loeblich, which has the peculiarity of producing

calcareous cysts (see, e.g., Montresor et al. 1997, 2003). *Scrippsiella* species have the same tabulation as a group of freshwater species currently placed in *Peridinium*. The species that build calcareous structures seem to form a monophyletic clade with a group of mainly heterotrophic species capable of ingesting particles or prey through a feeding tube, but not known to calcify: the Pfiesteriaceae (Gottschling et al. 2005). This led to the suggestion that the family name Thoracosphaeraceae be redefined to include all the calcareous dinoflagellates and the non-calcareous relatives presumably derived from them (Elbrächter et al. 2008).

The number of DNA sequences publicly available and stored centrally in GenBank increases steadily, enlarging the taxon sampling possibilities for phylogenetic studies. However, an important consideration about using deposited sequences is the need to be confident that the sequenced organisms were correctly identified.

Scanning and transmission electron microscopy. In the 1960s the scanning electron microscope (SEM) started to be used for observation of thecal structure in dinoflagellates (reviewed by Lewis and Dodge 1990). As seen before, the foundations of dinoflagellate taxonomy were created by light microscopy, which can be limiting when observing small structures and can lead to misinterpretations. With the general use of SEM, many taxa were re-evaluated and many new taxa were described more completely. In thecate taxa, the description of plate ornamentation, plate overlap, type of apical pore, number of cingular and, in some cases, sulcal plates were facilitated by the use of SEM.

Athecate taxa are much more delicate than thecate ones and SEM observations are heavily dependent upon the quality of the fixation and drying process. With the more general use of SEM for the observation of dinoflagellates it was discovered that the structure of the amphiesma and the types of apical grooves or furrows that ornament the athecate and thinly thecate forms are important taxonomic features (Daugbjerg et al. 2000, Moestrup et al. 2009b).

The first transmission electron microscopic (TEM) observations of dinoflagellates date from the 1950s. These were observations on the flagella (e.g., Pitelka and Schooley 1955), chromosomes (e.g., Grell and Wohlfarth-Bottermann

1957) and the theca (Fott and Ludvik 1956). The initial observations on the nucleus and flagella of dinoflagellates highlighted the peculiarity of this group of organisms and the need for further ultrastructural studies. Some of the first dinoflagellates to be studied more extensively by TEM were: *Karlodinium veneficum* (D. Ballantine) J. Larsen (Leadbeater and Dodge 1966, as *Woloszynskia micra* B. Leadbeater et J.D. Dodge), *Amphidinium carterae* Hulburt (Dodge and Crawford 1968), *Aureodinium pigmentosum* J.D. Dodge (Dodge 1967) and *Ceratium hirundinella* (O.F. Müller) Dujardin (Dodge and Crawford 1970). In the 1970s, several review articles on the general ultrastructure of dinoflagellates (Dodge 1971) and on more particular structures, e.g., chloroplasts, pyrenoids and food reserves (Dodge 1975, Dodge and Crawford 1971), and pusules (Dodge 1972) were published. Important revisions on several aspects concerning dinoflagellates, including ultrastructural features, were assembled during the 1980s in the books edited by Spector (1984. *Dinoflagellates*) and F. J. R. “Max” Taylor (1987. *The Biology of Dinoflagellates*).

The great majority of the ultrastructural works on dinoflagellates produced during the 1960s and 1970s treated the flagellar apparatus (including the basal bodies and roots, and fibrous material associated with them) as a sideline to the overall ultrastructural examination of the cell. It was only in the 1980s that renewed attention was given to this complex region of the cells and, in some works, three-dimensional reconstructions of the flagellar root apparatus were prepared from the information obtained by the TEM examination of serial sections. Among the first species to be examined in this way were *Oxyrrhis marina* Dujardin, *Woloszynskia* sp. and *Ceratium furcoides* (Levander) Langhans (Roberts 1985, Roberts and Timpano 1989, Roberts 1989). Details of the flagellar apparatus had been published for nearly a dozen species of dinoflagellates by the early 1990s (Roberts and Roberts 1991, Roberts et al. 1992). An attempt to incorporate flagellar apparatus and other cytosketon features into a phylogenetic framework was made by Roberts (1991).

Although ultrastructural features that are typical of dinoflagellates are widely known and it is often possible to recognize a member of the group from a single TEM micrograph, the finding of new structures or new aspects for some cell

components continues at a steady rate. This is an indication that there is still much to unravel about the ultrastructure of dinoflagellates.

GENERAL ULTRASTRUCTURE OF PERIDINIOIDS, GONYAULACOIDS AND WOLOSZYNSKIOIDS

In this section, a general comparison of peridinioids, gonyaulacoids and woloszynskioids is given on the basis of morphological and ultrastructural features of representatives from each group (see Table 1).

Peridinioids are here considered in the sense of Taylor (2004), as thecate dinoflagellates with five latitudinal plate series plus the cingular and sulcal series; cells tend to be bilaterally symmetrical and have two relatively large, subequal antapical plates and a single posterior sulcal plate in the hypotheca. In freshwater, *Peridinium* and *Peridiniopsis* (as defined in, e.g., Popovský and Pfiester 1990) are the most common peridinioid genera, whereas in marine and brackish waters *Heterocapsa*, *Scrippsiella*, *Pfiesteria* and *Protoperidinium* are some of the most widespread genera. The latter genus has a reduced number of cingular plates (three or four, depending on whether a small plate at the cingulum-sulcus boundary is counted as cingular), usually taken as a clear difference from *Peridinium*, in which it was included in past classifications (Balech 1974).

Particular attention is given to the type species of *Peridinium* (*P. cinctum*) and *Peridiniopsis* (*P. borgei*), *Tyrannodinium berolinense* (Lemmermann) Calado, Craveiro, Daugbjerg et Moestrup (formerly *Peridiniopsis berolinensis* (Lemmermann) Bourrelly), *Heterocapsa pygmaea* A.R. Loeblich, R.J. Schmidt et Sherley, *Scrippsiella minima* X. Gao et J.D. Dodge and *Bysmatrum arenicola* T. Horiguchi et Pienaar (Table 1).

Gonyaulacoids are basically similar to peridinioids in having the same number of latitudinal plate series but show significant left-handed torsion of the epitheca; the antapical plates and the first apical plate show considerable asymmetry (Taylor 2004). In this group, *Alexandrium catenella* (Whedon et Kofoid) Balech, *Gonyaulax spinifera* (Claparède et J. Lachmann) Diesing and *Protoceratium reticulatum* (Claparède et J. Lachmann) Bütschli are considered (Table 1).

The woloszynskioids are usually characterized by the cells being covered by many thin, often hexagonal plates, sometimes arranged in latitudinal series but too numerous to be described using the Kofoidian system of plate terminology (Moestrup et al. 2009a). In Fensome et al. (1993) these organisms were included in two different orders, the Gymnodiniales and Suessiales. Recent works confirmed that woloszynskioids are polyphyletic. Two new families, Tovelliaceae and Borghiellaceae, were created for some of the woloszynskioids and the family Suessiaceae was emended as a result of a revision of the group (Lindberg et al. 2005, Moestrup et al. 2009a). The Suessiaceae included in this summary are: *Biecheleria pseudopalustris* (J. Schiller) Moestrup, K. Lindberg et Daugbjerg, *B. baltica* Moestrup, K. Lindberg et Daugbjerg, *Biecheleriopsis adriatica* Moestrup, K. Lindberg et Daugbjerg, *Polarella glacialis* Montresor, Procaccini et Stoecker and *Symbiodinium natans* Gert Hansen et Daugbjerg. In the Tovelliaceae, *Tovellia coronata* (Wołoszyńska) Moestrup, K. Lindberg et Daugbjerg, *T. sanguinea* Moestrup, Gert Hansen, Daugbjerg, Flaim et D'Andrea, *Esoptrodinium gemma* Javornický[1] and *Jadwigia applanata* Moestrup, K. Lindberg et Daugbjerg and in the Borghiellaceae, *Borghiella dodgei* Moestrup, Gert Hansen et Daugbjerg and *Baldinia anauniensis* Gert Hansen et Daugbjerg are considered (Table 1). When relevant, comparisons are extended to other species.

Cell cover and tabulation. Peridinioids and gonyaulacoids are thecate (they have thick plates inside the amphiesmal vesicles) and have six latitudinal plate series (including the cingular series). Peridinioids always have two antapical plates of similar size and five (excepcionally six) postcincular plates. Gonyaulacoids, in contrast, have two antapical plates with considerable asymmetry, one being much smaller and shifted to the left as a result of torsion (sometimes considered a posterior intercalary plate), and six postcingular plates (Taylor 2004). In general, plate arrangement in gonyaulacoids is more asymmetrical that in peridinioids (Taylor 2004).

[1] *Esoptrodinium gemma* Javornický was described for *Bernardinium bernardinense* auctt. non Chodat (Javornický 1997). It assumes the existence of a mirror symmetrical species, with the transverse flagellum directed to the cell's right, that would be the true *Bernardinium bernardinense* Chodat (see Calado et al. 2006 for discussion).

Table 1. General comparison of morphology and fine structure of a selection of peridinioids, gonyaulacoids, Tovelliaceae, Borghiellaceae and Suessiaceae. +, present; –, not present; ?, no information, uncertain.

Features	peridinioids	gonyaulacoids	Tovelliaceae	Borghiellaceae	Suessiaceae
Number of latitudinal series plus sulcus[a]	6-7	6-7	ca. 9	16 or ca. 100 plates	7-15/20
Apical complex	– / +	+	ALP	– / PEV	– / EAV
Chloroplast	– / few to numerous, peripheral / lobes radiating from the centre	lobes radiating from the centre	numerous, peripheral / lobes radiating from the centre	numerous, peripheral / lobes radiating from the centre	numerous, peripheral
Pyrenoid[b]	– / one central or dorsal / several, with tubular structures derived from the thylakoids	central pyrenoid complex	– / central pyrenoid complex	– / central pyrenoid complex	one or several, with tubular structures derived from the thylakoids
Eyespot type[c]	– / A / B	–	C	B	E
BBs angle (°)	90 or less (100[d])	90 or more	90 or more	more than 90	more than 90
LC	+	–	–	–	–
SRC	– / +[e]	+	+	+	+
SMR, r2	+[f]	+	– / +	– / +	– / +
TMRE	one or more strands[g]	one strand	one or more strands	one strand	one strand

[a] Includes the cingulum and, in peridinioids and gonyaulacoids, anterior and posterior intercalary plate series; sulcal plates are included as a non-latitudinal series.
[b] Thylakoid-free areas in the chloroplast were not considered pyrenoids.
[c] Moestrup and Daugbjerg (2007).
[d] Ca. 100° in *Tyrannodinium berolinense*.
[e] Present only in *Heterocapsa pygmaea*.
[f] Not confirmed in *Heterocapsa pygmaea* and in *Bysmatrum arenicola.*
[g] With or without association with fibrous material.

Features	peridinioids	gonyaulacoids	Tovelliaceae	Borghiellaceae	Suessiaceae
LB-LMRc	–	–	– / +	+	+
TB-LMRc	– / +	– / +	–	+	– / +
BBc	–	+	–	+	? / +
Microtubular basket (MB)	– / +	–	–	–	–
Microtubular strand of the peduncle (MSP)	– / +	–	? / +	? / +	? / +
MSP homologue[h]	–	+	?	?	?
Peduncle	– / +	–	– / +	–	– / +
Pusule	pusular elements opening at large vesicles connected to the FCs / flattened vesicles	pusular elements opening at large vesicles connected to the FCs	long, coiled tube with numerous diverticula in middle or distal part	long, convoluted tube	long, convoluted tubes / pusule canals with pusular tubules
Trichocysts	+	+	+	–	–
Species considered	*Bysmatrum arenicola, Heterocapsa pygmaea, Peridinium cinctum, Peridiniopsis borgei, Scrippsiella minima, Tyrannodinium berolinense* **1**	*Alexandrium catenella, Gonyaulax spinifera, Protoceratium reticulatum* **2**	*Esoptrodinium gemma, Jadwigia applanata, Tovellia coronata, T. glabra, T. sanguinea* **3**	*Baldinia anauniensis, Borghiella dodgei* **4**	*Biecheleria baltica, B. pseudopalustris, Biecheleriopsis adriatica, Polarella glacialis, Symbiodinium natans* **5**

Abbreviations: ALP, apical line of narrow plates; PEV, pair of elongate amphiesmal vesicles; EAV, single elongate amphiesmal vesicle; BBs, basal bodies; LC, layered connective; SRC, striated root connective; SMR, single-stranted microtubular root; TMRE, transverse microtubular root extension; LB-LMRc, connective between LB and LMR; TB-LMRc, connective between TB and LMR; BBc, connective between basal bodies.

References: **1** Horiguchi and Pienaar (1988), Bullman and Roberts (1986), Calado et al. 1999, Calado and Moestrup (1997, 2002), Gao and Dodge (1991), Wedemayer and Wilcox (1984); **2** Hansen and Moestrup (1998), Hansen et al. (1996, 1997); **3** Calado et al. (2006), Roberts et al. (1995), Lindberg et al. (2005), Crawford and Dodge (1971), Moestrup et al. (2006); **4** Hansen et al. (2007), Moestrup et al. (2008); **5** Moestrup et al. (2009a, b), Montresor et al. (1999), Hansen and Daugbjerg (2009)

[h] Not associated with electron-opaque vesicles and not shown to extend into a peduncle.

In the Tovelliaceae, Borghiellaceae and Suessiaceae the amphiesmal vesicles are numerous, pentagonal or hexagonal, and contain thin plates. The number of latitudinal series varies from 7–16 (up to more than 20 in *Biecheleria pseudopalustris*) in the Suessiaceae and Borghiellaceae or is about 9 in the Tovelliaceae (Lindberg et al. 2005, Moestrup et al. 2008, Moestrup et al. 2009a).

Apical complex. One characteristic found in many dinoflagellates is the presence of a differentiated structure at the anterior end of the cell. In thecate taxa it typically includes a plate with some type of pore or aperture and is called an apical pore (or an apical pore complex). Dodge and Hermes (1981) described the apical pore in 15 genera of marine dinoflagellates studied by SEM, classified them into six different types, and proposed a new terminology for the plates comprising the apical pore structure. The same terminology will be used here: the 'cover plate' is a small, round or elongate plate that covers the pore; the 'pore plate' is a ring-shaped plate located around the cover plate; the 'canal plate' is typically rectangular and contacts the ventral edge of the pore plate. Toriumi and Dodge (1993) described the apical pore structure in 10 freshwater and marine genera of Peridiniaceae, based also on SEM observations, and classified them into four different types, further subdivided into sub-types, according to the number of sections of the 'apical collar' (a term applied to the raised margins of the plates surrounding the apical pore), the presence or absence of a rim around the pore, and how far the canal plate elongates into the pore plate.

Although the bulk of the peridinioids have an apical pore, the type species of *Peridinium*, *P. cinctum*, lacks one and forms, together with six other species, the subgenus Cleistoperidinium in Popovský and Pfiester (1990). When present, the apical pore complex is formed by a circular to elongated pore plate, the cover plate and the canal plate (Calado and Moestrup 2002, Gao and Dodge 1991).

In gonyaulacoids, an apical pore is always present but it is more variable: for example, in *Protoceratium reticulatum* the pore plate is elongate, with a narrow slit-like pore (Hansen et al. 1997) while in *Ceratium hirundinella* the pore plate is circular (Dodge and Crawford 1970, Calado and Larsen 1997); usually there is no canal plate.

The type of apical structure in athecate or thinly thecate forms is currently considered an important distinctive character at genus and family level (Daugbjerg et al. 2000, Lindberg et al. 2005). The structures involved have been named 'acrobase' or 'apical groove' in past literature (Biecheler 1952, Takayama 1985). The new families created for the woloszynskioid dinoflagelates differ in the types of apical apparatus. Members of the Tovelliaceae possess an apical line of narrow plates, which are ornamented with small thickenings (ALP sensu Lindberg et al. 2005). In the Borghiellaceae, the apical furrow, when present, comprises a pair of parallel elongated vesicles (PEV) and one of these has a central row of knobs (Moestrup et al. 2008). The Suessiaceae have been recently emended and the description of the family now includes an apical furrow apparatus comprising a single elongated and very narrow amphiesmal vesicle (EAV) surrounded by one to several very narrow amphiesmal vesicles on each side and a smaller vesicle at the ventral side (Moestrup et al. 2009a, Siano et al. 2010). *Baldinia anauniensis* and *Polarella glacialis* are two exceptions for the Borghiellaceae and Suessiaceae, respectively, since they do not seem to have any kind of apical furrow apparatus (Hansen et al. 2007, Montresor et al. 1999).

Nucleus. As seen above, the nucleus of dinoflagellates is easily recognized by the characteristic appearance of the permanently condensed chromosomes. The nuclear envelope is generally formed by a two-membrane structure with numerous, scattered nuclear pores. Although important variations have been found in the nuclei of the Gymnodiniales, notably the presence of nuclear pores restricted to peculiar folds of the nuclear envelope known as nuclear chambers (e.g., in *Gymnodinium* sensu stricto; Dodge and Crawford 1969, Hansen 2001, Hansen and Daugbjerg 2004, Hansen and Moestrup 2005) all peridinioids, gonyaulacoids and woloszynskioids examined show the more general nuclear type. The nucleus is generally large, rounded, ellipsoid or shaped like a curved sausage, and is variously located in the cell: in the hyposome (e.g., *Tyrannodinium berolinense*), in the dorsal part of the cell middle (e.g., *Peridinium cinctum*), in the episome (e.g., *Symbiodinium natans*), or even extending from epi- to hyposome (e.g., *Borghiella dodgei*) (Wedemayer and Wilcox 1984, Calado et al. 1997,

Calado et al. 1999, Hansen and Daugbjerg 2009, Moestrup et al. 2008). The position of the nucleus varies also within species of the same genus.

Chloroplasts and pyrenoids. Only approximately half the dinoflagellate species have chloroplasts, and their number, shape and distribution in the cell show some variation. The typical dinoflagellate chloroplast contains chlorophylls a and c, and peridinin as the main carotenoid pigment (Dodge 1975, Keeling 2004). The brown pigment fucoxanthin is present in some species instead of peridinin, e.g. *Karlodinium* spp., *Karenia* spp. and *Takayama* spp. (Schnepf and Elbrächter 1999, as species of *Gymnodinium*). The diatom nature of the symbiont that provided the fucoxanthin-containing chloroplast is firmly established for, e.g., *Kryptoperidinium foliaceum* (F. Stein) Er. Lindemann and *Peridiniopsis* cf. *kevei* Grigorszky (McEwan and Keeling 2004, Takano et al. 2008). In addition, species of *Lepidodinium* M.M. Watanabe, S. Suda, I. Inouye, Sawaguchi et Chihara have green chloroplasts derived from a prasinophyte (Watanabe et al. 1990, Hackett et al. 2004). The typical peridinin-containing chloroplast is bounded by three membranes, and contains thylakoids generally in groups of three (or sometimes two), running parallel to the longitudinal axis of the chloroplast (Dodge 1975, Schnepf and Elbrächter 1999, Keeling 2004). In some cases, as in *Gonyaulax spinifera*, grana (i.e. stacks of disk-shaped portions of thylakoids) were observed (Hansen et al. 1996)

Three different arrangements of chloroplasts in the dinoflagellates treated here were observed: 1) numerous chloroplast lobes disposed at the cell perifery without well-defined pyrenoids (although often with thylakoid-free areas), as in some peridinioids (e.g., *Peridinium cinctum*), Toveliaceae (e.g., *Jadwigia applanata*) and Borghiellaceae (e.g., *Borghiella dodgei*) (Calado et al. 1999, Lindberg et al. 2005, Moestrup et al. 2008); 2) numerous chloroplast lobes radiating from a central area with a complex pyrenoid, as in the Gonyaulacoids and some Toveliaceae (e.g., *Tovellia sanguinea*) and Borghiellaceae (e.g., *Baldinia anauniensis*) (Hansen and Moestrup 1998a, Moestrup et al. 2006, Hansen et al. 2007); 3) chloroplast profiles with more defined, sometimes stalked, pyrenoids (one or more), that in some cases are lined by starch sheaths (e.g., *Peridiniopsis borgei*, *Symbiodinium natans*) (Calado and Moestrup 2002, Hansen

and Daugbjerg 2009); these pyrenoids can be penetrated by cytoplasmic channels (e.g., *Bysmatrum arenicola, Heterocapsa* species) or by tubular, membrane-bounded structures, single or paired, that are continuous with thylakoids (e.g., *Scrippsiella minima*, *Biecheleria* species) (Horiguchi and Pienaar 1988, Iwataki et al. 2003, Gao and Dodge 1991, Moestrup et al. 2009a).

Eyespot. Dinoflagellates are an unusual group in having different types of eyespot, a cell structure that is constant in most algal lineages. In a recent review on dinoflagellate phylogeny and classification, earlier revisions of eyespot types found in dinoflagellates (Dodge 1984, Kawai and Kreimer 2000) were modified to accomodate recent findings (Moestrup and Daugbjerg 2007). In addition, some dinoflagellates, e.g., gonyaulacoids, heterotrophic peridinioids (*Tyrannodinium berolinense*) and *Heterocapsa pygmaea*, do not have any kind of eyespot (Wedemayer and Wilcox 1984, Bullman and Roberts 1986).

Moestrup and Daugbjerg (2007) illustrated five types of eyespot, which are described below. Eyespot type A is formed by osmiophilic globules located in a chloroplast lobe. This type was found in some peridinioids, e.g., *Peridinium cinctum* (Calado et al. 1999). Eyespot type B is similar to type A with an added vesicle with one layer of brick-like, probably crystalline units located between subthecal microtubules or the longitudinal microtubular root (LMR or r1) and the chloroplast lobe containing the osmiophilic globules. This type of eyespot was found in the Borghiellaceae and in the peridinioid *Peridiniopsis borgei* (Hansen et al. 2007, Calado and Moestrup 2002). Eyespot type C has osmiophilic globules more or less fused, sometimes grouped in layers, not connected to the chloroplast or surrounded by any membrane. This is characteristic of the Tovelliaceae (Calado et al. 2006, Moestrup et al. 2006). Eyespot type D is formed by osmiophilic globules enclosed by three membranes and is present in, e.g., *Kryptoperidinium foliaceum*, *Durinskia baltica* (Levander) Carty et El.R. Cox and in other species with a reduced diatom endosymbiont (Jeffrey and Vesk 1976, Tomas and Cox 1973). Eyespot type E consists of several layers of brick-like units delimited by membranes and characterizes the Suessiaceae (Moestrup et al. 2009a, Siano et al. 2010). This eyespot was also found in the heterotroph *Prosoaulax lacustris* (F.

Stein) Calado et Moestrup (Calado et al. 1998), a freshwater species that perhaps belongs in the same group.

Pusule. The pusule is a quite variable but distinctive structure that is formed by a system of apparently empty tubules, or vesicles, with a close association between their bounding membrane and the inner membrane of an enveloping vesicle. Although several functions have been proposed for the pusule, the most widely accepted is that it has an excretory and osmo-regulatory function (Dodge 1972). Dodge (1972) reviewed the types of pusules on the basis of 40 freshwater and marine dinoflagellates and classified them into seven types included in two categories: (1) pusules with vesicles that connected directly to the flagellar canal, or to collecting chambers, or to pusular tubes; (2) pusules constructed of tubules or sacks only, with or without invaginated walls.

In general, the pusule observed in thecate dinoflagellates (peridinioids and gonyaulacoids) consists of pusular elements (vesicles and/or tubes) discharging into one or two large vesicles or sacs that connect to the flagellar canals. *Gonyaulax spinifera*, *Protoceratium reticulatum, Peridinium cinctum* and *Peridiniopsis borgei* show this type of pusule (Hansen et al. 1996, 1996/1997, Calado et al. 1999, Calado and Moestrup 2002). In *Scrippsiella minima*, the pusule is somewhat different: instead of a large vesicle there is a group of more or less flattened vesicles connected to a relatively small collecting chamber (Gao and Dodge 1991).

The pusule in Tovelliaceae and Borghiellaceae is usually composed of a long, more or less coiled tube, with some small variations. In the Tovelliaceae *Esoptrodinium gemma* and *Tovellia coronata* the pusular tube has, in the distal part (i.e., more to the centre of the cell), numerous diverticula and in the latter species the inner membrane is covered by electron-opaque “knobs” (Calado et al. 2006, Lindberg et al. 2005). In the Borghiellaceae *Baldinia anauniensis* the pusular tube is located in a cavity of the pyrenoid and its proximal part is associated with numerous electron-opaque bodies (Hansen et al. 2007), which are not found in *Borghiella dodgei* (Moestrup et al. 2008). In the Suessiaceae there is larger variation in the type of pusule. *Biecheleriopsis adriatica* has two similar pusules, each associated with one flagellar canal, composed of one pusule canal and

several pusular tubules fusing into it; in *Symbiodinium natans* there are two convoluted tubular pusules, whereas in *Polarella glacialis* no pusule was found (Moestrup et al. 2009b, Hansen and Daugbjerg 2009, Montresor et al. 1999).

Flagellar apparatus. The flagellar apparatus in dinoflagellates is formed by a large number of components which may vary from taxon to taxon (see Fig. 5 for a schematic representation of a dinoflagellate flagellar apparatus); however, several basic components occur in most taxa. All dinoflagellates have two basal bodies (transverse, TB and longitudinal, LB) inserted at a very variable angle. In peridinioids, the angle is usually 90º or a little less; in *Heterocapsa pygmaea*, however, the angle is very small (ca. 20º) (Calado et al. 1999, Bullman and Roberts 1986). In Tovelliaceae, Borghiellaceae and Suessiaceae the angle is always larger than 90º (Calado et al. 2006, Moestrup et al. 2008, Hansen and Daugbjerg 2009) and in gonyaulacoids it is at least 90º, up to more than 145º (Hansen et al. 1996). In some species not belonging to the groups under focus, as *Gymnodinium cryophilum* and *A. rhynchocephalum*, the angle can be almost 180º (Wilcox et al. 1982, Farmer and Roberts 1989).

The most widespread components of the flagellar apparatus in dinoflagellates are the longitudinal microtubular root (LMR, r1 in Moestrup 2000), the transverse microtubular root (TMR, r3 in Moestrup 2000) and the transverse striated root and associated microtubule (TSRM, r4 in Moestrup 2000).

The LMR is formed by a strand of a variable number of microtubules (usually more than 15 in the groups considered here) that makes contact, in the proximal end, with the proximal-left side of the LB, and runs posteriorly in the sulcal area. The relatively large number of microtubules in this root makes it easily spotted in sections through the posterior side of the flagellar base area.

The TMR consists of one microtubule that associates with the anterior-proximal side of the TB, going from a parallel orientation relative to the basal body microtubules to a roughly anterior-dorsal orientation in the cell. The TMR typically nucleates one row of 12 to 35 microtubules (transverse microtubular extension, TMRE) that extend toward the dorsal side of the cell. However, in peridinioids some variant features of this extension were found. In *Peridiniopsis borgei* the distal part of the TMRE associates with a fibre and forms a cylinder around it; this

configuration extends along the surface of the central, large sac pusule toward the pyrenoid at the dorsal side of the cell (Calado and Moestrup 2002). In *Peridinium cinctum* the TMRE is formed by at least five rows of microtubules, nucleated by the TMR that loops around the flagellar canal and sac pusule (Calado et al. 1999). A remarkable specialization was found in the TMRE of the gymnodinioid genus *Lepidodinium*, where it closely associates with a fibre that links the LMR to the nucleus (called the nuclear fibrous connective) and extends all the way to the nuclear envelope (Hansen and Moestrup 2005).

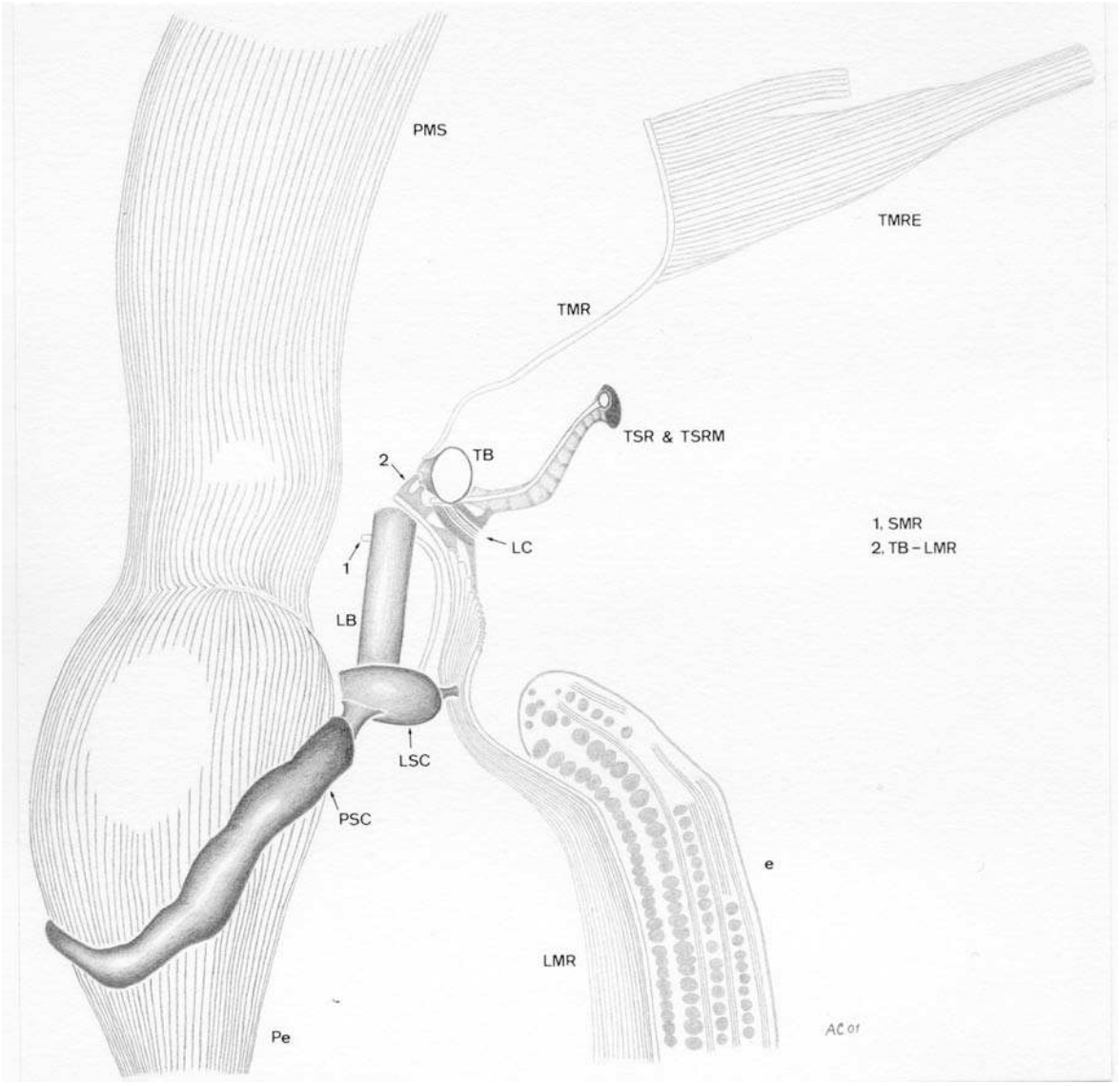

Fig. 5. Schematic representation of the flagellar apparatus of *Peridiniopsis borgei*, seen from the left side of the cell. LMR (r1), longitudinal microtubular root; SMR (r2), single–stranded

microtubular root; TMR (r3), transverse microtubular root; TSRM (r4), transverse striated root microtubule; TSR, transverse striated root; TMRE, transverse microtubular root extension; LB, longitudinal basal body; LC, layered connective; LSC, longitudinal striated collar; TB, transverse basal body; TB-LMR (=TB-LMRc), connective between TB and LMR. The microtubular strand of the peduncle (PMS), the peduncle (Pe), the peduncle striated collar (PSC) and the eyespot (e) are also represented. Adapted from Calado and Moestrup (2002).

The TSR is usually associated, at the anterior end, with the dorsal-posterior surface of the TB; it extends approximatly parallel to the TB and terminates close to the striated collar that limits the transverse flagellar canal (Hansen et al. 1997, Hansen and Daugbjerg 2009, Roberts et al. 1995). A single microtubule (TSRM) is usually seen along the entire length of the TSR, diverging from it proximally (Calado et al. 1999, Calado and Moestrup 2002).

A single-stranded microtubular root (SMR, r2 in Moestrup 2000) may also be present on the right side of the LB, approximately parallel to the LMR. It was found in all peridinioids studied in detail and in several gonyaulacoids, although not in *Peridiniella catenata* (Hansen and Moestrup 1998b). Although the presence of this root in some other dinoflagellate groups still needs to be clarified, it was clearly demonstrated in *Baldinia anauniensis* (Hansen et al. 2007).

In several dinoflagellate groups the basal bodies are sometimes, but not always, directly connected to each other by means of fibrous structures. In the peridinioids there is always a fibrous layered connective (LC) that associates the posterior-proximal side of the TB with the proximal end of the LB. This component is considered a significant peridinioid structure because it has not been found in other groups (Calado et al. 1999). On the other hand, all the other dinoflagellates observed in detail, with the exception of *Gymnodinium fuscum* (Ehrenberg) F. Stein and the swarmers of *Noctiluca scintillans* (Macartney) Kofoid (Hansen et al. 2000, Höhfeld and Melkonian 1995), have a fibrous connective (called the striated root connective, SRC or r1–r4 connective) linking the TSR and the LMR. The SRC is not present in peridinioids with the exception of *Heterocapsa pygmaea*, in which both a “bilayered connective” reminescent of the LC and a SRC were found (Bullman and Roberts 1986). As seen above, the taxonomic position of *Heterocapsa* may need to be reconsidered.

The TB and LB may be connected by more or less simple connective fibres to the LMR and this seems to be variable from group to group. Connectives between the LB and the ventral side of the LMR were not found in the peridinioids or gonyaulacoids, except in *Ceratium furcoides* (Roberts 1989), but they seem to be a regular feature in woloszynskioids, e.g., *Esoptrodinium gemma*, *Baldinia anauniensis*, *Symbiodinium natans* (Calado et al. 2006, Hansen et al. 2007, Hansen and Daugbjerg 2009). The connectives are usually very thin and connect individual triplets of the LB to several microtubules across the ventral side of the LMR. One or more connectives can be present linking the TB and the dorsal side of the LMR (TB-LMRc). They were found in some peridinioids, some gonyaulacoids and in Borghiellaceae (e.g., *Peridiniopsis borgei*, *Protoceratium reticulatum* and *Borghiella dodgei*), but not in the Tovelliaceae or Suessiaceae (Calado and Moestrup 2002, Hansen et al. 1997, Moestrup et al. 2008). In a number of cases, small connectives (not identifiable as a LC) were found between the two basal bodies, like in the gonyaulacoids, Borghiellaceae and some Suessiaceae (Hansen and Moestrup 1998a, Moestrup et al. 2008, Hansen and Daugbjerg 2009).

The flagellar canals are usually bordered by striated, complete or incomplete collars (transverse and longitudinal striated collars, TSC and LSC) at the point where the flagella exit the cell. In the gonyaulacoids and some peridinioids the collars are linked to each other by one or more striated connectives (Calado et al. 1999, Hansen et al. 1997); in addition, the collars of several woloszynskioids are linked to the ventral ridge, e.g., in *Borghiella dodgei* and *Jadwigia applanata* (Moestrup et al. 2008, Roberts et al. 1995).

Feeding apparatus. The presence of one or several microtubular strands in the ventral area of the cell, close, but not visibly connected, to the flagellar apparatus, has been a common observation in dinoflagellates studied in detail. In heterotrophic species, like *Tyrannodinium berolinense* and *Pfiesteria piscicida*, the food is ingested through a feeding tube supported by several such rows of microtubules (16 in *P. piscicida* to over 20 in *T. berolinense*), which overlap at the edges and are accompanied by elongated electron-opaque vesicles, forming the so-called “microtubular basket” (Calado and Moestrup 1997, Litaker et al. 2002). In

many species only one row of microtubules is present, also accompanied by electron-opaque vesicles (the microtubular strand of the peduncle, MSP). This is the case in some Tovelliaceae (*Tovellia* species, *Esoptrodinium*), Suessiaceae (*Symbiodinium natans*) and Borghiellaceae (*Baldinia anauniensis*) (Lindberg et al. 2005, Calado et al. 2006, Hansen and Daugbjerg 2009, Hansen et al. 2007). The somewhat particular MSP of *Peridiniopsis borgei* is made of a single strand of 75–80 microtubules on the ventral side (close to elongated electron-opaque vesicles) that, when extending to the interior of the cell, divides successively into two and then four strands, terminating between the pyrenoid and the sac pusule with the same number of microtubules as in the ventral region (Calado and Moestrup 2002). Another type of microtubular strand is formed by one row of microtubules not accompained by any electron-opaque vesicles. This type of microtubular strand is probably homologous with the strands of the peduncle (Hansen et al. 1996) although there is no indication that they are functional. This was observed in some gonyaulacoids like *Gonyaulax spinifera* and *Protoceratium reticulatum* (Hansen et al. 1996, 1997). In these cases, no protruded peduncle was seen.

AIMS OF THE WORK

Among thecate dinoflagellates, the presence or absence of an apical thecal pore and the number of plates in the cingulum have been often considered important phylogenetic markers at genus or family level. As presently conceived, *Peridinium*, the most widely represented dinoflagellate genus in freshwater, includes organisms with four different combinations of those features. The type species, *P. cinctum*, has five cingular plates and no apical pore; another group, exemplified by *P. bipes*, has five cingular plates and an apical pore; in yet another group, including e.g. *P. palatinum*, the number of cingular plates is six and an apical pore is absent; finally, species like *P. lomnickii* or *P. umbonatum* F. Stein have six cingular plates and an apical pore. The latter combination is also widespread in *Peridiniopsis* and in the marine genus *Scrippsiella*. With this in mind, the main propose of this work was to contribute to the knowledge of the peridinioid dinoflagellates in order to be able to attempt a revision of the group

using a combination of an ultrastructural and a molecular approach. In particular, the aims were:

1. Extending the knowledge on the fine structural organization of peridinioids through the detailed examination of the selected species;

2. Increasing the database of comparable gene sequences obtained from reliably identified members of the group, especially the LSU rDNA (domains D1-D6);

3. Inferring the phylogenetic affinities of peridinioid dinoflagellates from morphological, ultrastructural and molecular data;

4. Identifying reliable phylogenetic markers for the peridinioids and their subgroups recognized — aiming for a resulting classification that will not only reflect evolutionary relationship, but will also allow the prediction of features in related species not examined in detail;

5. Effecting the necessary taxonomic changes.

6. Achieving a better understanding of the evolution and present occurrence of heterotrophic feeding capabilities in the peridinioids and related groups resulting from unravelling the evolution of the peduncular system in the group.

REFERENCES

Baker, H. 1753. *Employment for the microscope*. Chapter XXIX. Of luminous water insects. R. Dodsley, London, pp. 399–406.

Balech, E. 1974. El género *"Protoperidinium"* Bergh, 1881 (*"Peridinium"* Ehrenberg, 1831, partim). *Rev. Mus. Argent. Cienc. Nat., Hidrobiol.* 4:1-79.

Biecheler, B. 1952. Recherches sur les Péridiniens. *Bull. Biol. Fr. Belg., Suppl.* 36: VI + 149 pp.

Bourrelly P. 1968. Notes sur les Péridiniens d'eau douce. *Protistologica* 4:5–13, pls I–II

Bourrelly P. 1970. *Les algues d'eau douce 3: Les algues bleues et rouges, les Eugléniens, Peridiniens et Cryptomonadines.* Boubée, Paris. 512 pp.

Bullman, V. & Roberts, K. R. 1986. Structure of the flagellar apparatus in *Heterocapsa pygmaea* (Pyrrophyta). *Phycologia* 25:558–71.

Calado, A. J., Craveiro, S. C. & Moestrup, Ø. 1998. Taxonomy and ultrastructure of a freshwater, heterotrophic *Amphidinium* (Dinophyceae) that feeds on unicellular protists. *J. Phycol.* 34:536–54.

Calado, A. J., Craveiro, S. C., Daugbjerg, N. & Moestrup, Ø. 2006. Ultrastructure and LSU rDNA-based phylogeny of *Esoptrodinium gemma* (Dinophyceae), with notes on feeding behavior and the description of the flagellar base area of a planozygote. *J. Phycol.* 42:434–52.

Calado, A. J., Hansen, G. & Moestrup, Ø. 1999. Architecture of the flagellar apparatus and related structures in the type species of *Peridinium*, *P. cinctum* (Dinophyceae). *Eur. J. Phycol.* 34:179–91.

Calado, A. J. & Larsen, J. 1997. On the identity of the type species of the genus *Ceratium* Schrank (Dinophyceae), with notes on *C. hirundinella*. *Phycologia* 36:500–5.

Calado, A. J. & Moestrup, Ø. 1997 Feeding in *Peridiniopsis berolinensis* (Dinophyceae): new observations on tube feeding by an omnivorous, heterotrophic dinoflagellate. *Phycologia* 36:47–59.

Calado, A. J. & Moestrup, Ø. 2002. Ultrastructural study of the type species of *Peridiniopsis*, *Peridiniopsis borgei* (Dinophyceae), with special reference to the peduncle and flagellar apparatus. *Phycologia* 41:567–84.

Cavalier-Smith, T. 1991. Cell diversification in heterotrophic flagellates. *In* Patterson, D. J. & Larsen, J. [Eds.] *The biology of free-living heterotrophic flagellates*. Clarendon Press, Oxford, pp. 113–31 (Systematic Association Special Volume No. 45).

Craveiro, S. C., Calado, A. J., Daugbjerg, N. & Moestrup, Ø. 2009. Ultrastructure and LSU rDNA-based revision of *Peridinium* group palatinum (Dinophyceae) with the description of *Palatinus* gen. nov. *J. Phycol.* 45:1175–1194.

Daugbjerg, N., Hansen, G., Larsen, J. & Moestrup, Ø. 2000. Phylogeny of some of the major genera of dinoflagellates based on ultrastructure and partial LSU rDNA sequence data, including the erection of three new genera of unarmoured dinoflagellates. *Phycologia* 39:302–17.

Dodge, J. D. 1966. The Dinophyceae. *In* Godward, M. B. E. [Ed.] *The chromosomes of the Algae*. Edward Arnold, London, pp. 96–115.

Dodge, J. D. 1967. Fine structure of the dinoflagellate, *Aureodinium pigmentosum* gen. et sp. nov. *Br. phycol. Bull.* 3:327–36.

Dodge, J. D. 1971. Fine structure of the Pyrrophyta. *Bot. Rev.* 37:481–508.

Dodge, J. D. 1972. The ultrastructure of the dinoflagellate pusule: A unique osmo-regulatory organelle. *Protoplasma* 75:285–302.

Dodge, J. D. 1975. A survey of chloroplast ultrastructure in the Dinophyceae. *Phycologia* 14:253–63.

Dodge, J. D. 1984. The functional and phylogenetic significance of dinoflagellate eyespots. *BioSystems* 16:259-67.

Dodge, J. D. 1987. Dinoflagellate ultrastructure and complex organelles: A. General ultrastructure. *In* Taylor, F. J. R. [Ed.] *The biology of dinoflagellates*. Blackwell Scientific Publ., Oxford, pp. 93–119 (Botanical Monographs Volume 21.)

Dodge, J. D. & Crawford, R. M. 1968. Fine structure of the dinoflagellate *Amphidinium carteri* Hulbert. *Protistologica* 4:231–42, pls 1–6.

Dodge, J. D. & Crawford, R. M. 1969. The fine structure of *Gymnodinium fuscum* (Dinophyceae). *New Phytol.* 68:613–8.

Dodge, J. D. & Crawford, R. M. 1970. The morphology and fine structure of *Ceratium hirundinella. J. Phycol.* 6:137–49.

Dodge, J. D. & Crawford, R. M. 1971. A fine-structural survey of dinoflagellate pyrenoids and food–reserves. *Bot. J. Linn. Soc.* 64:105–15.

Dodge, J. D. & Hermes, H. B. 1981. A scanning electron microscopical sudy of the apical pores of marine dinoflagellates (Dinophyceae). *Phycologia* 20:424–30.

Ehrenberg, C. G. 1830. Beiträge zur Kenntniss der Organisation der Infusorien und ihrer geographischen Verbreitung, besonders in Sibirien. *Abh. Königl. Akad. Wiss. Berlin (Phys. Kl.)* 1830:1–88, pls 1–8. [The journal was published in 1832, but was preceded by a separatum released on 13 August 1830.]

Ehrenberg, C. G. 1838. *Die Infusionsthierchen als vollkommene Organismen. Ein Blick in das tiefere organische Leben der Natur*. Leopold Voss, Leipzig. Germany, 547 pp., 64 pls.

Elbrächter, M., Gottschling, M., Hildebrand-Habel, T., Keupp, H., Kohring, R., Lewis, J., Meier, K. J. S., Montresor, M., Streng, M., Versteegh, G. J. M., Willems, H. & Zonneveld, K. 2008. Establishing an agenda for calcareous dinoflagellate research (Thorascophaeraceae, Dinophyceae) including a nomenclatural synopsis of generic names. *Taxon* 57:1289–303.

Farmer, M. A. & Roberts, K. R. 1989. Comparative analyses of the dinoflagellate flagellar apparatus. III. Freeze substitution of *Amphidinium rhynchocephalum. J. Phycol.* 25:280–92.

Fast, N. M., Xue, L., Bingham, S. & Keeling, P. J. 2002. Re-examining alveolate evolution using multiple protein molecular phylogenies. *J. Eukaryot. Microbiol*. 49:30–7.

Fensome R. A., Taylor F. J. R., Norris G., Sarjeant W. A. S., Wharton D. I. & Williams G. L. 1993. A classification of living and fossil dinoflagellates. *Micropaleontology*, *Special Publication* 7:1–351.

Flø Jørgensen, M., Murray, S. & Daugbjerg, N. 2004. *Amphidinium* revisited. I. Redefinition of *Amphidinium* (Dinophyceae) based on cladistic and molecular phylogenetic analyses. *J. Phycol*. 40:351–65.

Fott, B. & Ludvík, J. 1956. Über den submikroskopischen Bau des Panzers von *Ceratium hirundinella*. *Preslia* 28:278–80, pls 16–17.

Gaines, G. & Taylor, F. J. R. 1985. Form and function of the dinoflagellate transverse flagellum. *J. Protozool*. 32:290–6.

Gajadhar, A. A., Marquardt, W. C., Hall, R., Gunderson, J., Ariztia-Carmona, E. V. & Sogin, M. L. 1991. Ribosomal RNA sequences of *Sarcocystis muris*, *Theileria annulata* and *Crypthecodinium cohnii* reveal evolutionary relationships among apicomplexans, dinoflagellates, and ciliates. *Mol. Biochem. Parasitol*. 45:147–54.

Gao, X. & Dodge, J. D. 1991. The taxonomy and ultrastructure of a marine dinoflagellate, *Scrippsiella minima* sp. nov. *Brit. Phycol. J.* 26:21–31.

Gottschling, M., Keupp, H., Plötner, J., Knop, R., Willems, H. & Kirsch, M. 2005. Phylogeny of calcareous dinoflagellates as inferred from ITS and ribosomal sequence data. *Mol. Phylogenet. Evol*. 36:444–55.

Grell, K. G. & Wohlfarth-Bottermann, K. E. 1957. Licht- und elektronenmikroskopische Untersuchungen an dem Dinoflagellaten *Amphidinium elegans* n. sp. Z. Zellforsch. Mikrosk. *Anat*. 47:7–17.

Hackett, J. D., Anderson, D. M., Erdner, D. L. & Bhattacharya, D. 2004. Dinoflagellates: a remarkable evolutionary experiment. *Amer. J. Bot.* 91:1523–34.

Hansen, G. 2001. Ultrastructure of *Gymnodinium aureolum* (Dinophyceae): toward a further redefinition of *Gymnodinium sensu stricto*. *J. Phycol.* 37:612–23.

Hansen, G & Daugbjerg, N. 2004. Ultrastructure of *Gyrodinium spirale*, the type species of *Gyrodinium* (Dinophyceae), including a phylogeny of *G. dominans*, *G. rubrum* and *G. spirale* deduced from partial LSU rDNA sequences. *Protist* 155:271–94.

Hansen, G. & Daugbjerg, N. 2009. *Symbiodinium natans* sp. nov.: a “free-living” dinoflagellate from Tenerife (Northeast-Atlantic Ocean). *J. Phycol.* 45:251–263.

Hansen, G., Daugbjerg, N. & Henriksen, P. 2007. *Baldinia anauniensis* gen. et sp. nov.: a “new” dinoflagellate from Lake Tovel, N. Italy. *Phycologia* 46:86–108.

Hansen, G. & Moestrup, Ø. 1998a. Fine-structural characterization of *Alexandrium catenella* (Dinophyceae) with special emphasis on the flagellar apparatus. *Eur. J. Phycol.* 33:281–91.

Hansen, G. & Moestrup, Ø. 1998b. Light and electron microscopical observations on *Peridiniella catenata* (Dinophyceae). *Eur. J. Phycol.* 33:293–305.

Hansen, G. & Moestrup, Ø. 2005. Flagellar apparatus and nuclear chambers of the green dinoflagellate *Gymnodinium chlorophorum*. *Phycol. Res.* 53:169–81.

Hansen, G., Moestrup, Ø. & Roberts, K. R. 1996. Fine structural observations on *Gonyaulax spinifera* (Dinophyceae), with special emphasis on the flagellar apparatus. *Phycologia* 35:354–66.

Hansen, G., Moestrup, Ø. & Roberts, K. R. 1997. Light and electron microscopical observations on *Protoceratium reticulatum* (Dinophyceae). *Arch. Protistenkd.* 147:381–91.

Hansen, G., Moestrup, Ø. & Roberts, K. R. 2000. Light and electron microscopical observations on the type species of *Gymnodinium, G. fuscum* (Dinophyceae). *Phycologia* 39:365–76.

Hansen, P. J. & Calado, A. J. 1999. Phagotrophic mechanisms and prey selection in free-living dinoflagellates. *J. Eukaryot. Microbiol.* 46:382–9.

Hinnebusch, A. G., Klotz, L. C., Blanken, R. L. & Loeblich III, A. R. 1981. An evaluation of the phylogenetic position of the dinoflagellate *Crypthecodinium cohnii* based on 5S rRNA characterization. *J. Mol. Evol*. 17:334–47.

Höhfeld, I. & Melkonian, M. 1995. Ultrastructure of the flagellar apparatus of *Noctiluca miliaris* Suriray swarmers (Dinophyceae). *Phycologia* 34:508–13.

Horiguchi, T. & Pienaar, R. N. 1988. Ultrastructure of a new sand-dwelling dinoflagellate, *Scrippsiella arenicola* sp. nov. *J. Phycol.* 24:426–38.

Huber-Pestalozzi G. 1950. Cryptophyceen, Chloromonadinen, Peridineen. *In* Thienemann, A. [Ed.] *Die Binnengewässer* vol. 16, *Das Phytoplankton des Süsswassers. Systematik und Biologie*, part 3. Schweizerbart'sche Verlagsbuchhandlung, Stuttgart, Germany, 310 pp.

Iwataki, M., Botes, L., Sawaguchi, T., Sekiguchi, K. & Fukuyo, Y. 2003. Cellular and body scale structure of *Heterocapsa ovata* sp. nov. and *Heterocapsa orientalis* sp. nov. (Peridiniales, Dinophyceae). *Phycologia* 42:629–37.

Javornický, P. 1997. *Bernardinium* Chodat (Dinophyceae), an athecate dinoflagellate with reverse, right-handed course of the cingulum and transverse flagellum, and *Esoptrodinium* genus novum, its mirror-symmetrical pendant. *Arch. Hydrobiol. Suppl.* 122:29-42 (*Algol. Stud.* 87).

Jeffrey, S.W. & Vesk, M. 1976. Further evidence for a membrane-bound endosymbiont within the dinoflagellate *Peridinium foliaceum. J. Phycol.* 12: 450–5.

Kawai, H. & Kreimer, G. 2000. Sensory mechanisms. Phototaxes and light perception in algae. *In* Leadbeater, B.S.C. & Green, J.C. [Eds.] *The flagellates. Unity, diversity and evolution*. Taylor & Francis, New York, pp. 124-146. (Systematics Association Special Volume No. 59.)

Keeling, P. J. 2004. Diversity and evolutionary history of plastids and their hosts. *Amer. J. Bot.* 91:1481–93.

Kiselev, I. A. 1954. Pirofitovye vodorosli. *In* Gollerbakh, M. M. & Polîanskiĭ, V. I. [Eds.] *Opredelitel' presnovodnykh vodorosleĭ SSSR*, vol. 6. Sovetskaîa Nauka, Moskva, 212 pp.

Kofoid, C. A. 1907. The plates of *Ceratium* with a note on the unity of the genus. *Zool. Anz.* 32:177–83.

Kofoid, C. A. 1909. On *Peridinium steinii* Jörgensen, with a note on the nomenclature of the skeleton of the Peridinidae. *Arch. Protistenkd*. 16:25–47, pl 2.

Leadbeater, B. S. C. & Dodge, J. D. 1966. The fine structure of *Woloszynskia micra* sp. nov., a new marine dinoflagellate. *Br. phycol. Bull.* 3:1–17.

Leander, B. S. & Keeling, P. J. 2004. Early evolutionary history of dinoflagellates and apicomplexans (Alveolata) as inferred from HSP90 and actin phylogenies. *J. Phycol.* 40:341–50.

Lefèvre, M. 1932. Monographie des espèces d'eau douce du genre *Peridinium*. *Arch. Bot.* 2 (Mémoire 5):1–210.

Lewis, J. & Dodge, J. D. 1990. The use of the SEM in dinoflagellate taxonomy. *In* Claugher, D. [Ed.] *Scanning Electron Microscopy in Taxonomy and Functional Morphology.* Clarendon Press, Oxford, pp. 125–48. (Systematics Association Special Volume No. 41).

Lindberg, K., Moestrup, Ø. & Daugbjerg, N. 2005. Studies on woloszynskioid dinoflagellates I: *Woloszynskia coronata* re-examined using light and electron microscopy and partial LSU rDNA sequences, with description of *Tovellia* gen. nov. and *Jadwigia* gen. nov. (Tovelliaceae fam. nov.). *Phycologia* 44:416–40.

Litaker, R. W., Vandersea, M. W., Kibler, S. R., Madden, V. J., Noga, E. J. & Tester, P. A. 2002 Life cycle of the heterotrophic dinoflagellate *Pfiesteria piscicida* (Dinophyceae). *J. Phycol.* 38:442–463.

Loeblich, A. R. III. 1970. The amphiesma or dinoflagellate cell covering. *North Am. Paleont. Conv. Symp. Pt. G* 867–929.

Logares, R. 2007. *Microbial evolution: patterns of diversity in aquatic protists.* Doctoral thesis, Lund University, Sweden, 160 pp.

McEwan, M. L. & Keeling, P. J. 2004. HSP90, tubulin and actin are retained in the tertiary endosymbiont genome of *Kryptoperidinium foliaceum*. *J. Eukaryot. Microbiol.* 51:651–9.

Matviîenko, O.M. & Lytvynenko, R.M. 1977. Pirofitovi vodorosti — Pyrrophyta. *In* Hollerbakh, M.M. & Kondrat'îeva, N.V. [Eds.] *Vyznachnyk Prisnovodnykh Vodorosteĭ Ukraïns'koï RSR* 3 (2). Naukova Dumka, Kyïv. 386 pp.

Moestrup, Ø. 2000. The flagellate cytoskeleton. Introduction of a general terminology for microtubular flagellar roots in protists. *In* Leadbeater, B. S. C. & Green, J. C. [Eds.] *The*

flagellates. Unity, diversity and evolution. Taylor & Francis, New York, pp. 69–94. (Systematics Association Special Volume No. 59).

Moestrup, Ø. & Daugbjerg, N. 2007. On dinoflagellate phylogeny and classification. *In* Brodie J. & Lewis J. [Eds.] *Unravelling the algae, the past, present, and future of algal systematics.* CRC Press, Boca Raton, pp. 215–230. (Systematics Association Special Volume No. 75.

Moestrup, Ø., Hansen, G., Daugbjerg, N. 2008. Studies on woloszynskioid dinoflagellates III: on the ultrastructure and phylogeny of *Borghiella dodgei* gen. et sp. nov., a cold-water species from Lake Tovel, N. Italy, and on *B. tenuissima* comb. nov. (syn. *Woloszynskia tenuissima*). *Phycologia* 47:54–78.

Moestrup, Ø., Hansen, G., Daugbjerg, N., Flaim, G. & D'Andrea, M. 2006. Studies on woloszynskioid dinoflagellates II: On *Tovellia sanguinea* sp. nov., the dinoflagellate responsible for the reddening of Lake Tovel, N. Italy. *Eur. J. Phycol.* 41:47–65.

Moestrup, Ø., Lindberg, K. & Daugbjerg, N. 2009a. Studies on woloszynskioid dinoflagellates IV. The genus *Biecheleria* gen. nov. *Phycol. Res.* 57:203–20.

Moestrup, Ø., Lindberg, K. & Daugbjerg, N. 2009b. Studies on woloszynskioid dinoflagellates V. Ultrastructure of *Biecheleriopsis* gen. nov., with description of *Biecheleriopsis adriatica* sp. nov. *Phycol. Res.* 57:221–37.

Montresor, M., Procaccini, G. & Stoecker, D. K. 1999. *Polarella glacialis*, gen. nov., sp. nov. (Dinophyceae): Suessiaceae are still alive! *J. Phycol.* 35:186–97.

Montresor, M., Janofske, D. & Willems, H. 1997. The cyst-theca relationship in *Calciodinellum operosum* emend. (Peridiniales, Dinophyceae) and a new approach for the study of calcareous cysts. *J. Phycol.* 33:122-31.

Montresor, M., Sgrosso, S., Procaccini, G. & Kooistra, W.H.C.F. 2003. Intraspecific diversity in *Scrippsiella trochoidea* (Dinophyceae): evidence for cryptic species. *Phycologia* 42:56-70.

Morrill, L. C. & Loeblich, A. R. 1981. The dinoflagellate pellicular wall layer and its occurrence in the division Pyrrhophyta. *J. Phycol.* 17:315-23.

Müller, O. F. 1773. *Vermium terrestrium et fluviatilium, seu animalium Infusoriorum, Helminthicorum et Testaceorum, non marinorum, succincta historia*. 1 (1). Martini Hallager, Hauniae et Lipsiae. Preface, bibliography and a synopsis of classification (30 unnumbered pages), 135 pp.

Müller, O.F. 1776. *Zoologiae danicae prodromus, seu animalium Daniae et Norvegiae indigenarum characteres, nomina, et synonyma imprimis popularium*. Impensis auctoris, Hauniae. xxxii, 274 pp.

Müller, O. F. 1786. *Animalcula Infusoria fluviatilia et marina, quae detexit, systematice descripsit et ad vivum delineari curavit Otho Fridericus Müller, Regi Daniae quondam a consiliis*

conferentiae, pluriumque academiarum et societatum scientiarum sodalis, sistit opus hoc posthumum quod cum tabulis aeneis L. in lucem tradit vidua ejus nobilissima, cura Othonis Fabricii. Nicolai Mölleri, Hauniae. LVI, 367 pp, 50 pls. [With a 4-page foreword by Otho Fabricius.].

Murray, S., Flø Jørgensen, M., Ho, S. Y. W., Patterson, D. J. & Jermiin, L. S. 2005. Improving the analysis of dinoflagellate phylogeny based on rDNA. *Protist* 156:269–86.

Netzel, H. & Dürr G. 1984. Dinoflagellate cell cortex. *In* Spector, D. L. [Ed.] *Dinoflagellates*. Academic Press, London, pp. 43–105.

Pitelka, D. R. & Schooley, C. N. 1955. Comparative morphology of some protistan flagella. *Univ. Calif. Publ. Zool*. 61:79–128.

Popovský J. & Pfiester L. A. 1990. Dinophyceae (Dinoflagellida). *In* Ettl, H., Gerloff, J., Heynig, H. & Mollenhauer D. [Eds.] *Süsswasserflora von Mitteleuropa*, vol. 6. G. Fisher, Jena. 272 pp.

Roberts, K. R. 1985. The flagellar apparatus of *Oxyrrhis marina* (Pyrrophyta). *J. Phycol.* 21:641–55.

Roberts, K. R. 1991. The flagellar apparatus and cytoskeleton of dinoflagellates: organization and use in systematics. *In* Patterson, D. J. & Larsen, J. [Eds.] *The Biology of Free-living Heterotrophic Flagellates.* Clarendon Press, Oxford, pp. 285–302. (Systematics Association special volume 45).

Roberts, K. R. 1989. Comparative analyses of the dinoflagellate flagellar apparatus. II. *Ceratium hirundinella*. *J. Phycol.*, 25:270–80.

Roberts, K. R., Hansen, G. & Taylor, F. J. R. 1995. General ultrastructure and flagellar apparatus architecture of *Woloszynskia limnetica* (Dinophyceae). *J. Phycol.* 31:948–57.

Roberts, K. R. & Roberts, J. E. 1991. The flagellar apparatus and cytoskeleton of the dinoflagellates. A comparative overview. *Protoplasma* 164:105-22.

Roberts, K. R., Roberts, J. E. & Cormier, S. A. 1992. The dinoflagellate cytoskeleton. *In* Menzel, D. [Ed.] *The cytoskeleton of the algae.* CRC Press, London, pp. 19–38.

Roberts, K. R. & Timpano, P. 1989. Comparative analyses of the dinoflagellate flagellar apparatus. I. *Woloszynskia* sp.. *J. Phycol.* 25:26–36.

Saldarriaga, J. F., McEwan, M. L., Fast, N. M., Taylor, F. J. R. & Keeling, P. J. 2003. Multiple protein phylogenies show that *Oxyrrhis marina* and *Perkinsus marinus* are early branches of the dinoflagellate lineage. *Int. J. Syst. Evol. Microbiol.* 53:355–65.

Saldarriaga, J. F., Taylor, F. J. R., Cavalier-Smith, T., Menden-Deuer, S. & Keeling, P. J. 2004. Molecular data and the evolutionary history of dinoflagellates. *Eur. J. Protistol*. 40:85–111.

Saunders, G. W., Hill, D. R. A., Sexton, J. & Andersen, R. A. 1997. Small-subunit ribosomal RNA sequences from selected dinoflagellates: testing classical evolutionary hypotheses with molecular systematic methods. *In* Bhattacharya, D. [Ed.] *Origins of Algae and their Plastids*. Springer, New York, pp. 237–59.

Schiller, J. 1933. Dinoflagellatae (Peridineae) in monographischer Behandlung. *In* Kolkwitz, R. [Ed.] *Rabenhorst's Kryptogamen-flora von Deutschland, Österreich und der Schweiz*, 2nd ed., 10(3). Part 1. Akademische Verlagsgesellschaft, Leipzig. 617 pp.

Schiller, J. 1937. Dinoflagellatae (Peridineae) in monographischer Behandlung. *In* Kolkwitz, R. [Ed.] *Rabenhorst's Kryptogamen-flora von Deutschland, Österreich und der Schweiz*, 2nd ed., 10(3). Part 2. Akademische Verlagsgesellschaft, Leipzig. 589 pp.

Schnepf, E & Elbrächter, M. 1999. Dinophyte chloroplasts and phylogeny – A review. *Grana* 38:81–97.

Schrank, F. v. P. 1793. Mikroskopische Wahrnehmungen. *Der Naturforscher (Halle)* 27:26–37, pl. 3, figs 10–23.

Siano, R., Montresor, M., Probert, I., Not, F. & de Vargas, C. 2010. *Pelagodinium* gen. nov. and *P. béii* [sic] comb. nov., a dinoflagellate symbiont of planktonic foraminifera. *Protist* 161:385–99.

Spector, D. L. [Ed.] 1984. *Dinoflagellates*. Academic Press, Inc., Orlando, Florida, 545 pp.

Stein, F. 1883. *Der Organismus der Infusionsthiere nach eigenen Forschungen in systematischer Reihenfolge bearbeitet. III. Abtheilung. Die Naturgeschichte der Flagellaten oder Geisselinfusorien. II. Hälfte. Die Naturgeschichte der arthrodelen Flagellaten. Einleitung und Erklärung der Abbildungen*. Wilhelm Engelmann, Leipzig. 30 pp., 25 pls.

Takano, Y., Hansen, G., Fujita, D. & Horiguchi, T. 2008. Serial replacement of diatom endosymbionts in two freshwater dinoflagellates, *Peridiniopsis* spp. (Peridiniales, Dinophyceae). *Phycologia* 47:41–53.

Takayama, H. 1985. Apical grooves of unarmored dinoflagellates. *Bull. Plankton Soc. Jpn.* 32:129–40.

Taylor, F. J. R. 1987. General group characteristics; special features of interest; short history of dinoflagellate study. *In* Taylor, F. J. R. [Ed.] *The biology of dinoflagellates*. Blackwell Scientific Publ., Oxford, pp. 1–23 (Botanical Monographs Volume 21.)

Taylor, F. J. R. 2004. Illumination or confusion? Dinoflagellate molecular phylogenetic data viewed from a primarily morphological standpoint. *Phycol. Res*. 52:308–24.

Thompson R. H. 1951. A new genus and new records of freshwater Pyrrophyta in the Desmokontae and Dinophyceae. *Lloydia* 13:277–99.

Tomas, R. N. & Cox, E. R. 1973. Observations on the symbiosis of *Peridinium balticum* and its intracellular alga. I. Ultrastructure. *J. Phycol*. 9:304–23.

Toriumi, S. & Dodge, J. D. 1993. Thecal apex structure in the Peridiniaceae (Dinophyceae). *Eur. J. Phycol.* 28:39–45.

Van de Peer, Y. & De Wachter, R. 1997. Evolutionary relationships among the eukaryotic crown taxa taking into account site-to-site rate variation in 18S rRNA. *J. Mol. Evol.* 45:619–30.

Van de Peer, Y., Van der Auwera, G. & De Wachter, R. 1996. The evolution of Stramenopiles and Alveolates as derived by "substitution rate calibration" of small ribosomal subunit RNA. *J. Mol. Evol.* 42:201–10.

Watanabe, M. M., Suda, S., Inouye, I., Sawaguchi, T. & Chihara, M. 1990. *Lepidodinium viride* gen. et sp. nov. (Gymnodiniales, Dinophyta), a green dinoflagellate with a chlorophyll a- and b-containing endosymbiont. *J. Phycol.* 26:741–51.

Wedemayer, G. J. & Wilcox, L. W. 1984. The ultrastructure of the freshwater colorless dinoflagellate *Peridiniopsis berolinense* (Lemm.) Bourrelly. *J. Protozool.* 31:444–53.

Wilcox, L. W., Wedemayer, G. J. & Graham, L. E. 1982. *Amphidinium cryophilum* sp. nov. (Dinophyceae), a new freshwater dinoflagellate. II. Ultrastructure. *J. Phycol.* 18:18–30.

Zhang, H., Bhattacharya, D. & Lin, S. 2005. Phylogeny of dinoflagellates based on mitochondrial cytochrome *b* and nuclear small subunit rDNA sequence comparisons. *J. Phycol*. 41:411–20.

Zhang, H., Bhattacharya, D. & Lin, S. 2007. A three-gene dinoflagellate phylogeny suggests monophyly of Prorocentrales and a basal position for *Amphidinium* and *Heterocapsa*. *J. Mol. Evol*. 65:463–74.

CHAPTER 2

ULTRASTRUCTURE AND LSU RDNA-BASED REVISION OF *PERIDINIUM* GROUP PALATINUM (DINOPHYCEAE) WITH THE DESCRIPTION OF *PALATINUS* GEN. NOV.

Craveiro, S.C., Calado, A.J., Daugbjerg, N. & Moestrup, Ø. 2009. Ultrastructure and LSU rDNA-based revision of *Peridinium* group palatinum (Dinophyceae) with the description of *Palatinus* gen. nov. *Journal of Phycology* 45 (5): 1175-1194.

ABSTRACT

The name *Peridinium palatinum* Lauterborn currently designates a freshwater peridinioid with 13 epithecal and six cingular plates, and no apical pore complex. Freshwater dinoflagellate floras classify it in *Peridinium* group palatinum together with *P. pseudolaeve* M. Lefèvre. General ultrastructure, flagellar apparatus, and pusular components of *P. palatinum* were examined by serial section TEM and compared to *P. cinctum* (O. F. Müll.) Ehrenb. and *Peridiniopsis borgei* Lemmerm., respectively, types of *Peridinium* and *Peridiniopsis*. Partial LSU rDNA sequences from *P. palatinum*, *P. pseudolaeve* and several peridinioids, woloszynskioids, gymnodinioids, and other dinoflagellates were used for a phylogenetic analysis. General morphology and tabulation of taxa in group palatinum were characterized by SEM. Differences in plate numbers, affecting both the epitheca and the cingulum, combine with differences in plate ornamentation and a suite of internal cell features to suggest a generic-level distinction between *Peridinium* group palatinum and typical *Peridinium*. The branching pattern of the phylogenetic tree is compatible with this conclusion, although with low support from bootstrap values and posterior probabilities, as are sequence divergences estimated between species in group palatinum, and typical *Peridinium* and *Peridiniopsis*. *Palatinus* nov. gen. is proposed with the new combinations *Palatinus apiculatus* nov. comb. (type species; syn. *Peridinium palatinum*), *P. apiculatus* var. *laevis* nov. comb., and *P. pseudolaevis* nov. comb. Distinctive characters for *Palatinus* include a smooth or slightly granulate, but not areolate, plate surface, a large central pyrenoid penetrated by cytoplasmic channels and radiating into chloroplast lobes, and the presence of a peduncle-homologous microtubular strand. *Palatinus* cells exit the theca through the antapical-postcingular area.

Key index words: Dinophyceae; *Glenodinium apiculatum*; LSU rDNA; *Palatinus apiculatus*; *Peridinium palatinum*; phylogeny; ultrastructure

Abbreviations: ab, accumulation body; b, bacteria; Ch, chloroplast; D, dictyosome; E, eyespot; gv, granulose vesicles; LB, longitudinal basal body; LC, layered connective; LF, longitudinal flagellum; LFC, longitudinal flagellar canal; LMR, longitudinal microtubular root; LSC,

longitudinal striated collar; LSP, longitudinal sac pusule; N, nucleus; nu, nucleolus; O, oil; P, pyrenoid; pt, pusular tube; s, starch; SBc, striated basal body connective; T, trichocyst; TB, transverse basal body; TF, transverse flagellum; TFC, transverse flagellar canal; TMR, transverse microtubular root; TMRE, transverse microtubular root extension; TSC, transverse striated collar; TSP, transverse sac pusule; TSR, transverse striated root; TSRM, transverse striated root microtubule

INTRODUCTION

As currently defined, the genus *Peridinium* Ehrenb. includes thecate dinoflagellates mostly found in freshwater ponds and swamps. *Peridinium* species share a hypotheca with two similar-sized antapical plates and five postcingular plates and are artificially separated from species of *Peridiniopsis* Lemmerm. by the presence of two to three, rather than zero to one, intercalary plates in the epitheca. Classification of species within *Peridinium* in most 20th-century freshwater dinoflagellate floras incorporates two subdivision levels; the first is the establishment of two groups based on the presence or absence of an apical pore, originally proposed as sections *Poroperidinium* and *Cleistoperidinium* by Lemmermann (1910) and later raised to subgenera by Lefèvre (1932). Each of these subdivisions of the genus is then divided into sets of species, which in general correspond to (or are derived from) the ‘‘groupes’’ originally established by Lefèvre (1932). Species in each group have similar epithecal arrangements in terms of number, symmetry, and contacts between plates (Lefèvre 1932, Huber-Pestalozzi 1950, Bourrelly 1970, Starmach 1974). Although generally not regarded as formal taxa (Popovský and Pfiester’s 1990 use of the term section to designate them is unwarranted), the groups are practical in narrowing down the possibilities when identifying species. However, associations based only on epithecal features do not always result in monophyletic assemblages. This is illustrated by the epithecal tabulation scheme of *Glochidinium penardiforme* (Er. Lindem.) Boltovskoy, which closely matches that of *Peridiniopsis borgei*, suggesting that the two species belong to the same group (Lefèvre 1932, Huber-Pestalozzi 1950, Popovský and Pfiester 1990); in contrast, the presence of three cingular plates in *G. penardiforme* and six cingular plates in *P. borgei* sets the two species quite apart (Bourrelly 1968, Imamura and Fukuyo 1990, Boltovskoy 1999).

Comparison of species currently included in *Peridinium* with species in related genera (e.g., *Peridiniopsis*, *Glochidinium*, *Protoperidinium* Bergh, *Scrippsiella* Balech ex A.R. Loebl.) suggests the need for revision of the peridinioid group of dinoflagellates. Reconsideration of the phylogenetic affinities of the peridinioids should preferably be based on a combination of complete thecal composition, internal cell structure, and molecular methods. The present article addresses the species included in *Peridinium* group palatinum (Lefèvre 1932, Huber-Pestalozzi 1950, Kiselev 1954, Starmach 1974, Popovský and Pfiester 1990). Lefèvre named the group after the most common of the included species, for which he used the name *P. palatinum*, although he cited as synonym *P. apiculatum* (Ehrenb.) Er. Lindemann (Lefèvre 1932, p. 102). It is perhaps a consequence of Lefèvre's (1932) magistral monograph that later authors used Lauterborn's name for the species while acknowledging the synonyms proposed by Lindemann (1928), despite the priority of the epithet apiculatum over palatinum. The taxonomic and nomenclatural issues surrounding these names are explained in the Discussion.

Although the fine structure of peridinioid cells, in particular the character-rich flagellar base area, is known from few species only, these include the type species of *Peridinium* and *Peridiniopsis* (Calado et al. 1999, Calado and Moestrup 2002). In addition, the database of partial LSU rDNA from dinoflagellates has grown to include numerous comparison points from which phylogenetic hypotheses may be derived (Calado et al. 2006, Moestrup et al. 2006, 2008, Hansen et al. 2007).

MATERIALS AND METHODS

Palatinus apiculatus occurs commonly in Danish lakes, mostly between October and April. In Portugal, the species was only found in significant numbers in a pond near Vista Alegre, Aveiro, in February 2005. Most of the observations documented herein are from a large population collected from the ponds Kollelev Mose and Kollelev Hul, north of Copenhagen, in October 1994, and from two cultured strains: AJC1, started from the Kollelev Mose sample and grown in L16 medium (Lindström 1991) supplemented with vitamins according to Popovský and

Pfiester (1990); and K-34, from the Scandinavian Culture Centre for Algae and Protozoa, started in March 1990 from a freshwater lake in North Sealand, Denmark, initially grown in soil–water medium and later transferred to L16. Cultures were maintained at 14ºC, 16:8 light:dark photoperiod and a photon flux density of ~20 µmol · m^{-2} · s^{-1}.

Palatinus apiculatus var. *laevis* was obtained from the Microbial Culture Collection at National Institute for Environmental Studies, Japan, as strain NIES-1405, originally identified as *Peridinium pseudolaeve*.

Palatinus pseudolaevis was collected from a pond near Store Magleby, Amager, Denmark, in April 1995, and isolated into culture (strain AJC6) as indicated above for AJC1. Growth in the culture was always moderate, and the strain was eventually lost in 1999.

Light microscopy. Light micrographs were taken using a Zeiss Axioplan 2 imaging light microscope (Carl Zeiss, Oberkochen, Germany) equipped with a DP70 Olympus camera (Olympus Corp., Tokyo, Japan).

Semi-thin sections (500 nm) for LM were cut with glass knives from the resin blocks used for TEM. Sections were dried on a coverslip, stained with 1% toluidine blue, and mounted in Entellan® (Merck KGaA, Darmstadt, Germany).

Scanning electron microscopy. Both field material preserved in 2% glutaraldehyde and cultured material fixed with Lugol's solution overnight were prepared for SEM. Cells were collected onto Isopore polycarbonate membrane filters with 5 or 8 µm pore size (Millipore Corp., Billerica, MA, USA), rinsed with distilled water, dehydrated through a graded ethanol series, and criticalpoint-dried. The dry filters were attached onto stubs with double-sided adhesive tape, sputter-coated with gold–palladium or platinum–palladium, and examined using JEOL JSM-6335F (JEOL Ltd., Tokyo, Japan) and Hitachi S-4100 (Hitachi High-Technologies Corp., Tokyo, Japan) scanning electron microscopes.

Transmission electron microscopy. Two fixation schedules were used: (1) Cells from the 1994 Kollelev Hul sample were transferred with a micropipette into 2% glutaraldehyde in 0.1 M sodium cacodylate, pH 7.4, for 1 h. Following centrifugation (Sigma 302 K centrifuge; Sigma, Osterode／Harz, Germany) and a wash in buffer, cells were postfixed overnight in 0.5% osmium tetroxide prepared

in the same buffer. The material was dehydrated through a graded ethanol series and propylene oxide and embedded in Spurr's resin. (2) Swimming cells of *P. apiculatus* from culture K-34 were picked up and transferred to a mixture of 1% glutaraldehyde and 0.5% osmium tetroxide (final concentrations) in 0.1 M phosphate buffer, pH 7.2, for ~30 min. After one rinse in buffer, cells were embedded in 1.5% agar and postfixed in 0.5% osmium tetroxide overnight. The agar blocks were dehydrated through a graded ethanol series and propylene oxide and embedded in Epon. Serial sections were prepared using a diamond knife on Reichert Ultracut E and EM UC6 ultramicrotomes (Leica Microsystems, Wetzlar, Germany). Ribbons of sections were picked up with slot grids, placed on Formvar film, and stained with uranyl acetate and lead citrate. Serial sections of four cells were examined using a JEOL JEM 1010 transmission electron microscope.

Determination of the LSU rDNA sequences from Palatinus *species*. Partial LSU rDNA sequences for *P. apiculatus* and *P. pseudolaevis* were obtained as described in Daugbjerg et al. (2000).

DNA of Peridiniopsis borgei. Extracted (total genomic) DNA of a clonal culture (PBSK-1) of the type species of *Peridiniopsis* (viz. *P. borgei*) was kindly provided by Ramiro Logares. The culture was originally isolated in 2005 by Karin Rengefors from a water sample collected in Stora Kalkbrottsdammen near Malmö, SW Sweden.

Determination of the LSU rDNA sequence from P. borgei. PCR amplification and temperature cycle conditions were as outlined in Moestrup et al. (2008). PCR fragments were purified using a NucleoFast 96 PCR Kit (Macherey-Nagel GmbH & Co. KG, Düren, Germany) following the recommendations of the manufacturer. A final concentration of 500 ng of the PCR product was air-dried and together with primers sent to the sequencing service at Macrogen (Seoul, Korea) for determination in both directions. The sequencing primers used were D1R, D2C, D3A, D3B, and 28-1483R (for primer sequences, see Daugbjerg et al. 2000 and Hansen et al. 2000).

Sequence alignment. The *P. borgei* sequence was added to a data matrix comprising 35 nuclear-encoded LSU rDNA sequences from a diverse assemblage of dinoflagellates retrieved from GenBank (see Table S1 in the supplementary

material). Except for the five pfiesteriaceans, the retrieved sequences have previously been determined by our group and used in a number of separate studies (e.g., Daugbjerg et al. 2000, Hansen and Daugbjerg 2004, Bergholtz et al. 2006, Moestrup et al. 2008). The LSU rDNA sequences were aligned using information from the secondary structure with domains and interdomains forming stems and loops as suggested by De Rijk et al. (2000). The alignment comprised 1,439 base pairs, but domain D2 was too variable to be aligned unambiguously. Therefore, this fragment was deleted, thus leaving 1,076 positions to be included in the phylogenetic analyses. The sequence data matrix was manually edited using MacClade (ver. 4.08, Maddison and Maddison 2003).

Outgroup. Ciliates (viz. *Tetrahymena pyriformis* and *T. thermophila*) were used for outgroup rooting as molecular studies have revealed these protozoans to form a sister group to the dinoflagellates (e.g., van de Peer et al. 1996).

Phylogenetic analyses. The aligned sequence data matrix was subjected to two different methods of phylogeny reconstruction, namely, maximum likelihood (ML) and Bayesian analysis (BA). We used MrModeltest (Nylander 2004) to select the best model among 24 defined models of nucleotide substitution. Following hierarchical likelihood ratio tests, the best-fit model was GTR+I+G, and the value and shape parameter for the proportion of invariable sites (pinvar = 0.2889) and the gamma distribution (shape = 0.5785), respectively, were used in both ML and BA. We used the online version of PhyML (Guindon and Gascuel 2003) available from the Montpellier bioinformatics platform at http://www.atgc-montpellier.fr/phyml/. One hundred replicates for bootstrap analyses were run, and a 50% majority-rule consensus tree was calculated using consense from the Phylip package ver. 3.68 (Felsenstein 2008). This provided bootstrap support values for the branching pattern (Fig. 14). BA was performed using MrBayes (ver. 3.1.2, Ronquist and Huelsenbeck 2003) with a general-time-reversible (GTR) substitution model with base frequencies and substitution rate matrix estimated from the data. In total, 2 million Markov Chain Monte Carlo (MCMC) generations with four parallel chains (three heated and one cold) were performed. A tree was sampled every 50th generation. According to AWTY (Wilgenbusch et al. 2004), the Bayesian analysis had been running long enough as the plots of posterior

probabilities of all splits for paired MCMC runs converged using the compare command (plot not shown). Plotting the log-likelihood values as a function of generations in a spreadsheet, the lnL values reached a stationarity level at ~ –9.035 after 10.050 generations. Trees below this level were omitted, and the burn-in thus comprised 39.800 trees. These were imported into PAUP* (ver. 4b10, Swofford 2003), and a 50% majority-rule consensus tree was constructed (tree not shown). Posterior probabilities were mapped onto the bootstrap tree derived from the PhyML analysis.

RESULTS

The organisms examined in this work displayed important differences from typical *Peridinium* species, involving both the theca and the internal organization of the cells. They cannot be accommodated in any existing genus of peridinioid dinoflagellates and are therefore classified in the following new genus.

Palatinus Craveiro, Calado, Daugbjerg et Moestrup gen. nov.

Dinoflagellata autotrophica, thecata, non parasitica. Formula kofoidiana thecarum 4′, 2a, 7″, 6c, 5s, 5‴, 2⁗, porus apicalis carens. Patellae laeves vel subtiliter ad grosse granulatae, sed haud areolatae. Lobi chloroplasti ex pyrenoide centrali radians. Pyrenoides canalibus cytoplasmatibus penetratus. Stigma in lobo chloroplasto subter sulcum sito. Filum microtubulare pedunculare praesens sed vesiculae concomitantes carens et tenus superficie cellulae non accedens (pedunculum non extendans). Cellulae ex theca liberatis per hypovalvam prope antapicem.

Typus generis: Palatinus apiculatus (Ehrenb.) Craveiro, Calado, Daugbjerg et Moestrup comb. nov., hic designatus.

Thecate, autotrophic, free-living dinoflagellates. Kofoidian plate formula: 4′, 2a, 7″, 6c, 5s, 5‴, 2⁗, apical pore complex absent. Plate surface smooth or finely to coarsely granulate, but not with ridges that form areolae. Chloroplast lobes radiating from a central, branching pyrenoid penetrated by cytoplasmic channels. Eyespot located in a chloroplast lobe beneath the sulcus. Microtubular strand homologous to peduncle microtubules of other dinoflagellates present, but lacking accompanying vesicles and not reaching the cell surface (not extending into a

peduncle). Dividing or ecdysing cells exiting the theca through the antapical-postcingular area.

Type species: Palatinus apiculatus (Ehrenb.) Craveiro, Calado, Daugbjerg et Moestrup comb. nov., designated here.

Etymology: The generic name is derived from the specific epithet of *Peridinium palatinum*, so named in allusion to the Palatinate (Pfalz, in German), the southwest region of Germany where Lauterborn (1896) originally found the species. As the name of a genus, the term is treated as a noun and takes the masculine gender (Lewis and Short 1879).

Note: The choice of the generic name *Palatinus* aims to preserve the link to the specific epithet long used for the type species, while replacing it with its long-accepted older synonym (see Discussion). Conservation of the specific epithet *palatinum* does not seem desirable as the generic name is being changed. The original publication by Ehrenberg (1838) of illustrations where the species can be recognized, against the absence of illustrations accompanying Lauterborn's original description of *Peridinium palatinum*, and the recent use of the legitimate name *Peridinium apiculatum* (Ehrenb.) Claparède et J. Lachmann (Hansen and Flaim 2007), also speak for the application of the priority principle in this case.

Palatinus apiculatus (Ehrenb.) Craveiro, Calado, Daugbjerg et Moestrup comb. nov. (Fig. 2, a–e).

Basionym: Glenodinium apiculatum Ehrenberg 1838. Infusionsthierchen, p. 258, pl. XXII, fig. XXIV (reproduced here in grayscale as Fig. 1).

Homotypic synonyms: Peridinium apiculatum (Ehrenb.) Claparède and J. Lachmann (1859, p. 404); *Properidinium apiculatum* (Ehrenb.) Meunier (1919, p. 60); ''*Peridinium apiculatum* (Ehrenb.) Er. Lindemann'' (1928, p. 260), later isonym.

Heterotypic synonyms: Peridinium palatinum Lauterborn (1896, p. 17); *Peridinium marssonii* Lemmermann (1900a, p. 28); *Peridinium anglicum* G. S. West (1909, pp. 187–90, fig. 23).

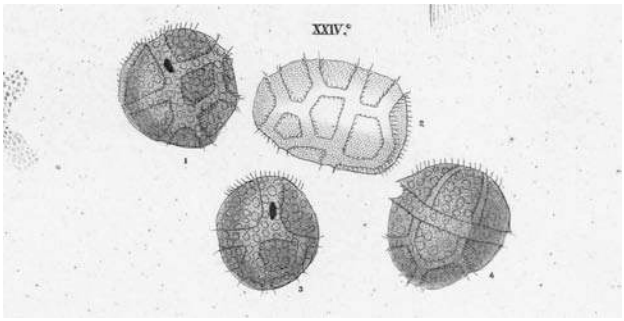

Fig. 1. *Glenodinium apiculatum*. Reproduced from Ehrenberg (1838, pl. XXII, fig. XXIV). Same size as the original drawing.

Palatinus apiculatus var. ***laevis*** (Huitfeldt-Kaas) Craveiro, Calado, Daugbjerg et Moestrup comb. nov. (Fig. 13, a–c).

Basionym: Peridinium laeve Huitfeldt-Kaas 1900. Vid.-Selsk. Skr. [Christiania], Math.-Naturv. Kl. 1900 No. 2:4, figs. 1–5.

Homotypic synonyms: Peridinium palatinum f. *laeve* (Huitfeldt-Kaas) Er. Lindemann (1925a, p. 478); *Peridinium apiculatum* f. *laeve* (Huitfeldt-Kaas) Er. Lindemann (1928, p. 260); ‘‘*Peridinium palatinum* f. *laeve* (Huitfeldt-Kaas) M. Lefèvre’’ (1932, p. 105), later isonym.

Note: This taxon has often been ranked as a forma by the modern authors that recognize it. However, we doubt the usefulness of having two infraspecific categories for unicellular organisms, particularly when choice of rank has been irregular and inconsistent (see established varieties and forms of freshwater dinoflagellates in, e.g., Starmach 1974). We therefore use the higher-ranking varietas.

Palatinus pseudolaevis (M. Lefèvre) Craveiro, Calado, Daugbjerg et Moestrup comb. nov. (Fig. 13, d–i).

Basionym: Peridinium pseudolaeve M. Lefèvre 1926. Rev. Algol. 2:341, pl. XI, figs. 6–9, ‘pseudo-laeve’.

Note: Lefèvre (1926, pp. 338–41) noted that *P. pseudolaeve* had been illustrated under the name *P. laeve* by Lindemann (1920, p. 128, fig. 18). However, he later (Lefèvre 1932, p. 108) cited in error Lindemann (1919), which does not contain any illustration showing *P. pseudolaeve* characters. The erroneous citation has been repeatedly copied (Schiller 1937, Starmach 1974, Popovský and Pfiester 1990).

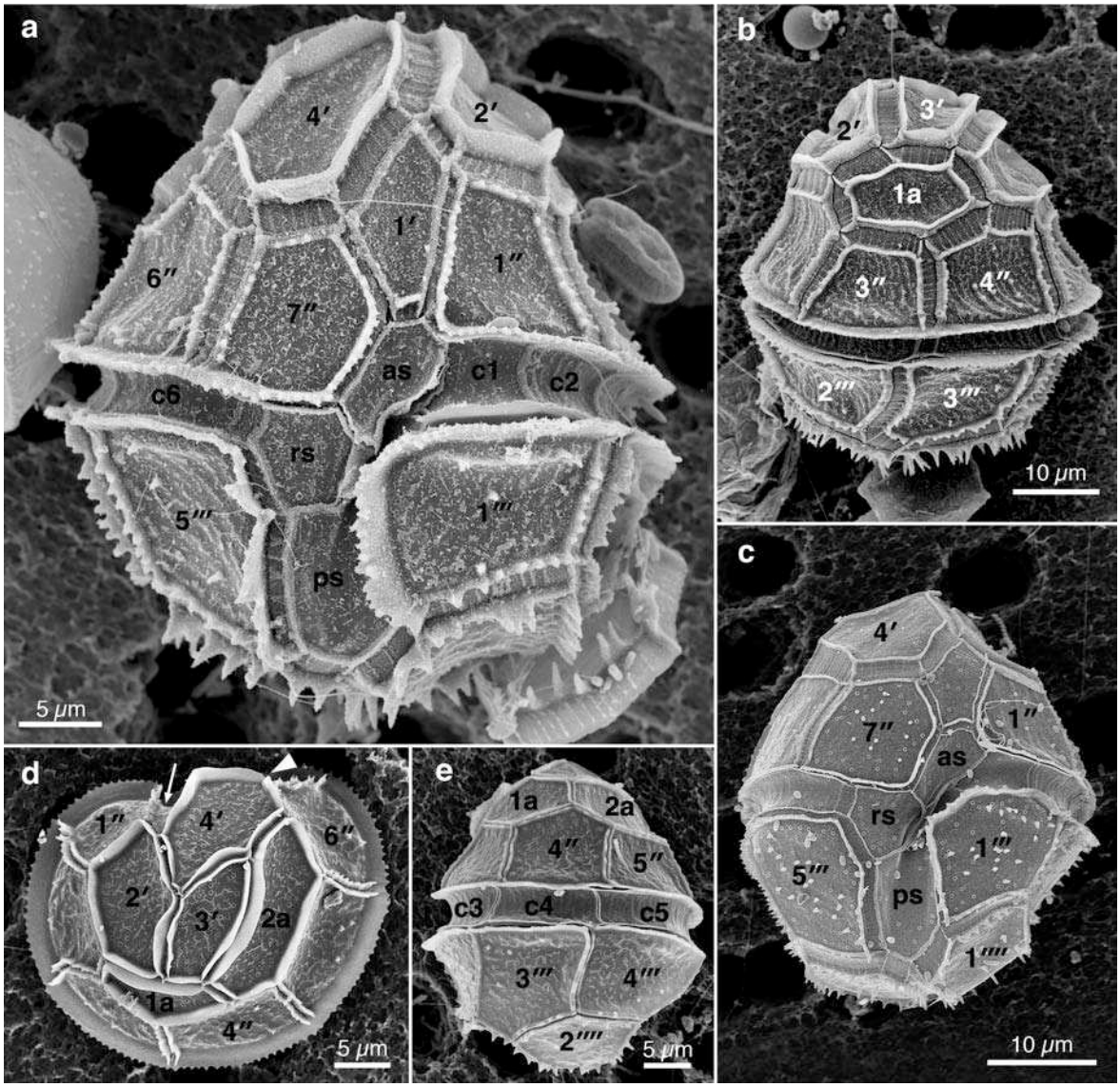

Fig. 2. *Palatinus apiculatus*, SEM. All cells from field samples except cell in (c), which is from strain K- 34. as, anterior, rs, right, and ps, posterior sulcal plates. (a) Ventral view of a strongly ornamented cell; note the shorter cingular plates c1 and c2 positioned for the most part above plate 1‴. (b) Dorsal view. (c) Ventral view. (d) Apical view showing the asymmetric arrangement of the apical and intercalary plates. The thin arrow indicates the plate 1′, and the arrowhead indicates the position of plate 7″. (e) Dorsal view of small cell with narrow sutures between the plates.

Observations of Palatinus apiculatus*. Morphology and thecal structure*: Cell size was mostly in the range of 32–48 μm long, 28–42 μm wide, and 23–28 μm thick, with the largest values measured in heavily ornamented field specimens with sutures up to 3 μm wide. The cells were ovoid, with the hypotheca more rounded than the tapering, somewhat conical epitheca, and were nearly flat on the ventral

side (Fig. 2, a–e). In ventral view the epitheca showed a characteristic twist to the left relative to the hypotheca, leaving plate 7″ vertically aligned with the right sulcal plate and plate 1′ in line with the right side of plate 1‴ (Fig. 2, a and c). The four apical and the two intercalary plates usually showed a markedly asymmetric arrangement, centered around an elongate 3′, oriented from dorsal-left to ventral-right and pointed on the ventral side (Fig. 2d). Intercalary plate 2a was the longest, oriented roughly parallel to 3′ and contacting plates 4″, 5″, and 6″ (Fig. 2d). In well-ornamented cells, the edges of the five uppermost plates (2′, 3′, 4′, 1a, 2a) were raised to form smooth flanges up to 2 μm high (Fig. 2, a, b, and d); the edges of the remaining epithecal plates were less raised and were provided with granules or short, blunt spines (Fig. 2, a, b, and d).

The cingulum was a distinct groove that circled the cell transversely, descending about its own width at the distal (right-ventral) end. The first two cingular plates were short, both essentially positioned above plate 1‴ (Fig. 2a). Plates c3–c6 were roughly aligned with plates 2‴–5‴, respectively (Fig. 2, a and e). Dissection of the sulcus revealed four larger plates (Fig. 2, a and c, only three sulcal plates indicated) and a smaller one intercalated between the right and left sulcal plates and the posterior plate; both this small so-called accessory plate and the left sulcal plate were usually concealed in intact thecae of *P. apiculatus* and were easier to see in specimens of *P. apiculatus* var. *laevis* and *P. pseudolaevis* (see below).

The sulcus was bordered by the raised edges of plates 1‴ and 5‴ (Fig. 2, a and c). The edges of postcingular and antapical plates were provided with conical spines, which reached up to 2.5 μm long in the antapical area of heavily ornamented cells(Fig. 2a). Shorter and blunter spines were scattered along the surface of some plates, especially in the hypotheca (Fig. 2, a–e).

Elongated groups of tiny granules usually gave a rough appearance to the plate surface of field-collected specimens (Figs. 2, a and b; 3a), whereas cells from cultures looked smoother (Fig. 2c). Numerous pores with raised rims were distributed on the surface of all plates, especially near their margins; the outer pore opening was ~200–250 nm in diameter and was sometimes associated with a trichocyst (Fig. 3b). When viewed in SEM, most pores contained a round structure

in the middle (Fig. 3a, arrow); in TEM, this probably corresponded to a cylindrical, hollow structure, located between the plasma membrane and the amphiesmal vesicle, and associated with a granular, subthecal vesicle (Fig. 3c).

The sutures between plates varied from thin lines in small specimens (Fig. 2e) to bands up to 2.5– 3 µm wide in large cells (Figs. 2, a–c; 3a). Cross-striations in the sutures were visible, but not striking, in high resolution LM (not shown). In SEM, the striations were lines 0.15–0.2 µm wide placed some 0.8–0.9 µm apart (Fig. 3a).

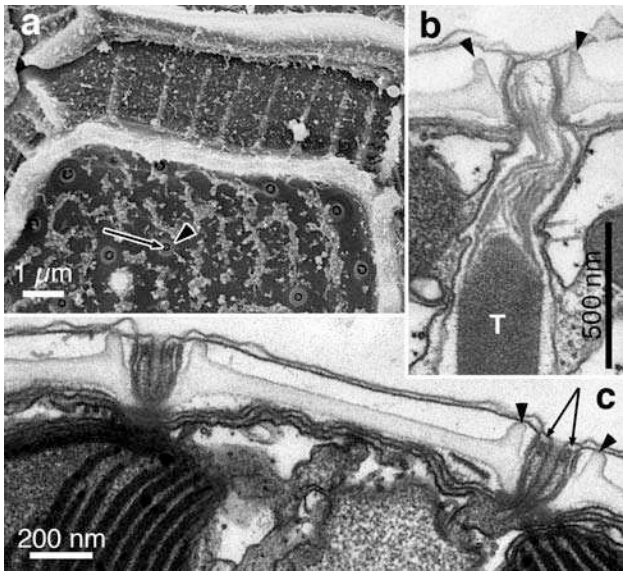

Fig. 3. *Palatinus apiculatus*, thecal structure. (a) Plate surface showing pores (arrowhead points to pore rim) containing round structures (arrow). Note the thin striations on the suture. SEM. (b) Section through a pore connected to a trichocyst (T). Arrowheads point to pore rim. TEM. (c) Pores connected to cylindrical hollow structure (arrows). TEM.

Dividing or recently divided cells exited the theca through the antapex, leaving the empty thecae with missing or displaced antapical and sometimes also postcingular plates (not shown). Although division stages were rarely seen in the cultures, unarmored, swimming dividing cells were abundant in the dense populations collected from Kollelev. Figure 4 shows the typical appearance of these naked division stages, with the posterior ends of the forming cells diverging in an asymmetrical way; the shallow left side of the cingulum was barely visible in SEM (Fig. 4a, arrow), and two recently divided nuclei were readily evidenced by lightly staining with acetocarmine (Fig. 4b).

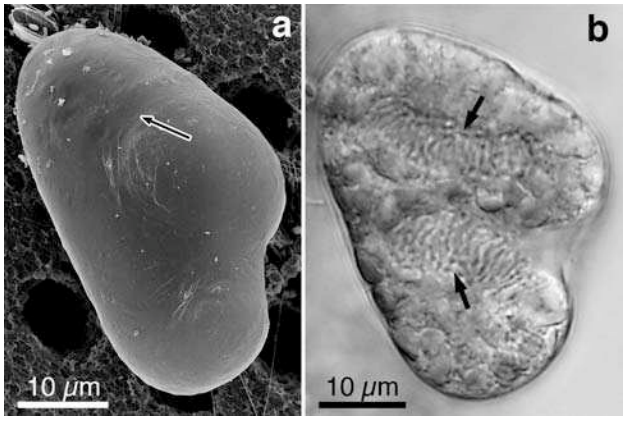

Fig. 4. *Palatinus apiculatus*. Division in a naked, motile stage. (a) Ventral view, SEM. The arrow indicates the left part of the cingulum. (b) Light micrograph showing the two recently separated nuclei (arrows). Lightly stained with acetocarmine.

General structure in LM and TEM: The cell surface was nearly covered with brownish chloroplast lobes, which radiated from a central pyrenoid (Figs. 5, a and b; 6, a and b). The nucleus was transversely elongated and occupied the dorsal part of the cell at cingulum level, slightly invading the epicone (Figs. 5, a and b; 6, a and c). Swimming cells usually contained a large vesicle on the ventral-right side, here called a longitudinal sac pusule (LSP; see below) (Figs. 5a; 6, c and d); this was often lacking in immotile specimens. Oil droplets were found in the peripheral part of the cell, mostly in the epicone, whereas starch grains accumulated mainly in the hypocone (Fig. 6a). Bacteria were plentiful in the cytoplasm of cultured cells, especially near the central pyrenoid, between the radiating chloroplast lobes (Figs. 6, a–c; 7a), and in the ventral region (Fig. 8a). Bacteria were also found inside the nucleus of some cells (Figs. S1, b and c, in the supplementary material).

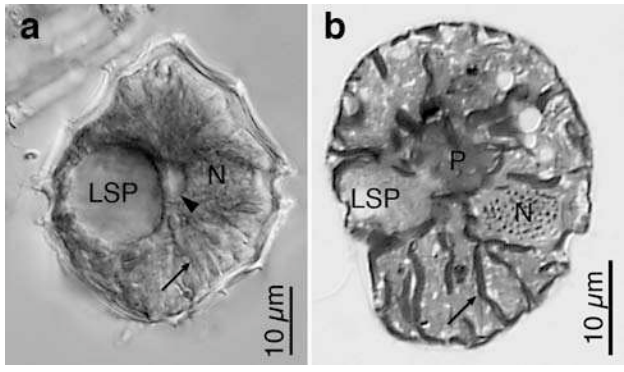

Fig. 5. *Palatinus apiculatus*, general view in LM. Thin arrows indicate chloroplast lobes radiating from the center. N, nucleus; LSP, longitudinal sac pusule. (a) Ventral view of a whole, fixed cell. The arrowhead points to the extended transverse flagellar canal (transverse sac pusule). (b) Semithin section through the longitudinal axis, viewed from the cell's left. P, central pyrenoid.

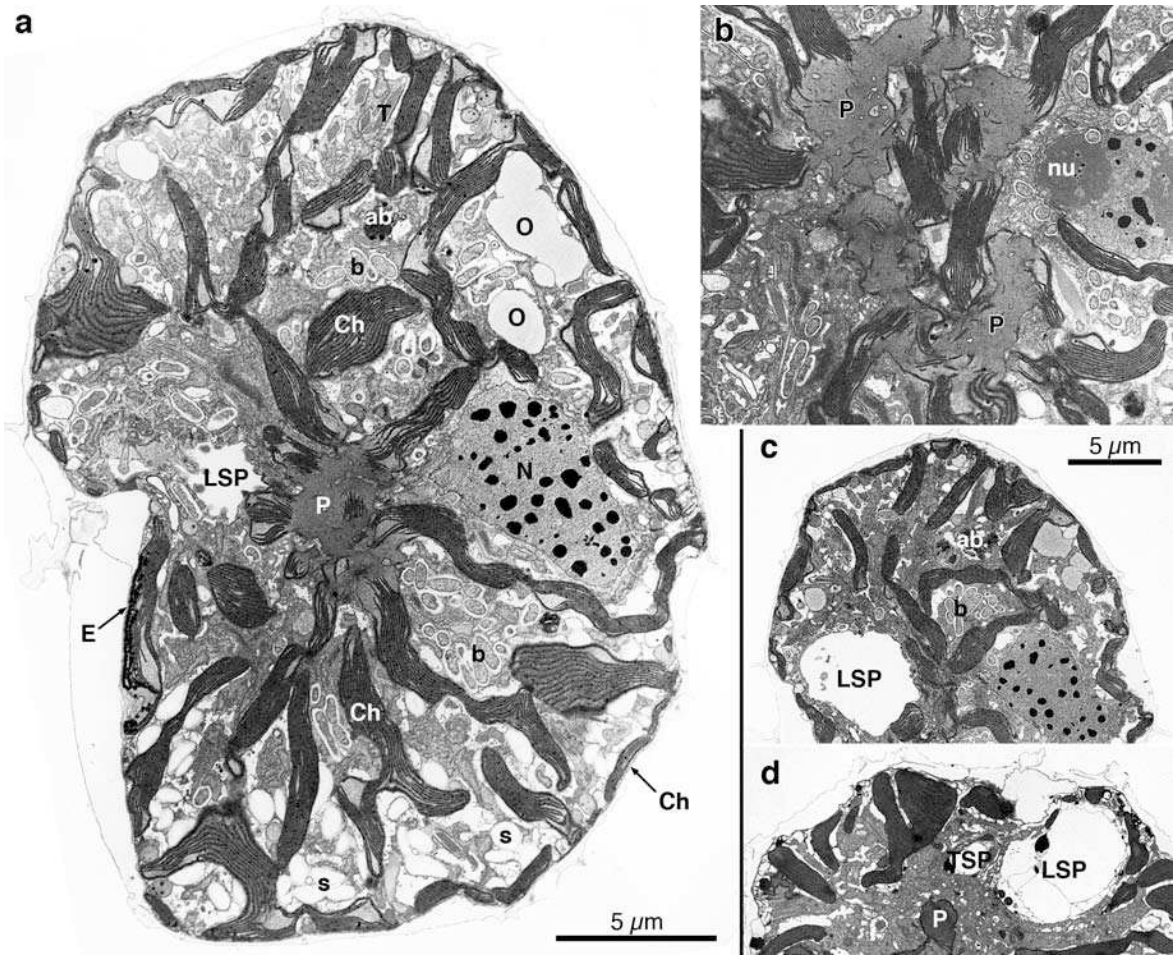

Fig. 6. *Palatinus apiculatus*, general ultrastructure, TEM. (a) Longitudinal section viewed from the cell's left showing the central pyrenoid (P) and the radiating chloroplast lobes (Ch), groups of bacteria (b), the nucleus (N), the eyespot (E) in the ventral region, and the left side of the longitudinal sac pusule (LSP); oil droplets (O) are visible in the epicone and starch grains (s) in the hypocone. (b) Detail of the central pyrenoid (P) sectioned through its peripheral, branching part, showing scattered thylakoid lamellae and cytoplasmic tubes. Scale bar as in (a). (c) Longitudinal section of the same cell as in (a), but farther to the right side, showing the LSP occupying most of the midventral area. (d) Approximately transverse section viewed from the anterior-right side of the cell, showing the LSP and the much smaller (but not collapsed) transverse sac pusule (TSP). Cell fixed from field material. Scale bar as in (c). ab, accumulation body; nu, nucleolus.

In all cases, bacteria were bounded by two membranes and surrounded by an electron-translucent area ~20–80 nm thick, with no external membranes separating them from either the cytoplasm or the nucleoplasm of the dinoflagellate (Figs. S1c; 8c). Dictyosomes were scattered around the central pyrenoid (Fig. 7a)

and near the nucleus (Fig. S1c). Trichocysts were common in the peripheral cytoplasm (Figs. 6a; 7a). Accumulation bodies with unrecognizable contents were present in the epicone (Fig. 6, a, c). Two types of vesicles were common along the surface, apparently discharging their contents into amphiesmal vesicles: round vesicles containing what seemed to be whorls of membranous material (Fig. 7d), and ellipsoid vesicles with a granular matrix and several lumps of electron-opaque material (Fig. 7, a, d). Vesicles with fibrillar contents of the type usually associated with flagellar hairs were seen in close association with dictyosomes; Figure S1a documents traffic of small vesicles between a dictyosome and a fibrillar vesicle. Vesicles containing crystal-like bodies were common throughout the cytoplasm (Fig. 8a), including the ventral area near the basal bodies (Fig. S2, b and d, in the supplementary material).

Chloroplast, pyrenoid, and eyespot: Chloroplast lobes radiated from the central pyrenoid in all directions and ramified into further lobes, establishing what was probably a single chloroplast network (Figs. 5b; 6, a–c; 7a). Upon reaching the peripheral cytoplasm, the lobes extended tangentially, covering most of the surface (Figs. 5b; 6a). Sections through the center of the cell showed the three-thylakoid lamellae regularly arranged in evenly spaced, parallel alignments (Fig. 7a). In some chloroplast lobes, the peripheral lamella surrounded the internal lamellae in a way reminiscent of the girdle lamellae of heterokonts (Fig. 7b). The central pyrenoid extended somewhat into the radiating lobes, giving a fragmented appearance in sections through its periphery (Fig. 6b). The pyrenoid matrix contained a few scattered thylakoid lamellae and was traversed by cytoplasmic channels of irregular shape (Figs. 6, a, b; 7a); Fig. 7c shows two such cytoplasmic channels lined by the three membranes of the chloroplast envelope. Thylakoid-free areas were also present in some peripheral chloroplast lobes (Fig. 7a).

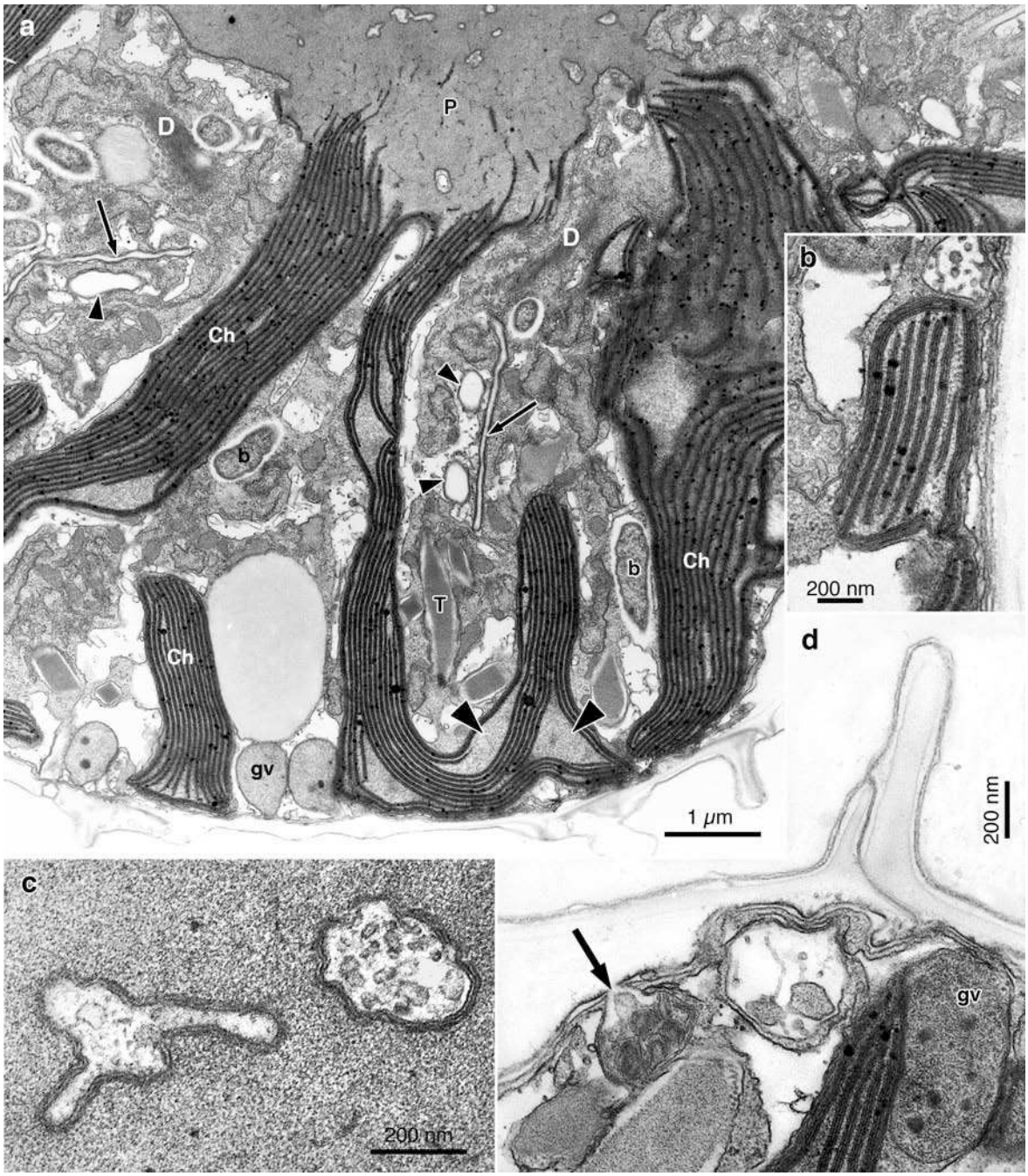

Fig. 7. *Palatinus apiculatus*, general ultrastructure. gv, granular vesicle; T, trichocyst. (a) Longitudinal section showing part of the central pyrenoid (P), chloroplast lobes (Ch) with some areas free of thylakoids (large arrowheads), and dictyosomes (D). Thin arrows point to the flat pusular vesicles, and small arrowheads indicate pusular tubes. (b) Detail of a chloroplast lobe with a peripheral lamella overlapping the ends of internal lamellae. (c) Cytoplasmic tubes in the pyrenoid, bounded by three membranes. (d) Vesicles with membranous contents (the arrow marks a connection with an amphiesmal vesicle) and vesicles with granular contents (gv), both common along the cell surface.

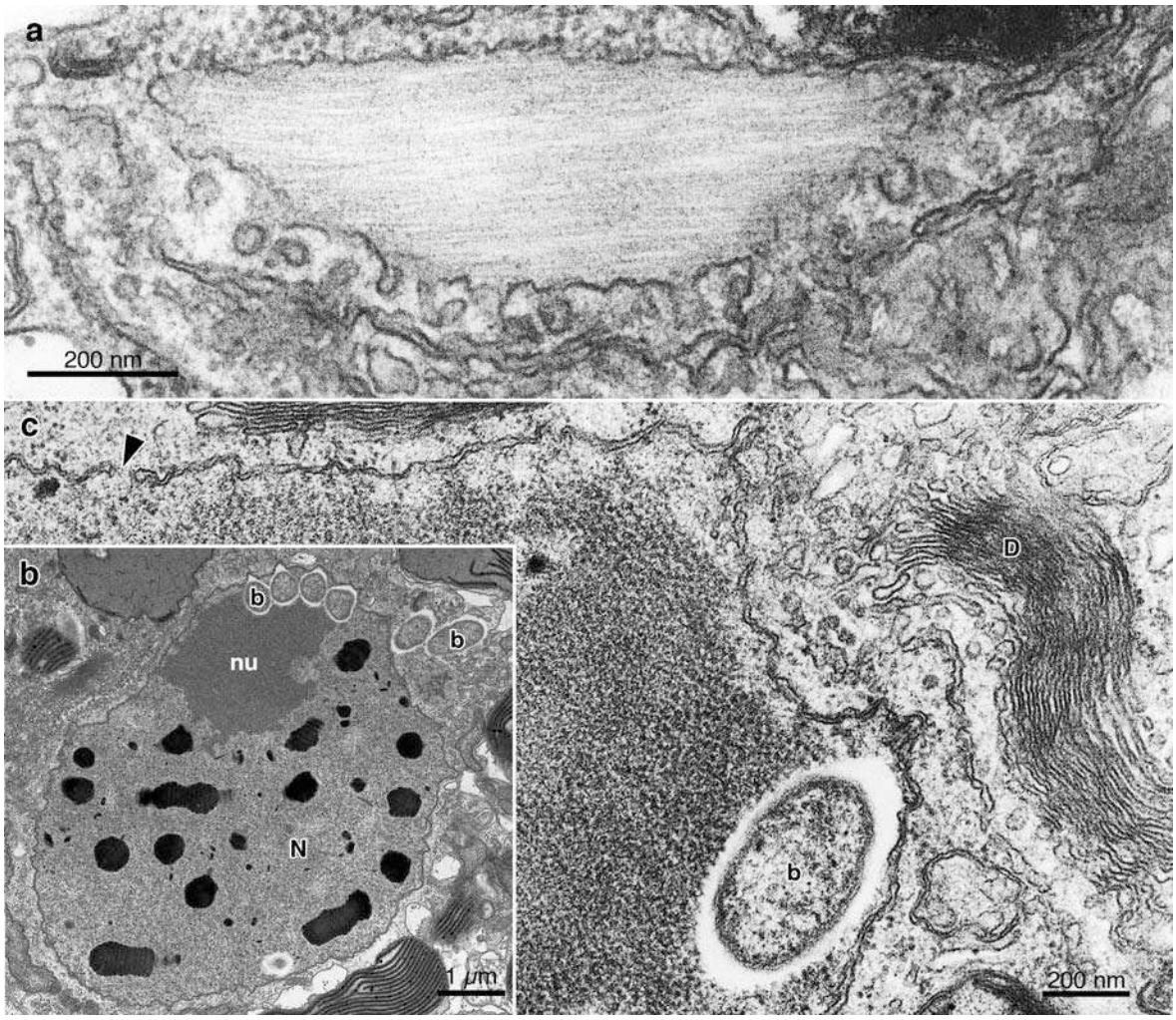

Fig. S1. *Palatinus apiculatus*, ultrastructure. (a) Fibrillar vesicle adjacent to a dictyosome, apparently receiving dictyosome-derived vesicles. (b) Overview of the nucleus (N) with a group of bacteria (b) adjacent to the nucleolus (nu). (c) Detail of an intranuclear bacterium located between the nucleolus and the nuclear envelope. The arrowhead points to a nuclear pore. D, dictyosome.

The eyespot was usually visible with the light microscope, although often faintly, as a reddish area nearly 5 µm long located in the upper part of the sulcus. It consisted mainly of one to two layers of globules along the ventral surface of a chloroplast lobe, placed directly underneath the chloroplast envelope (Fig. 8, a and b). Although layers of globules oriented parallel to the surface were in general not separated by thylakoids, some layers turned obliquely inward, alternating with obliquely oriented thylakoid lamellae (Fig. 8, a and b). The size of individual globules ranged from 80 to 130 nm.

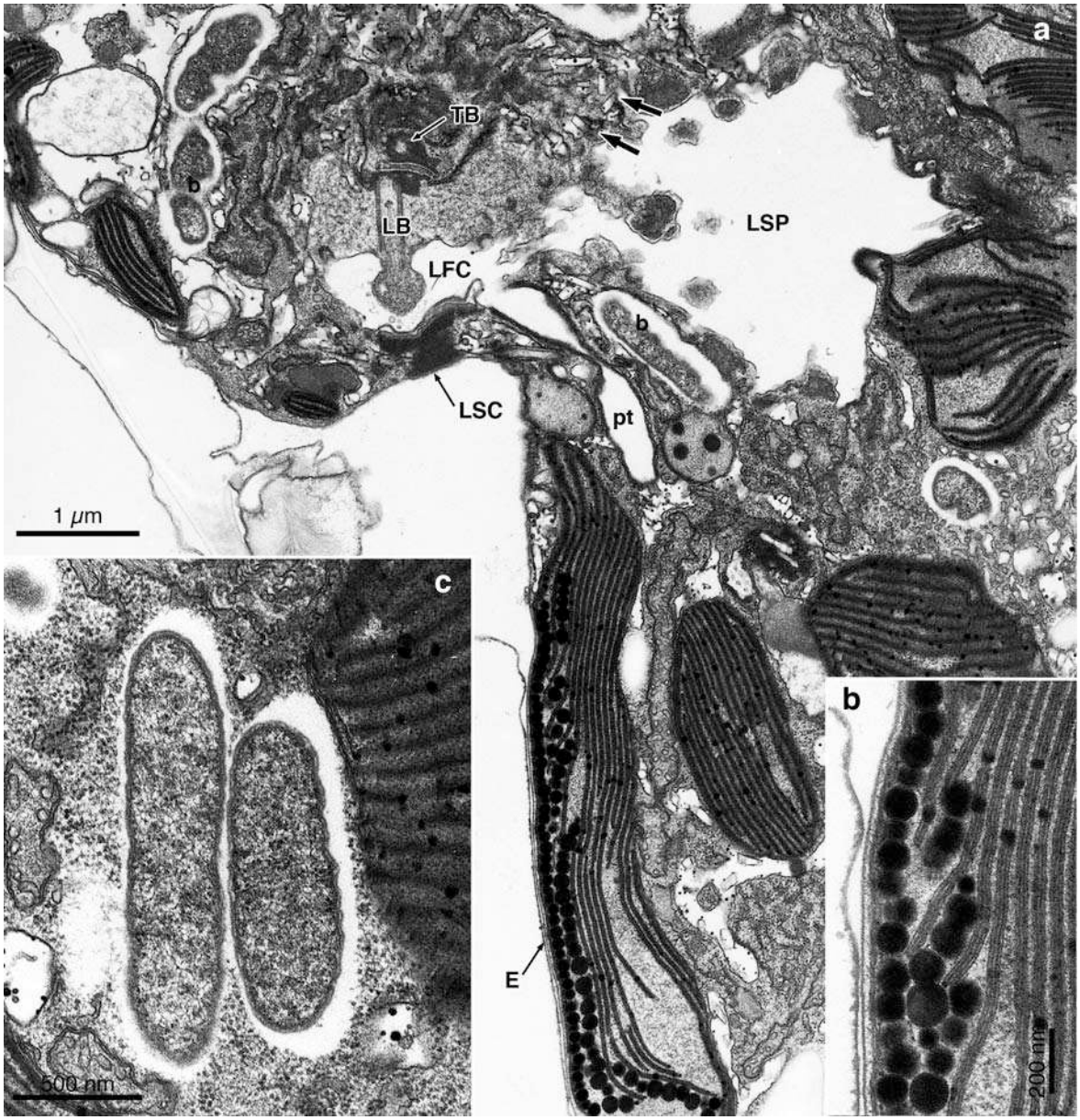

Fig. 8. *Palatinus apiculatus*, ultrastructure of the ventral area. (a) Longitudinal section showing the eyespot (E) and the basal bodies (LB and TB). Note the connection of the longitudinal sac pusule (LSP) and of a pusular tube (pt) to the longitudinal flagellar canal (LFC). LSC, longitudinal striated collar; b, bacteria. The arrows indicate vesicles with crystal-like contents. (b) Layers of globules in the eyespot, the inner layer repeatedly bending inward along obliquely oriented thylakoid lamellae. (c) Bacteria, bounded by two membranes and surrounded by an electron-translucent area.

Pusular system: Typical pusular elements, that is, membrane-bounded compartments wrapped in a vesicle, were of two kinds: roughly cylindroid tubes with the lumen some 150–300 nm in diameter, and flat vesicles with relatively straight profiles up to nearly 4 μm long (Fig. 7a). The tubes opened at the flagellar

canals and radiated from the ventral area, with some twists and turns along their path but without ramifications. A single tube connected to the dorsal-posterior side of the longitudinal flagellar canal (LFC) and extended into the posterior-ventral- left part of the cell (Fig. 8a). Two tubes extended from the transverse flagellar canal, one roughly parallel to the tube originating at the LFC, but deeper into the cell, and the other oriented toward the anterior-ventral area (Fig. S2, a, b and d; see the proximal ends of the tubes in the diagram of Fig. 9). The flat vesicles extended parallel to the three tubes (Fig. 7a) but were absent from the flagellar base area. We could not demonstrate continuity between the flat vesicles and the tubes nor any other structure. Two large vesicles were connected to the flagellar canals and were therefore labeled sac pusules in the sense of earlier light microscopists, as explained by Calado et al. (1999). The largest of these was a round vesicle up to > 10 µm in diameter, located on the ventral-right side of the cell and connected to the LFC (Figs. 5a; 6, c and d; 8a). Whereas the connection between this LSP and the LFC was rather wide in cells initially fixed with glutaraldehyde alone, it was constricted to a narrow bridge when osmium tetroxide was included in the first fixation (Fig. 8a). The transverse flagellar canal (TFC) extended into a much smaller vesicle, which was sometimes visible with the light microscope (Fig. 5b) but was collapsed in cells fixed with the mixture of glutaraldehyde and osmium tetroxide (compare Fig. 6d with Fig. S2, a–f). Although profiles of endoplasmic reticulum were common along the surface of the sac pusules, direct connection between the sac pusules and typical pusular elements was not observed.

Flagellar apparatus: A diagram of the flagellar apparatus and related structures of *P. apiculatus* as seen from the cell's left is given in Figure 9. The same point of view is illustrated in a series of sections progressing from left to right in Figures S2, 10, and 11. A slightly different view, from an anterior-left perspective, is given in Figure 12. As estimated from serial sections, the basal bodies formed an angle of about 80º–85º. Each flagellum exited the cytoplasm into an area bounded by a single membrane and connected to the exterior by a pore; complete rings of fibrous material, which appeared striated in some views and were labeled striated collars, surrounded the pores of these so-called flagellar

canals. Figures S2f and 12a show fibrous material extending from the transverse striated collar (TSC) that established continuity between the two collars.

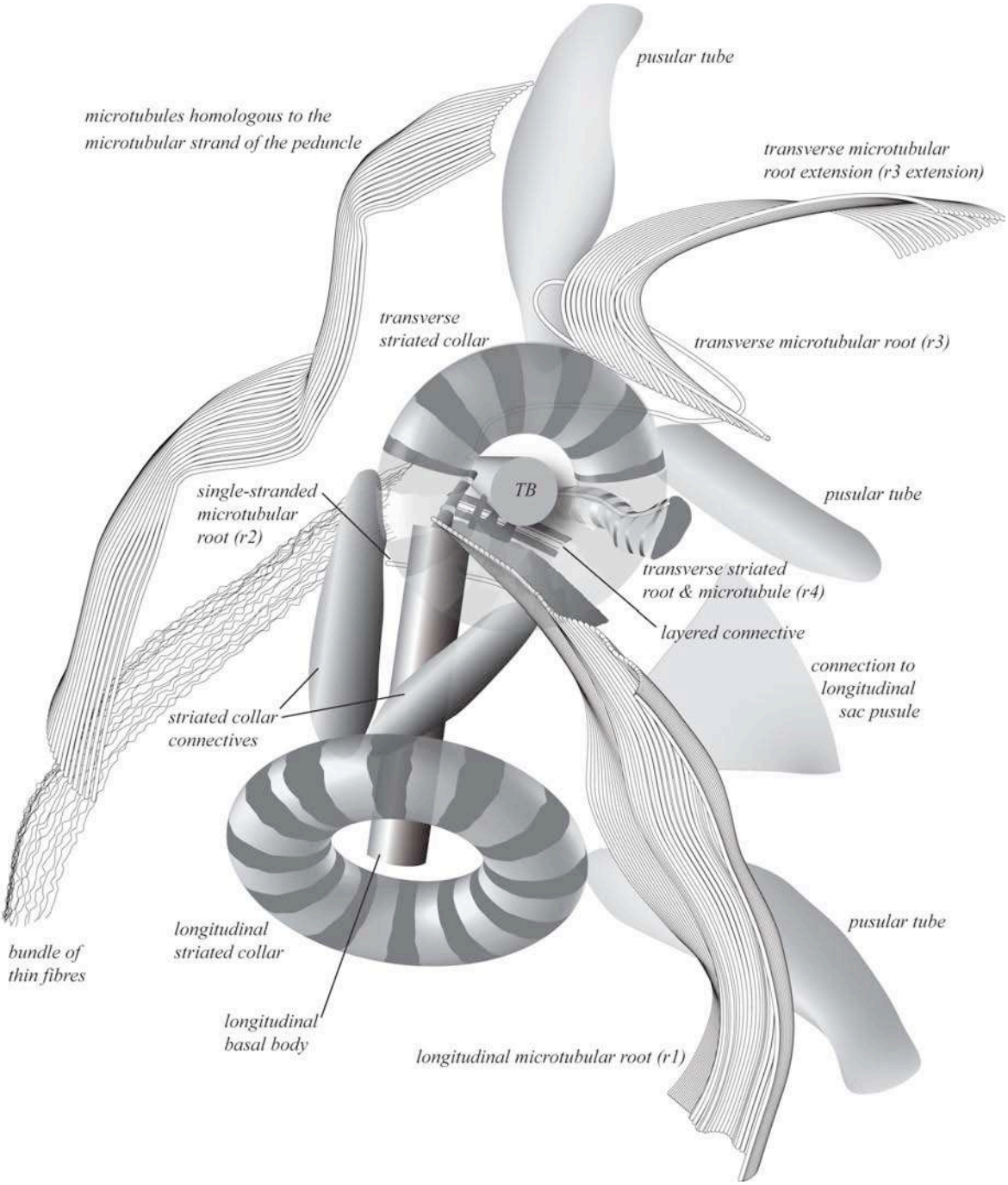

Fig. 9. *Palatinus apiculatus*. Schematic representation of the flagellar apparatus and adjacent structures as viewed from the cell's left (transverse basal body, TB, in cross-section).

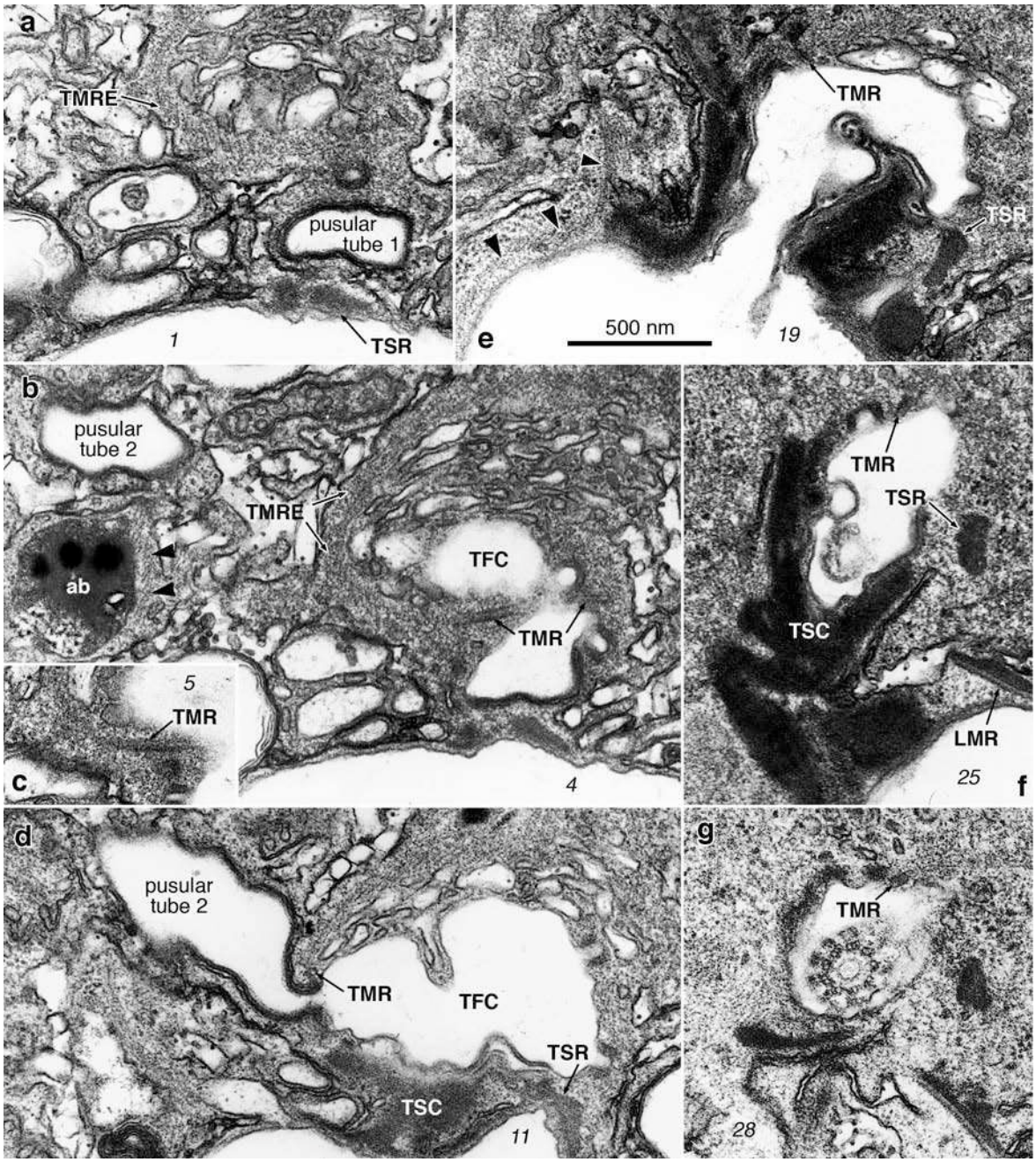

Fig. S2. *Palatinus apiculatus*, flagellar apparatus. Nonadjacent serial sections proceeding from left to right, viewed from the cell's left. Small slanted numbers refer to the section number. (a– d) Two pusular tubes connect to the transverse flagellar canal (TFC). The transverse microtubular root (TMR) and its microtubular extension (TMRE) are visible at this level, both encircling the TFC. A strand of microtubules, marked with arrowheads, is seen in (b), adjacent to an accumulation body (ab), and continues in (d–e). Note the left (distal) end of the transverse striated root (TSR) near the transverse striated collar (TSC). LMR, longitudinal microtubular root.

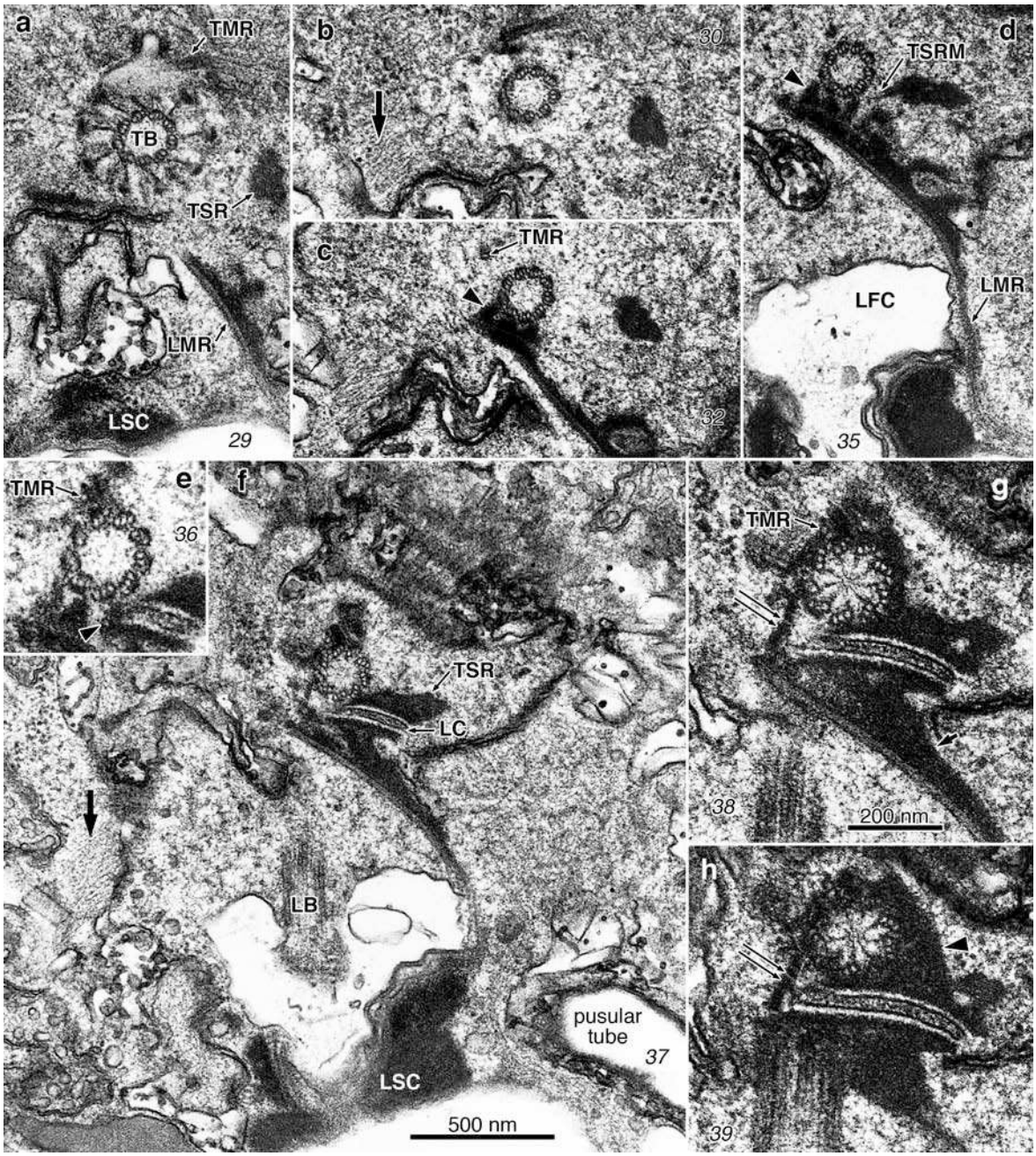

Fig. 10. *Palatinus apiculatus*, flagellar apparatus. Same series as in Figure S2 (in the supplementary material). Small slanted numbers refer to the section number. Proximal part of the transverse microtubular root (TMR), approaching and connecting to the anterior face of the transverse basal body (TB). The thick arrow in (b) and (f) points to a bundle of thin fibers extending along the flagellar base area, on the ventral side. (a–e) The transverse striated root (TSR) approaches the TB from the posterior-dorsal side. The TSR microtubule (TSRM) diverges from the fibrous portion of the root and connects to the posterior layer of the layered connective [LC; arrowhead in (e)]. The triple connection between the TB and electron-opaque material on the dorsal face of the LMR is marked with an arrowhead in (c) and (d). (f–h) A fiber connects the TB with the proximal end of the LMR [double arrow in (g) and (h)], apparently extending to the

longitudinal basal body (LB) in (h). Arrowhead in (h), electron-opaque material extending from the LC and surrounding the base of the TB. LMR, longitudinal microtubular root.

A multistranded microtubular root extended from the basal body region, along the surface of the sulcus, toward the antapex. We refer to it as the longitudinal microtubular root (LMR; designated r1 in Moestrup 2000), and its principal associations are shown in Figure 10. The rightmost microtubule of the LMR associated obliquely with the proximal part of the longitudinal basal body (LB) (Fig. 10, g and h). We estimated about five LMR microtubules at this proximal level, and the number increased gradually to an estimated 40 in the sulcal region, overlying the eyespot. The LMR passed along the surface of the longitudinal striated collar (LSC), to which it was probably attached, although a distinct fiber between the two structures was not seen (Fig. 10, d and f). The dorsal side of the proximal part of the LMR was covered with a layer of electron-opaque material (Figs. S2, f and g; 10, a–h), from which three fibers extended toward three or four triplets of the TB, some 500–600 nm from its base (Fig. 10, c and d). A layered connective (LC) linked this dorsal layer of the LMR with the proximal end of the transverse basal body (TB) (Fig. 10, f–h). A single fiber connected one of the triplets of the proximal part of the TB and the rightmost microtubules of the LMR and continued toward the base of the LB (Fig. 10, g and h). Figure 10, g and h, and 11a show the LC extending to the right beyond the LMR and directly connecting the two basal bodies. In exact cross-sections of the structure (i.e., longitudinal sections of the cell), the LC was ~120 nm thick with two outer electron-opaque layers 30 nm thick and two middle layers, each thinner than a unit membrane, limiting an area with discontinuous electron-opaque material (Fig. 10h). The LC extended for nearly 500 nm along the left-right axis and slightly less along the ventral-dorsal axis (Figs. 10, f–h; 11, a and b).

A single-stranded microtubular root (SMR; r2 in Moestrup 2000) was oriented parallel to the LMR and extended from the right side of the LB to near the dorsal side of the LSC (Fig. 11, b–d).

A layer of electron-opaque material, apparently continuous with the upper layer of the LC, surrounded the base of the TB, linking the two opposite sides where roots associate with this basal body (Figs. 10, g and h; 11a). On the apical,

slightly ventral side of the TB, a single microtubule ran parallel to the triplet microtubules for some 300 nm (Fig. 10, e–h), then turned away and took a sharp turn to the left, passing around the TFC next to a row of collared pits, spiraling anticlockwise for about one and a half turns (Figs. S2, a–g; 10, a–c). This transverse microtubular root (TMR; r3 in Moestrup 2000) nucleated one or two rows of about 20 microtubules, the TMR extension (TMRE), which curved around the anterior part of the TFC and continued toward the pyrenoid for ~1.4 µm (Fig. S2, a–d).

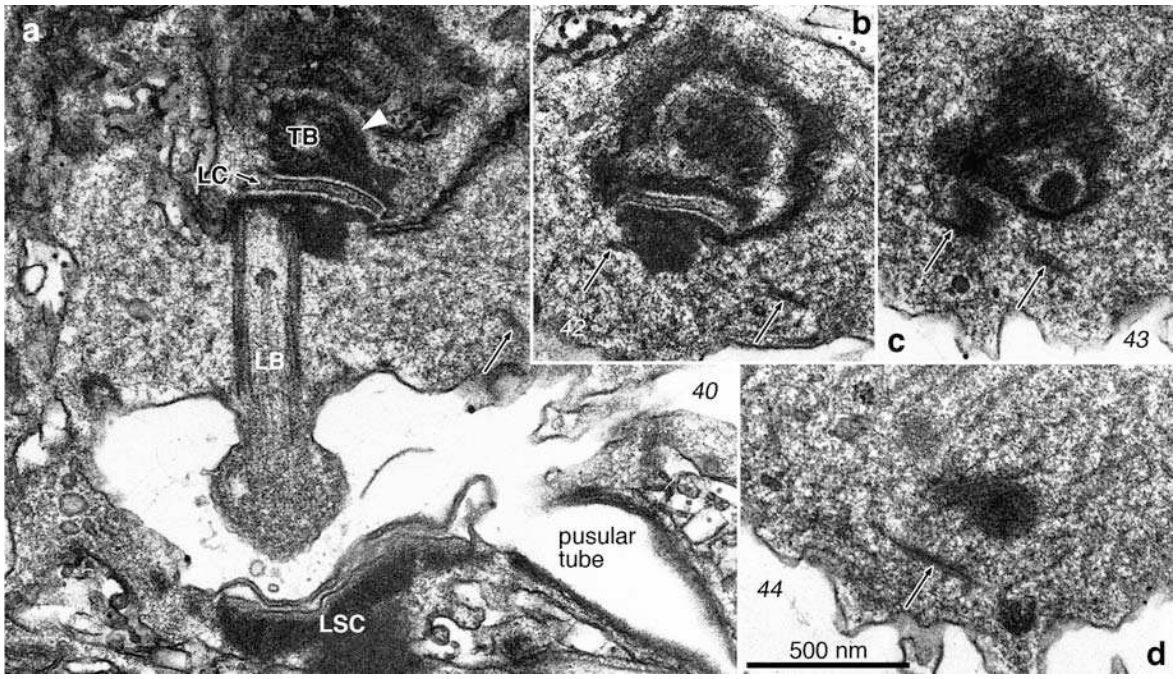

Fig. 11. *Palatinus apiculatus*, flagellar apparatus. Same series as Figure S2 (in the supplementary material) and Figure 10. Small slanted numbers refer to the section number. Single-stranded microtubular root (arrows) associated with the right hand side of the longitudinal basal body (LB). The proximal end of the transverse basal body (TB) is covered by electron-opaque material [arrowhead in (a)] that contacts also the upper layer of the layered connective (LC). LSC, longitudinal striated collar.

A fiber associated with the dorsal-posterior side of the TB and with the anterior layer of the LC extended toward the cell's left for 2.5 µm and terminated on the surface, near the left end of the TSC (Figs. S2, a, b, d–g; 10, a–f). This was identified as the transverse striated root (TSR) and was accompanied by a

microtubule (TSRM; r4 in Moestrup 2000), which diverged from the fiber near the proximal end and connected with the posterior layer of the LC (Fig. 10, d, e). A conspicuous set of concentric arcs of electron-opaque material, roughly centered on the TB, partly occupied the area anterior to the proximal end of this basal body (Figs. 10, f–h; 11, a–c).

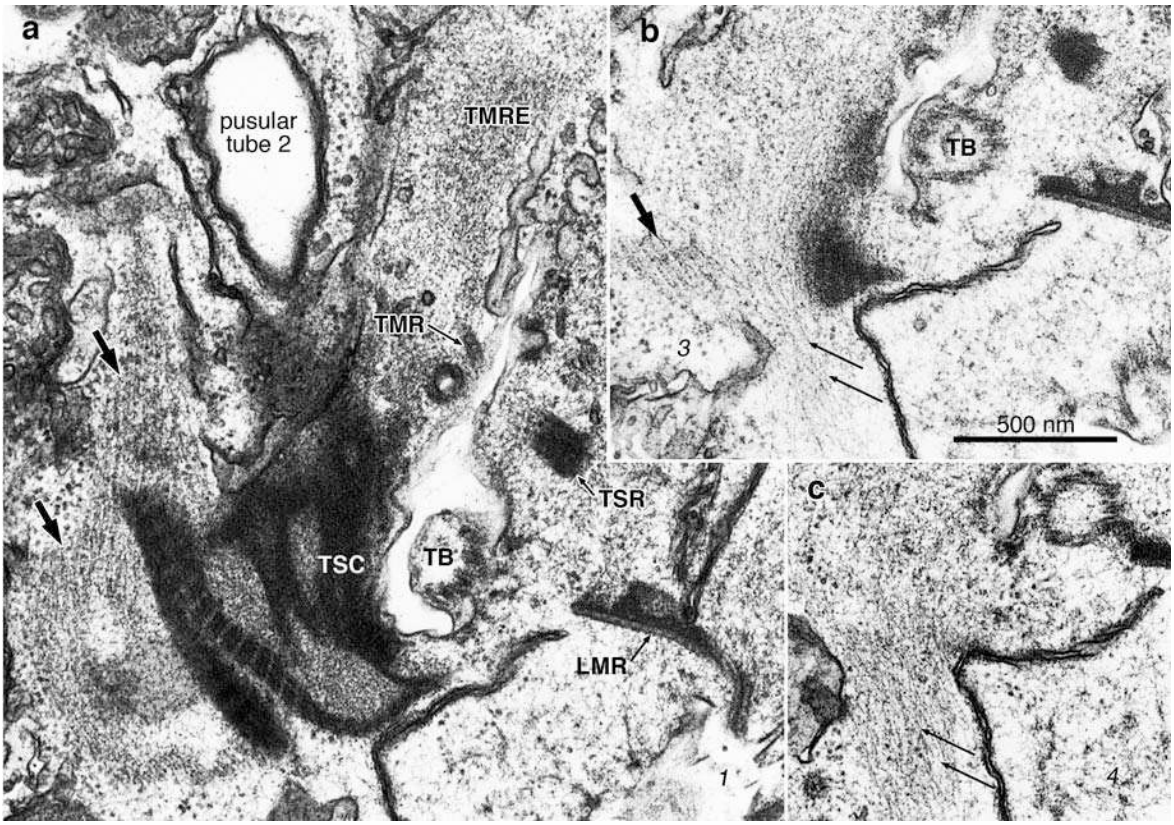

Fig. 12. *Palatinus apiculatus*, flagellar apparatus. Nonadjacent serial sections proceeding from anterior-left to posterior-right, viewed from the left. Strand of microtubules adjacent to the flagellar base area (thick arrows) and a roughly parallel bundle of thin fibers (thin arrows) that extends beyond the posterior end of the microtubules. The microtubular strand runs adjacent to fibrous material extending from the transverse striated collar (TSC). LMR, longitudinal microtubular root; TB, transverse basal body; TMR, transverse microtubular root; TMRE, transverse microtubular root extension; TSR, transverse striated root.

A strand of about 16 microtubules was seen near the flagellar collars and roots without visible connections to these structures. It was present near the TMR and TMRE microtubules (Fig. S2b) and continued toward the posterior-ventral side, bending near the surface of the TSC and barely reaching the level of the LSC

(Figs. S2e; 12, a and b), but it did not extend beyond these areas. An accumulation body was usually adjacent to this row of microtubules (Fig. S2b). A bundle of thin fibers coming from near the TSC seemed to extend beyond the posterior ends of the microtubules toward the posterior-ventral side, ending near the ventral cell surface (Figs. 10, b, c, and f; 12, b and c).

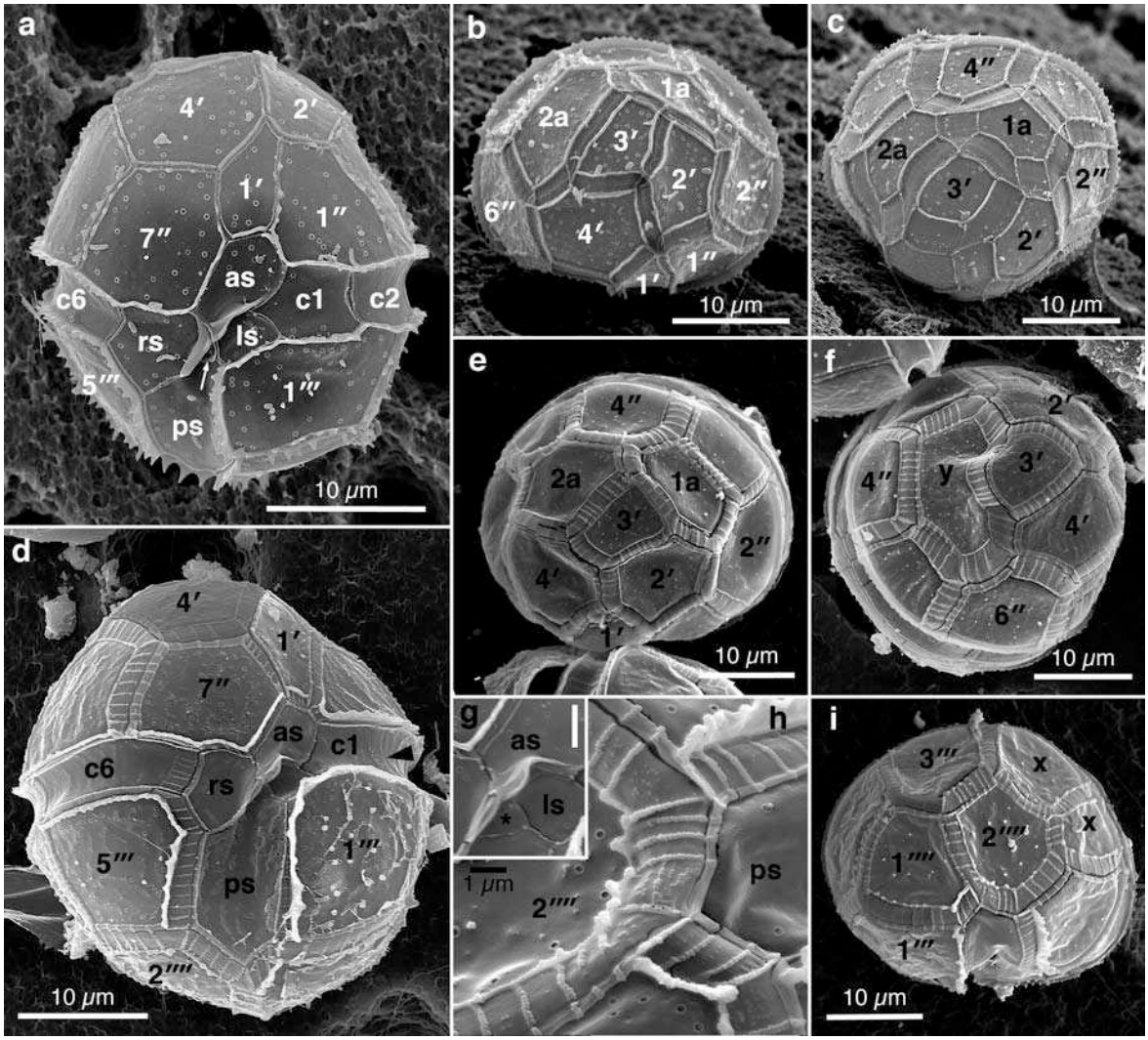

Fig. 13. *Palatinus apiculatus* var. *laevis* (a-c) and *P. pseudolaevis* (d-i), SEM. All cells from cultures. as, anterior, rs, right, ls, left, and ps, posterior sulcal plates. (a) Ventral view. (b, c) Apical views showing large sutures with thin cross-striations. The apical plates show a more symmetric arrangement than in *P. palatinus*. (d) Ventral view. (e) Apical view with the characteristic symmetric arrangement of the four apical and two intercalary plates. (f) Apical view showing plate variation; one transversely elongate plate (y) occupies the position of the two intercalary plates. (g) Detail of the sulcal plates showing the small accessory plate (*). Scale bar, 2 μm. (h) Detail of plate and suture surfaces. (i) Antapical view. Plate variation; plate 4‴ (or perhaps 3‴) appears subdivided (plates marked with x).

Morphology and thecal structure of Palatinus apiculatus *var.* laevis *(strain NIES-1405)*. Most specimens fell in the length range of 26-30 µm and were somewhat less elongate than the populations examined of *P. apiculatus.* Other than that, their overall characteristics were similar to cultured material of *P. apiculatus*, including the very thinly striated sutures in larger specimens and the presence of distinct spines in the hypotheca (Fig. 13, a-c). Figure 13b shows slightly raised borders of apical plates similar to those of cultured *P. apiculatus* (compare with Fig. 2c). However, the apical and intercalary plate pattern varied from nearly totally symmetric (Fig. 13c) to slightly asymmetric with plate 3′ somewhat elongate in a dorsal-left to ventral- right orientation (Fig. 13b), without reaching the marked asymmetry seen in *P. apiculatus*. The left side of the sulcus was usually less excavated than in *P. apiculatus*, making it easier to document the left and accessory sulcal plates (Fig. 13a).

Morphology and thecal structure of Palatinus pseudolaevis. Most cells were 28–37 µm long, 25–35 µm wide, and 24–28 µm thick. The cells were ellipsoidal, slightly flattened dorsoventrally, with the epitheca and hypotheca of similar size. The general appearance was usually smoothly convex (Fig. 13d); the concavity of plates seen in Figure 13, e, f, h, and i, is an artifact produced during electron microscopical observation. The cells displayed the characteristic twist to the left of the epitheca relative to the hypotheca, as described for *P. apiculatus* (Fig. 13d). The tabulation matched that of *P. apiculatus* in terms of number and position of plates, but the apical arrangement of plates was regularly symmetrical (Fig. 13e). The cingulum descended near the right-ventral side about a cingular width (Fig. 13d). Although bordered by the raised edges of plates 1‴ and 5‴, the sulcus was usually wide enough to allow visibility of all five sulcal plates (Figs. 13, d and g). Scattered granules or short, blunt spines ornamented some of the thecal plates, particularly in the hypotheca (Figs. 13, d and i), but no conical spines were present. Sutures between plates were distinctly striated, with individual cross-lines just over 0.2 µm thick and topped by a row of small granules (Fig. 13h). The cells exited the theca through the antapex (not shown).

Cells with variant tabulations were relatively common in the culture. Variations most commonly affected epithecal plates, particularly the fusion of the

two intercalary plates (Fig. 13f, plate marked y). Figure 13i shows a more uncommon variation, in which there are six postcingular plates, apparently caused by the duplication of plate 4‴ (or perhaps 3‴).

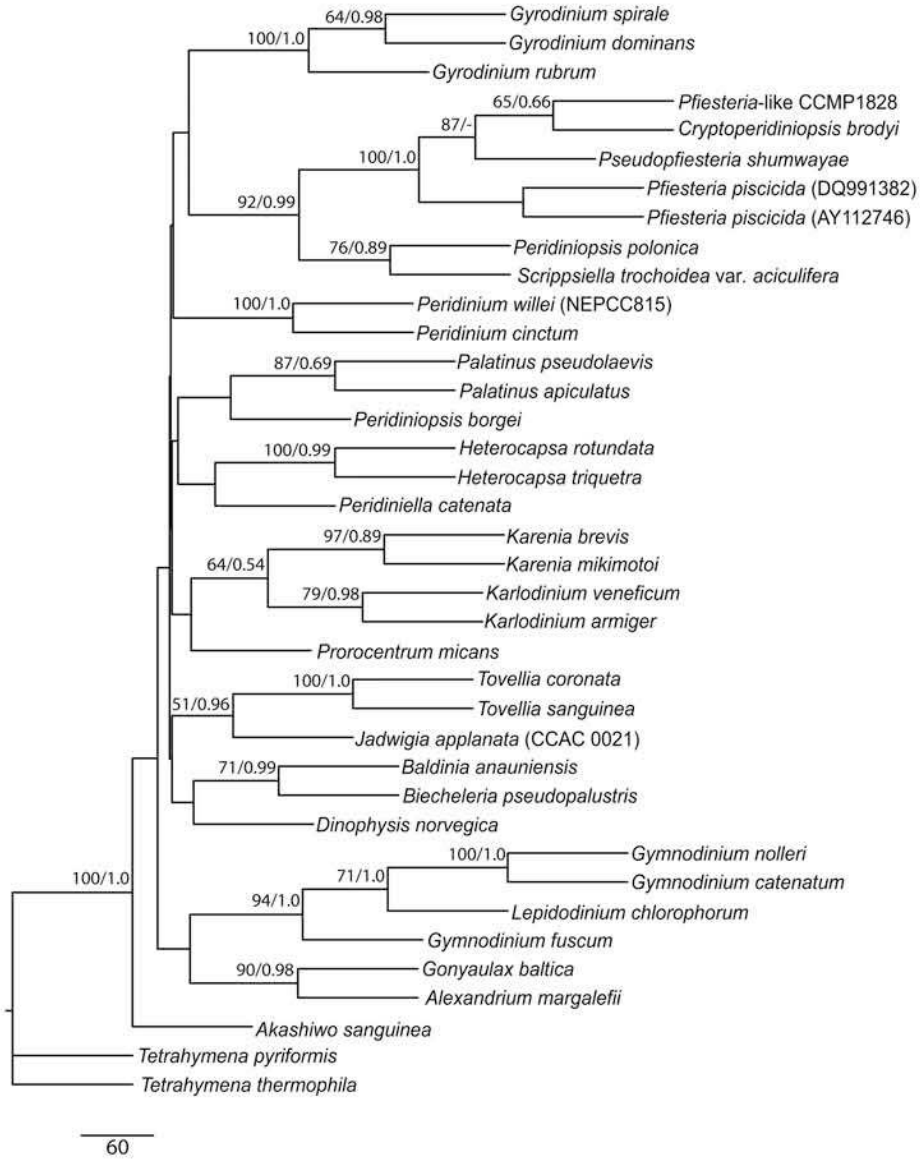

Fig. 14. Phylogenetic tree based on maximum-likelihood (ML) bootstrap analysis (PhyML) of nuclear-encoded LSU rDNA sequences from a diverse assemblage of dinoflagellates including the new genus *Palatinus*. The tree was rooted using two ciliate species of the genus *Tetrahymena*. MrModeltest suggested GTR+G+I as the best-fit nucleotide substitution model and the settings proposed by the program were used in PhyML analysis. Support for nodes was estimated by bootstrap (100 replications in ML) and posterior probabilities in Bayesian analysis. Only bootstrap

values ≥50% and posterior probabilities ≥0.5 are written to the left of nodes. The branch lengths are proportional to the number of character changes.

Molecular phylogeny. The tree topology obtained from ML using PhyML is illustrated in Figure 14. The deepest branches in the tree are very short and without support from bootstrap analysis (<50%) and posterior probabilities (<0.5). Hence, the relationships at this level cannot be established with confidence. However, there is support for the branching pattern of the terminal taxa, and in a few cases, their sister group relationships. With respect to the relationship between the taxa of interest in this study, PhyML analysis suggests the two species of *Palatinus* to be related to *Peridiniopsis borgei*. The relationship between *Palatinus* spp. and *Peridinium cinctum* and *P. willei* seems distant (Fig. 14), even though this is not supported by any of the methods applied here as measure of branch support. Thus, the ML analysis does not propose a phylogenetic relationship (i.e., a most recent common ancestor) between *Palatinus* and *Peridinium* as would be expected considering the potential level of taxonomic resolution provided in this data set.

Table 1. Sequence divergence estimates in percent between *Palatinus* spp., *Peridinium* spp., and *Peridiniopsis borgei*. Estimates based on 991 base pairs of the nuclear-encoded LSU rDNA sequences. Uncorrected distances (P-values from PAUP*) are provided above the diagonal, and distance values calculated using the Kimura-2-parameter model are given below the diagonal.

	Palatinus apiculatus	*Palatinus pseudolaevis*	*Peridiniopsis borgei*	*Peridinium cinctum*	*Peridinium willei*
P. apiculatus	—	6.7	11.5	17.1	19.4
P. pseudolaevis	7.3	—	11.1	17.7	19.7
P. borgei	12.6	12.1	—	19.5	21.4
P. cinctum	19.7	20.5	23.0	—	9.5
P. willei	22.8	23.1	25.8	10.3	—

Sequence divergence. Estimates of sequence divergence in percent provide a simple measure of relationship as similar nucleotide sequences are expected to mirror relatedness. However, in cases of lateral gene transfer, similar sequences will (in most cases) misleadingly suggest a close relationship. Here the

sequence divergence estimates for pairwise comparisons between the two species belonging to *Peridinium* and *Palatinus*, respectively, and *Peridiniopsis borgei* are shown in Table 1. Depending on the method used to calculate the sequence divergence, the values between *Palatinus* spp. (6.7%, 7.3%) and *Peridinium* spp. (9.5%, 10.3%) are significantly lower than the values obtained from comparisons between the two genera (17.1%, 19.7% and 19.7%, 23.1%). The sequence divergence estimates between *Palatinus* spp. and *P. borgei* were 11.1%, 11.5% and 12.1%, 12.6%, and considerably higher values were seen when comparing *Peridinium* spp. and *P. borgei* (19.5%, 21.4% and 23.0%, 25.8%). The sequence divergence values in percent given as numbers above are based on uncorrected distances (P-values in PAUP*) and the Kimura-2-parameter model, respectively.

DISCUSSION

Taxonomy and nomenclature of Palatinus *species*. The original descriptions of *Peridinium palatinum* and *P. marssonii* display significant similarities between the two species, notably the absence of areolations on the thecal plates, the ‘‘wing-like’’ raised borders of the epithecal plates, and the more or less spiny posterior ends of the cells (Lauterborn 1896, Lemmermann 1900a). However, the lack of illustrations and of defined tabulation patterns rendered the identities of both species uncertain, and the two names were listed in equal standing in a compilation by Lemmermann (1900b). The publication of illustrations and a tabulation formula for *P. marssonii* (Lemmermann 1910, pp. 658, 678), although inaccurate (see below), followed by Schilling’s (1913) inclusion of *P. palatinum* in a list of uncertain species, were probably responsible for the limited use of the latter name during the following years (e.g., Bachmann 1911, Lindemann 1919).

The interpretation of *P. laeve* was facilitated by illustrations and an accurate tabulation scheme, showing the apex of the cell with four plates symmetrically arranged around a square, central plate (Huitfeldt-Kaas 1900). In contrast, the tabulation described for the epitheca of *P. anglicum* was erroneous and misleading, as pointed out by Lindemann (1919, p. 259). The arrangement of the 11 plates recognized in the apical view of *P. anglicum* (West 1909) closely

matched the tabulation later described for *P. marssonii* (Lemmermann 1910), except that the plate labeled ventral-apical contacts the precingular plate 6 in *P. anglicum*. Lemmermann's (1910) statement that the right dorsal-apical plate of *P. marssonii* contacted precingular plate 7 disagrees with the ventral view of the theca included, just as the regular-looking ventral and dorsal views of *P. anglicum* disagree with the interpretation of the tabulation by West (1909, fig. 23C, p. 190) and Lemmermann (1910, p. 679). However, the apical views of the two species given by these authors can easily be matched to the epithecal arrangements of the plates later ascribed to *P. palatinum*, by presuming that the steepness of the ventral side of the theca conceals plates 1′ and 7″ (compare with Fig. 2d, relabeling plates 2′, 3′, and 4′ as r, va, and 7 pr, respectively).

Lindemann (1919) reviewed the group ''*Peridinium-laeve-marssoni-anglicum*'' and concluded that features such as a slight difference in the size of the antapical plates and the concavity or convexity of plates, previously used as discriminating characters, were not reliable, and that species distinction could only be based on the tabulation of the epitheca. Although noting the good correspondence between the diagnoses of *P. palatinum* and *P. marssonii*, Lindemann (1919) left *P. palatinum* out of the discussion for lack of figures to clarify its features. All the variant forms in the group were classified in a single species, for which he used the name *P. laeve*, with both *P. marssonii* and *P. anglicum* ranked as subspecies; several variations in plate tabulation, mainly affecting the position of sutures and contacts between plates, were described as varieties, classified mainly in subsp. *marssonii* (Lindemann 1919, 1920).

Lindemann eventually became convinced that *P. palatinum* was conspecific with *P. laeve*, a synonymy previously indicated by Lauterborn (1910, p. 498), and started using the former name (Lindemann 1924, 1925a); his statement that *P. marssonii* was identical to *P. palatinum* was substantiated by the study of samples given to him by Lauterborn (Lindemann 1925b, p. 189). Although Lindemann did not formally recombine the infraspecific taxa previously recognized under *P. laeve* with *P. palatinum*, he did distinguish the asymmetric arrangement of plates around the long, triangular plate 3′ of *P. palatinum* from the symmetric disposition seen at the apex of *P. laeve*, which he named *P. palatinum* f. *laeve* (Huitfeldt-Kaas) Er.

Lindemann (1925a, p. 478, 1925b, p. 189). The high proportion of nearly symmetric cells of strain NIES-1405, analyzed in the present study, in contrast with the regularity of strongly asymmetric cells in the populations examined of *Palatinus apiculatus*, suggests this symmetry to be a stable, inheritable feature and supports the recognition of an independent taxon.

Although Lefèvre (1926) confirmed Lindemann's observations and agreed, in general, with his taxonomic decisions, he also detected a new, unnoticed taxon among the previous illustrations of *P. laeve*– like cells with a symmetric apex. On the basis of observations in fig. 18 in Lindemann (1920, p. 128) and his own study of material collected in Haute-Savoie, French Alps, by Georges Deflandre, Lefèvre (1926, p. 341) described the new species *P. pseudolaeve*, using the markedly striated intercalary bands as a specific character. Although, as shown in Figure 2, a and b, the sutures of *Palatinus apiculatus* are not completely smooth, striations appear rather faint in classical, bright-field LM and are usually not represented in published drawings of the species (Lefèvre 1932, Starmach 1974, Popovskký and Pfiester 1990); notable exceptions are Skuja (1930, pl. I, figs. 8, 9, as *Peridinium anglicum*) and Wołoszyńska (1952, pl. XVII, figs. 6, 9). The more rounded, less compressed shape, the absence of flanges bordering the epithecal plates, and the lack of strong spines in the hypotheca combine with the distinctly striated sutures and the symmetrical arrangement of the apical plates to make *Palatinus pseudolaevis* a clearly recognizable species.

Lindemann (1928) brought *Glenodinium apiculatum* into the context of this group by noting that both *Peridinium marssonii* and *P. palatinum* were identical to this species, described by Ehrenberg (1838). Without first-hand knowledge of *G. apiculatum*, Stein (1878, p. 92, 1883) had regarded it as a developmental stage of *Peridinium tabulatum* Ehrenb. However, the smooth theca, the raised edges of the epithecal plates, the spiny posterior end of the cells, and the epitheca with the typical twist toward the left, as seen in Ehrenberg's original illustrations (see Fig. 1), all match the current concept of *Peridinium palatinum*, and Lindemann's (1928) proposed synonymy has not been disputed.

Although the name *P. apiculatum* ''(Ehrenb.) Er. Lindemann'' was used by contemporary authors (Höll 1928, Eddy 1930), Lefèvre (1932) retained *P.*

palatinum as the correct name for the species; whether this decision was idiosyncratic or had some nomenclatural basis was not explained. One possible nomenclatural consideration would be that *P. apiculatum* Penard (Penard 1891, p. 51, pl. III, figs. 3–13) would have priority over Lindemann's (1928) combination. However, the original transfer of *Glenodinium apiculatum* to *Peridinium* dates back to Claparède and Lachmann (1859), with the consequence that Penard's *P. apiculatum* is a later homonym, and therefore illegitimate, and Lindemann's intended new combination *P. apiculatum* is a later isonym, without nomenclatural status (McNeill et al. 2006, Art. 6, Note 2).

Meunier (1919) transferred *G. apiculatum* Ehrenb. to the newly described genus *Properidinium*, erected to receive a diverse assemblage of marine and freshwater species with only 13 epithecal plates. Although arguably illegitimate (it included the type species of *Heterocapsa* F. Stein), the genus was later typified by Loeblich and Loeblich (1966, p. 51), who selected *Properidinium avellana* Meunier as lectotype. Lebour (1925, p. 108) treated *P. avellana* as a species of *Peridinium*, and Balech (1974, p. 54) transferred it to *Protoperidinium* Bergh; the presence of an elongated apical pore complex was documented by Wall and Dale (1968, pl. 4, fig. 1), who obtained thecae from the germination of cysts identical to *Chytroeisphaeridia cariacoensis* D. Wall. The cyst was subsequently transferred to *Brigantedinium* P. C. Reid (Reid 1977, p. 434). Fensome et al. (1993) considered *Properidinium* to be a synonym of *Archaeperidinium* Jörgensen, which they assigned, together with *Brigantedinium*, to a family characterized by the presence of only four plates in the cingulum, and with no affinity with the group of species studied herein.

Morphology and ultrastructure. Although the arrangement of the chloroplast, with lobes radiating from a central pyrenoid, is a striking feature in axial sections of *Palatinus apiculatus*, it is relatively difficult to perceive in whole cells, probably because the pyrenoid is not enveloped by a layer of starch. Cytoplasmic channels penetrating the pyrenoid matrix are common in several groups of chlorophytes (e.g., Dodge 1973) but have been described in few dinoflagellates; these include species of *Heterocapsa* (Dodge and Crawford 1971, Horiguchi 1995, Tamura et al. 2005) and *Bysmatrum arenicola* Horiguchi et Pienaar (Horiguchi and Pienaar

1988). However, another species with peridinioid affinities, *Peridiniopsis borgei*, has been shown to lack cytoplasmic channels in the pyrenoid (Calado and Moestrup 2002).

The eyespot of *P. apiculatus* belongs to type A sensu Moestrup and Daugbjerg (2007), defined to include eyespots consisting of rows of electron-opaque globules inside a chloroplast lobe located in the sulcal area. Diversity within this type of eyespot includes variation in size and in number of rows of globules, from the relatively small-sized eyespots of, for example, *Peridinium cinctum* and *Baldinia anauniensis*, with a single or two ill-defined rows, to large types as in *Peridiniopsis borgei*, with up to six rows (Calado et al. 1999, Calado and Moestrup 2002, Hansen et al. 2007). In *Palatinus apiculatus*, the eyespot is about as long as in *P. borgei*, although it shows only two longitudinal and the unusual oblique rows of globules. A layer of crystal-like (brick-like) material was found between the eyespot-containing chloroplast lobe and the LMR (r1 flagellar root) of both *P. borgei* and *B. anauniensis*, but not in *P. apiculatus*.

Bacteria are commonly found inside dinoflagellate cells, both in the cytoplasm and, more rarely, in the nucleus (Silva and Franca 1985). Although cultured cells of *P. apiculatus* did not show signs of being harmed by the large numbers of bacteria they contained, their presence did not seem to be required because no bacteria were detected in cells fixed from a field sample. The number of intracellular bacteria had no significant effect on the growth or survival of cultured *Heterocapsa circularisquama* T. Horiguchi (Maki and Imai 2001).

Cytoplasmic vesicles containing bundles of thin fibers are a regular feature of dinoflagellate cells and, following Leadbeater (1971), are generally interpreted as being involved in the formation of flagellar hairs. Figure S1a supports the idea that dictyosomes are involved in the maturation of these fibrillar vesicles (Leadbeater 1971).

Microtubular strands located near the flagellar base area, but not attached to flagellar roots, have been found in most dinoflagellates examined in detail. Dinoflagellates that have such rows of microtubules fall into two groups: the ones with several overlapping rows capable of extending into an external tube commonly used for food uptake, as shown for *Peridiniopsis berolinensis*

(Lemmerm.) Bourrelly (Calado and Moestrup 1997), and those with a single row of microtubules, which vary in number from nearly 80 in *Peridiniopsis borgei* (Calado and Moestrup 2002) to about 26 in the small-celled *Prosoaulax lacustris* (F. Stein) Calado et Moestrup (Calado et al. 1998, as *Amphidinium lacustre* F. Stein non auctt.; see Calado and Moestrup 2005). Although it is not clear what function these microtubular strands have in some species, the use of microtubule-driven peduncles for feeding, probably involving the electron-opaque vesicles usually located along the microtubules, is well documented (Hansen and Calado 1999). Judging from its position and orientation, the microtubular strand positioned adjacent to the flagellar base area of *P. apiculatus* is interpreted as homologous to the rows of microtubules involved in peduncle extension in other dinoflagellates. The short length of the microtubules, not reaching the cell surface, the lack of accompanying vesicles, and the absence of a definite exit location for a peduncle, such as a striated collar, suggest that the microtubular strand of *P. apiculatus* is nonfunctional, perhaps an evolutionary leftover.

Comparison with typical Peridinium. The genus *Peridinium* is typified by *P. cinctum* (O. F. Müll.) Ehrenb., currently classified in group cinctum together with *P. gatunense* Nygaard and *P. raciborskii* Wołosz. Group willei, comprising *P. willei* Huitfeldt- Kaas and *P. volzii* Lemmerm., differs from species of group cinctum in having the epithecal plates disposed symmetrically relative to the ventral–dorsal axis (Popovský and Pfiester 1990). The general appearance of the cells and the tabulation features are otherwise similar in the two groups, and *P. willei* consistently pairs with *P. cinctum* in DNA-derived phylogenetic schemes (Fig. 14 and, e.g., Calado et al. 2006, Moestrup et al. 2008). The features common to all these species, as far as they are known, therefore represent typical *Peridinium* characters.

Peridinium group palatinum is separated from other groups of species without an apical pore by the presence of two, rather than three, anterior intercalary plates (e.g., Bourrelly 1970, Popovský and Pfiester 1990). As seen in the present work, this correlates with other differences from typical *Peridinium* features. The presence of six cingular plates in *Palatinus*, against five in typical *Peridinium*, would by itself warrant a separate generic status to *Palatinus* species

in a widely followed practice initiated by Balech for marine dinoflagellates (Balech 1959). However, given the high number of thecate species for which cingular details had not been reported, Bourrelly (1968, 1970, pp. 52–3) did not adopt the number of cingular plates as a generic level character in his account of the freshwater dinoflagellates. Another notable aspect of the theca of *Palatinus* is the smooth or finely granulate surface of the plates, with no traces of the ridges that form the areolate pattern seen in typical *Peridinium* species (e.g., Hickel and Pollingher 1988, Olrik 1992, Calado et al. 1999).

Cells of *Peridinium* sensu Popovský and Pfiester (1990) shed the theca when they divide, and sometimes also without dividing, a process known as ecdysis (e.g., Taylor 1987). The way the theca opens for the exiting cells is quite regular within a species (Lefèvre 1932, p. 21). In *P. cinctum*, *P. willei*, and *P. volzii*, an operculum formed by the dorsal half of the epitheca breaks off, made of plates 3′, 1a, 2a, 3a, 3″, 4″, 5″, as reported by Boltovskoy (1973, 1975)—who applied the term archeopyle to the theca rather than to the cyst—and repeatedly confirmed by us (A. Calado and S. Craveiro, unpublished observations). The theca of *P. gatunense* opens along the upper edge of the cingulum (Boltovskoy 1973). In contrast, thecae of *Palatinus* species break open in the antapical area.

The occurrence of cells dividing in an athecate, swimming stage, reported here for dense *P. apiculatus* populations in the Kollelev ponds, was previously described by West (1909, p. 189) from Warwickshire, middle England, who saw in this division mode ‘‘the reason for the occurrence of prodigious numbers of active individuals’’ in Bracebridge Pool, in April. Although this division in the swimming stage seems restricted to rapidly growing, dense populations, and the more common exit of already divided cells from the parent theca may also occur in *P. apiculatus*, it is noteworthy that a similar division strategy has never been reported, even for dense populations of any other species.

The most striking difference between the internal structure of *Palatinus* and typical *Peridinium* is the connection of peripheral lobes to a central, branching pyrenoid described in the present work, in contrast with the entirely peripheral plastid system reported for *P. cinctum* (Spector and Triemer 1979, Calado et al. 1999) and *P. gatunense* (Messer and Ben-Shaul 1969, as *P. westii* Lemmerm.).

Seo and Fritz (2002) documented a diel migration of chloroplasts (or chloroplast lobes) in *P. volzii*, located at the periphery during the dark phase and retreating toward the center of the cell, with the pyrenoid-containing areas inward, during the light phase, but without connecting into a single entity.

Ultrastructural details of typical *Peridinium* species for comparison with *Palatinus apiculatus* are only available from *Peridinium cinctum*. The structure documented in Figure 3, a and c, in the thecal pores of *P. apiculatus* was not found in a detailed study of the theca of *P. cinctum* (Dürr 1979). The well-defined pusular tubes occurring in *P. apiculatus* were not present *in P. cinctum*. In the latter species, numerous irregularly shaped pusular tubes and vesicles were directly linked to the flagellar canals and sac pusules, and abundant profiles of pusular elements were present in the ventral area (Calado et al. 1999). The comparatively more localized pusular system of *P. apiculatus* suggests a different strategy for establishing a large contact area between pusule and cytoplasm, perhaps mainly through the surface of the spreading wrapping vesicles.

P. cinctum was found to lack a microtubular strand homologous to those involved in peduncle formation in other dinoflagellates (Calado et al. 1999). In contrast, such a microtubular system was observed in all cells of *P. apiculatus* examined in the present work (see above). The distinct fibers connecting the TB to the dorsal side of the LMR and the aspect of the LC in cross-section, as documented here for *P. apiculatus*, are reminiscent of similar structures in *Peridiniopsis borgei*, which they resemble more than those of *P. cinctum* (Calado and Moestrup 2002). Taken together, these features and the chloroplast organization with a large, central pyrenoid, suggest that *P. apiculatus* has retained more plesiomorphic characters from the common ancestor to *Peridinium* and *Peridiniopsis* than *P. cinctum*.

The molecular phylogeny presented in Figure 14 complements the comparison of morphological features outlined above and also suggests the separation of the two *Palatinus* species from the *P. cinctum* group. Although this molecular phylogenetic indication is weakened by the low bootstrap values and posterior probabilities supporting the branching pattern, the ML analysis did propose a somewhat distant relationship between typical *Peridinium* and a clade

comprising *P. borgei* and the *Palatinus* species. Additionally, the sequence divergence estimates indicated that the percentage difference between *Palatinus* and *Peridinium* is in the same range as that seen at the genus level for other dinoflagellates (N. Daugbjerg, pers. observation). We therefore interpret that the LSU rDNA sequence data provide indirect support to the morphological reasoning for erecting the new genus *Palatinus*. Future gene sequence analyses, preferably of nonribosomal nuclear and mitochondrial genes, should be performed to elucidate further the evolutionary history and phylogeny of *Palatinus* and species belonging to the *P. cinctum* group.

S. C. C. was supported by a Ph.D. fellowship from the financing program POCI, Portugal (SFRH ⁄BD⁄ 16794 ⁄ 2004), and by a grant from the European Commission's (FP 6) Integrated Infrastructure Initiative programme SYNTHESYS (DK-TAF) during July–September 2008. Ø. M. gratefully acknowledges a grant from the Villum-Kann Rasmussen Foundation. We thank Ramiro Logares for sending an extracted DNA sample of *Peridiniopsis borgei*.

REFERENCES

Bachmann, H. 1911. *Das Phytoplankton des Süßwassers mit besonderer Berücksichtigung des Vierwaldstättersees*. Gustav Fischer, Jena, Germany, 213 pp., 15 pls.

Balech, E. 1959. Two new genera of dinoflagellates from California. *Biol. Bull*. 116:195–203.

Balech, E. 1974. El género *"Protoperidinium"* Bergh, 1881 (*"Peridinium"* Ehrenberg, 1831, partim). *Rev. Mus. Argent. Cienc. Nat. Hidrobiol*. 4:1–79.

Bergholtz, T., Daugbjerg, N., Moestrup, Ø. & Fernández-Tejedor, M. 2006. On the identity of *Karlodinium veneficum* and description of *Karlodinium armiger* sp. nov. (Dinophyceae), based on light- and electron microscopy, nuclear-encoded LSU rDNA and pigment composition. *J. Phycol*. 42:170–93.

Boltovskoy, A. 1973. Formacion del arqueopilo en tecas de dinoflagelados. *Rev. Esp. Micropaleontol*. 5:81–98.

Boltovskoy, A. 1975. Estructura y estereoultraestructura tecal de dinoflagelados. II. *Peridinium cinctum* (Müller) Ehrenberg. *Physis Secc. B* 34:73–84.

Boltovskoy, A. 1999. The genus *Glochidinium* gen. nov., with two species: *G. penardiforme* comb. nov. and *G. platygaster* sp. nov. (Peridiniaceae). *Grana* 38:98–107.

Bourrelly, P. 1968. Note sur *Peridiniopsis borgei* Lemm. *Phykos* 7:1–2.

Bourrelly, P. 1970. *Les algues d'eau douce 3: Les algues bleues et rouges, les Eugléniens, Péridiniens et Cryptomonadines*. Boubée, Paris, 512 pp.

Calado, A. J., Craveiro, S. C., Daugbjerg, N. & Moestrup, Ø. 2006. Ultrastructure and LSU rDNA-based phylogeny of *Esoptrodinium gemma* (Dinophyceae), with notes on feeding behavior and the description of the flagellar base area of a planozygote. *J. Phycol*. 42:434–52.

Calado, A. J., Craveiro, S. C. & Moestrup, Ø. 1998. Taxonomy and ultrastructure of a freshwater, heterotrophic *Amphidinium* (Dinophyceae) that feeds on unicellular protists. *J. Phycol*. 34:536–54.

Calado, A. J., Hansen, G. & Moestrup, Ø. 1999. Architecture of the flagellar apparatus and related structures in the type species of *Peridinium*, *P. cinctum* (Dinophyceae). *Eur. J. Phycol*. 34:179–91.

Calado, A. J. & Moestrup, Ø. 1997. Feeding in *Peridiniopsis berolinensis* (Dinophyceae): new observations on tube feeding by an omnivorous, heterotrophic dinoflagellate. *Phycologia* 36:47–59.

Calado, A. J. & Moestrup, Ø. 2002. Ultrastructural study of the type species of *Peridiniopsis*, *Peridiniopsis borgei* (Dinophyceae), with special reference to the peduncle and flagellar apparatus. *Phycologia* 41:567–84.

Calado, A. J. & Moestrup, Ø. 2005. On the freshwater dinoflagellates presently included in the genus *Amphidinium*, with a description of *Prosoaulax* gen. nov. *Phycologia* 44:112–9.

Claparède, E. & Lachmann, J. 1859. Études sur les Infusoires et les Rhizopodes. *Mém. Inst. Natl. Geneve* 6:261–482, pls. 14–24.

Daugbjerg, N., Hansen, G., Larsen, J. & Moestrup, Ø. 2000. Phylogeny of some of the major genera of dinoflagellates based on ultrastructure and partial LSU rDNA sequence data, including the erection of three new genera of unarmoured dinoflagellates. *Phycologia* 39:302–17.

De Rijk, P., Wuyts, J., van der Peer, Y., Winkelmans, T. & de Wachter, R. 2000. The European large subunit ribosomal RNA database. *Nucleic Acids Res*. 28:117–8.

Dodge, J. D. 1973. *The Fine Structure of Algal Cells*. Academic Press, London, xii + 261 pp.

Dodge, J. D. & Crawford, R. M. 1971. A fine-structural survey of dinoflagellate pyrenoids and food-reserves. *Bot. J. Linn. Soc*. 64:105–15.

Dürr, G. 1979. Elektronenmikroskopische Untersuchungen am Panzer von Dinoflagellaten. II. *Peridinium cinctum*. *Arch. Protistenkd*. 122:88–120.

Eddy, S. 1930. The fresh-water armored or thecate dinoflagellates. *Trans. Am. Microsc. Soc*. 49:277–321.

Ehrenberg, C. G. 1838. *Die Infusionsthierchen als vollkommene Organismen. Ein Blick in das tiefere organische Leben der Natur*. Leopold Voss, Leipzig, Germany, 547 pp., 64 pls.

Felsenstein, J. 2008. *Phylogeny Inference Package (PHYLIP). Version 3.68*. University of Washington, Seattle. http://evolution.genetics.washington.edu/phylip.html (last accessed 17 June 2009).

Fensome, R. A., Taylor, F. J. R., Norris, G., Sarjeant, W. A. S., Wharton, D. I. & Williams, G. L. 1993. A classification of living and fossil dinoflagellates. *Micropaleontology*, Special Publication Number 7, 351 pp.

Guindon, S. & Gascuel, O. 2003. PhyML – a simple, fast, and accurate algorithm to estimate large phylogenies by maximum likelihood. *Syst. Biol.* 52:696–704.

Hansen, P. J. & Calado, A. J. 1999. Phagotrophic mechanisms and prey selection in free-living dinoflagellates. *J. Eukaryot. Microbiol*. 46:382–9.

Hansen, G. & Daugbjerg, N. 2004. Ultrastructure of *Gyrodinium spirale*, the type species of *Gyrodinium* (Dinophyceae), including a phylogeny of *G. dominans*, *G. rubrum* and *G. spirale* deduced from partial LSU rDNA sequences. *Protist* 155:271–94.

Hansen, G., Daugbjerg, N. & Henriksen, P. 2000. Comparative study of *Gymnodinium mikimotoi* and *Gymnodinium aureolum* comb. nov. (= *Gyrodinium aureolum*) based on morphology, pigment composition, and molecular data. *J. Phycol*. 36: 394–410.

Hansen, G., Daugbjerg, N. & Henriksen, P. 2007. *Baldinia anauniensis* gen. et sp. nov.: a 'new' dinoflagellate from Lake Tovel, N. Italy. *Phycologia* 46:86–108.

Hansen, G. & Flaim, G. 2007. Dinoflagellates of the Trentino Province, Italy. *J. Limnol*. 66:107–41.

Hickel, B. & Pollingher, U. 1988. Identification of the bloomforming *Peridinium* from lake Kinneret (Israel) as *P. gatunense* (Dinophyceae). *Br. Phycol. J.* 23:115–9.

Höll, K. 1928. Oekologie der Peridineen. Studien u¨ber den Einfluß chemischer und physikalischer Faktoren auf die Verbreitung der Dinoflagellaten im Süßwasser. *Pflanzenforschung* 11:I–VI. 1–105.

Horiguchi, T. 1995. *Heterocapsa circularisquama* sp. nov. (Peridiniales, Dinophyceae): a new marine dinoflagellate causing mass mortality of bivalves in Japan. *Phycol. Res*. 43:129–36.

Horiguchi, T. & Pienaar, R. N. 1988. Ultrastructure of a new sanddwelling dinoflagellate, *Scrippsiella arenicola* sp. nov. *J. Phycol*. 24:426–38.

Huber-Pestalozzi, G. 1950. Cryptophyceen, Chloromonadinen, Peridineen. *In* Thienemann, A. [Ed.] *Die Binnengewässer*, vol. 16. E. Schweizerbart'sche Verlagsbuchhandlung, Stuttgart, Germany, 310 pp.

Huitfeldt-Kaas, H. 1900. Die limnetischen Peridineen in norwegischen Binnenseen. *Vid. Selsk. Skr. [Christiania] Math. Naturv. Kl*. 2:1–7, 1 pl.

Imamura, K & Fukuyo, Y. 1990. *Peridinium penardiforme* Lindemann. In Fukuyo, Y., Takano, H., Chihara, M. & Matsuoka, K. [Eds.] *Red Tide Organisms in Japan – An Illustrated Taxonomic Guide*. Uchida Rokakuho, Tokyo, pp. 52–3.

Kiselev, I. A. 1954. Pirofitovye vodorosli. *In* Gollerbakh, M. M. & Polîànskiĭ, V. I. [Eds.] *Opredelitel' presnovodnykh vodorosleĭ SSSR*, vol. 6. Sovetskaîà Nauka, Moskva, p. 212.

Lauterborn, R. 1896. Diagnosen neuer Protozoen aus dem Gebiete des Oberrheins. *Zool. Anz*. 19:14–8.

Lauterborn, R. 1910. Die Vegetation des Oberrheins. *Verh. Naturh. Med. Ver. Heidelberg N.F.* 10:450–502.

Leadbeater, B. S. C. 1971. The intracellular origin of flagellar hairs in the dinoflagellate *Woloszynskia micra* Leadbeater & Dodge. *J. Cell Sci*. 9:443–51.

Lebour, M. V. 1925. *The Dinoflagellates of Northern Seas*. Marine Biological Association of the United Kingdom, Plymouth, UK, vii + 250 pp.

Lefèvre, M. 1926. ('1925') Contribution à la flore des Pèridiniens de France. *Rev. Algol*. 2:327–42, pls. XI–XII.

Lefèvre, M. 1932. Monographie des espèces d'eau douce du genre *Peridinium*. *Arch. Bot*. 2(Mémoire 5):1–210.

Lemmermann, E. 1900a. Beiträge zur Kenntniss der Planktonalgen. III. Neue Schwebalgen aus der Umgegend von Berlin. *Ber. Deutsch. Bot. Ges*. 18:24–32.

Lemmermann, E. 1900b. Beiträge zur Kenntniss der Planktonalgen. VIII. Peridiniales aquae dulcis et submarinae. *Hedwigia* 39:115–21.

Lemmermann, E. 1910. *Kryptogamenflora der Mark Brandenburg. Bd. 3. Algen I (Schizophyceen, Flagellaten, Peridineen).* Gebrüder Borntraeger, Leipzig, Germany, 712 pp.

Lewis, C. T. & Short, C. 1879. *A Latin Dictionary Founded on Andrews' Edition of Freund's Latin Dictionary*. Oxford University Press, Oxford, UK, xiv + 2019 pp.

Lindemann, E. 1919. Untersuchungen über Süßwasserperidineen und ihre Variationsformen. *Arch. Protistenk*. 39:209–62, pl. 17.

Lindemann, E. 1920. Untersuchungen u¨ber Su¨ßwasserperidineen und ihre Variationsformen II. *Arch. Naturg. Sec. A* 84:121–94.

Lindemann, E. 1924. Peridineen des Alpenrandgebietes. *Bot. Arch*. 8:297–303.

Lindemann, E. 1925a. Peridineen des Oberrheins und seiner Altwässer. *Bot. Arch*. 11:474–81.

Lindemann, E. 1925b. III. Klasse: Dinoflagellatae (Peridineae). *In* Schoenichen, W. [Ed.] *[Eyferth's] Einfachste Lebensformen des Tier- und Pflanzenreiches*, 5th ed., vol. 1, Spaltpflanzen, Geißellinge, Algen, Pilze. Hugo Bermühler Verlag, Berlin-Lichterfelde, Germany, pp. 144–95.

Lindemann, E. 1928. Vorläufige Mitteilung. *Arch. Protistenk*. 63: 259–60.

Lindström, K. 1991. Nutrient requirements of the dinoflagellate *Peridinium gatunense*. *J. Phycol*. 27:207–19.

Loeblich Jr., A. R. & Loeblich III, A. R. 1966. Index to the genera, subgenera, and sections of the Pyrrhophyta. *Stud. Trop. Oceanogr*. 3:i–ix, 1–94.

Maddison, D. R. & Maddison, W. P. 2003. *MacClade* 4. Sinauer Associates Inc., Publishers, Sunderland, Massachusetts.

Maki, T. & Imai, I. 2001. Relationships between intracellular bacteria and the bivalve killer dinoflagellate *Heterocapsa circularisquama* (Dinophyceae). *Fish. Sci.* 67:794–803.

McNeill, J., Barrie, F. R., Burdet, H. M., Demoulin, V., Hawksworth, D. L., Marhold, K., Nicolson, D. H., et al. [Eds.] 2006. *International Code of Botanical Nomenclature (Vienna Code), Adopted by the Seventeenth International Botanical Congress, Vienna, Austria, July 2005*. A.R.G. Gantner Verlag, Ruggell, Liechtenstein, xviii + 568 pp. (Regnum Vegetabile 146).

Messer, G. & Ben-Shaul, Y. 1969. Fine structure of *Peridinium westii* Lemm., a freshwater dinoflagellate. *J. Protozool*. 16:272–80.

Meunier, A. 1919. Microplankton de la Mer Flamande. 3me Partie. Les Péridiniens. *Mém. Mus. R. Hist. Nat. Belg*. 8:1–116, pls. 15–21.

Moestrup, Ø. 2000. The flagellate cytoskeleton. Introduction of a general terminology for microtubular flagellar roots in protists. *In* Leadbeater, B. S. C. & Green, J. C. [Eds.] *The Flagellates. Unity, Diversity and Evolution*. Taylor & Francis, New York, pp. 69–94 (Systematics Association Special Volume No. 59).

Moestrup, Ø. & Daugbjerg, N. 2007. On dinoflagellate phylogeny and classification. *In* Brodie, J. & Lewis, J. [Eds.] *Unravelling the Algae: The Past, Present, and Future of Algal Systematics*. CRC Press, Boca Raton, Florida, pp. 215–30 (Systematics Association Special Volume No. 75).

Moestrup, Ø., Hansen, G. & Daugbjerg, N. 2008. Studies on woloszynskioid dinoflagellates III: on the ultrastructure and phylogeny of *Borghiella dodgei* gen. et sp. nov., a cold-water species from Lake Tovel, N. Italy, and on *B. tenuissima* comb. nov. (syn. *Woloszynskia tenuissima*). *Phycologia* 47:54–78.

Moestrup, Ø., Hansen, G., Daugbjerg, N., Flaim, G. & d'Andrea, M. 2006. Studies on woloszynskioid dinoflagellates II: on *Tovellia sanguinea* sp. nov., the dinoflagellate responsible for the reddening of Lake Tovel, N. Italy. *Eur. J. Phycol*. 41:47–65.

Nylander, J. A. A. 2004. *MrModeltest v2*. Program distributed by the author. Evolutionary Biology Centre, Uppsala University, Uppsala, Sweden.

Olrik, K. 1992. Ecology of *Peridinium willei* and *P. volzii* (Dinophyceae) in Danish lakes. *Nord. J. Bot*. 12:557–68.

van de Peer, Y., van der Auwera, G. & De Wachter, R. 1996. The evolution of stramenopiles and alveolates as derived by ''substitution rate calibration'' of small ribosomal subunit RNA. *J. Mol. Evol*. 42:201–10.

Penard, E. 1891. Les Péridiniacées du Léman. *Bull. Trav. Soc. Bot. Genève* 6:1–63, pls, I–V.

Popovský, J. & Pfiester, L. A. 1990. Dinophyceae (Dinoflagellida). *In* Ettl, H., Gerloff, J., Heynig, H. & Mollenhauer, D. [Eds.] *Süßwasserflora von Mitteleuropa*, vol. 6. Gustav Fischer, Jena, Germany, 272 pp.

Reid, P. C. 1977. Peridiniacean and glenodiniacean dinoflagellate cysts from the British Isles. *Nova Hedwigia* 29:429–63.

Ronquist, F. & Huelsenbeck, J. P. 2003. MRBAYES 3: Bayesian phylogenetic inference under mixed models. *Bioinformatics* 19:1572–4.

Schiller, J. 1937. Dinoflagellatae (Peridineae) in monographischer Behandlung. *In* Kolkwitz, R. [Ed.] *Rabenhorst's Kryptogamenflora von Deutschland, Österreich und der Schweiz*, 2nd ed., vol. 10 (3). Part 2. Akademische Verlagsgesellschaft, Leipzig, Germany, 589 pp.

Schilling, A. J. 1913. Dinoflagellatae (Peridineae). *In* Pascher, A. [Ed.] *Süsswasser-Flora Deutschlands, Österreichs und der Schweiz*, vol. 3. Gustav Fischer, Jena, Germany, 66 pp.

Seo, K. S. & Fritz, L. 2002. Diel changes in pyrenoid and starch reserves in dinoflagellates. *Phycologia* 41:22–8.

Silva, E. S. & Franca, S. 1985. The association dinoflagellate-bacteria: their ultrastructural relationship in two species of dinoflagellates. *Protistologica* 21:429–46.

Skuja, H. 1930. ('1929') Süsswasseralgen von den westestnischen Inseln Saaremaa und Hiiumaa. *Acta Hort. Bot. Univ. Latv*. 4: 1–76, pls. I–III.

Spector, D. L. & Triemer, R. E. 1979. Ultrastructure of the dinoflagellate *Peridinium cinctum* f. *ovoplanum*. I. Vegetative cell ultrastructure. *Am. J. Bot*. 66:845–50.

Starmach, K. 1974. Cryptophyceae, Dinophyceae, Raphidophyceae. *In* Starmach, K. & Siemińska, J. [Eds.] *Flora Słodkowodna Polski*, vol. 4. Państwowe Wydawnictwo Naukowe, Warszawa, 520 pp.

Stein, F. 1878. *Der Organismus der Infusionsthiere nach eigenen Forschungen in systematischer Reihenfolge bearbeitet. III. Abtheilung. Die Naturgeschichte der Flagellaten oder Geisselinfusorien. I. Hälfte. Den noch nicht Abgeschlossenen allgemeinen Theil nebst Erklärung der sämmtlichen Abbildungen enthaltend*. Wilhelm Engelmann, Leipzig, Germany, 154 pp., 24 pls.

Stein, F. 1883. *Der Organismus der Infusionsthiere… III. Abtheilung. II. Hälfte. Die Naturgeschichte der arthrodelen Flagellaten. Einleitung und Erklärung der Abbildungen*. Wilhelm Engelmann, Leipzig, Germany, 30 pp., 25 pls.

Swofford, D. L. 2003. *PAUP* Phylogenetic Analysis Using Parsimony (*and Other Methods), version 4*. Sinauer Associates, Sunderland, Massachusetts.

Tamura, M., Iwataki, M. & Horiguchi, T. 2005. *Heterocapsa psammophila* sp. nov. (Peridiniales, Dinophyceae), a new sanddwelling marine dinoflagellate. *Phycol. Res*. 53:303–11.

Taylor, F. J. R. 1987. Dinoflagellate morphology. *In* Taylor, F. J. R. [Ed.] *The Biology of Dinoflagellates*. Botanical Monographs Volume 21. Blackwell Scientific Publ., Oxford, UK, pp. 24– 91.

Wall, D. & Dale, B. 1968. Modern dinoflagellate cysts and evolution of the Peridiniales. *Micropaleontology* 14:265–304.

West, G. S. 1909. A biological investigation of the Peridinieae of Sutton Park, Warwickshire. *New Phytol*. 8:181–96.

Wilgenbusch, J. C., Warren, D. L. & Swofford, D. L. 2004. AWTY: a system for graphical exploration of MCMC convergence in Bayesian phylogenetic inference. http://ceb.csit.fsu.edu/awty (last accessed 17 June 2009).

Wołoszyńska, J. 1952. Bruzdnice Tatr i Karpat Wschodnich (Peridineae montium Tatrensium et Carpathorum Orientalium). *Acta Soc. Bot. Pol*. 21:311–6, pls. I–XVII.

SUPPLEMENTARY MATERIAL

Figures S1 and S2, published online as supplementary material, were here reproduced in their natural position in the text.

Table S1. Alphabetic list of dinoflagellates included in the phylogenetic analyses. The ciliates comprising the outgroup are included below. Genbank accession numbers for the nuclear-encoded LSU rDNA sequences are given for each species.

Species name	GenBank number
Akashiwo sanguinea (Hirasaka) Gert Hansen et Moestrup	AF260396
Alexandrium margalefii Balech	AY154957
Baldinia anauniensis Gert Hansen et Daugbjerg	EF052683
Biecheleria pseudopalustris (J. Schiller) Moestrup, K. Lindberg et Daugbjerg	AF260402
Cryptoperidiniopsis brodyi Steidinger, Landsberg, P. L. Mason, Vogelbein, Tester et Litaker	DQ991380
Dinophysis norvegica Claparède et J. Lachmann	AY571375
Gonyaulax baltica Ellegaard, J. M. Lewis et I. Harding	AF260388
Gymnodinium catenatum H. W. Graham	AF200672
Gymnodinium fuscum (Ehrenberg) F. Stein	AF200676
Gymnodinium nolleri Ellegaard et Moestrup	AF200673
Gyrodinium dominans Hulburt	AY571370
Gyrodinium rubrum (Kofoid et Swezy) Y. Takano et T. Horiguchi	AY571369
Gyrodinium spirale (Bergh) Kofoid et Swezy	AY571371
Heterocapsa rotundata (Lohmann) Gert Hansen	AF260400
Heterocapsa triquetra (Ehrenberg) F. Stein	AF260401
Jadwigia applanata (CCAC0021) Moestrup, K. Lindberg et Daugbjerg	AY950447
Karenia brevis (C. C Davis) Gert Hansen et Moestrup	AF200677
Karenia mikimotoi (Miyake et Kominami ex Oda) Gert Hansen et Moestrup	AF200681
Karlodinium armiger Bergholtz, Daugbjerg et Moestrup	DQ114467
Karlodinium veneficum (D. Ballantine) J. Larsen	DQ114466

Lepidodinium chlorophorum (Elbrächter et Schnepf) Gert Hansen, Botes et de Salas	AF200669
Palatinus apiculatus (Ehrenberg) Craveiro, Calado, Daugbjerg et Moestrup (syn. *Peridinium palatinum*)	AF260394
Palatinus pseudolaevis (M. Lefèvre) Craveiro, Calado, Daugbjerg et Moestrup (syn. *Peridinium pseudolaeve*)	AF260395
Peridiniella catenata (Levander) Balech	AF260398
Peridiniopsis borgei Lemmermann	FJ236464
Peridiniopsis polonica (Wołoszyńska) Bourrelly	EF205010
Peridinium cinctum Ehrenberg	AF260385
Peridinium willei Huitfeldt-Kaas (strain: NEPCC815)	EF205012
Pfiesteria piscicida Steidinger et Burkholder	DQ991382
Pfiesteria piscicida Steidinger et Burkholder	AY112746
Pfiesteria-like CCMP 1828	AY590476
Prorocentrum micans Ehrenberg	AF260377
Pseudopfiesteria shumwayae Glasgow et Burkholder	AY245694
Scrippsiella trochoidea var. *aciculifera* Montresor	AF260393
Tovellia coronata (Wołoszyńska) Moestrup, K. Lindberg et Daugbjerg	AY950445
Tovellia sanguinea Moestrup, Gert Hansen, Daugbjerg, Flaim et D'Andrea	DQ320627
Outgroup	
Tetrahymena pyriformis (Ehrenberg) Lwoff	X54004
Tetrahymena thermophila Nanney et McCoy	X54512

CHAPTER 3

ULTRASTRUCTURE AND LSU RDNA-BASED PHYLOGENY OF *PERIDINIUM LOMNICKII* AND DESCRIPTION OF *CHIMONODINIUM* GEN. NOV. (DINOPHYCEAE)

Craveiro, S.C., Calado, A.J., Daugbjerg, N., Hansen, G. & Moestrup, Ø. (submitted to *Protist*). Ultrastructure and LSU rDNA-based Phylogeny of *Peridinium lomnickii* and Description of *Chimonodinium* gen. nov. (Dinophyceae). — *Inclusion in this thesis is not intended as effective publication of the new taxa proposed in the manuscript.*

ABSTRACT

Several populations of *Peridinium lomnickii* were examined by SEM and serial section TEM. Comparison with typical *Peridinium*, *Peridiniopsis*, *Palatinus* and *Scrippsiella* species revealed significant structural differences, congruent with phylogenetic hypotheses derived from partial LSU rDNA sequences. *Chimonodinium* gen. nov. is described as a new genus of peridinioids, characterized by the Kofoidian plate formula Po, cp, x, 4′, 3a, 7″, 6c, 5s, 5‴, 2⁗, the absence of pyrenoids, the presence of a microtubular basket with four or five overlapping rows of microtubules associated with a small peduncle, a pusular system with well-defined pusular tubes connected to the flagellar canals, and the production of non-calcareous cysts. Serial section examination of *Scrippsiella trochoidea*, here taken to represent typical *Scrippsiella* characters, revealed no peduncle and no associated microtubular strands. The molecular phylogeny placed *C. lomnickii* comb. nov. as a sister group to a clade composed of *Thoracosphaera* and the pfiesteriaceans. Whereas the lack of information on fine structure of the swimming stage of *Thoracosphaera* leaves its affinities unexplained, *C. lomnickii* shares with the pfiesteriaceans the presence of a microtubular basket and the unusual connection between two plates on the left side of the sulcus, involving extra-cytoplasmic fibres.

Key words: *Chimonodinium*; Dinophyceae; LSU rDNA; *Peridinium lomnickii*; phylogeny; *Scrippsiella trochoidea*; ultrastructure

Abbreviations: apc, apical pore complex; as, anterior sulcal plate; Ch, chloroplast; cp, cover plate; d, dictyosomes; E, eyespot; EV, elongated vesicle; f, fiber; LB, longitudinal basal body; LC, layered connective; LF, longitudinal flagellum; LFC, longitudinal flagellar canal; LMR, longitudinal microtubular root; ls, left sulcal plate; LSC, longitudinal striated collar; mt, mitochondria; N, nucleus; o, oil droplets; P, pyrenoid; pl, platelets; pp, pore plate; ps, posterior sulcal plate; PSC, peduncular striated collar; rs, right sulcal plate; SCc, striated collar connective; SMR, single microtubular root; T, trichocyst; TB, transverse basal body; TF, transverse flagellum; TFC, transverse flagellar canal; TMR, transverse microtubular root; TMRE, transverse microtubular root extension; TSC, transverse striated collar; TSR, transverse striated root; TSRM, transverse striated root microtubule; x, canal plate

INTRODUCTION

Peridinium lomnickii Wołoszyńska was originally described from ponds in the southeastern Polish region of Lwów (called Lemberg in the original German text), now Lviv, southwest Ukraine (Wołoszyńska 1916). The original description included mention of numerous chloroplasts and a central, oval nucleus. The report on the tabulation, combined with five drawings of the theca showing all major and some of the furrow plates, allow unambiguous identification of the species (Wołoszyńska 1916). A distinct preference for the winter period was noted for *P. lomnickii*, which attained its maximum development and formed blooms during the colder months (Wołoszyńska 1916, pp 264, 268).

Peridinium lomnickii has been reported from Europe, North America, Tasmania and Japan (Eddy 1930; Lefèvre 1932; Lewis and Dodge 2002; Ling et al. 1989; Senzaki and Horiguchi 1994). It was found abundantly in samples from shallow ponds shortly after thaw (Lindemann 1920, 1924) and was reported to occur mainly in cold waters with low organic content (Grigorszky et al. 2003b).

The current classification of *Peridinium* Ehrenberg, based on features of the theca, holds together species with and without an apical pore complex and with varying numbers of plates in epithecal and cingular Kofoidian series, while excluding species with a number of anterior intercalary plates smaller than two (Bourrelly 1970; Starmach 1974; Popovský and Pfiester 1990). The bulk of the excluded species possess an apical pore complex and are grouped in *Peridiniopsis* Lemmermann (Popovský and Pfiester 1990). Although plate arrangement in the furrows has been little used in the taxonomic organization of recent freshwater dinoflagellate floras (e.g. Lewis and Dodge 2002) the furrows are generally regarded as more conservative than other areas of the theca and formed the basis for the segregation of several marine genera (for a brief summary of the use in taxonomy of cingular plate number see Bourrelly 1968; Sournia 1986). The type species of *Peridinium*, *P. cinctum* (OF Müller) Ehrenberg, with five cingular plates and no apical pore, may therefore be more distantly related to *P. lomnickii* and other species of *Peridinium* and *Peridiniopsis* with six cingular plates and an apical pore than these species are among themselves. The ordering of *Peridinium* species into several distantly related groups in phylogenetic

hypotheses based on SSU and LSU rDNA analyses (Logares et al. 2007) likewise suggests the need for revising generic boundaries within the peridinioids if a taxonomy reflecting phylogeny is to be achieved. This should preferably be based on the combination of external morphology, internal fine structure and DNA-derived phylogenies of representatives of various peridinioid groups.

For decisions to be made concerning the taxonomic position of *P. lomnickii* its features must be compared in detail with the typical features of closely related peridinioid genera. Ultrastructural data including the character-rich flagellar base area are available for *P. cinctum* and the type species of *Peridiniopsis*, *P. borgei* Lemmermann (Calado et al. 1999; Calado and Moestrup 2002). In addition, species of the marine genus *Scrippsiella* Balech ex AR Loeblich have a thecal organization that closely matches that of *P. lomnickii*; however, available ultrastructural information on *Scrippsiella* species (Bibby and Dodge 1973, 1974; Gao et al. 1989; Gao and Dodge 1991; Kalley and Bisalputra 1971; Roberts et al. 1987) is insufficient to allow the comparison of critical features and we therefore add new observations on *S. trochoidea* (F Stein) AR Loeblich.

The partial LSU rDNA sequence of *Peridinium lomnickii* was added to the database of peridinioid sequences compiled in recent contributions for the revision of *Peridinium* and allied genera (Calado et al. 2009; Craveiro et al. 2009) and used for phylogeny reconstruction with maximum likelihood and Bayesian analysis methods.

RESULTS

Peridinium lomnickii - External morphology

Cells of *Peridinium lomnickii* were egg-shaped, very slightly flattened dorsoventrally (Figs 1A–D, 2A, 2B). The cingulum was nearly equatorial, with a minor downward shift at the distal end, and divided the theca into a larger helmet-shaped epitheca and a smaller, smoothly round hypotheca (Fig. 1A, 1B). The sulcus did not penetrate the epitheca and ended posteriorly a little beyond the ventral edge of the antapical plates (Figs 1A, 2A, 2B). Cell dimensions were similar in the populations studied, from Denmark, Portugal, Sweden and

Greenland, and mostly fell within the range of 27–38 µm long and 22–32 µm wide, with a length:width ratio of 1.0–1.2.

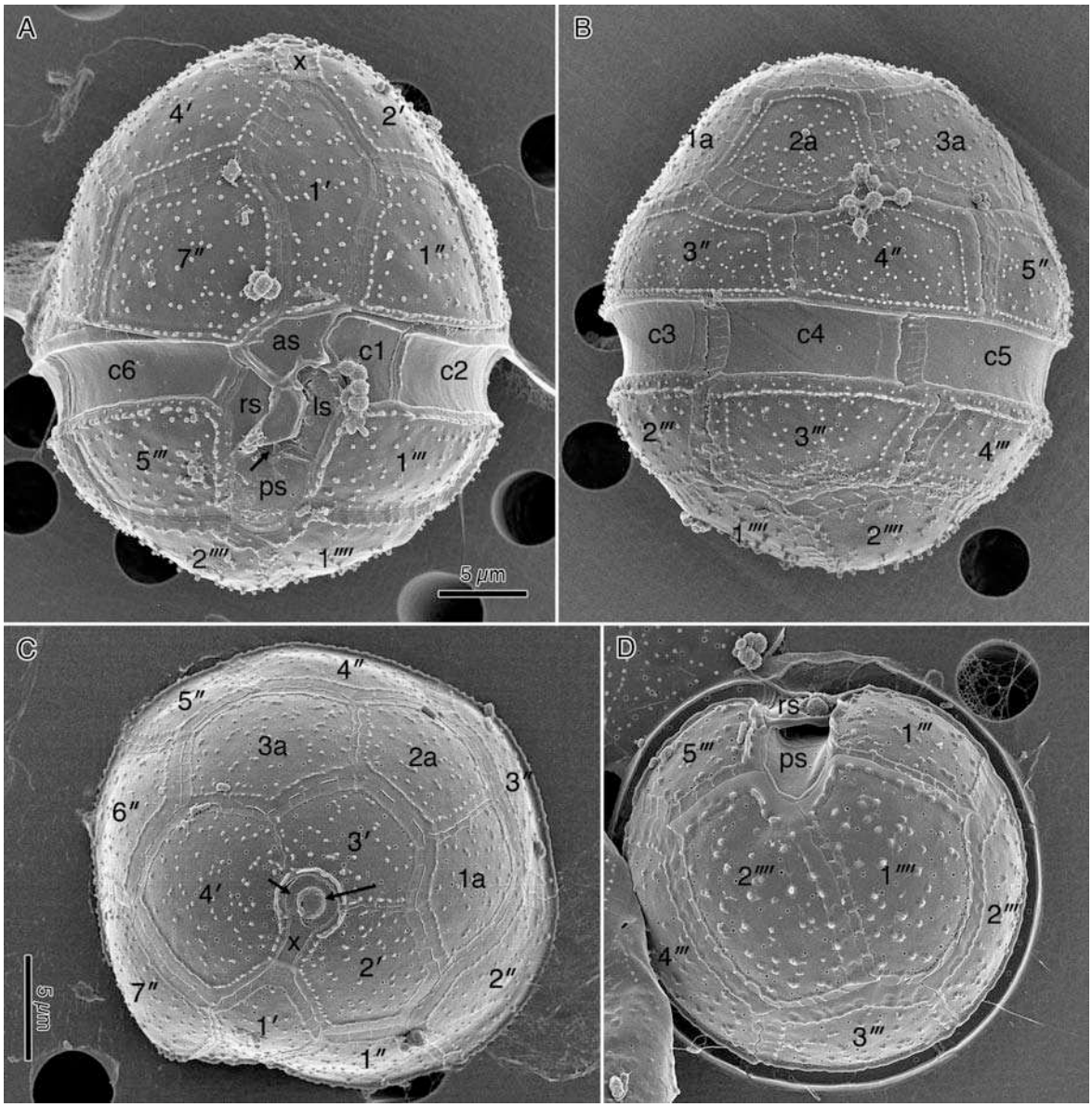

Fig.1. *Peridinium lomnickii*, SEM. Material from Sweden (A—C) and Greenland (D). The plates are marked in Kofoidian notation. **A**. Ventral view. The arrow points to the accessory plate in the sulcal region, partially covered by the right sulcal plate (rs) and x marks the canal plate near the apex. **B**. Dorsal view. Scale bar as in A. **C**. Apical view showing the apical pore complex with the canal plate (x) indenting the pore plate (small arrow) on the ventral side. The long arrow points to the rim around the cover plate. **D**. Antapical view. Scale bar as in C.

Tabulation was the usual for this species. The arrangement of the epithecal plates was roughly symmetrical, with a slight clockwise twist of the four apical plates imposed by the larger size of plate 3a relative to the other two intercalary plates, as seen in apical view (Fig. 1C). Three platelets made up the apical pore complex; the canal plate (marked x in Fig. 1C) deeply notched the ventral side of the circular pore plate, and a distinct rim surrounded the cover plate that obstructed the pore (Fig. 1C). The cingulum contained six plates, of which the small c1 impinged on the left side of the anterior sulcal area (Figs 1A, 1B, 2A, 2B). Five plates were visible in the sulcus; four larger plates occupied anterior, posterior, left and right of the sulcal area and a small platelet was just visible between the right, left and posterior sulcal plates (Figs 1A, 2A, 2B). The left side of the right sulcal plate was raised in a flap-like extension covering the middle part of the sulcus (Figs 1A, 1D, 2B).

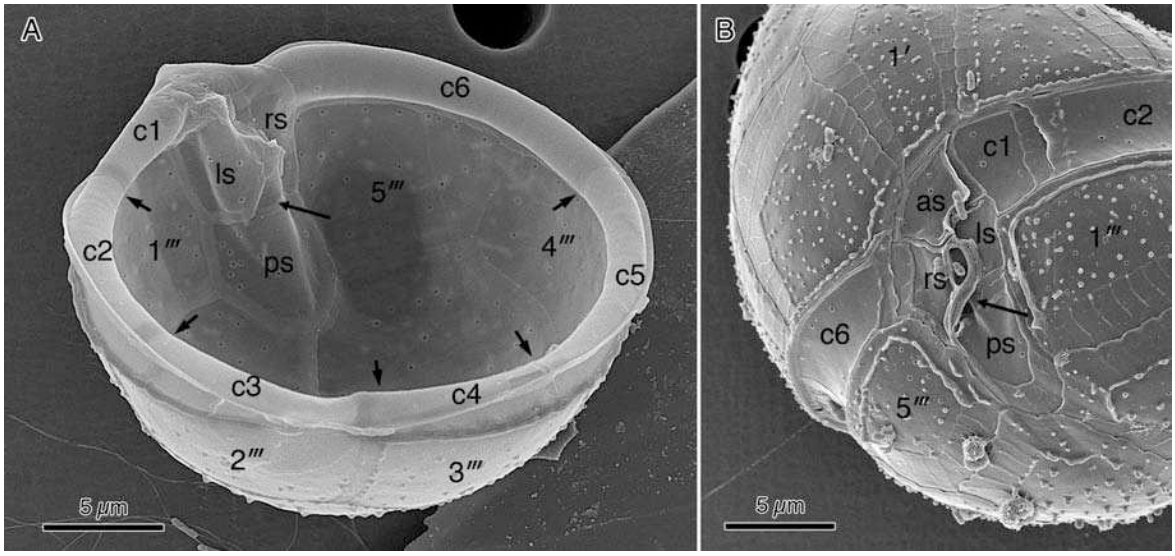

Fig. 2. *Peridinium lomnickii*, SEM. Material from Greenland (A) and Sweden (B). The long arrow in both images points to the small sulcal accessory plate. **A**. Internal view of the hypotheca. Small arrows indicate the five sutures separating the six cingular plates (c1-c6). **B**. Ventral view of the sulcal region.

The surface of all major plates, both in the epitheca and in the hypotheca, was ornamented with small, conical or somewhat capitate spines that were uniformly scattered in the middle and arranged in rows along the edges of plates,

especially those bordering the furrows. The spines were more prominent in the hypotheca, sometimes reaching over 0.5 µm in the antapical plates (Figs 1A–D, 2B). Plates of the apical pore complex, and cingular and sulcal plates were smooth. Circular perforations some 140 nm in diameter were randomly distributed on all thecal plates except in the apical pore complex (Figs 1A–D, 2A, 2B). Sutures between the plates ranged from narrow up to 4 µm wide and showed thin cross-striations with a 0.5–1 µm spacing (Figs 1B, 2B).

Ecdysed thecae broke up regularly along the anterior edge of cingulum and sulcus, sometimes remaining attached along the sulcus-epitheca boundary (Fig. 1A). An intact hypotheca with cingulum and sulcus in place is shown in Fig. 2A.

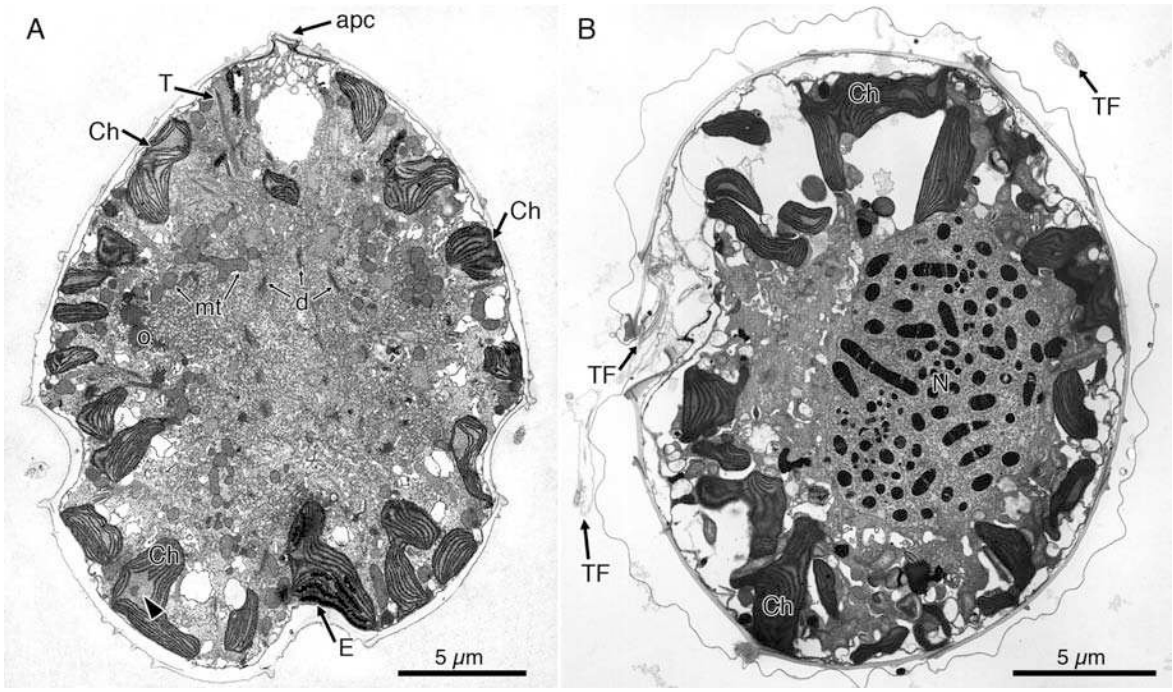

Fig. 3. *Peridinium lomnickii*, TEM. General views, showing the results of two different fixation protocols. **A**. Longitudinal section, viewed from the dorsal side, showing the location near the cell surface of chloroplast lobes (Ch), some with thylakoid-free areas (arrowhead), the eyespot (E) in the sulcal region, the apical pore complex (apc), and dictyosomes (d) and mithocondria profiles (mt) in the central region. Few oil droplets (o) can be seen in the epicone. T, trichocyst. Cell fixed initially with a mixture of 1% glutaraldehyde and 0.5% osmium tetroxide **B**. Transverse section at cingulum level (apical view), near the emergence point of the transverse flagellum (TF), showing the dorsal location of the nucleus (N) and the distribution of chloroplast lobes (Ch). Initial fixation with 2% glutaraldehyde alone.

General internal fine structure

As seen in axial longitudinal and transverse sections of the cells, the chloroplast network was restricted to the peripheral cytoplasm whereas the central part displayed abundant dictyosomes, small vesicles and mitochondrial profiles (Fig. 3A, 3B). Although thylakoid-free areas were visible in some chloroplast lobes no distinct pyrenoids were found.

The ellipsoid nucleus was located at cingulum level on the dorsal-left side of the cell (Fig. 3B). Oil droplets were visible mainly in the epicone and a few starch grains in the hypocone (not shown). Vesicles with disorganized contents (so-called accumulation bodies) were present in the epicone of all cells examined (not shown). Trichocysts were common in the peripheral cytoplasm (Fig. 3A).

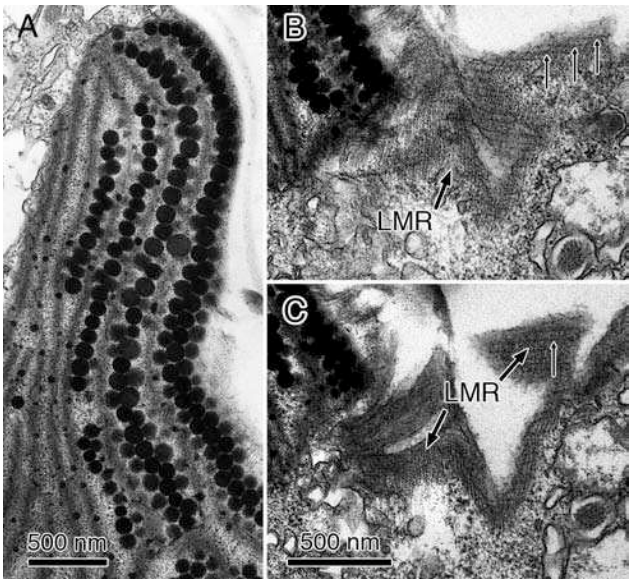

Fig. 4. *Peridinium lomnickii*, TEM. Eyespot region. **A**. Eyespot-containing choroplast lobe, with four rows of globules intercalated with thylakoids. **B** and **C**. Adjacent, grazing longitudinal sections through the sulcal region showing a cross-striation (thin arrows) on the surface of the longitudinal microtubular root (LMR). Both to the same scale.

An eyespot was located underneath the right-hand side of the sulcus (seen in dorsal view in Fig. 3A). It was contained in a chloroplast lobe and consisted of four or five layers of globules intercallated with thyllacoid lamellae (Fig. 4A). Individual globules were 80–150 nm in diameter and the midlines of adjacent

layers were 190–240 nm apart. The eyespot was overlaid with the microtubules of the longitudinal multistranded root 1, which displayed thin cross-lines in this area (Fig. 4B, 4C).

The ventral area, near the insertion of the flagella, showed striated fibres, microtubules and pusular elements in the form of convoluted tubes wrapped in a vesicle (Fig. 5A, 5B). The proximal parts of the emergent flagella were contained in a tube-like area limited externally by the flap-like extension of the right sulcal plate, which attached by means of extra-cytoplasmic fibres to the middle of the left sulcal plate (Fig. 5A, 5C).

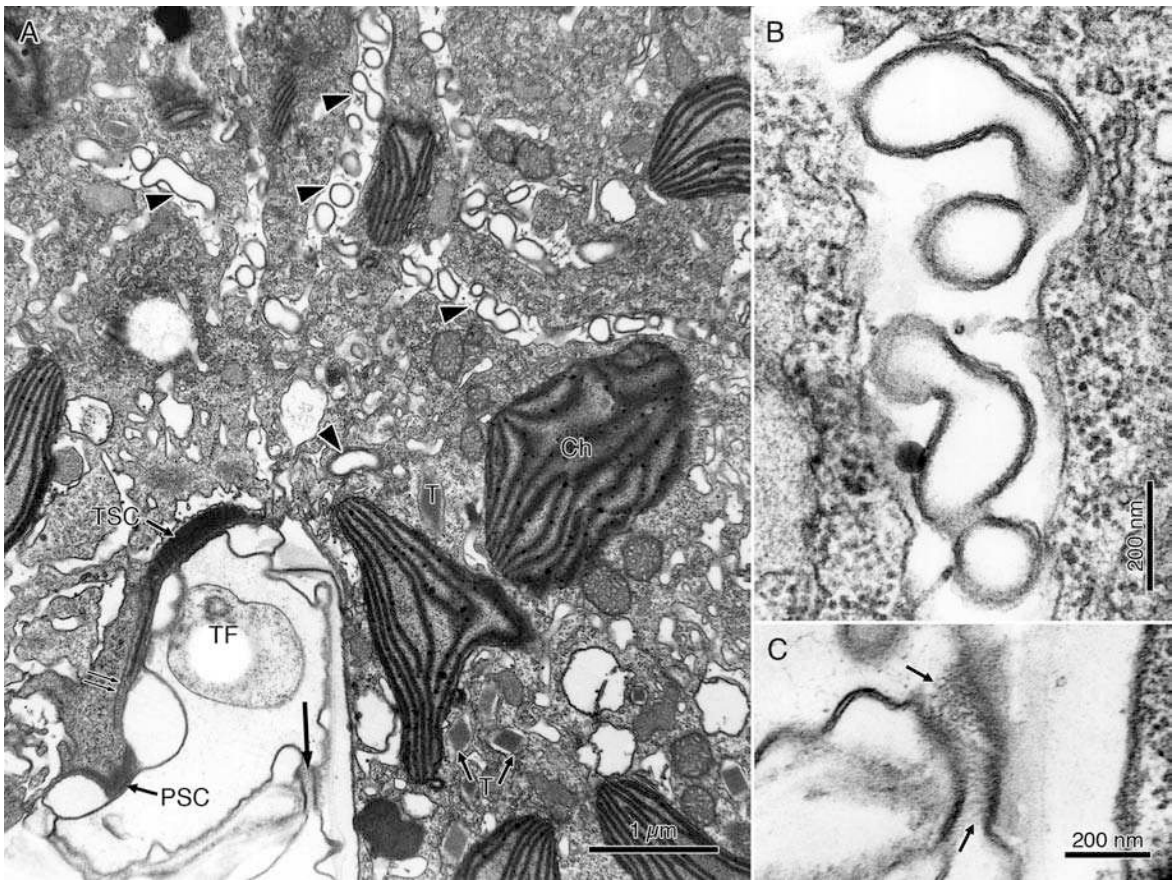

Fig. 5. *Peridinium lomnickii*, TEM. **A**. Approximately ventral view showing the convoluted pusular tubes (arrowheads). One row of microtubules of the microtubular basket (double arrow) and the peduncle striated collar (PSC) are visible on the bottom-left part of the image. A tubular area surrounds the proximal part of the transverse flagellum (TF), closed externally by a connection between the plasmalemma at the edge of a sulcal plate and near the middle of another (long arrow). **B**. Higher magnification of a pusular tube and its envelopping vesicle. **C**. Detail of the thin fibres (arrows) making the connection indicated in A.

Apical fibrous complex

The apical fibrous complex consisted of a group of fibres and an apparently continuous fibrous layer underlying the apical pore complex (Fig. 6A–E). Proceeding from ventral to dorsal, a group of parallel fibres extended for about 1.5 µm, increasing in number from a single fibre near the mid-ventral edge of plate x (Fig. 6A) to a seemingly continuous layer underneath the pore plate (Fig. 6B–E). A single fibre ran under the ventral-dorsal axis of the cover plate (Fig. 6C), converging with the fibrous layer under the pore plate on the ventral side and terminating near the middle of the cover plate. The dorsal side of the suture between the cover and pore plates was underlain by a curved fibre (not shown). Amphiesmal vesicles (or perhaps only one) were present between the cover and pore plate amphiesmal vesicles, and formed a rim around the cover plate (Fig. 6C).

In the apical region the cytoplasm was rich in 0.3–0.4 µm globose vesicles with 0.8–1 µm long tubular connections to the cover and pore plate amphiesmal vesicles (Fig. 6C). A larger vesicle was found beneath the apical region in one cell (Fig. 3A).

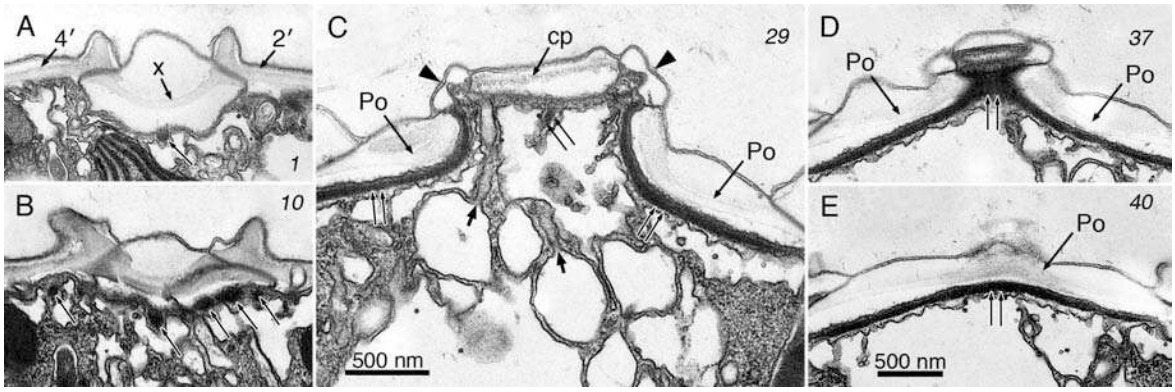

Fig. 6. *Peridinium lomnickii*, TEM. Apical pore complex. Longitudinal serial sections proceeding toward the dorsal side of the cell. The small slanted numbers refer to the section number. **A**. The canal plate (x) is seen between apical plates two and four. A single fibre is visible in cross section (arrow) under the canal plate. **B**. A larger number of fibres underlying the dorsal edge of the canal plate (arrows). **C**. Section through the cover plate (cp) and the pore plate (Po). The amphiesmal vesicle forming the rim that surrounds the cp is indicated by arrowheads. Fibres underlying the pore plate and the middle of the cover plate are marked with double arrows. Several vesicles with

tubular extensions converging toward the cp are marked with short arrows. **D** and **E**. Fibres on the dorsal edge of the cp and underneath the Po (double arrows). A, B, D and E to the same scale.

Peduncle and supporting microtubules

The relative position of basal bodies and roots, peduncle and supporting microtubules, and fibrous material making up collars and connectives is shown schematically in left view in Fig. 7.

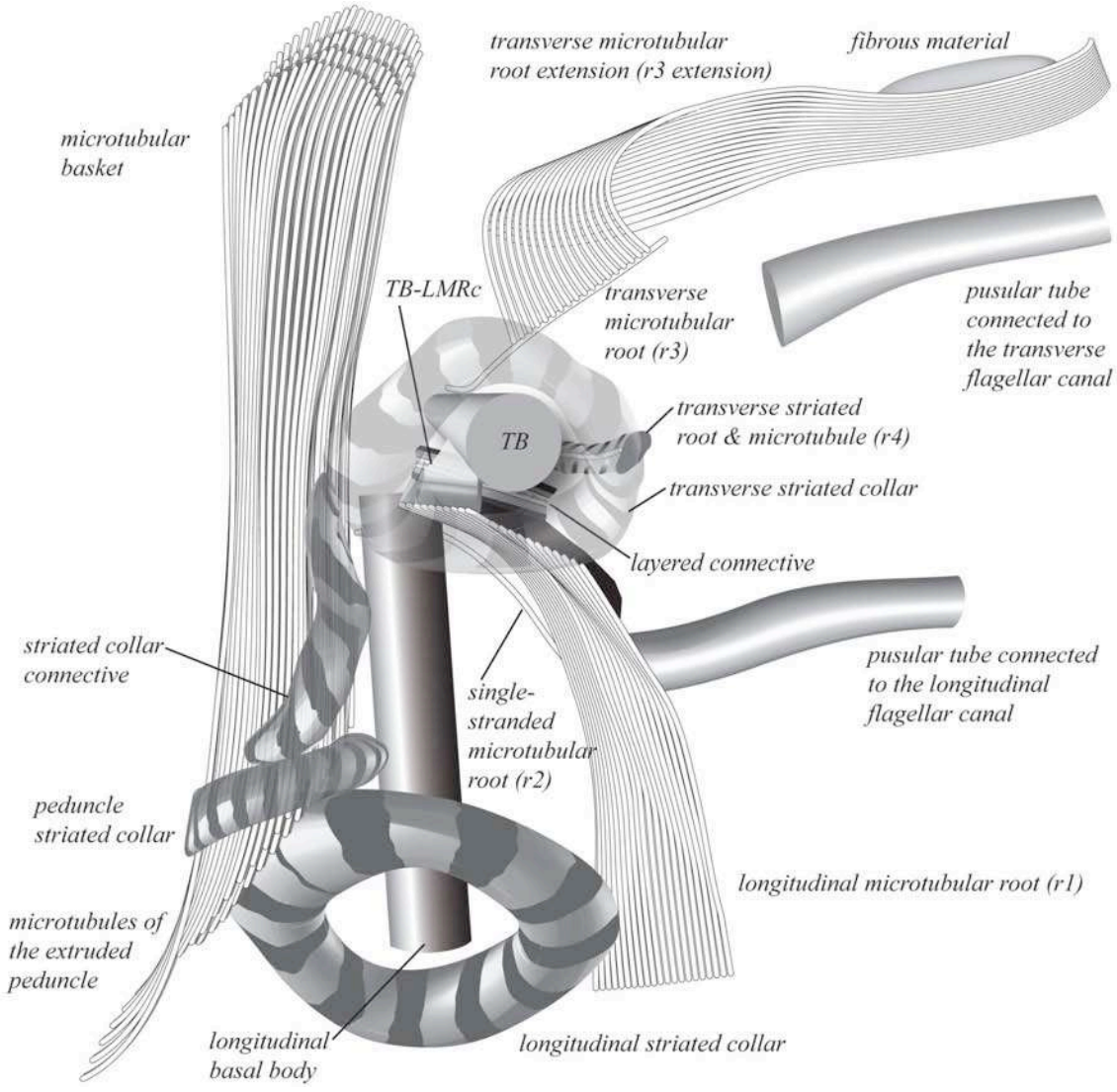

Fig. 7. Schematic reconstruction of the flagellar apparatus, microtubular basket and pusular tubules of *Peridinium lomnickii*, as seen from the left side of the cell (TB, transverse basal body). The transverse and peduncle striated collars, and the fibrous connective between them are rendered transparent to show underlying structures.

Fig. 8. *Peridinium lomnickii*, TEM. Peduncle area. **A**. Emergence area of the peduncle seen from dorsal-left. TF, transverse flagellum. **B–D**. Non-adjacent, longitudinal serial sections from a different cell viewed with a similar perspective. Small slanted numbers indicate the section number. A small peduncle formed by cytoplasm and microtubules (arrow) and limited by a single membrane extends through the peduncle striated collar (PSC). A striated collar conective (SCc) links the transverse striated collar (TSC) and the PSC. The supporting microtubules continue within the cytoplasm parallel to the collars and connective (arrow).

A small peduncle some 800 nm long and 350-600 nm wide protruded from the cytoplasm roughly between the two flagellar canal openings. This cytoplasmic extension was lined by a single membrane and contained one or two rows of microtubules. A complete ring of fibrous material (peduncle striated collar, PSC) surrounded the base of the peduncle and was linked to both flagellar striated collars by fibrous extensions (Figs 7, 8A–D). The small peduncle was only detected in sections of material initially fixed in a mixture containing osmium

tetroxide and always appeared surrounded by sulcal plates (Figs 5A, 8A). The microtubules extended internally forming a so-called microtubular basket (MB) composed of four or five parallel rows of microtubules (Figs 7, 9A–D). Each microtubular row was composed of 8–25 microtubules (most commonly 15) and the MB had a total of 55–70 microtubules (Fig. 9E). Although vesicles were absent from the extruded peduncles examined, conspicuous elongated vesicles (EV) extended from near the peduncle base along the MB, widening from little more than a microtubular width to near 100 nm in their proximal portion (Fig. 9A–D).

Fig. 9. *Peridinium lomnickii*, TEM. Microtubular basket (peduncle-related microtubules). Same series of sections as Fig. 8B–D (except the insert E). Small slanted numbers refer to the section

number. **A–C**. Four rows of microtubules (arrows) parallel to a group of elongated vesicles (EV). All to the same scale. **D**. The microtubules (arrow) and the elongated vesicles (EV) diverge as they continue toward the inner cytoplasm of the epicone. **E**. Transverse section through the inner portion of the microtubular basket of another cell, some 12 µm away from the area of emergence of the peduncle, showing five nearly parallel rows of microtubules.

Vesicles and microtubules extended along the ventral surface toward the apex for about 2 µm before curving into the apical part of the cytoplasm; some 5 µm further into the cell the EV diverged slightly toward the cell's right and terminated without any obvious connection to another structure (Fig. 9). Electron-opaque material lining the inside of the wider portions of the vesicles is visible in Fig. 9 C. The four or five rows of the MB continued in an apical-dorsal direction for another 6 µm or so, apparently with a more windy path, and ended near the anterior side of the nucleus without visibly associating with any structure. Accumulation bodies were present near the proximal part of the MB (not shown).

Flagellar apparatus

The arrangement of the flagellar apparatus is shown in serial sections with a dorsal-right to ventral-left orientation in Figs. 10 and 11. Some flagellar roots are shown in different orientations in Figs. 12 and 13.

The basal bodies formed an angle of 85-90º, with the proximal end of the transverse basal body (TB) slightly overlapping the proximal end of the longitudinal basal body (LB) (Fig. 7). Each flagellum emerged from the cytoplasm into a so-called flagellar canal, a surface depression lined by a single membrane and limited externally by a ring of fibrous material (Figs 7, 8C–D).

A row of microtubules contacted obliquely with the left base of the LB and extended underneath the sulcus toward the antapex (Figs 7, 10, 11A–D). The number of microtubules in this longitudinal microtubular root (LMR; designated r1 in Moestrup 2000) increased from about 10 near the LB (Fig. 11D) to about 35 more distally (Fig. 10C). The proximal end of the LMR was partly lined on the dorsal side by an electron-opaque layer 60 nm thick, from which thin fibres stretched out for about 120 nm toward the posterior-proximal surface of the TB (Figs 7, labelled TB-LMRc; 11D, double arrow). Right below this TB-LMR connective a more extensive layer of electron-opaque material covered the dorsal

surface of the LMR, extended across the base of the LB and connected with the posterior face of the so-called layered connective (LC) (Figs 10C–D, 11A–C).

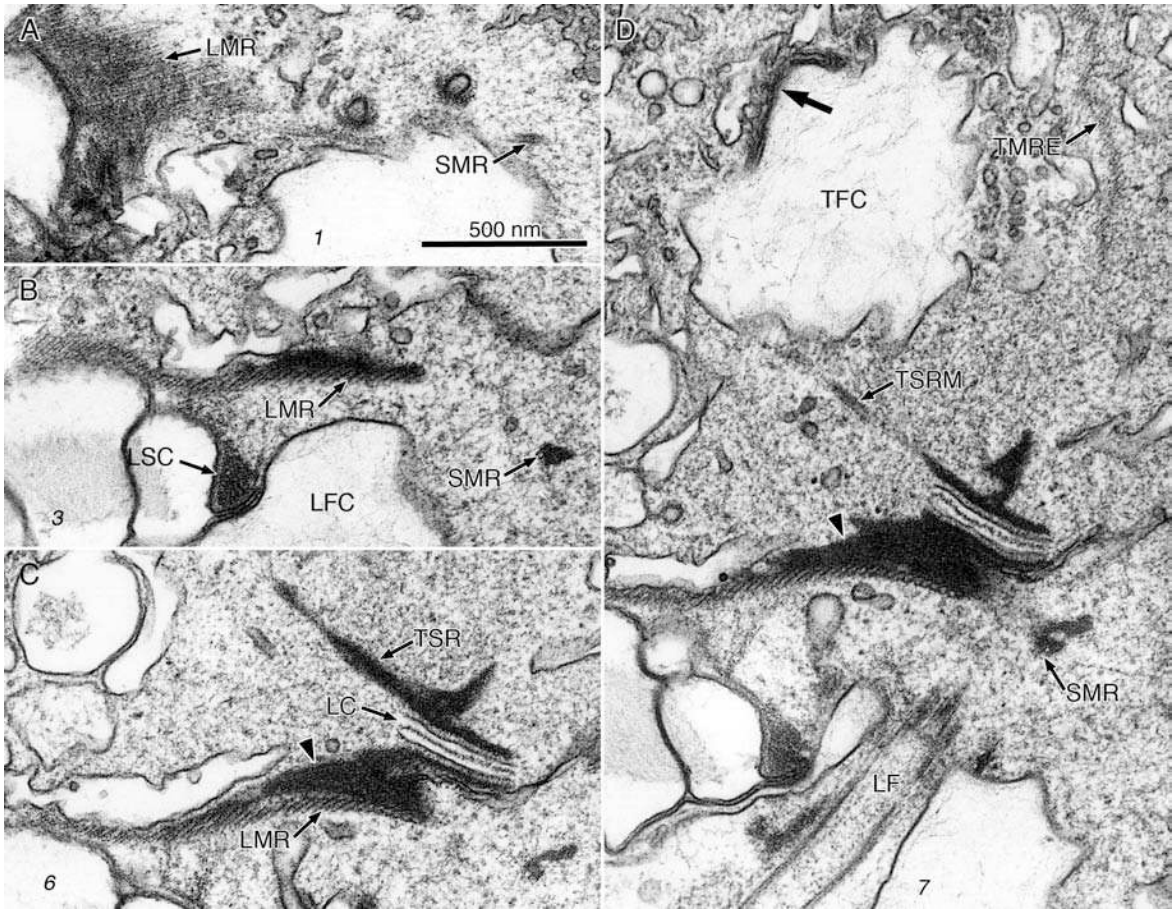

Fig. 10. *Peridinium lomnickii*, TEM. Flagellar apparatus. **A–D**. Non-adjacent, nearly longitudinal serial sections proceeding toward the ventral side of the cell, in dorsal view. Small slanted numbers refer to the section number. All to the same scale. The single-stranded microtubular root (SMR) follows a path roughly parallel to the longitudinal microtubular root (LMR) and is visible in all sections. Electron-opaque material covering the dorsal side of the LMR is indicated in C and D (arrowhead). A pusular tube (marked with an arrow in D) connects with the transverse flagellar canal (TFC). LC, layered connective; LF, longitudinal flagellum; LFC, longitudinal flagellar canal; LSC, longitudinal striated collar; TMRE, the transverse microtubular root extension; TSR, transverse striated root; TSRM, microtubule of the transverse striated root.

When seen in cross-section (i.e., in longitudinal sections of the cell) the layered connective was approximately 160 nm thick, with an electron-translucent inner part some 50 nm thick limited by two distinct electron-opaque layers, each thinner than

a unit membrane, and with a distinct layer of less compact electron-opaque material along the middle; two 30-nm layers of electron-opaque material formed the anterior and posterior limits of the LC, apparently linked by bands of 20-nm long fibres to the inner part of the structure (Figs 10C, 10D, 11A, 11B).

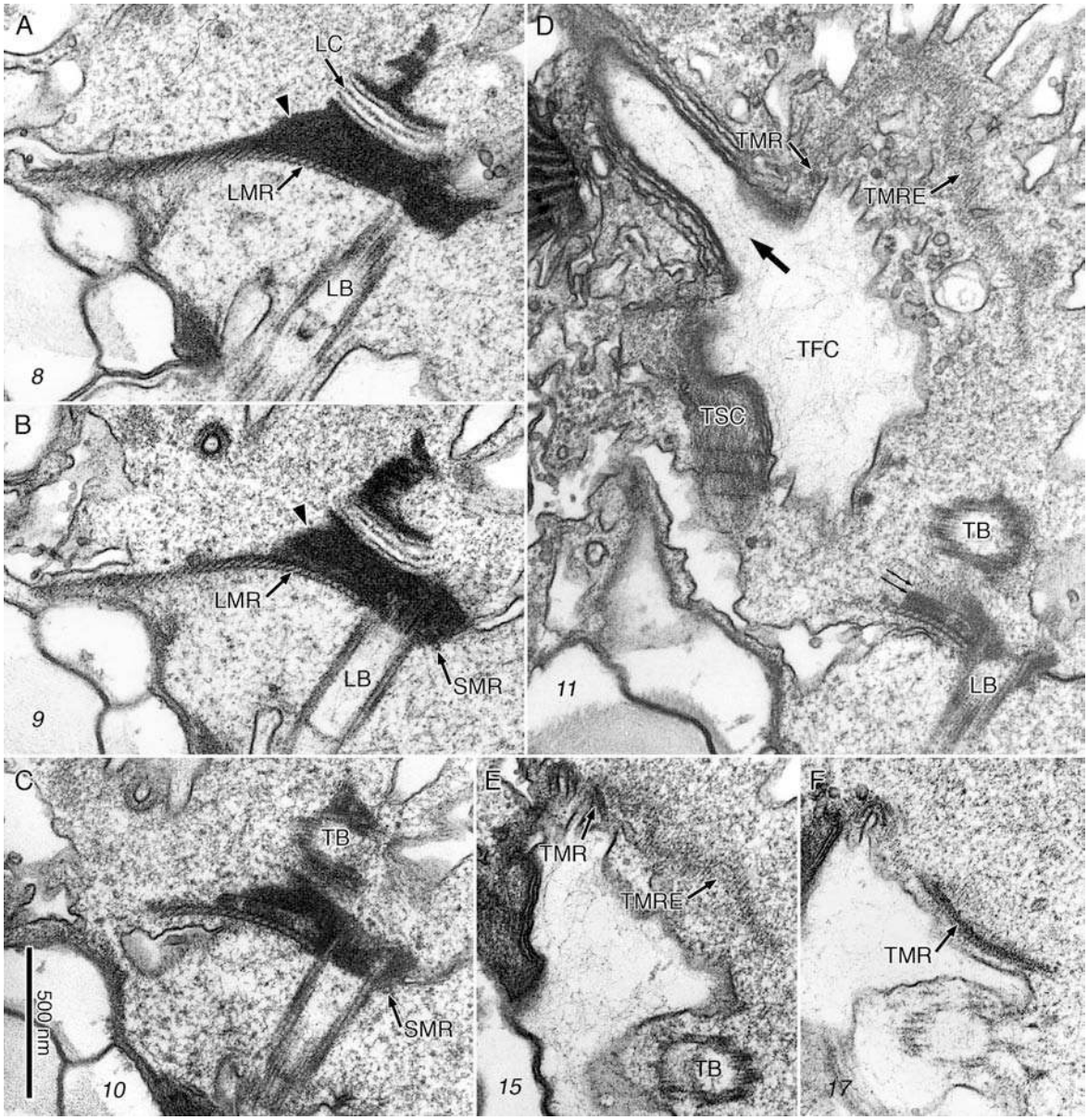

Fig. 11. *Peridinium lomnickii*, TEM. Flagellar apparatus. **A–F**. Continuation of the series of sections shown in Fig. 10. Small slanted numbers refer to the section number. All to the same scale. The single-stranded microtubular root (SMR) ends in the right-proximal side of the longitudinal basal body (LB), in an almost perpendicular orientation in relation to it (C). The electron-opaque material (arrowheads in A and B) on the dorsal side of the longitudinal microtubular root (LMR) connects

with the layered connective (LC). A pusular tube (arrow) connecting with the transverse flagellar canal (TFC) and a connective between the LMR and the transverse basal body (TB) (double arrow) are seen in D. The transverse microtubular root (TMR) and the microtubules which it nucleates (TMRE) are visible in D–F.

The LC extended for ca. 400 nm along the left-right axis of the cell and slightly less along the ventral-dorsal axis. The anterior electron-opaque layer of the LC was continuous with similar-looking material extending around the base of the TB (Figs 10C, 10D, 11A–C).

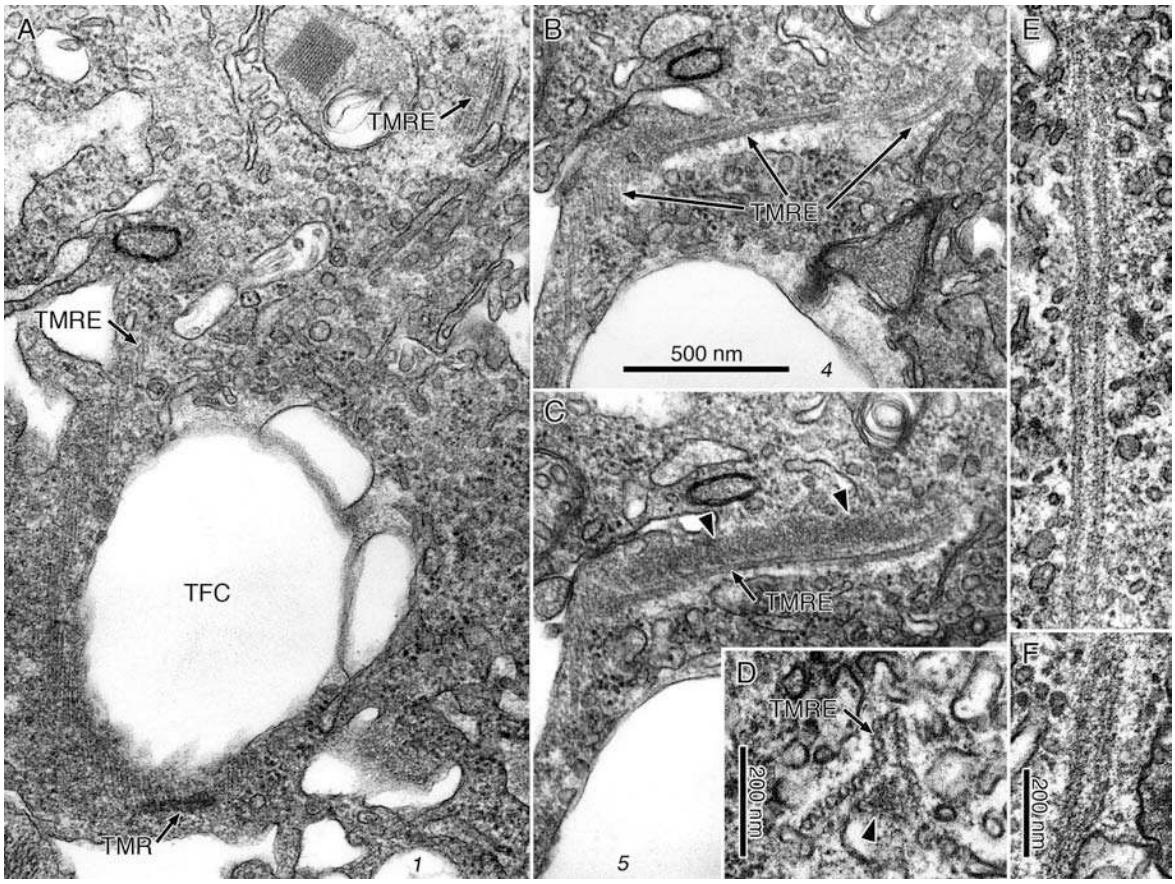

Fig. 12. *Peridinium lomnickii*, TEM. Flagellar apparatus, transverse microtubular root extension (TMRE). **A–C**. Non-adjacent, transverse serial sections, in apical view, of the transverse microtubular root (TMR) and TMRE. The TMR is seen in A, ventral to the transverse flagellar canal (TFC). The TMRE extends along the right side of the TFC toward the back of the cell and then curves to the cell's left. In the dorsal side of the LFC the dorsal face of the TMRE associates with fibrous material (arrowheads). Small slanted numbers refer to the section number. All to the same scale. **D–F**. Three different aspects of the TMRE in longitudinal sections of the same cell. In D the

TMRE is seen in cross section with the microtubules forming an open ring wrapped around fibrous material (arrowhead), some 3 µm from the basal body area. An approximately longitudinal section of the TMRE is shown in E. In the oblique view shown in F the TMRE seems to form a closed ring. E and F are about 5 µm away from the basal body area. A–C and E to the same scale.

A single-stranded microtubular root (SMR; r2 in Moestrup 2000) associated obliquely with the right side of the LB, extended parallel to the LMR for about 1 µm, and terminated near the connection between a pusular tube and the longitudinal flagellar canal (Figs 7, 10A–D, 11A–C).

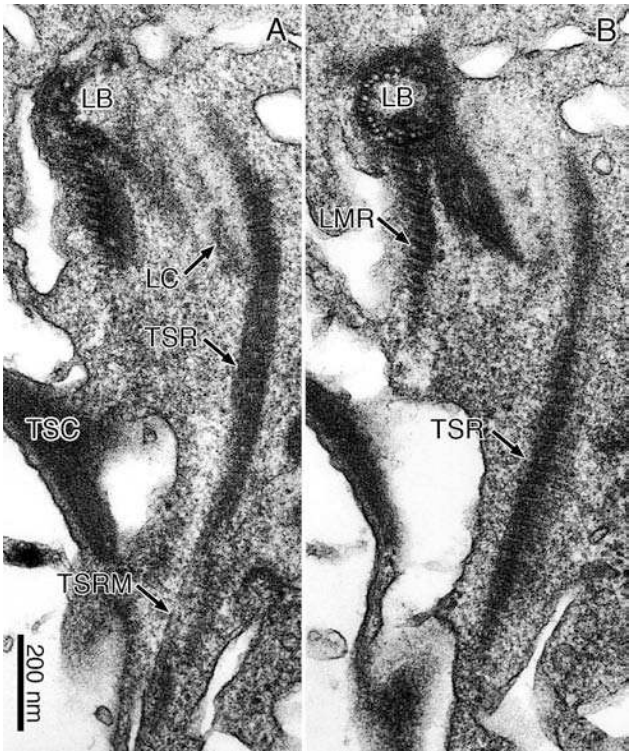

Fiig. 13. *Peridinium lomnickii*, TEM. Flagellar apparatus, transverse striated root (TSR). **A** and **B**. Apical view of adjacent transverse sections, somewhat tilted to show the longitudinal basal body (LB) in cross section. The transverse striated root microtubule (TSRM) is visible along the TSR. LC, layered connective; LMR, longitudinal microtubular root; TSC, transverse striated collar. Both figures to the same scale.

Another root initially composed of a single microtubule extended from the anterior surface of the TB and gradually curved upward and around the ventral-right side of the transverse flagellar canal (TFC) for some 700 nm; this transverse

microtubular root (TMR; r3 in Moestrup 2000) then slightly descended on the oposite side of the TFC, along a row of collared pits, and terminated near the emergence of a pusular tube (Figs 7, 11D–F). An extension of about 20 microtubules started at the distal part of the TMR, curved around the anterior surface of the TFC and bent toward the dorsal side, where the microtubules associated with fibrous material (Figs 7, 11D–F, 12A–D). The extension microtubules continued beyond this point for some 5 µm in the anterior direction and eventually terminated near an accumulation body and the proximal end of the MB (not shown). In the distal tract of the TMR-extension the microtubular strand closed into a flat ring and the associated fibre was no longer visible (Fig. 12E, 12F).

A striated fibre (transverse striated root, TSR) associated with the anterior layer of the LC and the proximal-posterior end of the TB, and extended along the dorsal side of the transverse striated collar (TSC) for up to 1.3 µm, toward the cell's left (Figs 7, 13A, 13B). A single microtubule (TSRM; r4 in Moestrup 2000) accompanied the TSR for most of its length (Figs 10D, 13A), but diverged from it near the proximal end (not shown).

Pusular system

The general aspect of the pusular system in the ventral area is shown in Fig. 5. The pusular elements were tubular membrane-bounded compartments wrapped in a vesicle (Fig. 5B). A single tube opened at each flagellar canal (Fig. 7). The three pusular membranes were close together in the nearly straight segment that connected with each flagellar canal (Figs 10D, 11D, arrow). The tubes had an inner diameter of about 190 nm in this part. After some 1.5 µm the tubes became extensively bent and the wrapping vesicle became wider (Fig. 5A, 5B). The pusular tube attached to the TFC extended roughly to the ventral-left, whereas the tube linked to the LFC went to the dorsal-right side of the cell. In their terminal, inner parts the tubes seemed to flatten out and were perhaps ramified (Fig. 9D).

Cyst morphology

Peridinium lomnickii cysts (examined mainly from culture SCCAP K-1151) were 30–35 µm long and 24–29 µm wide, with roughly the same shape as the

motile cell. A strong wall, nearly 1.5 µm thick, was apparent beneath the theca of recently-formed cysts (Fig. 14A, 14B). Cyst contents were generally colourless except for a red body usually present in the middle of the epicone (Fig. 14B, arrow).

Scrippsiella trochoidea: Cyst morphology

Cysts of the strain of *Scrippsiella trochoidea* examined are shown in Fig. 14C–E. They were ovoid, 39–41(–49) µm long and 27–29 µm wide, with a calcareous outer wall furnished with generally triangular spines with irregular bases and pointed or blunt tips (Fig. 14C, 14E). The contents were colourless except for the presence of a red body (Fig. 14D, arrow).

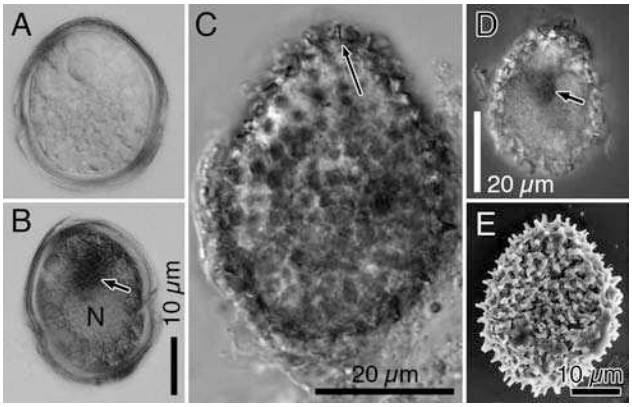

Fig. 14. Cysts of *Peridinium lomnickii* from Sweden (A–B) and of *Scrippsiella trochoidea* (C–E) from culture KF2N16. **A** and **B**. Light micrographs of two cysts with thick, unornamented wall. The cyst in B shows a dark red body (arrow) and the nucleus (N). Both images to the same scale. **C** and **D**. Light micrographs of calcareous cysts with triangular spines (long arrow in C) and a red body (short arrow in D). **E**. SEM of an ovoid calcareous cyst.

Fine structure of motile cells

Cells were ovoid with a round hypocone and a conical epicone. General fine-structural features are shown in longitudinal and transverse sections in Fig. 15A and 15B, respectively. Chloroplast profiles, few in number but relatively large, lined most of the cell surface; thylakoid-free chloroplast areas were visible here and there and at least two larger, starch-covered pyrenoids projected inward from the peripheral lobes (Fig. 15A, 15B). The pyrenoids were penetrated by tubular, membrane-bounded structures, single or paired, that seemed to be continuous

with thylakoids (Fig. 15F, 15G). An eyespot up to 1.5 µm long, composed of 1–2 rows of globules, was present in a chloroplast lobe in the sulcal region (Fig. 15E). Longitudinal sections through the cell apex showed thin fibres flanking the slightly projecting apical pore region (Fig. 15C, f). The nucleus was located at the central-dorsal part of the cell, at cingulum level (Fig. 15B). A large part of the right mid-ventral cytoplasm was occupied by the pusule, composed of tubular and flattened, ramified vesicles that radiate from the flagellar base area (Fig. 15B, 15D).

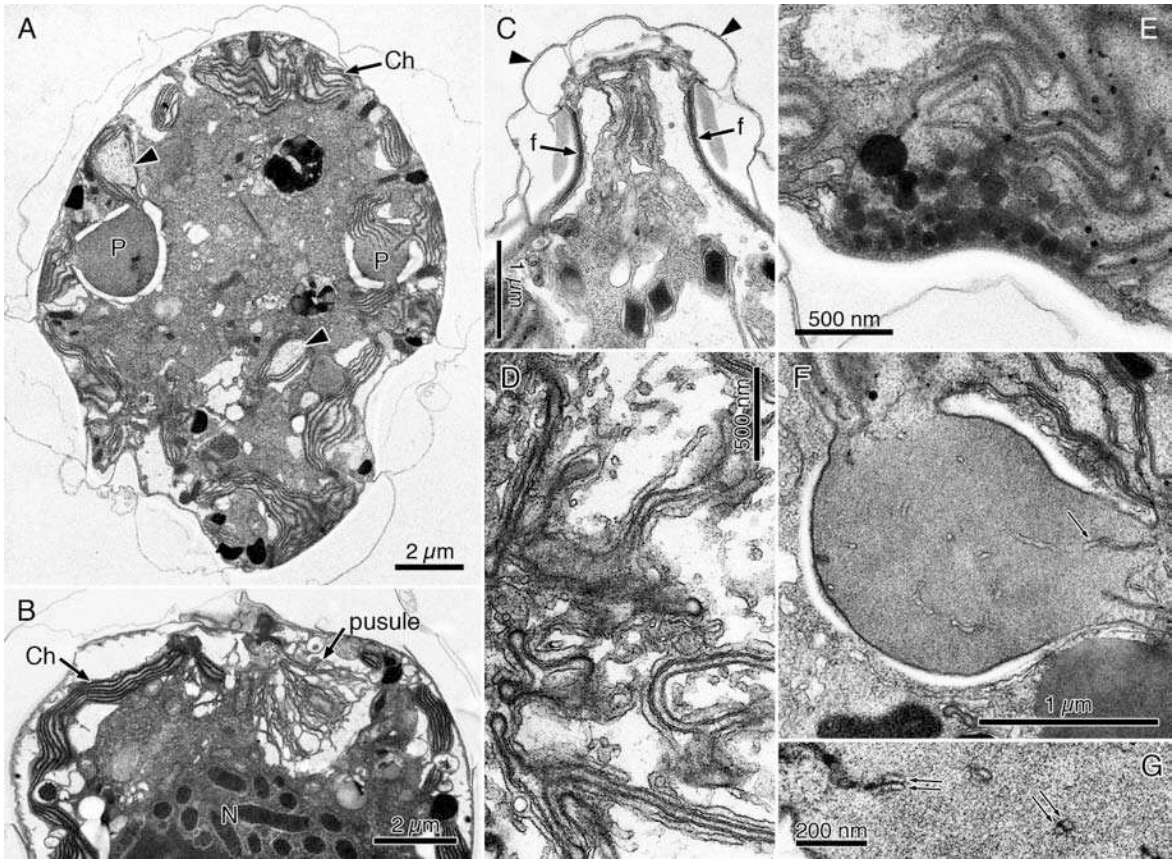

Fig. 15. *Scrippsiella trochoidea*, TEM. **A.** Longitudinal section showing the general organization. Note the multiple-stalked pyrenoids (P) with sheaths of starch. Ch, chloroplast lobes. Areas of chloroplast lobes without thylakoids are indicated by arrowheads. **B**. Transverse section at cingulum level (apical view), showing the pusule and the nucleus (N). **C**. Longitudinal section through the somewhat projecting apical pore complex, showing fibres (f) of the apical fibrous complex and amphiesmal vesicle profiles (arrowheads) between the vesicles containing the pore plate and the cover plate. **D**. Detail of the pusule with the appearance of flat vesicles. **E**. Eyespot formed by a row of globules located in a chloroplast lobe. **F**. Multiple-stalked pyrenoid with tubular

structures apparently continuous with the thylakoids (arrow). **G**. Detail of the pyrenoid matrix with simple or double (double arrow) tubular structures.

Although four cells were examined, neither a microtubular basket nor a microtubular strand that could be associated with a peduncle were found.

The flagellar apparatus contained the typical peridinioid elements, including a LC (Fig. 16A), and is not described further. However, the areas of emergence of both flagella were distinctive in having what appeared to be 5–6 platelets defining narrow, cylindrical canals that the flagella seemed to squeeze through; these platelets were contained in vesicles with the same appearance as the amphiesmal vesicles of other plates, but they were positioned in layers and were made of a distinct, somewhat fibrous-looking material (Fig. 16).

Fig. 16. *Scrippsiella trochoidea*, TEM. Exit pores of the flagella. **A**. Longitudinal flagellum (LF) exiting through a canal lined by at least four platelets (pl) in a more internal position relative to the surrounding sulcal plates. The appearance of the platelets is consistently different from that of the outer thecal plates (arrowheads). LC, layered connective; LMR, longitudinal microtubular root; LSC, longitudinal striated collar. **B**. Transverse flagellum (TF) squeezed in a canal formed by platelets (pl). TSC, transverse striated collar.

Molecular phylogeny

In the LSU rDNA based phylogeny including 32 dinoflagellate genera *Peridinium aciculiferum* and *Peridinium lomnickii* form two early diverging lineages related to *Thoracosphaera*, *Tyrannodinium* and the other three pfiesteriaceans (Fig. 17). This cluster of dinoflagellates is well supported in terms of posterior probabilites (PP=1.0) but has only little support from bootstrap analysis (BS=57%). The sister group relationship between these 7 genera of dinoflagellates and the group containing *Scrippsiella* spp. and *Peridiniopsis polonica* is well supported both in terms of posterior probabilities and bootstrap values (PP=0.98 and BS=94%). However, the phylogenetic positioning of *Peridinium lomnickii* as a sister group to *Thoracosphaera, Tyrannodinium* and other pfiesteriaceans is not highly supported (PP=0.59 and BS<50%).

Sequence divergence

A pair-wise comparison based on 1513 base pairs of the LSU rRNA gene in *Peridinium lomnickii* and a representative assemblage of nine of the most closely related dinoflagellates is shown in Table 1. The overall sequence divergence in the LSU rRNA genes of *P. lomnickii* and *P. aciculiferum* is < 2%, whereas the sequence divergence between *P. lomnickii/P. aciculiferum* and *Scrippsiella trochoidea* is 3.5–3.7%. There is a ≈ 5-6% sequence divergence between *P. lomnickii* and *Tyrannodinum*, *Thoracosphaera*, *Pfiesteria* and *Peridiniopsis polonica*. Table 1 also illustrates that *P. lomnickii* is distantly related to the type species of *Peridinium* (*P. cinctum*), as the sequence divergence is 14 or 15.7%, depending on the method used to estimate the divergence. Both sequence divergence estimates between *P. lomnickii* and *P. borgei* are slightly smaller, but still relatively large: 9.8 and 10.7%.

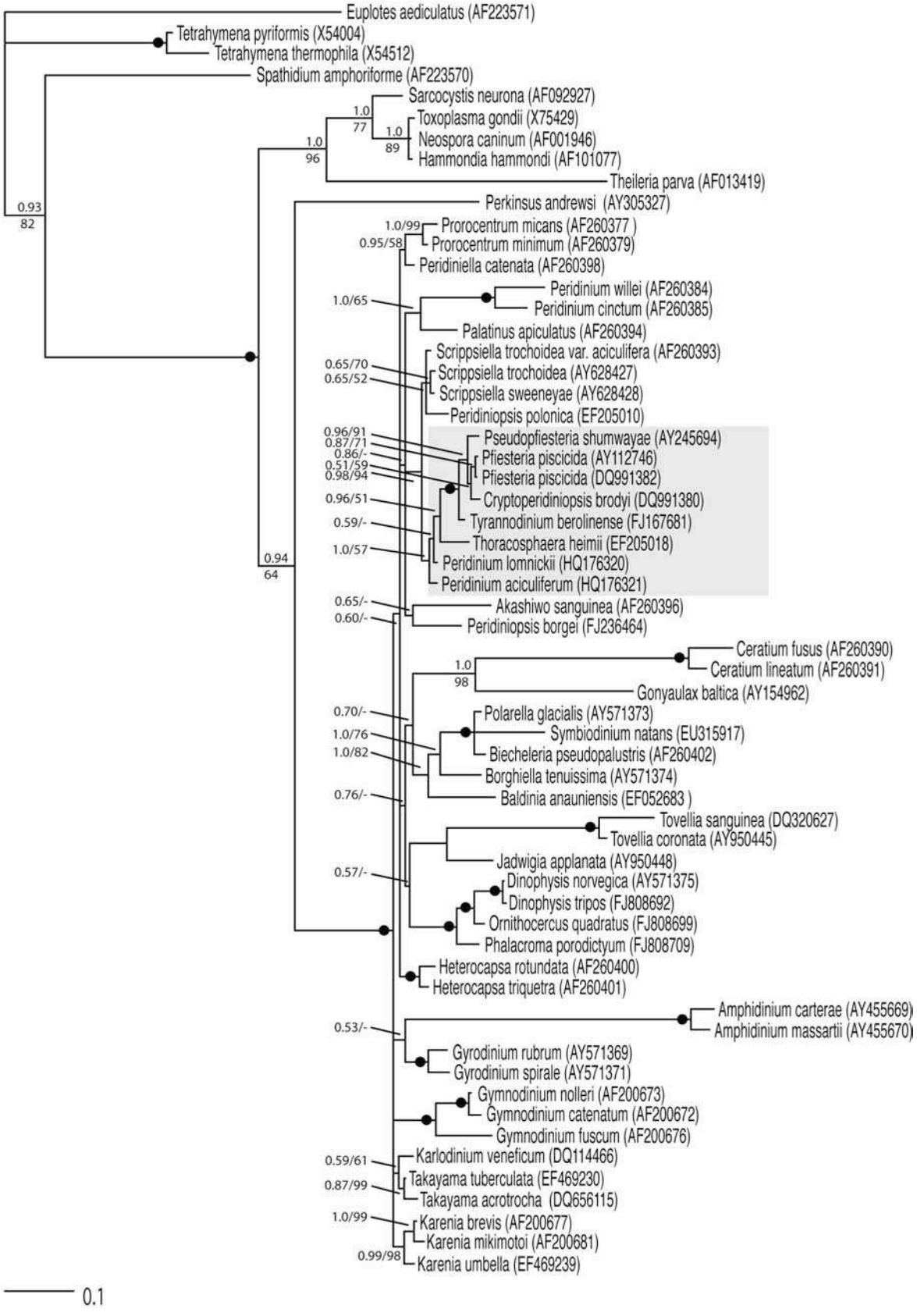

Fig. 17. Phylogeny of *Peridinium lomnickii* and 47 other species of dinoflagellates from Bayesian inference of nuclear-encoded LSU rRNA sequences. The alignment included 1158 base pairs.

Four ciliates, five Apicomplexa and *Perkinsus* formed the outgroup taxa. Branch support values given to the left of internodes are from posterior probabilities (≥ 0.5) and maximum likelihood bootstrap analyses with 100 replications (≥ 50%). Maximum branch support (posterior probability = 1 and 100% in ML bootstrap) is indicated by filled black circles. Branch lengths are proportional to the number of character changes.

Taxonomic descriptions

Chimonodinium Craveiro, Calado, Daugbjerg, Gert Hansen et Moestrup gen. nov.

Dinoflagellata autotrophica, thecata, non parasitica. Formula kofoidiana thecarum Po, cp, x, 4′, 3a, 7″, 6c, 5s, 5‴, 2⁗. Patellae laeves vel granulatae vel spinulosae, sed haud areolatae. Lobi chloroplasti in strato externo cytoplasmatis distributa, sine pyrenoidibus. Stigma in lobo chloroplasti subter sulcum sito. Fila microtubularia peduncularia quadrifariam vel quinquefariam (alveus microtubularis dictus), ad extremum ventrales vesiculis fuscis (per microscopium electronicum visae) concomitatis. Pusula tubularis saltem prope canales flagellares, ad pars profunda convoluta et complanata. Theca cinguli superiorem marginem dehiscens. Cysta ovoidea vel ellipsoidea cum pariete crassa non calcarea.

Typus generis: Chimonodinium lomnickii (Wołoszyńska) Craveiro, Calado, Daugbjerg, Gert Hansen et Moestrup comb. nov., hic designatus.

Thecate, autotrophic free-living dinoflagellates. Kofoidian plate formula: Po, cp, x, 4′, 3a, 7″, 6c, 5s, 5‴, 2⁗. Plate surface with granules or short spines and trichocyst pores, but not areolated. Chloroplast lobes near the surface, not connected in the cell centre, without distinct pyrenoids. Eyespot located in a chloroplast lobe beneath the sulcus. Small extruded peduncle present, supported by a microtubular basket of 4 or 5 rows of microtubules extending into the anterior part of the epicone, accompanied in their distal part by elongated vesicles with electron-opaque contents. Pusular system formed by two vesicle-wrapped tubes, each one connected to one of the flagellar canals; tubes convoluted and flat in the more internal cytoplasm. Dividing or ecdysing cells exiting the theca through an opening along the anterior edge of the cingulum. Resting cyst oval to ellipsoid, with a non-calcareous, thick wall.

Table 1. Sequence divergence estimates in percent between *Chimonodinium lomnickii*, *Thoracosphaera heimii* and some peridinioids. Uncorrected distances (P-values from PAUP*) are provided below the diagonal, and distance values calculated using the Kimura-2-parameter model are given above the diagonal.

	Peridinium cinctum	*Palatinus apiculatus*	*Scrippsiella trochoidea*	*Peridiniopsis polonica*	*Pfiesteria piscicida*	*Tyrannodinium berolinense*	*Thoracosphaera heimii*	*Peridiniopsis borgei*	*Peridinium aciculiferum*	*Chimonodinium lomnickii*
P. cinctum	—	15.3	15.0	16.0	17.6	17.4	17.2	19.1	15.9	15.7
P. apicul.	13.7	—	8.7	10.3	10.5	10.9	10.5	11.3	8.5	8.2
S. trochoid.	13.4	8.2	—	5.6	6.8	6.8	6.9	10.5	3.7	3.7
P. polonica	14.2	9.6	5.3	—	8.6	8.2	8.6	12.0	5.7	6.0
P. piscicida	15.5	9.7	6.5	8.1	—	3.5	7.3	12.0	4.8	5.2
T. berol.	15.3	10.1	6.5	7.7	3.4	—	6.7	12.7	5.2	5.3
T. heimii	15.2	9.7	6.5	8.1	6.9	6.4	—	11.8	6.0	5.8
P. borgei	16.6	10.3	9.7	11.0	11	11.5	10.8	—	11.2	10.7
P. acicul.	14.2	8.0	3.5	5.5	4.6	5.0	5.7	10.2	—	1.8
C. lomnickii	14.0	7.7	3.6	5.7	5.0	5.1	5.6	9.8	1.7	—

Type species: *Chimonodinium lomnickii* (Wołoszyńska) Craveiro, Calado, Daugbjerg, Gert Hansen et Moestrup comb. nov., designated here.

Etymology: from Greek χειμων, "winter", after Wołoszyńska's original notes on the period of greatest abundance of the type species. The termination *–dinium*, originally from Greek δινη, "vortex", is common in names of dinoflagellates.

Chimonodinium lomnickii (Wołoszyńska) Craveiro, Calado, Daugbjerg, Gert Hansen et Moestrup comb. nov.

Basionym: *Peridinium lomnickii* Wołoszyńska 1916, Bull Int Acad Sci Cracovie, Cl Sci Math Nat, sér. B 1915 (8–10), p. 267, pl. 10, figs 25–29.

Homotypic synonym: *Glenodinium lomnickii* (Wołoszyńska) Er. Lindemann (1925, pp 162, 168, 169).

Heterotypic synonym: *Peridinium lomnickii* var. *punctulatum* Er. Lindemann (1924, p. 436, pl. 21, figs 1–6; '*punktulatum*').

Chimonodinium lomnickii var. ***splendidum*** (Wołoszyńska) Craveiro, Calado, Daugbjerg, Gert Hansen et Moestrup comb. nov.

Basionym: *Peridinium lomnickii* var. *splendidum* Wołoszyńska 1916, Bull Int Acad Sci Cracovie, Cl Sci Math Nat, sér. B 1915 (8–10), p. 268, pl. 10, figs 30–40 ('*splendida'*).

Homotypic synonym: *Glenodinium lomnickii* var. *splendidum* (Wołoszyńska) Er. Lindemann (1928, p. 260).

Chimonodinium lomnickii var. ***wierzejskii*** (Wołoszyńska) Craveiro, Calado, Daugbjerg, Gert Hansen et Moestrup comb. nov.

Basionym: *Peridinium wierzejskii* Wołoszyńska 1916, Bull Int Acad Sci Cracovie, Cl Sci Math Nat, sér. B 1915 (8–10), p. 269, pl. 11, figs 1–8.

Homotypic synonym: *Glenodinium lomnickii* var. *wierzejskii* (Wołoszyńska) Er. Lindemann (1928, p. 260).

DISCUSSION

A brief note on the taxonomy of *Chimonodinium*

The populations we report on closely match the original description of *Peridinium lomnickii* (Wołoszyńska 1916), including the distinct size difference between epi- and hypotheca. *Peridinium wierzejskii* was described in the same

article with features very similar to *P. lomnickii*, but more spherical (i.e., less elongate and less flattened dorsoventrally) and with epi- and hypotheca of the same size (Wołoszyńska 1916). The exiguity of the features separating the two taxa was noted by Lindemann (1920, 1924, 1925). However, after transferring *P. lomnickii* to *Glenodinium* because of the indistinctness of thecal plates in intact specimens, Lindemann (1928) recognized *P. wierzejskii* at variety level. Lefèvre (1932) retained this group of taxa in *Peridinium* and recognized *P. wierzejskii* as an independent species on the basis of the morphological differences originally given by Wołoszyńska (1916), and was followed by subsequent monographers (e.g., Schiller 1935; Huber-Pestalozzi 1950; Starmach 1974). Popovský and Pfiester (1990) recognized it again as a variety under the name "P. lomnickii var. wierzejskii (Wołoszyńska) Lindemann", a combination not validly published.

Peridinium lomnickii var. *splendidum* was originally described as a larger, much more flattened form than typical *P. lomnickii*, with thick borders to the furrows and an asymmetry derived from a right cell side larger than the left (Wołoszyńska 1916). The variety has been generally recognized (e.g., Lefèvre 1932; Schiller 1935; Huber-Pestalozzi 1950; Starmach 1974), but not reported. Although it is tempting to consider all these taxa as variations within the life cycle of a single species, as done by Grigorszky et al. (2003a), to reliably merge them as synonyms it would be important to recognize cells fitting the diagnostic characters given for *P. wierzejskii* and *P. lomnickii* var. *splendidum* within populations of *P. lomnickii* (preferably in unialgal culture), and not only a gradation in thecal thickness. However, even in thecae containing cysts, which presumably developed form the planozygote stage, we did not find the large size, the dorsoventral flattening or the asymmetry described for var. *splendidum*; nor could we demonstrate spherical cells with equal-sized epi- and hypotheca in the populations we studied.

The citation of *Chalubinskia tatrica* Wołoszyńska as a synonym of *P. lomnickii*, as done by Popovský and Pfiester (1990) and Grigorszky et al. (2003a), is unjustified. Both the species and the genus *Chalubinskia* Wołoszyńska were based on a single empty theca, which the author decided to describe because of the uniqueness of having a hypotheca with three post-cingular and a single

antapical plate (Wołoszyńska 1916, p. 276, pl. 13, figs 1–8). The specimen was probably abnormal and the genus ill-founded (Schiller 1935; Bourrelly 1970). Although the identity of *C. tatrica* with *P. lomnickii* was mentioned as possible (Schiller 1935), the relatively elongate outline, the somewhat produced apex, the smooth theca and the presence of stout spines on the edges of hypothecal plates are much more suggestive of *P. aciculiferum* Lemmermann, as noted by Wołoszyńska (1936, p. 195).

General structure of *C. lomnickii*

The general features of *C. lomnickii* were typical for dinoflagellates. The eyespot displayed an unusually large number of layers of globules, surpassed only by *Peridiniopsis borgei*, which, however, differs in being overlaid by a vesicle with a layer of brick- or crystal-like units (Calado and Moestrup 2002). The significance of the thin cross-lines on the ventral surface of the LMR in the sulcal area is unknwon; similar lines were reported from the woloszynskioids *Prosoaulax lacustris* (F. Stein) Calado et Moestrup, *Jadwigia applanata* Moestrup, K. Lindberg et Daugbjerg, and *Tovellia coronata* (Wołoszyńska) Moestrup, K. Lindberg et Daugbjerg, but also from the peridinioid *Tyrannodinium berolinense* (Lemmermann) Calado, Craveiro, Daugbjerg et Moestrup (Calado et al. 1998, Roberts et al. 1995a, Lindberg et al. 2005, Wedemayer and Wilcox 1984).

The flagellar apparatus showed all the regular features of peridinioids, notably the single microtubule that associates with the right-hand side of the LB (SMR, r2), of general occurrence in peridinioids and gonyaulacoids, and the layered connective, only found in peridinioids, that presumably takes up the function of the striated connective between LMR and TSR found in other dinoflagellate groups (Calado et al. 2006, 2009). The band of thin fibres extending from electron-opaque material on the dorsal side of the LMR toward the TB (TB-LMRc) is in the position of the well-defined fibres that link the same flagellar apparatus components in *P. borgei*, *Tyrannodinium berolinense* and *Palatinus apiculatus* (Ehrenberg) Craveiro, Calado, Daugbjerg et Moestrup (Calado and Moestrup 2002, Calado et al. 2009, Craveiro et al. 2009).

In a review of apical pore complexes of Peridiniaceae based on SEM, Toriumi and Dodge (1993) included the rim around the pore (between the pore

plate and the actual pore, or the cover plate if it has not detached) as a constant feature in the group. Judging from its location and size, the profiles of amphiesmal vesicles shown on the edges of the cover plate in *C. lomnickii* (Fig. 6C) correspond to the rim visible in SEM. The presence in the apical pore complex of amphiesmal vesicles additional to the ones containing the plates has not been reported previously, although amphiesmal profiles matching the ones shown here are visible in Roberts et al. (1987) in their fig. 3, representing *Heterocapsa pygmaea* A.R. Loeblich, R.J. Schmidt et Sherley, and especially in their fig. 14, representing *Scrippsiella sweeneyae* A.R. Loeblich. The same aspect is present in our material of *S. trochoidea* (Fig. 15C). Although further examination of apical pores of dinoflagellates by TEM is necessary to evaluate the occurence of supplementary amphiesmal vesicles, examination of published material suggests that they are absent in some gonyaulacoids (e.g., Hansen et al. 1996). The inclusion of *C. lomnickii* in a group of species with the pore plate not indented by the canal plate (Toriumi and Dodge 1993), contrary to the observations we report here, is not documented by the figure given, which does not show the boundary between the relevant plates (Toriumi and Dodge 1993, fig. 27), and we regard it as a mistake.

Comparison with *Peridinium*, *Palatinus* and *Peridiniopsis*

External cell features pertaining to *Peridinium* sensu stricto are those shared by the type species, *P. cinctum*, with other species in groups cinctum and willei, which differ essentially in degree of symmetry of the epithecal tabulation (Craveiro et al. 2009). Internal fine structure, including the flagellar base area, is known only from *P. cinctum* in enough detail for comparison with *Chimonodinium* (Calado et al. 1999). Both internal and external detailed analyses are available from the type species of *Palatinus* Craveiro, Calado, Daugbjerg et Moestrup, *P. apiculatus*, and *Peridiniopsis*, *P. borgei* (Craveiro et al. 2009; Calado and Moestrup 2002).

The presence or absence of an apical pore complex has long been the basis of the major subdivision of *Peridinium* sensu lato (Lemmermann 1910; Lefèvre 1932) and clearly separates *C. lomnickii* from both *Peridinium* sensu stricto and *Palatinus*. The occurrence of an apical pore in species currently

classified in *Peridiniopsis*, which have 6 plates in the cingulum (Bourrelly 1968, 1970), suggests a closer proximity to *Chimonodinium*, although they all display a smaller number of epithecal plates. The thecal plate organization of *P. borgei* is somewhat peculiar in having only three plates contacting the apical pore, which combines with unusual internal features (Calado and Moestrup 2002) to suggest that it may be phylogenetically distant from other so-called *Peridiniopsis*. The presence of a diatom-like endosymbiont in *Peridiniopsis penardii* (Lemmermann) Bourrelly and *P.* cf. *kevei* Grigorszky also indicates that species currently placed in *Peridiniopsis* form a heterogeneous group with uncertain affinities (Takano et al. 2008).

Additional aspects concerning the theca that separate *Chimonodinium* from *Peridinium* sensu stricto are the different ornamention of plates, generally covered with areolate ridges in species of groups cinctum and willei, and the way the theca breaks open for cells to exit (see discussion in Craveiro et al. 2009). *Peridinium gatunense* Nygaard, apparently a close relative of *P. cinctum*, stands out as an exception because its theca opens along the anterior edge of the cingulum (Boltovskoy 1973), just as in *Chimonodinium*. Thecae of *Peridiniopsis borgei* and *Tyrannodinium berolinense* open in a similar way to *Chimonodinium*, whereas the cells of *Palatinus* species exit the theca through the antapical area (Calado et al. 2009, Craveiro et al. 2009).

The general cell structure of *Chimonodinium*, particularly the chloroplast organization, is essentially the same as in *Peridinium* sensu stricto (Calado et al. 1999, Craveiro et al. 2009) and contrasts both with the organization of *Peridiniopsis borgei*, with a large, starch-enveloped pyrenoid on the dorsal side of the cell, and of *Palatinus*, with radiating chloroplast lobes connected to a central, branching pyrenoid (Calado et Moestrup 2002, Craveiro et al. 2009).

In contrast with the numerous vesicles opening into the large sac pusules in the ventral areas of *Peridinium cinctum* and *Peridiniopsis borgei* (Calado et al. 1999, Calado and Moestrup 2002), typical pusular elements in *C. lomnickii* were restricted, at least near the flagellar canals, to well-defined, non-collapsed tubes about 190 nm wide. This type of pusule resembles the one described from

Palatinus apiculatus, although three pusular tubes, rather than two, were found in that species (Craveiro et al. 2009).

Chimonodinium appears closer to *Peridiniopsis borgei* than to either *Peridinium* sensu stricto or *Palatinus* in having a well-developed system of microtubules associated with a peduncle (see below) and in the particular organization of the microtubular extension to flagellar root 3 (the TMRE). In *P. borgei* 23 microtubules of the TMRE reorganize from a flat strand near its nucleation site on the TMR to a cylindrical arrangement with a fibrous core that extends around the central sac pusule toward the back of the cell (Calado and Moestrup 2002). Although the association of the TMRE with fibrous material is much more poorly defined in *Chimonodinium*, it still suggests a closer relationship between the two genera than the molecular tree of Fig. 17 displays. However, statistical support for the clade containing *P. borgei* is relatively low, and other molecular markers may be needed to further clarify its phylogeny.

Comparison with *Scrippsiella*

The similarity between the tabulation of *C. lomnickii* and that found in species of *Scrippsiella* makes an ultrastructural comparison desirable. The genus *Scrippsiella* was originally described by Balech (1959) and later validated in botanical nomenclature by the addition of a Latin diagnosis (Loeblich 1965). Only one species, *S. sweeneyae* (as '*sweeneyi*') was initially included and it is therefore the type of the genus. Vegetative cells of currently recognized *Scrippsiella* species resemble each other considerably and the morphology of the calcareous cysts (or sometimes the comparison of DNA sequences) is often required for reliable identification (D'Onofrio et al. 1999). No information on cysts of *S. sweeneyae* was given by Balech (1959) and the distinction from vegetative cells of *S. trochoidea* relies on subtle variations of some plates (Balech 1988, p. 159). Whether *S. trochoidea* is closely related or, as discussed by Fine and Loeblich (1976) and Janofske (2000), is identical to *S. sweeneyae*, its fine-structural characters are here taken as representative of *Scrippsiella.*

Several cytoplasmic features separate *S. trochoidea* from *C. lomnickii*. Whereas *C. lomnickii* lacks pyrenoids, starch-enveloped pyrenoids were represented in the original drawings of *S. sweeneyae* (Balech 1959) and are

among the prominent features of vegetative *Scrippsiella* cells. The tubular structures, apparently continuous with thylakoids, that invade the pyrenoid matrix of *S. trochoidea* are similar to those reported from *S. minima* X. Gao et J.D. Dodge (Gao and Dodge 1991). The well-defined pusular tubes opening at the flagellar canals of *C. lomnickii* contrast with the higher number of less orderly, ramified vesicles shown here for *S. trochoidea*. The report of short and wide tubes in the pusule of *S. sweeneyae* by Dodge (1972) may be related to differences in fixation or in viewing angle; the aspect illustrated (Dodge 1972, fig. 11) bears no resemblance to the pusular tubes of *C. lomnickii* and we suggest that its description as a tubular pusule with invaginations is misleading. The pusule of *S. minima* was depicted as a group of vesicles radiating from the ventral area (Gao and Dodge 1991, fig. 13).

Recent phylogenetic studies have consistently shown that *Scrippsiella* species, together with other calcareous forms, share a clade with a group of non-calcareous tube feeders, the pfiesteriaceans (Meier et al. 2007, Gottschling et al. 2008, Calado et al. 2009). Pfiesteriacean feeding tubes are supported by overlaping rows of microtubules that form the so-called microtubular basket (Hansen and Calado 1999). However, although a less elaborate microtubular basket was found in *C. lomnickii*, none was present in the cells of *S. trochoidea* examined. In view of the widespread occurrence in dinoflagellates of peduncle-related microtubular strands, secondary loss seems the plausible explanation for the absence of a microtubular basket or a peduncular microtubular strand in *Scrippsiella.*

The emergence of the flagella through thin canals lined by odd-looking plates, as reported here for *S. trochoidea*, is unusual and brings to mind the canal plates of *Prorocentrum* (Roberts et al. 1995b, Mohammad-Noor et al. 2007). Among thecate dinoflagellates provided with furrows, similar-looking plates have only been reported from *Bysmatrum arenicola* T. Horiguchi et Pienaar (Horiguchi and Pienaar 1988, as “Scrippsiella arenicola”, nom. inval.).

The features mentioned above, together with the absence of a calcareous cyst in *C. lomnickii*, agree with the molecular phylogeny in placing *Chimonodinium* separate from *Scrippsiella* (see below).

Molecular phylogeny versus phenotype

The tree topology shown in Fig. 17 groups *Scrippsiella* species on a sister clade to the one containing both *Chimonodinium* and the pfiesteriaceans. On the face of the extensive physiological differences between the largely heterotrophic, predatory or parasitic pfiesteriaceans (Calado et al. 2009) and the autotrophic *Chimonodinium*, a closer relationship between these groups than between *Chimonodinium* and *Scrippsiella* is unexpected. However, two non-trivial phenotypic features support this relationship: one is the presence in *Chimonodinium* of several rows of microtubules related to the peduncle, making up a relatively small microtubular basket, whereas other photosynthetic peridinioids examined have either a single microtubular strand or none at all (Craveiro et al. 2009); the other is the connection between the edge of one sulcal plate and the middle of another, involving extra-cytoplasmic fibres. This type of plate contact was first described in *Tyrannodinium berolinense* (Calado and Moestrup 1997) and seems to be associated with the contact between the peduncle cover plate and the left side of the sulcus, presumably providing the necessary flexibility to accomodate the highly dynamic feeding tube of pfiesteriaceans (Calado et al. 2009).

The position of the calcareous *Thoracosphaera* as a sister clade to the pfiesteriaceans is consistent with published results (Gottschling et al. 2005, 2008). *Thoracosphaera* is unusual in that the vegetative (dividing) stage resembles the cyst stage of dinoflagellates producing calcareous cysts (Tangen et al. 1982, Inouye and Pienaar 1983). Detailed examination of the flagellate stage of *Thoracosphaera* is needed to verify if fine-structural characters corroborate the phylogetic position suggested by molecular phylogenies.

Although *Chimonodinium lomnickii* and *Peridinium aciculiferum* appear closely related in terms of their LSU rRNA gene sequences (Table 1), the molecular phylogeny suggests that *C. lomnickii* and *P. aciculiferum* do not form sister taxa (Fig 17). Rather, *P. aciculiferum* takes a basal position forming a sister taxon to a large assemblage comprising pfiesteriaceans, *Thoracosphaera* and *Chimonodinium*. *Peridinium aciculiferum* is commonly regarded as closely related to *C. lomnickii* (e.g., Popovský and Pfiester 1990) and the small sequence

divergence suggests that its transfer to *Chimonodinium* would be justified. However, the preliminary observation of a complete series of sections through the well-preserved ventral area of a *P. aciculiferum* cell showed neither a microtubular basket nor the pusular system found in *C. lomnickii*, raising doubts about the relationship between the two species. Further observations, preferably complemented with the analysis of additional molecular markers, are needed to clarify the phylogenetic position of *P. aciculiferum*. Also in need of taxonomic revision, judging from the affinities displayed in the molecular tree, is *Peridiniopsis polonica*, which appears related to *Scrippsiella*, although it is not known to produce calcareous cysts.

METHODS

Biological material: Populations of *Chimonodinium lomnickii* from four locations were studied: Salamandersøen, North Jutland, Denmark collected in October 1994 by the late Tyge Christensen; Lake Helen, near Kangerlussuaq (Søndre Strømfjord), Greenland, collected in March 2001; small pond near Ugglehult, Aneboda, Sweden, collected as cysts in the sediment in October 2001; and Pateira de Fermentelos, a lake near Aveiro, Portugal, collected in February 2006. Clonal cultures of *C. lomnickii* were established from vegetative cells from the Greenland sample, and from germinating cysts isolated from the Swedish sample (the latter deposited as SCCAP K-1151).

The culture of *Scrippsiella trochoidea* (KF2N16) used in this work was initiated from a cyst isolated from 11-cm depth (dated 1986) in core sediment from Koljö Fjord, north of Göteborg, Sweden, collected in March 2005. The cyst germinated in TL25 culture medium.

Light microscopy: Light micrographs were taken on a Zeiss Axioskop light microscope with a Zeiss Axiocam HRc digital camera (Carl Zeiss, Oberkochen, Germany).

Scanning electron microscopy: Cultured cells of *Chimonodinium lomnickii* (from Greenland and Sweden) were fixed in 3.7% formalin neutralized by $NaHCO_3$ to pH 7.5, for at least one hour. Cells were concentrated on 5 µm pore Isopore polycarbonate membrane filters, washed for one hour in distilled water,

dehydrated with a graded ethanol series and critical point dried in a Baltec CPD-030 (Balzers, Liechtenstein). The dried filters were glued onto stubs, sputter-coated with platinum-palladium and examined in a Jeol JSM-6335F (Jeol Ltd., Tokyo, Japan) scanning electron microscope.

The *Scrippsiella trochoidea* cysts were collected and micrographed in a microscope preparation, and then air dried on the removed coverslip. The coverslip was glued onto a stub, sputter-coated with platinum-palladium and examined in a Jeol JSM-5400 (Jeol Ltd., Tokyo, Japan).

Transmission electron microscopy: Two different fixation schedules were used for *Chimonodinium lomnickii*: (1) cells from the Danish field sample were fixed for 1 hour in 2% glutaraldehyde in 0.1 M Na-cacodylate buffer (pH 7.4). After centrifugation and two washes in the same buffer cells were post-fixed in buffered 0.5% osmium tetroxide overnight. Following a wash in buffer, cells were dehydrated through a graded ethanol series and propylene oxide and embedded in Spurr's resin; (2) swimming cells of *C. lomnickii* from the field sample from Portugal were picked up with a micropipette and transferred to a mixture of 1% glutaraldehyde and 0.5% osmium tetroxide (final concentrations) in 0.1 M phosphate buffer, pH 7.2, for ca. 30 minutes. After one rinse in buffer, cells were embedded in 1.5% agar and post-fixed in 0.5% osmium tetroxide overnight. The agar blocks were dehydrated through a graded ethanol series and propylene oxide and embedded in Epon. Serial sections, in both cases, were prepared with a diamond knife on a Reichert Ultracut E and an EM UC6 ultramicrotomes (Leica Microsystems, Wetzlar, Germany). Ribbons of sections were picked up with slot grids, placed on Formvar film and stained with uranyl acetate and lead citrate. Serial sections of four cells were examined with a Jeol JEM 1010 (Jeol Ltd., Tokyo, Japan) transmission electron microscope.

Swimming cells from *Scrippsiella trochoidea* culture (KF2N16) were picked up and fixed for 30 minutes in 1% glutaraldehyde and 0.5% osmium tetroxide (final concentrations) in 0.2 M cacodylate buffer, pH 7.2. After one rinse in buffer, cells were embedded in 1.5% agar, washed once in a 1:1 mixture of 0.2 M and 0.1 M cacodylate buffer and washed again in pure 0.1 M cacodylate buffer. Post-fixation was in 1% osmium tetroxide in 0.1 M cacodylate buffer for two hours. The agar

blocks were dehydrated as described above and embedded in Spurr's resin. The rest of the procedure was the same as for both *Chimonodinium lomnickii* fixations.

Determination of nuclear-encoded LSU rRNA sequence: For this study we determined the LSU rRNA sequence of two thecate species of dinoflagellate (viz. *Chimonodinium lomnickii* and *Peridinium aciculiferum*). Total genomic DNA was extracted from a clonal isolate of *P. aciculiferum* originating from Lake Tovel (North Italy). For this we used the CTAB extraction methods as previously outlined in Daugbjerg et al. (2000). The LSU rDNA sequence of *C. lomnickii* was obtained from single-cell PCR of cells isolated from Pateira de Fermentelos, a shallow lake near Aveiro, Portugal. This sequence obtained was 100% identical to one from a clonal isolate of *C. lomnickii* originating from a lake near Kangerlussuaq (Greenland). Since the sequences were indistinguishable we only included one in the phylogeny. The conditions used here for setting-up and running PCR were similar to those already provided in Calado et al. (2009) and Hansen and Daugbjerg (2004).

Sequence alignment: In order to infer the phylogeny of *Chimonodinium lomnickii* and *Peridinium aciculiferum* we added their LSU rDNA sequence to an alignment comprising a diverse assemblage of other dinoflagellate species. Thus, the phylogeny is based on analysis of a total of 32 genera and 45 species of dinoflagellates. Genbank accession numbers for all taxa included are given in Fig. 17. Information from the secondary structure of the mature RNA molecule sensu Lenaers et al. (1989) was incorporated in the alignment. Due to ambiguous alignment of the variable domain D2 this fragment was excluded prior to the phylogenetic analyses. The data matrix was edited manually using MacClade (ver. 4.08, Maddison and Maddison 2003) and included 1158 base pairs.

Outgroup: Numerous phylogenetic studies of eukaryotes have shown that the ciliates and Apicomplexa form sister groups to the dinoflagellates (e.g. Baldauf 2008). Hence, to polarize the ingroup of dinoflagellates we used 4 species of ciliates, 5 species of Apicomplexa and *Perkinsus* as outgroup taxa.

Phylogenetic analyses: Bayesian analysis (BA) was performed using MrBayes (ver. 3.1.2, Ronquist and Huelsenbeck 2003) and maximum likelihood (ML) by using PhyML (ver. 3.0, Guindon and Gascuel 2003). In BA we used $2*10^6$

generations and every 50th generation a tree was sampled. BA analyses were carried out on the freely available Bioportal (www.bioportal.uio.no). To evaluate the burn-in value we plotted the LnL values as a function of generations. The burn-in occurred after 20.050 generations, thus 401 trees were removed leaving 39600 trees for generating a 50% majority-rule consensus in PAUP* (Swofford 2003). For ML analysis we applied the parameter settings obtained from MrModeltest (ver. 2.3, Nylander 2004). PhyML was run via the online version available on the Montpellier bioinformatics platform at http://www.atgc-montpellier.fr/phyml. The robustness of the tree topology was evaluated using bootstrapping with 100 replications.

ACKNOWLEDGEMENTS

SCC was supported by a Ph.D. fellowship from the financing program POCI, Portugal (SFRH/BD/16794/2004) and by a grant from the European Commission's (FP 6) Integrated Infrastructure Initiative programme SYNTHESYS (DK-TAF) during July-September 2008. ND thanks the Carlsberg Foundation for equipment grants. The *Scrippsiella trochoidea* culture was established during the project "Changes in community structure and microevolution in marine protists" and was kindly provided by Nina Lundholm and Marianne Ellegaard. Henrik Levinsen provided the sample collected in Greenland and Karin Lindberg established the culture originating from cysts collected in Sweden.

REFERENCES

Baldauf S (2008) An overview of the phylogeny and diversity of eukaryotes. J Syst Evol **46:** 263–273

Balech E (1959) Two new genera of dinoflagellates from California. Biol Bull **116**: 195–203

Balech E (1988) Los dinoflagelados del Atlántico Sudoccidental. Publ Espec Inst Esp Oceanogr **1**: 1-310

Bibby BT, Dodge JD (1973) The ultrastructure and cytochemistry of microbodies in dinoflagellates. Planta **112**: 7–16

Bibby BT, Dodge JD (1974) The fine structure of the chloroplast nucleoid in *Scrippsiella sweeneyae* (Dinophyceae). J Ultrastruct Res **48**: 153–161

Boltovskoy A (1973) Formacion del arqueopilo en tecas de dinoflagelados. Rev Esp Micropaleont **5**: 81–98

Bourrelly P (1968) Notes sur les Péridiniens d'eau douce. Protistologica **4**: 5–13

Bourrelly P (1970) Les algues d'eau douce **3**: Les algues bleues et rouges, les Eugléniens, Peridiniens et Cryptomonadines. Boubée, Paris

Calado AJ, Craveiro SC, Moestrup Ø (1998) Taxonomy and ultrastructure of a freshwater heterotrophic *Amphidinium* (Dinophyceae) that feeds on unicellular protists. J Phycol **34**: 536–554

Calado AJ, Craveiro SC, Daugbjerg N, Moestrup Ø (2006) Ultrastructure and LSU rDNA-based phylogeny of *Esoptrodinium gemma* (Dinophyceae), with notes on feeding behavior and the description of the flagellar base area of a planozygote. J Phycol **42**: 434–452

Calado AJ, Craveiro SC, Daugbjerg N, Moestrup Ø (2009) Description of *Tyrannodinium* gen. nov., a freshwater dinoflagellate closely related to the marine *Pfiesteria*-like species. *J. Phycol.* **45**: 1195-1205

Calado AJ, Hansen G, Moestrup Ø (1999) Architecture of the flagellar apparatus and related structures in the type species of *Peridinium*, *P. cinctum* (Dinophyceae). Eur J Phycol **34**: 179–191

Calado AJ, Moestrup Ø (1997) Feeding in *Peridiniopsis berolinensis* (Dinophyceae): new observations on tube feeding by an omnivorous, heterotrophic dinoflagellate. Phycologia **36**: 47–59

Calado AJ, Moestrup Ø (2002) Ultrastructural study of the type species of *Peridiniopsis*, *Peridiniopsis borgei* (Dinophyceae), with special reference to the peduncle and flagellar apparatus. Phycologia **41**: 567–584

Craveiro SC, Calado AJ, Daugbjerg N, Moestrup Ø (2009) Ultrastructure and LSU rDNA-based revision of *Peridinium* group palatinum (Dinophyceae) with the description of *Palatinus* gen. nov. *J. Phycol.* **45**: 1175-1194

Daugbjerg N, Hansen G, Larsen J, Moestrup Ø (2000) Phylogeny of some of the major genera of dinoflagellates based on ultrastructure and partial LSU rDNA sequence data, including the erection of three new genera of naked dinoflagellates. Phycologia **39**: 302–317

Dodge JD (1972) The ultrastructure of the dinoflagellate pusule: A unique osmo-regulatory organelle. Protoplasma **75**: 285–302

D'Onofrio G, Marino D, Bianco L, Busico E, Montresor M (1999) Toward an assessment on the taxonomy of dinoflagellates that produce calcareous cysts (Calciodinelloideae, Dinophyceae): a morphological and molecular approach. J Phycol **35**: 1063–1078

Eddy S (1930) The fresh-water armored or thecate dinoflagellates. Trans Amer Microsc Soc **49**: 277–321

Fine KE, Loeblich AR III (1976) Similarity of the dinoflagellates *Peridinium trochoideum*, *P. faeroense* and *Scrippsiella sweeneyae* as determined by chromosome numbers, cell division studies and scanning electron microscopy. Proc Biol Soc Wash **89**: 275–288

Gao X, Dodge JD (1991) The taxonomy and ultrastructure of a marine dinoflagellate, *Scrippsiella minima* sp. nov. Br Phycol J **26**: 21–31

Gao X, Dodge JD, Lewis J (1989) An ultrastructural study of planozygotes and encystment of a marine dinoflagellate, *Scrippsiella* sp. Br Phycol J **24**: 153–165

Gottschling M, Keupp H, Plötner J, Knop R, Willems H, Kirsch M (2005) Phylogeny of calcareous dinoflagellates as inferred from ITS and ribosomal sequence data. Mol Phylogenet Evol **36**: 444–455

Gottschling M, Renner SS, Meier KJS, Willems H, Keupp H (2008) Timing deep divergence events in calcareous dinoflagellates. J Phycol **44**: 429–438

Grigorszky I, Krienitz L, Padisák J, Botics G, Vasas G (2003a) Redefinition of *Peridinium lomnickii* Woloszynska (Dinophyta) by scanning electron microscopical survey. Hydrobiologia **502**: 349–355

Grigorsky I, Borics G, Padisák J, Tótmérész B, Vasas G, Nagy S, Borbély G (2003b) Factors controlling the occurrence of Dinophyta species in Hungary. Hydrobiologia **506–509**: 203–207

Guindon S, Gascuel O (2003) A simple, fast, and accurate algorithm to estimate large phylogenies by maximum likelihood. Syst. Biol. **52**: 696–704

Hansen G, Daugbjerg N (2004) Ultrastructure of *Gyrodinium spirale*, the type species of *Gyrodinium* (Dinophyceae), including a phylogeny of *G. dominans*, *G. rubrum* and *G. spirale* deduced from partial LSU rDNA sequences. Protist **155**: 271–294

Hansen G, Moestrup Ø, Roberts, KR (1996) Fine structural observations on *Gonyaulax spinifera* (Dinophyceae), with special emphasis on the flagellar apparatus. Phycologia **35**: 354–366

Hansen PJ, Calado AJ (1999) Phagotrophic mechanisms and prey selection in free-living dinoflagellates. J Eukaryot Microbiol **46**: 382–389

Horiguchi T, Pienaar RN (1988) Ultrastructure of a new sand-dwelling dinoflagellate, *Scrippsiella arenicola* sp. nov. J Phycol **24**: 426–438

Huber-Pestalozzi G (1950) Cryptophyceen, Chloromonadinen, Peridineen. In Thienemann A (ed.) Die Binnengewässer vol. 16, Das Phytoplankton des Süsswassers. Systematik und Biologie, part 3. Schweizerbart'sche Verlagsbuchhandlung, Stuttgart, Germany, 310 pp

Inouye I, Pienaar RN (1983) Observations on the life cycle and microanatomy of *Thoracosphaera heimii* (Dinophyceae) with special reference to its systematic position. S Afr J Bot **2**: 63–75

Janofske D (2000) *Scrippsiella trochoidea* and *Scrippsiella regalis*, nov. comb. (Peridiniales, Dinophyceae): a comparison. J Phycol **36**: 178–189

Kalley JP, Bisalputra T (1971) *Peridinium trochoideum*: the fine structure of the thecal plates and associated membranes. J Ultrastruct Res **37**: 521–531

Lefèvre M (1932) Monographie des espèces d'eau douce du genre *Peridinium*. Arch Bot **2**, Mémoire 5: 1–210, pl 1–6

Lemmermann E (1910) Kryptogamenflora der Mark Brandenburg. Bd. **3**. Algen I (Schizophyceen, Flagellaten, Peridineen). Gebrüder Borntraeger, Leipzig.

Lenaers G, Maroteaux L, Michot B, Herzog M (1989) Dinoflagellates in evolution. A molecular phylogenetic analysis of large subunit ribosomal RNA. J. Mol. Evol. **29**: 40–51

Lewis JM, Dodge JD (2002) Phyllum Pyrrophyta (Dinoflagellates). In John DM, Whitton BA, Brook AJ (eds) The Freshwater Algal Flora of the British Isles. Cambridge University Press, Cambridge, pp 186–207

Lindberg K, Moestrup Ø, Daugbjerg N (2005) Studies on woloszynskioid dinoflagellates I: *Woloszynskia coronata* re-examined using light and electron microscopy and partial LSU rDNA sequences, with description of *Tovellia* gen. nov. and *Jadwigia* gen. nov. (Tovelliaceae fam. nov.). Phycologia **44**: 416–440

Lindemann E (1920) Untersuchungen über Süßwasserperidineen und ihre Variationsformen II. Arch Naturg, section A, **84**: 121–194

Lindemann E (1924) Neue oder wenig bekannte Protisten. X. Neue oder wenig bekannte Flagellaten. IX. Mitteilungen über nicht genügend bekannte Peridineen. Arch Protistenkd **47**: 431–439, pl 21

Lindemann E (1925) III. Klasse: Dinoflagellatae (Peridineae). In Schoenichen, W. (ed.) [Eyferth's] Einfachste Lebensformen des Tier- und Pflanzenreiches, 5th ed., **1**. Spaltpflanzen, Geißellinge, Algen, Pilze. Bermühler, Berlin, pp 144-195

Lindemann E (1928) Vorläufige Mitteilung. Arch Protistenkd **63**: 259–260

Ling HU, Croome RL, Tyler PA (1989) Freshwater dinoflagellates of Tasmania, a survey of taxonomy and distribution. Br Phycol J **24**: 111–129

Loeblich AR III (1965) Dinoflagellate nomenclature. Taxon **14**: 15–18

Logares R, Shalchian-Tabrizi K, Boltovskoy A, Rengefors K (2007) Extensive dinoflagellate phylogenies indicate infrequent marine-freshwater transitions. Mol Phylogenet Evol **45**: 887–903

Maddison DR, Maddison WP (2003) MacClade 4. Sinauer Associates, Inc. Publishers. Sunderland, Massachusetts, U.S.A.

Meier KJS, Young JR, Kirsch M, Feist-Burkhardt S (2007) Evolution of different life-cycle strategies in oceanic calcareous dinoflagellates. Eur J Phycol **42**: 81–89

Moestrup Ø (2000) The flagellate cytoskeleton. Introduction of a general terminology for microtubular flagellar roots in protists. In Leadbeater BSC, Green JC (eds) The flagellates. Unity, diversity and evolution. Taylor & Francis, New York, pp 69–94. (Systematics Association Special Volume No. 59)

Mohammad-Noor N, Moestrup Ø, Daugbjerg N (2007) Light, electron microscopy and DNA sequences of the dinoflagellate *Prorocentrum concavum* (syn. *P. arabianum*) with special emphasis on the periflagellar area. Phycologia **46**: 549–564

Nylander JAA (2004) MrModeltest v2. Program distributed by the author. Evolutionary Biology Centre, Uppsala University

Popovský J, Pfiester LA (1990) Dinophyceae (Dinoflagellida). In Ettl H, Gerloff J, Heynig H, Mollenhauer D (eds) Süßwasserflora von Mitteleuropa **6**. Gustav Fischer, Jena

Roberts KR, Hansen G, Taylor FJR (1995a) General ultrastructure and flagellar apparatus architecture of *Woloszynskia limnetica* (Dinophyceae). J Phycol **31**: 948–957

Roberts KR, Heimann K, Wetherbee R (1995b) The flagellar apparatus and canal structure in *Prorocentrum micans* (Dinophyceae). Phycologia **34**: 313–322

Roberts KR, Timpano P, Montegut AE (1987) The apical pore fibrous complex: a new cytological feature of some dinoflagellates. Protoplasma **137**: 65–69

Ronquist F, Huelsenbeck JP (2003) MRBAYES 3: Bayesian phylogenetic inference under mixed models. Bioinformatics **19**: 1572–1574

Schiller J (1935) Dinoflagellatae (Peridineae) in monographischer Behandlung. In Kolkwitz R (ed.) Rabenhorst's Kryptogamen-flora von Deutschland, Österreich und der Schweiz, 2nd ed., **10** (3), Part 2 (Lief. 2), pp. 161–320. Akademische Verlagsgesellschaft, Leipzig

Senzaki S, Horiguchi T (1994). A taxonomic survey of freshwater dinoflagellates of Nagano prefecture, Japan. Jpn J Phycol **42**: 29–42

Sournia A (1986) Atlas du Phytoplankton Marin. **1**. Introduction, Cyanophycées, Dictyochophycées, Dinophycées et Raphidophycées. CNRS, Paris

Starmach K (1974) Cryptophyceae, Dinophyceae, Raphidophyceae. In Starmach K, Siemińska J (eds) Flora Słodkowodna Polski **4**. Państwowe Wydawnictwo Naukowe, Warszawa, Kraków, pp 1–520

Swofford DL (2003) PAUP* Phylogenetic analysis using parsimony (*and other methods). Version 4. Sinauer Associates, Sunderland, Massachusetts

Takano Y, Hansen G, Fujita D, Horiguchi T (2008) Serial replacement of diatom endosymbionts in two freshwater dinoflagellates, *Peridiniopsis* spp. (Peridiniales, Dinophyceae). Phycologia **47**: 41–53

Tangen K, Brand LE, Balckwelder PL, Guillard RRL (1982) *Thoracosphaera heimii* (Lohmann) Kamptner is a dinophyte: observations on its morphology and life cycle. Mar Micropaleontol **7**: 193–212

Toriumi S, Dodge JD (1993) Thecal apex structure in the Peridiniaceae (Dinophyceae). Eur J Phycol **28**: 39–45

Wedemayer GJ, Wilcox LW (1984) The ultrastructure of the freshwater colorless dinoflagellate *Peridiniopsis berolinense* (Lemm.) Bourrelly. J Protozool **31**: 444–453

Wołoszyńska J (1916) Polnische Süßwasser-Peridineen. Bull Int Acad Sci Cracovie, Cl Sci Math Nat, sér B **1915** (8–10): 260–285, pl 10–14

Wołoszyńska J (1936) Die Algen der Tatraseen und Tümpel. III. Peridineen im Winterplankton einiger Tatraseen. Arch Hydrobiol i Ryb **10**: 188–196, 1 pl

CHAPTER 4

DESCRIPTION OF *TYRANNODINIUM* GEN. NOV., A FRESHWATER DINOFLAGELLATE CLOSELY RELATED TO THE MARINE *PFIESTERIA*-LIKE SPECIES

Calado, A.J., Craveiro, S.C., Daugbjerg, N. & Moestrup, Ø. 2009. Description of *Tyrannodinium* gen. nov., a freshwater dinoflagellate closely related to the marine *Pfiesteria*-like species. *Journal of Phycology* 45 (5): 1195-1205.

ABSTRACT

On the basis of morphological (light and electron microscopy) as well molecular data, we show that the widely distributed freshwater dinoflagellate presently known as *Peridiniopsis berolinensis* is a member of the family Pfiesteriaceae, an otherwise marine and estuarine family of dinoflagellates. *P. berolinensis* is a close relative of the marine species, which it resembles in morphology, mode of swimming, food-uptake mechanism, and partial LSU rRNA sequences. It differs from all known genera of the family in plate tabulation. *P. berolinensis* is only distantly related to the type species of *Peridiniopsis*, *P. borgei*, and is therefore transferred to the new genus *Tyrannodinium* as *T. berolinense* comb. nov. *T. berolinense* is a very common freshwater flagellate that feeds vigorously on other protists and is able to consume injured metazoans much larger than itself. Production of toxins has not been reported.

Key index words: dinoflagellates; *Peridiniopsis berolinensis*; *Pfiesteria*; Pfiesteriaceae; *Tyrannodinium*

Abbreviations: apc, apical pore complex; BA, Bayesian analysis; cp, closing platelet; LC, layered connective; LMR, longitudinal microtubular root; ML, maximum likelihood; p, peduncle; pc, peduncle cover plate; Po, pore plate; PP, posterior probabilities; sa sd, sm, sp, ss, anterior, right, medium, posterior, and left sulcal plates, respectively; SMR, single-stranded microtubular root; TB, transverse basal body; TMR, transverse microtubular root; TMRE, transverse microtubular root extension; TSR, transverse striated root; TSRM, transverse striated root microtubule; x, canal plate

INTRODUCTION

The family Pfiesteriaceae was formally described in 1996 to accommodate the new genus *Pfiesteria*, a purportedly fish-killing dinoflagellate that attracted unprecedented attention from the general public. The original defining features of the family were centered on a complex, multiphasic life cycle, which included flagellate, amoeboid, and cyst stages (e.g., Burkholder et al. 1992, Steidinger et al. 1996). This set of characters made the group rather exclusive in the sense that other dinoflagellates with features that would fit the new group could not be found. However, the following years saw the description of new species of Pfiesteriaceae for which a multiphasic life cycle could not be demonstrated, placing the emphasis

on the characters of the flagellate stage, especially the feeding mode and the tabulation of the theca (Parrow and Burkholder 2003b, Jeong et al. 2005, Steidinger et al. 2006). The flagellate, thinly thecate cells became known as ‘‘cryptoperidiniopsoids,’’ in allusion to the peridinioid type of tabulation occurring in members of *Peridiniopsis* (Parrow and Burkholder 2003a). The recently demonstrated affinity of the parasitoid marine dinoflagellate genus *Paulsenella* to *Pfiesteria* and *Amyloodinium* (Kühn and Medlin 2005) highlights the feeding mode as a good phylogenetic marker for the group. The pfiesteriaceans are phylogenetically related to the calcareous dinoflagellates, such as *Thoracosphaera heimii* and species of *Scrippsiella* (Gottschling et al. 2005, Meier et al. 2007, Elbrächter et al. 2008).

As shown in the present study, the family Pfiesteriaceae is not restricted to the marine environment. On the basis of ultrastructural observations and supported by partial sequencing of LSU rRNA, we show that the species presently known as *P. berolinensis* is a close relative of the marine members of the Pfiesteriaceae. *P. berolinensis* was first described from Germany just over 100 years ago (Lemmermann 1900, as *Peridinium berolinense*), and it is a common dinoflagellate in freshwater ponds and lakes, reported from Europe, Africa, North America, and Japan (e.g., West 1907, Thompson 1951, Senzaki and Horiguchi 1994, Calado and Moestrup 1997). It feeds vigorously on other organisms, including algae, injured nematodes and other metazoans, even cells of its own kind (Calado and Moestrup 1997). It shares the feeding mechanism employed with its marine relations and is attracted to its prey by a chemosensory mechanism (Calado and Moestrup 1997) as in the marine species (e.g., Spero 1985). *P. berolinensis* differs from the marine species in details of the plate pattern and in LSU rRNA sequence. It constitutes a separate genus and species, described here as *T. berolinense* gen. et comb. nov.

Notes on the generic names used. (1) There is some discussion whether *Pseudopfiesteria* and *Pfiesteria* constitute separate genera (Marshall et al. 2006, Place et al. 2008). Pending additional evidence, we have followed Place et al. (2008) and retained the two genera, which differ in epithecal tabulation. (2) The genus *Stoeckeria* was published in a journal with a zoological tradition and fulfills

the requirements for availability (validity of publication) under the International Code of Zoological Nomenclature (Jeong et al. 2005). However, the use of the term ‘‘Dinophyceae’’ in the title is an incongruous link to botanical nomenclature, under which the name would be invalidly published for lack of Latin. We assume from the lack of a Latin diagnosis that it was not the authors’ intention to publish the new genus under the Botanical Code and therefore accept the name.

MATERIALS AND METHODS

Biological material. *T. berolinense* was collected in small lakes and ponds (incl. artificial lakes and fish ponds) in Portugal, Denmark, and Poland. Cells used for LM and SEM were collected in February 2008 from the artificial lake in ‘‘Baixa de Santo Antoónio,’’ Aveiro, Portugal, where it appears throughout the year. Cells for TEM were collected in April 1995 from ponds in Portugal and Denmark (Calado and Moestrup 1997). Cells for DNA sequencing originated at Pieskowa Skała near Cracow, Poland, collected 22 August 2007.

Light and electron microscopy. Light micrographs were taken with a Zeiss Axiophot light microscope (Carl Zeiss GmbH, Jena, Germany) using Kodak Technical Pan film (Eastman Kodak Company, Rochester, NY, USA) and a Zeiss Axioplan 2 imaging equipped with a DP70 Olympus camera (Olympus Corp., Tokyo, Japan).

SEM preparations followed two schedules of fixation: one to retain the flagella and the peduncle (1), and the other to remove the outermost membrane to show the plates (2). (1) Swimming cells were picked up with a micropipette into 1 mL of filtered lake water. They were fixed by addition of 0.5 mL of a fixative comprising a 1:3 mixture of saturated HgCl2 and 2% OsO4. Cells were collected on 8 µm pore-size Isopore polycarbonate membrane filters in a Swinnex filter holder (Millipore Corp., Billerica, MA, USA), washed with distilled water for 30 min, dehydrated through a graded ethanol series, and critical-point-dried. The dried filters were glued onto stubs, sputter-coated with gold-palladium, and examined in a Hitachi S-4100 scanning electron microscope (Hitachi High-Technologies Corp., Tokyo, Japan). (2) Swimming cells were transferred to 25% ethanol and fixed for

45 min. After collecting the cells in the filters, dehydration was completed, and the schedule followed as in (1).

TEM of feeding and nonfeeding cells was performed as described in Calado and Moestrup (1997).

Single-cell PCR and LSU rRNA sequencing. Cells of *T. berolinense* from field samples collected in Poland were isolated by pipetting and double rinsed in distilled water. Individual cells were transferred to 0.2 mL PCR tubes containing 8 µL of ddH2O. Prior to performing single-cell PCR, 5 µL of 10X Taq buffer [67 mM Tris-HCl, pH 8.5, 2 mM MgCl2, 16.6 mM (NH4)2SO4, and 10 mM β-mercaptoethanol] was added to each tube, and the material heated to 94ºC for 11 min. The tubes were placed on ice, and PCR reagents added to perform a 50 µL reaction (see Daugbjerg et al. 2000, Hansen et al. 2000, Hansen and Daugbjerg 2004 for PCR reagents, reaction conditions, and primer sequences). Despite using a dinoflagellate-specific primer (‘‘Dino-ND’’), the primary PCR reaction provided no visible DNA fragments when loaded onto a 1.5% agarose gel containing ethidium bromide and viewed on a UV light table. Therefore, nested and seminested PCR was performed using 1 µL from the first PCR reaction as template in two new PCR reactions with different sets of primer combinations (D1R-D3B and D3A-28-1483, respectively). The volume, PCR reagents, and temperature profile were identical to those of the primary PCR reactions. However, the nested and seminested PCR reactions only used 18 cycles. Nested and seminested PCR resulted in DNA fragments of correct size based on a molecular marker (viz. Phi X175 HAEIII). All DNA fragments were purified using NucleoFast 96 PCR Kit (Macherey-Nagel GmbH & Co. KG, Düren, Germany), following the manufacturer’s recommendations. PCR product (500 ng) was air-dried overnight and sent to the sequencing service at Macrogen (Seoul, Korea) for determination in both directions using five primers (see Table 1 in Hansen et al. 2007 for primer sequences).

Phylogenetic analyses. A data matrix comprising nuclear-encoded LSU rRNA sequences from 46 species of dinoflagellates was assembled to examine the phylogeny of *T. berolinense*. A diverse assemblage of outgroup taxa were included to polarize the dinoflagellate ingroup. Hence, four ciliates, five

apicomplexans, and *Perkinsus* formed the outgroup. GenBank accession numbers for all species analyzed phylogenetically are given in Figure 7. The data matrix excluded the highly divergent domain D2 (sensu Lenaers et al. 1989) as this DNA fragment was too variable to allow unambiguous alignment among all of the 56 alveolates included. The remaining 1,176 base pairs incorporated information from the secondary structure of the mature RNA molecule forming stems and loops as suggested by de Rijk et al. (2000). The final data matrix was edited manually in MacClade ver. 4.08 (Maddison and Maddison 2003) and analyzed phylogenetically using Bayesian analysis (BA) and maximum likelihood (ML) as implemented in PhyML 3.0 (Guindon and Gascuel 2003). Bayesian analysis (BA) was performed using MrBayes ver. 3.1.2 (Ronquist and Huelsenbeck 2003) with 2 million generations (Ronquist and Huelsenbeck 2003). Every 50th generation, a tree was sampled, and the burnin was evaluated by plotting the LnL values as a function of generations in a spreadsheet. The burn-in occurred after 20,050 generations, and, therefore, 401 trees were discarded, leaving 39,600 trees for estimating posterior probabilities (PP). The PP values were obtained from a 50% majority-rule consensus of the saved trees using PAUP* (Swofford 2003). In ML, we used the parameter settings suggested by MrModeltest ver. 2.3 (Nylander 2004). The ML analysis was run using the online version available on the Montpellier bioinformatics platform located at http:// www/atgc-montpellier.fr/phyml. To evaluate the robustness of the tree topology in ML, we used bootstrapping with 100 replications.

RESULTS

General morphology and tabulation. Cells of *T. berolinense* are generally round, slightly compressed dorsoventrally, and mostly in the range of 20–37 µm long. A large nucleus occupies most of the hypocone, and food items are often seen in the epicone (Figs. 1a and 2a). Chloroplasts and eyespot are absent. Nonswimming, aflagellate stages, during which the theca detaches from the protoplast (so-called temporary cysts), are common. Cells divide into two in the temporary cyst stage, usually before exiting the parent theca. The theca opens

along the cingular-epithecal sutures with the undivided sulcus linking the two halves (Fig. 1b).

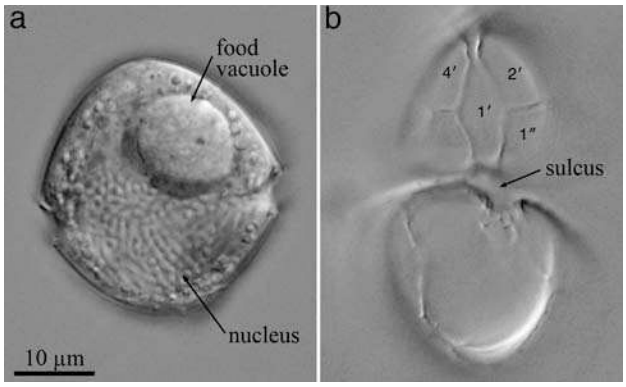

Fig. 1. LM of *Tyrannodinium berolinense*. The scale bar applies to both panels. (a) Optical section through a cell containing a food vacuole with apparently digested contents. (b) Ventral view of open theca showing the epi- and hypotheca linked by the unbroken sulcus.

Details of cell morphology and plate arrangement are shown in Figures 3–5. The longitudinal flagellum and the peduncle (feeding tube) protrude from within a cavity in the upper half of the sulcus, lined externally by an unusual plate called the peduncle cover plate (pc; Figs. 2a; 3, a and b; and 4a).

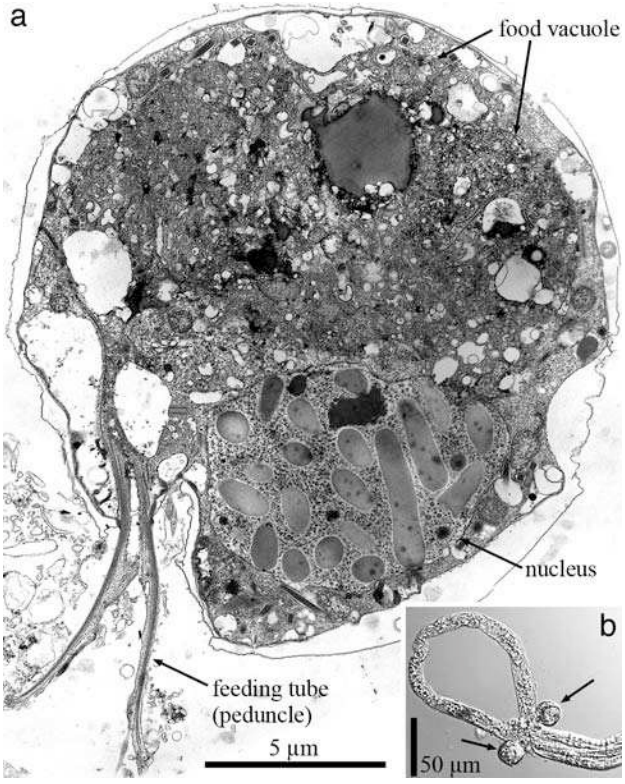

Fig. 2. Feeding *Tyrannodinium berolinense*. (a) TEM of cell fixed while feeding, viewed from the left. (b) Two cells (arrows) feeding on an experimentally injured nematode (details in Calado and Moestrup 1997).

Five other plates are visible in the sulcal area, three of them partially hidden behind the pc (Figs. 4a and 5a). The transverse, undulating flagellum extends to

the cell's left along a nearly circular groove (the cingulum), which is lined by six plates (Figs. 3, a–c; 4a; and 5).

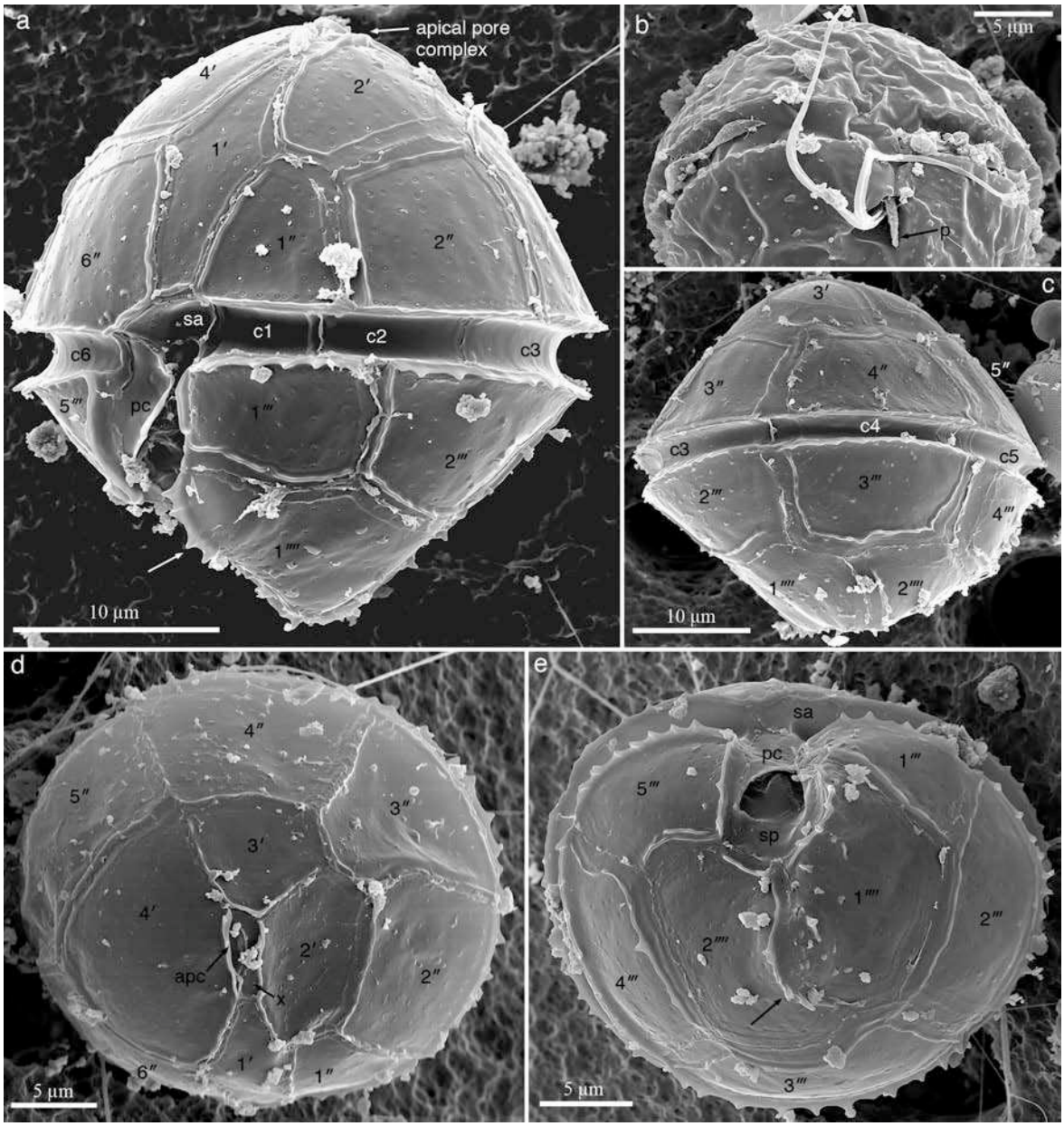

Fig. 3. Morphology and plate arrangement of *Tyrannodinium berolinense* (SEM). (a) Left-ventral view. The peduncle cover plate (pc) is detached on its left edge, probably as an artifact. The arrow points to the spiny flange on the left edge of the sulcus. (b) Ventral-posterior view of a planozygote showing the two longitudinal flagella and the peduncle (p) emerging from the sulcal cavity (preparation schedule 1). (c) Dorsal view. (d) Apical view. (e) Antapical view. The antapical flange is indicated by the arrow. apc, apical pore complex; sa, anterior sulcal plate; sp, posterior sulcal plate.

Large cells with well-developed thecae usually show two granular or spiny flanges, one antapical and another on the posterior left side of the sulcus (Fig. 3, a and e, arrows). An apical pore complex (apc), which is slightly deviated toward the cell's left, tops the epitheca; it comprises three platelets (Figs. 3, a and d; and 4b). Four so-called apical plates are asymmetrically arranged around the apc, with the dorsal, 3′ plate much smaller than its neighbors and somewhat displaced to the cell's left (Figs. 3d and 5c). Six precingular plates complete the epitheca (Figs. 3d and 5c). The hypotheca is made up of the five postcingular and two antapical plates that are typical of peridinioids but is marked by the presence of a wavy suture between the antapical plates (Figs. 3e and 5d).

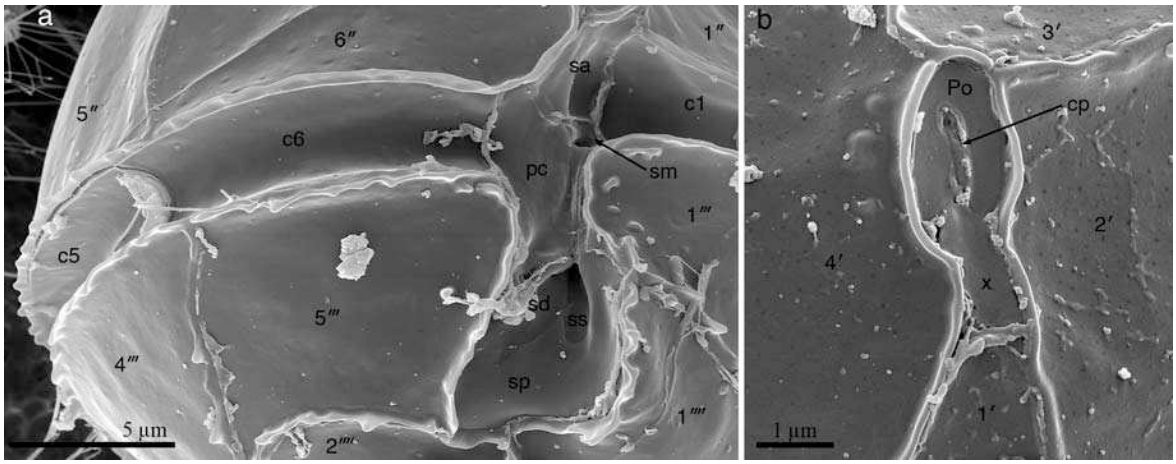

Fig. 4. Details of the sulcal and apical areas (SEM). Plate abbreviations as in Figure 5. (a) Sulcus and ventral-right part of the cingulum. (b) Apical pore complex. cp, closing platelet; pc, peduncle cover plate; Po, pore plate; sa, sd, sm, sp, ss, respectively anterior, right, medium, posterior, and left sulcal plates; x, canal plate.

The flagellar apparatus. Four microtubule-containing roots associate with the flagellar bases (Fig. 6). One microtubule extends from the apical surface of the transverse basal body (TB) and nucleates a dome-shaped row of microtubules directed toward the cell's left (TMR*f*3 and TMRE in Fig. 6, a–e). One multistranded root extends longitudinally beneath the sulcus, and its proximal part is linked through fibrous material to the TB and to a layered structure; the apical part of this layered connective associates with the TB and with a transverse fibrous root that runs along a microtubule (Fig. 6, c–e). A single microtubule

associates with the right-hand side of the longitudinal basal body and arches in a dorsal-posterior direction for about 1 µm (Fig. 6, f and g; for further information on the arrangement and nomenclature of peridinioid flagellar roots, see Calado and Moestrup 2002).

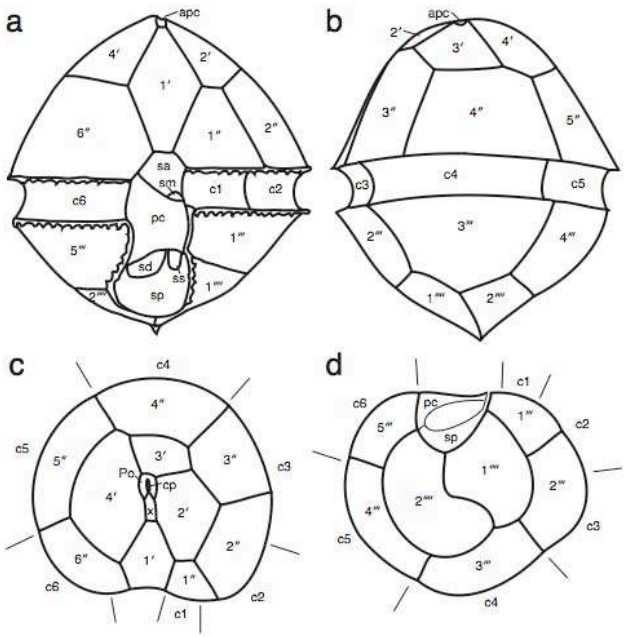

Fig. 5. Diagrammatic view of morphology and plate arrangement. Plate numbering follows Kofoidian notation. Modified from Wołoszyńska (1916, pl. 13, figs. 22, 23, 25, 26). (a) Ventral view. apc, apical pore complex; pc, peduncle cover plate; sa, sulcal anterior; sd, sulcal right; sm, sulcal medium; sp, sulcal posterior; ss, sulcal left. (b) Dorsal view. (c) Apical view. Po, pore plate; cp, closing platelet; x, canal plate. (d) Antapical view.

The sulcal cavity and the peduncle cover plate are shown in oblique section in Figure 6h; the pc is linked along the right edge of the sulcus by a normal plate suture, whereas along the left side, the connection involves numerous thin fibers that extend between the plasma membrane areas covering the parts in contact (Fig. 6i).

LSU rRNA-based phylogeny. Figure 7 illustrates the phylogenetic tree inferred from a Bayesian analysis of nuclear-encoded LSU rRNA sequences from 46 species of dinoflagellates and 10 outgroup taxa comprising ciliates, Apicomplexa, and *Perkinsus*. The phylogenetic analysis revealed that *T. berolinense* formed a highly supported sister taxon to the clade with *Pfiesteria* and *Cryptoperidiniopsis* (PP = 1.0). In ML bootstrap analysis (BS), this relationship was also highly supported (BS = 100%). The coccoid species *Thoracosphaera heimii* formed a highly supported sister to *Tyrannodinium* and the two pfiesteriacean species (PP = 1.0, BS = 93%). *Scrippsiella trochoidea* and *Peridiniopsis polonica*

made a highly supported sister group to the clade comprising *Thoracosphaera*, *Tyrannodinium*, and the pfiesteriaceans (PP = 1.0, BS = 95%). The type species of the genus *Peridiniopsis*, *P. borgei*, was also included in this study, and it was related to three species of *Peridinium* (*P. willei*, *P. cinctum*, and *P. palatinum*). However, this topology was poorly supported by the posterior probability in BA (PP = 0.59) and not at all in ML bootstrap analysis (<50%). Yet *P. borgei* was distantly related to *T. berolinense* (=*P. berolinensis*). The most divergent branches for the dinoflagellate ingroup formed a large polytomy (i.e., no support for the tree topology).

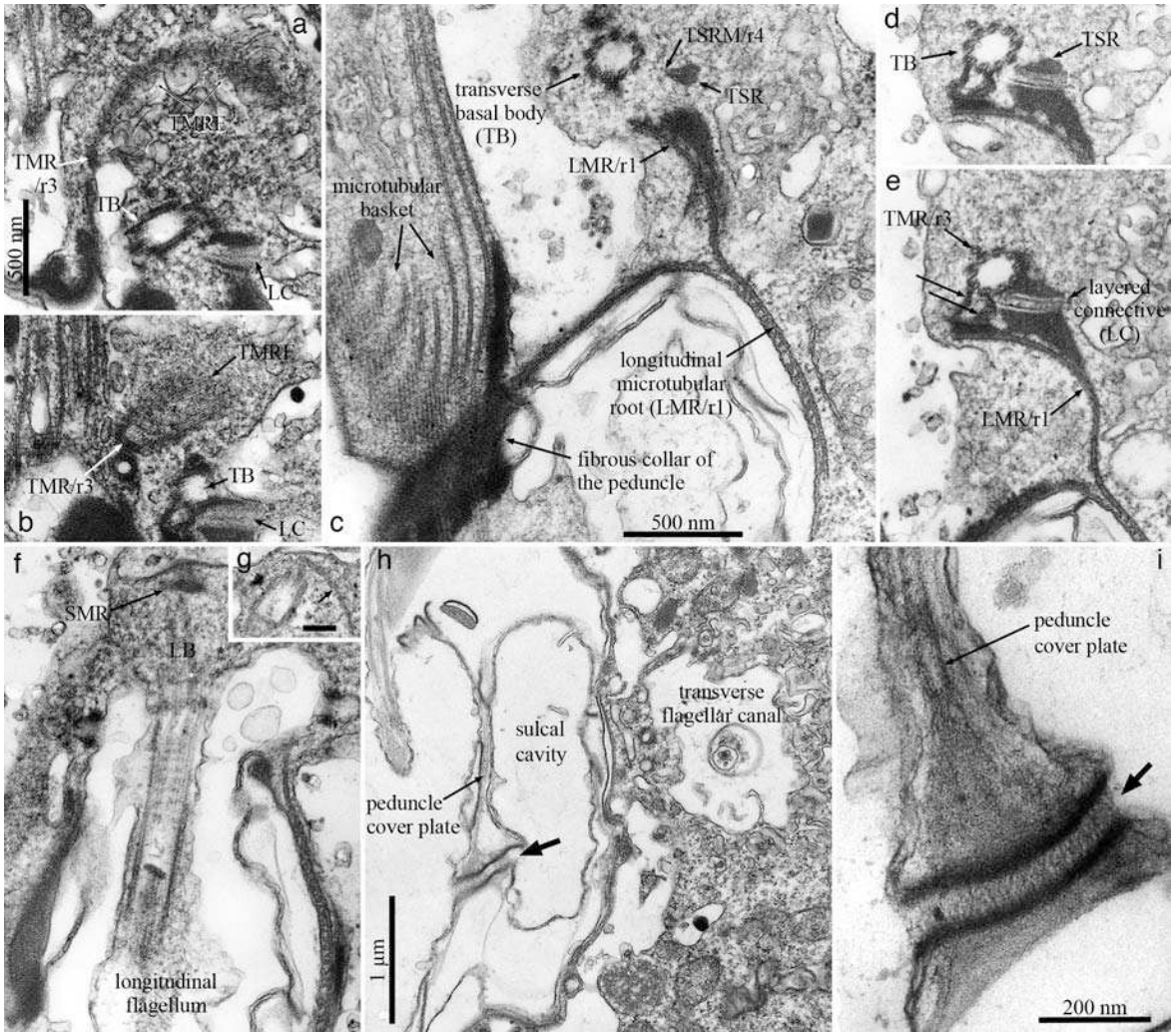

Fig. 6. Flagellar apparatus of *Tyrannodinium berolinense* (TEM). Sections from two series progressing from left to right with the cell's longitudinal axis slightly more tilted toward the observer in panels (a, b, g). (a, b) The arched microtubular extension (TMRE) of the transverse microtubular

root (TMR／r3). (c–e) Roots on the left side of the basal bodies and their interconnections. Two fibrous connectives link the transverse basal body (TB) to electron-opaque material on the dorsal side of the longitudinal microtubular root (LMR) (arrows). Both the TB and the transverse striated root (TSR) are connected to the LMR through a layered connective (LC). (f, g) The single microtubule (arrows) associating with the right-hand side of the longitudinal basal body (LB). (h, i) Oblique section through the sulcal cavity showing the unusual fibrous connection along the left edge of the peduncle cover plate (thick arrows).

The estimated sequence divergence between *T. berolinense*, *Pfiesteria piscicida*, and *Cryptoperidiniopsis brodyi* is given in Table 1. *P. piscicida* and *C. brodyi* diverged from each other by only 3.3%, whereas *T. berolinense* diverged from both species by about 5%. This sequence divergence is also reflected in the branching topology among these dinoflagellates (Fig. 7). A significantly higher sequence divergence was estimated when comparing *Tyrannodinium*, *Pfiesteria*, and *Cryptoperidiniopsis* to *Peridiniopsis*. Here, the divergence was 16%–18%.

Table 1. Sequence divergence estimates. Uncorrected ("p") distances are given above the diagonal in percentage.

	Tyrannodinium berolinense	*Pfiesteria piscicida*	*Cryptoperidiniopsis brodyi*	*Peridiniopsis borgei*
T. berolinense	—	5.0	4.9	17.8
P. piscicida		—	3.3	16.5
C. brodyi			—	17.36
P. borgei				—

DISCUSSION

Ultrastructure. Four flagellar roots with the characteristics shown here for *T. berolinense* have previously been found in the peridinioid species analyzed (Calado et al. 1999, Calado and Moestrup 2002). Roots 1, 3, and 4 are present in nearly all dinoflagellates examined, both naked and thecate, whereas the distribution of root 2 seems restricted to two thecate groups (gonyaulacoids and peridinioids; Hansen et al. 1996, Calado and Moestrup 2002) and some woloszynskioids, for example, the recently described *Baldinia anauniensis* Gert Hansen et Daugbjerg (Hansen et al. 2007). In contrast, the layered connective

linking roots 1 and 4, and the proximal portion of the TB, apparently replacing the more slender and widespread striated root connective of other dinoflagellates (src; e.g., Calado et al. 2006), has only been found in peridinioids and in *Kryptoperidinium foliaceum*, a species containing a diatom type of symbiont (Dodge and Crawford 1969).

The microtubules associated with peduncle formation and the two well-defined fibers linking r1 to the TB suggest a closer relationship of *T. berolinense* to *P. borgei* than to *P. cinctum*, which lacks these features (Calado et al. 1999, Calado and Moestrup 2002). However, the peduncle in *P. borgei* is a flat structure rather than a tube, and its supporting microtubules are arranged in a single row that turns around the upper-left side of the cell before dividing consecutively into two and four smaller rows, ending near a large central vesicle (Calado and Moestrup 2002). The cylindrical arrangement of 23 microtubules of the TMRE, surrounding a rod of fibrous material, is so far also known exclusively from P. borgei (Calado and Moestrup 2002) and contrasts with the simple and much shorter domeshaped extension to r3 found in *T. berolinense*.

The parallel arrangement of basal bodies and some flagellar roots in a planozygote of *T. berolinense* was documented by Wedemayer and Wilcox (1984). This finding is consistent with the organization described in detail for the planozygote of *Esoptrodinium gemma* (=*Bernardinium bernardinense*; Calado et al. 2006), although it is not known whether both transverse flagella also converge to a single flagellar canal in *Tyrannodinium*.

Studies on previously unrecognized pfiesteriaceans. The attraction to injured organisms and the mechanisms of capture, food uptake, and the underlying ultrastructural features, as reported for *T. berolinense* (Calado and Moestrup 1997), are remarkably similar to those described from a brackish water species examined in detail by Spero in the 1980s under the name *Gymnodinium fungiforme* (Spero and Morée 1981, Spero 1982, 1985). Although it is clear that *G. fungiforme* sensu Spero is a pfiesteriacean, the lack of diagnostic tabulation features makes it impossible to decide whether it belongs to any of the other named species of the group.

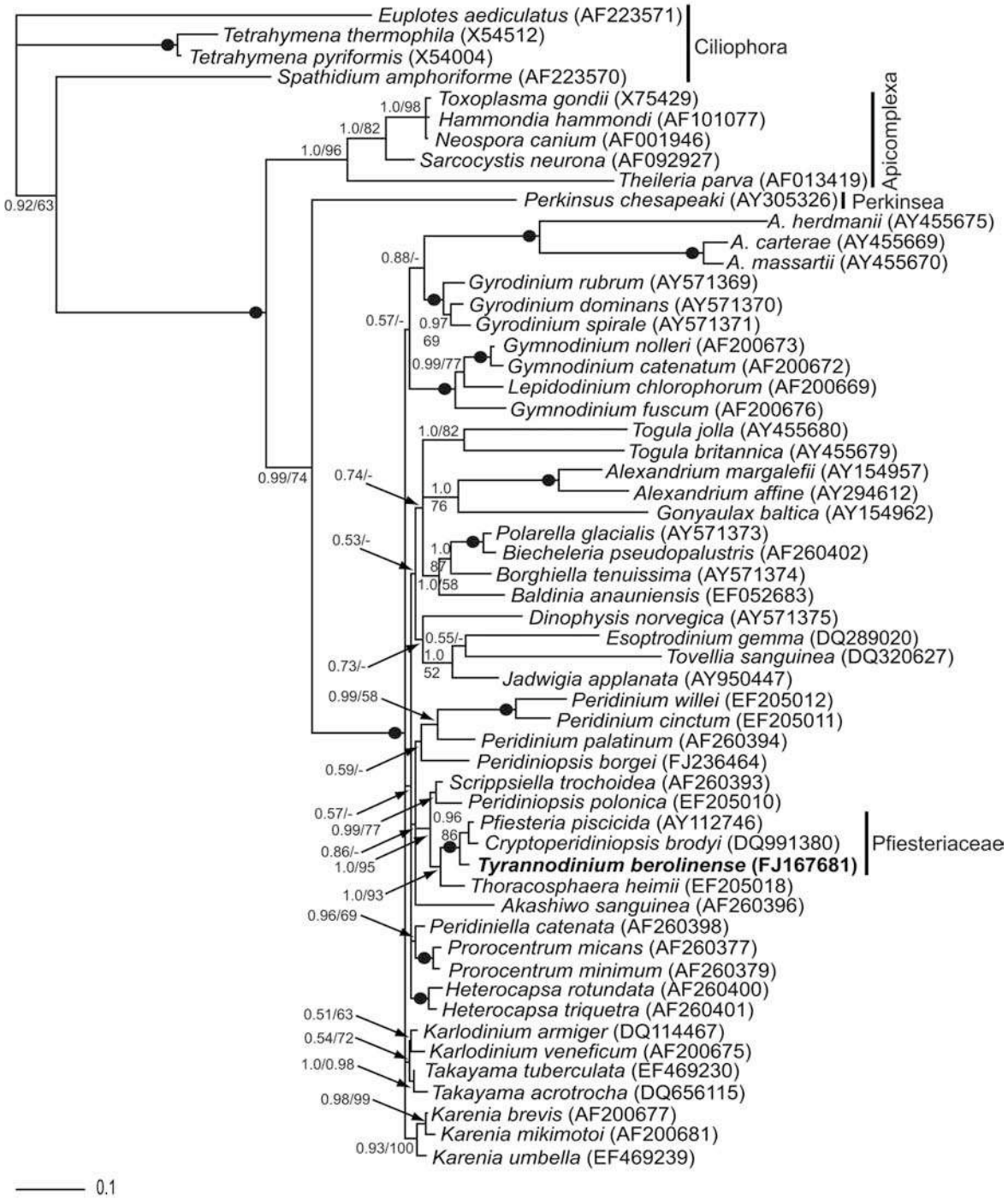

Fig. 7. Phylogeny of *Tyrannodinium berolinense* inferred from Bayesian analysis of nuclear-encoded LSU rRNA sequences from 46 species of dinoflagellates. Four ciliates, five apicomplexans, and *Perkinsus* formed the outgroup taxa. The first numbers to the left of internal nodes are posterior probabilities from Bayesian analysis. The last numbers are bootstrap values (>50%) from maximum likelihood (PhyML) with 100 replicates. GenBank accession numbers are

written in parentheses. Three species belonging to the genus *Amphidinium* are listed as *A. herdmanii*, *A. carterae*, and *A. massartii* due to space limitations.

As originally described from Russian waters by Anisimova (1926), *G. fungiforme* resembles the unnamed isolate known as ‘‘Bullet’’ (ODU034, VDH034S, Seaborn et al. 2006, fig. 1, E and F).

Comparison with other pfiesteriaceans. The single most notable feature of the pfiesteriaceans is undoubtedly their physiology. All known species are predators or ectoparasites, while autotrophy remains unknown. The genera *Pfiesteria*, *Pseudopfiesteria*, *Tyrannodinium*, *Cryptoperidiniopsis*, *Paulsenella*, *Luciella*, and *Stoeckeria* share many characteristics, including cell structure, way of swimming, and the food-uptake mechanism employed. They are morphologically very similar in average size and shape, although size varies considerably depending on how recently food uptake has taken place. The nucleus fills most of the hypocone. Cells congregate and swarm around the prey, which may be unicellular protists (algae and protozoa), injured metazoans, or fish. In culture, blood cells (fish or human blood cells) have been used as food. The species exhibit a characteristic mode of swimming, comprising a rotating movement near the prey, the axis of movement being the dorsoventral cell axis (*Paulsenella*: Drebes and Schnepf 1982; *Cryptoperidiniopsis*: Parrow and Burkholder 2003a; *Tyrannodinium*: Calado and Moestrup 1997—see also Movies S1 and S2 in the supplementary material). The way of attachment is only documented in a few cases, but an attachment filament has been shown to be present in *T. berolinensis* (Calado and Moestrup 1997) and *Luciella masanensis* (Jeong et al. 2007). Whether trichocysts are involved in prey capture remains unknown, but trichocysts are known to be present in *Pfiesteria* (Steidinger et al. 1996), *Tyrannodinium* (Calado and Moestrup 1997), and *Paulsenella* (Schnepf et al. 1985).

Cells are attracted to their prey by chemotaxis, documented so far in *Paulsenella* (Schnepf and Drebes 1986), *Tyrannodinium* (Calado and Moestrup 1997), *Pseudopfiesteria* (Vogelbein et al. 2002), *Cryptoperidiopsis brodyi* (Steidinger et al. 2006), and *Gymnodinium fungiforme* (Spero 1985). It is likely to be a characteristic of most if not all members of the family, and cells are attracted

by many organic compounds. For a detailed account, see Vogelbein et al. (2002). Once contact has been established with the prey, food is sucked up through a feeding tube supported internally by overlapping rows of microtubules, also known as a ‘‘microtubular basket.’’ This structure is presently known from *Paulsenella* (Schnepf et al. 1985), *Gymnodinium fungiforme* (Spero 1982), *Tyrannodinium* (Calado and Moestrup 1997), *Pfiesteria* (Litaker et al. 2002), *Pseudopfiesteria* (Marshall et al. 2006), and *Amyloodinium* (Lom and Lawler 1973). In *Amyloodinium*, the microtubular basket develops into the ‘‘tentacle’’ or ‘‘root-like process’’ described by Brown and Hovasse (1946). The microtubular basket is probably a characteristic of the family, although it may not be confined to the Pfiesteriaceae. The term was coined for another heterotrophic species, *Crypthecodinium cohnii*, by Kubai and Ris (1969), and although the information on the phylogenetic relationships of this species is contradictory, there is no indication that it is phylogenetically related to the Pfiesteriaceae (e.g., Murray et al. 2005, Parrow et al. 2006). The microtubular basket was also illustrated in strains from South Africa identified as *Gyrodinium lebouriae* (Lee 1977), but the phylogenetic relationships of this material remain unknown.

Amyloodinium ocellatum stands out from the other members of the Pfiesteriaceae in several respects, notably its complex life cycle, which includes a pyriform, so-called trophont, attached to fish gills and skin by a basal, flattened plate from whose borders numerous rhizoids penetrate into the host (Lom and Lawler 1973). The trophont stage changes into a cyst (tomont) the contents of which divide into as many as 256 motile cells (dinospores) that serve as the infection stage. Other pfiesteriaceans appear to have a different life cycle, comprising only the motile vegetative feeding cell, gametes, and cysts. The cyst is the meiotic stage (recognized by nuclear cyclosis), and the cyst contents divide into 2, 4, or 8 cells, which are released as motile, haploid feeding cells (Litaker et al. 2002, Parrow and Burkholder 2003b, 2004). In the SSU rRNA molecular tree published by Litaker et al. (1999), *Amyloodinium* forms a sister group to the other pfiesteriaceans.

Structurally, members of the Pfiesteriaceae differ from other dinoflagellates most particularly in the presence of a distinct plate, sometimes known as the

peduncle cover plate, covering the proximal part of the sulcus. It has been found in all species examined in detail, but it does not, to our knowledge, occur outside the family. We speculate that its function may be to confer structural support to the proximal part of the peduncle, which is an area of intense activity during feeding. A comparative overview of the epithecal tabulations of known pfiesteriacean genera is given in Figure 8.

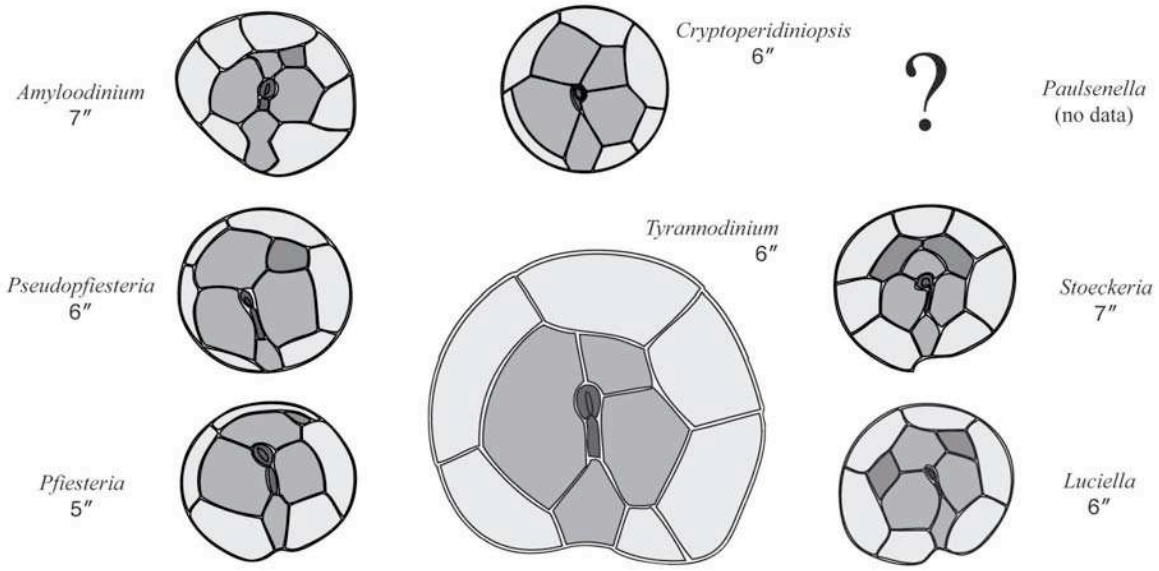

Fig. 8. Pfiesteriacean epithecal tabulations. Kofoidian series of plates are shown in different gray tones. Adapted from Landsberg et al. (1994, *Amyloodinium*), Steidinger et al. (2006, *Cryptoperidiniopsis*), Mason et al. (2007, *Luciella*), Litaker et al. (2005, *Pfiesteria* and *Pseudopfiesteria*), Jeong et al. (2005, *Stoeckeria*), and Wołoszyńska (1916, *Tyrannodinium*).

We conclude that *T. berolinense* is a freshwater member of the Pfiesteriaceae. It represents yet another case of a branch of dinoflagellates having left the marine environment in which the group originated to enter freshwater (cf. Logares et al. 2007). *T. berolinense* cells may be locally numerous, and numbers as high as 600,000 cells · L^{-1} have been recorded (B. Meyer in Weisse and Kirchhoff 1997). It has been assessed to feed on cryptomonad cells at a rate of 0.7–0.8 cells · h^{-1} for moderately starved cells (Weisse and Kirchhoff 1997), making it quantitatively important for the energy budget of the freshwater systems, especially when occurring in bloom proportions. Toxicity has not been documented.

TAXONOMIC DESCRIPTIONS

***Tyrannodinium* Calado, Craveiro, Daugbjerg et Moestrup gen. nov.**

Dinoflagellati heterotrophi, aquae dulcis, cibum haurientes nutritorio canale sustento microtubulorum ordinibus impositis. Nucleus commune dinokaryon est atque fere omnem hypoconum occupat. Cellulae theca satis subtili tectae, formula kofoidiana thecarum Po, cp, x, 4′, 0a, 6″, 6c, pc, 5+ s, 5‴, 0p, 2‴″. Cingulum equatoriale, quasi circulare, leviter motum. Cellulae divisio in cystis caducis fit. Theca iuxta cinguli superiorem marginem patet. Per sexum procreatio planozygotae duobus flagellis longitudinalibus gignit. Hypnozygota ignota.

Freshwater, heterotrophic dinoflagellates that ingest food through a feeding tube supported by overlapping rows of microtubules. Nucleus a typical dinokaryon, occupying most of the hypocone. Cells covered by a relatively thin theca with the Kofoidian plate formula Po, cp, x, 4′, 0a, 6″, 6c, pc, 5+ s, 5‴, 0p, 2‴″. Cingulum equatorial, nearly circular, with small displacement. Cell division in temporary cysts, theca opening along upper edge of the cingulum. Sexual reproduction resulting in planozygotes with two longitudinal flagella. Hypnozygote unknown.

Type species: Tyrannodinium berolinense (Lemmermann) Calado, Craveiro, Daugbjerg et Moestrup comb. nov., designated here.

Etymology: Latin *tyrannus* (from Greek τυραννος), ‘‘tyrant,’’ in allusion to the ruthless feeding behavior. The termination –*dinium*, originally from Greek δινη, ‘‘vortex,’’ is commonly applied to dinoflagellates.

***Tyrannodinium berolinense* (Lemmermann) Calado, Craveiro, Daugbjerg et Moestrup comb. nov.**

Basionym: Peridinium berolinense Lemmermann 1900 Ber. Deutsch. Bot. Ges. 18, p. 308 (no figure).

Neotype: Since Lemmermann (1900) did not provide an illustration and no original material is extant, the name *P. berolinense* has no type. The illustrations provided by Lemmermann (1910, figs. 17– 20 on p. 672) included a ventral and an antapical view of the cell but did not show the epithecal tabulation. Wołoszyńska (1916, pl. 13, figs. 22–26) provided a group of figures accurately representing morphology and tabulation of the species. Identification guides have repeatedly reproduced Wołoszyńska’s drawings, solidly linking them to our concept of the

species. Figure 5 is based on Wołoszyńska's figures, modified to include all the plates as shown by modern methods. We therefore designate Figure 5 as the type of *P. berolinense*.

Homotypic synonyms: Glenodinium berolinense (Lemmermann) Er. Lindemann (1925, pp. 162, 164); *Peridiniopsis berolinensis* (Lemmermann) Bourrelly (1968, p. 9).

***Tyrannodinium berolinense* var. *apiculatum* (Lemmermann) Calado, Craveiro, Daugbjerg et Moestrup comb. nov.**

Basionym: Peridinium berolinense var. *apiculatum* Lemmermann in West (1907, p. 188, pl. 9, fig. 3).

Note: This rarely reported form was described with a more conical epicone than the type and a concave antapex provided with two spines. Although the stability of these characters is uncertain, the size range given by Lemmermann (West 1907), 41–42 x 40– 41 µm, exceeds the dimensions we found in large planozygotes. Wołoszyńska (1916), who also recognized the taxon, reported a tabulation similar to the type, but represented a cell with a pointed, rather than concave, antapex.

We thank Dr. Elżbieta Wilk-Woźniak and Prof. Konrad Wołowski, Cracow, for assistance and hospitality when visiting and collecting near Cracow, Poland, August 2007. We acknowledge financial assistance as grants from the financing program POCI, Portugal to S. C. C. (SFRH ⁄BD ⁄ 16794 ⁄ 2004), and from the Villum-Kann Rasmussen Foundation to Ø. M. Prof. Antonella Inama, Trentino, Italy, kindly prepared the Latin diagnosis. We thank Ramiro Logares for sending an extracted DNA sample of *Peridiniopsis borgei*.

REFERENCES

Anisimova, N. W. 1926. Novye Peridineae, naĭdennye v solenykh vodoemakh Staroĭ Russy (Novgorod. gub.). *Russ. Gidrobiol. Zhurn.* 5:188-92 [in Russian; German version on pp. 192-3: Neue Peridineae aus den Salzgewässern von Staraja Russa (Gouv. Nowgorod).]

Bourrelly, P. 1968. Notes sur les Péridiniens d'eau douce. *Protistologica* 4:5-13.

Brown, E. R. & Hovasse, R. 1946. *Amyloodinium ocellatum* Brown, a peridinian parasite on marine fishes. A complementary study. *Proc. Zool. Soc. Lond.* 116:33-46.

Burkholder, J. M., Noga, E. J., Hobbs, C. W., Glasgow, H. B. Jr. & Smith, S. A. 1992. New 'phantom' dinoflagellate is the causative agent of major estuarine fish kills. *Nature* 358:407-10.

Calado, A. J., Craveiro, S. C., Daugbjerg, N. & Moestrup, Ø. 2006. Ultrastructure and LSU rDNA-based phylogeny of *Esoptrodinium gemma* (Dinophyceae), with notes on feeding behavior and the description of the flagellar base area of a planozygote. *J. Phycol.* 42:434-52.

Calado, A. J., Hansen, G. & Moestrup, Ø. 1999. Architecture of the flagellar apparatus and related structures in the type species of *Peridinium*, *P. cinctum* (Dinophyceae). *Eur. J. Phycol.* 34:179-91.

Calado, A. J. & Moestrup, Ø. 1997. Feeding in *Peridiniopsis berolinensis* (Dinophyceae): new observations on tube feeding by an omnivorous, heterotrophic dinoflagellate. *Phycologia* 36:47-59.

Calado, A. J. & Moestrup, Ø. 2002. Ultrastructural study of the type species of *Peridiniopsis*, *Peridiniopsis borgei* (Dinophyceae), with special reference to the peduncle and flagellar apparatus. *Phycologia* 41:567-84.

Daugbjerg, N., Hansen, G., Larsen, J. & Moestrup, Ø. 2000. Phylogeny of some of the major genera of dinoflagellates based on ultrastructure and partial LSU rDNA sequence data, including the erection of three new genera of naked dinoflagellates. *Phycologia* 39:302-17.

Dodge, J. D. & Crawford, R. M. 1969. Observations on the fine structure of the eyespot and associated organelles in the dinoflagellate *Glenodinium foliaceum*. *J. Cell Sci.* 5:479-93.

Drebes, G. & Schnepf, E. 1982. Phagotrophy and development of *Paulsenella* cf. *chaetoceratis* (Dinophyta), an ectoparasite of the diatom *Streptotheca thamesis*. *Helgol. Meeresunter.* 35:501-14.

Elbrächter, M., Gottschling, M., Hildebrand-Habel, T., Keupp, H., Kohring, R., Lewis, J., Meier, K. J. S. et al. 2008. Establishing an agenda for calcareous dinoflagellate research (Thoracosphaeraceae, Dinophyceae) including a nomenclatural synopsis of generic names. *Taxon* 57:1289-303.

Gottschling, M., Keupp, H., Plötner, J., Knop, R., Willems, H. & Kirsch, M. 2005. Phylogeny of calcareous dinoflagellates as inferred from ITS and ribosomal sequence data. *Mol. Phylogenet. Evol.* 36:444-55.

Guindon, S. & Gascuel, O. 2003. A simple, fast, and accurate algorithm to estimate large phylogenies by maximum likelihood. *Syst. Biol.* 52:694-704.

Hansen, G. & Daugbjerg, N. 2004. Ultrastructure of *Gyrodinium spirale*, the type species of *Gyrodinium* (Dinophyceae), including a phylogeny of *G. dominans*, *G. rubrum* and *G. spirale* deduced from partial LSU rDNA sequences. *Protist* 155:271-94.

Hansen, G., Daugbjerg, N. & Henriksen, P. 2000. Comparative study of *Gyrodinium mikimotoi* and *Gymnodinium aureolum*, comb. nov. (=*Gyrodinium aureolum*), based on morphology, pigment composition, and molecular data. *J. Phycol*. 36:394-410.

Hansen, G., Daugbjerg, N. & Henriksen, P. 2007. *Baldinia anauniensis* gen. et sp. nov.: a 'new' dinoflagellate from Lake Tovel, N. Italy. *Phycologia* 46:86-108.

Hansen, G., Moestrup, Ø. & Roberts, K. R. 1996. Fine structural observations on *Gonyaulax spinifera* (Dinophyceae), with special emphasis on the flagellar apparatus. *Phycologia* 35:354-66.

Jeong, H. J., Kim, J. S., Park, J. Y., Kim, J. H., Kim, S., Lee, I., Lee, S. H., Ha, J. H. & Yih, W. H. 2005. *Stoeckeria algicida* n. gen., n. sp. (Dinophyceae) from the coastal waters off southern Korea: morphology and small subunit ribosomal DNA gene sequence. *J. Eukaryot. Microbiol*. 52:382-90.

Jeong, H. J., Ha, J. H., Yoo, Y. D., Park, J. Y., Kim, J. H., Kang, N. S., Kim, T. H., Kim, H. S., & Yih, W. H. 2007. Feeding by the *Pfiesteria*-like heterotrophic dinoflagellate *Luciella masanensis*. *J. Eukaryot. Microbiol.* 54:231-41.

Kubai, D. F. & Ris, H. 1969. Division in the dinoflagellate *Gyrodinium cohnii* (Schiller). A new type of nuclear reproduction. *J. Cell Biol*. 40:508-28.

Kühn, S. F. & Medlin, L. K. 2005. The systematic position of the parasitoid marine dinoflagellate *Paulsenella vonstoschii* (Dinophyceae) inferred from nuclear-encoded small subunit ribosomal DNA. *Protist* 156:393-8.

Landsberg, J. H., Steidinger, K. A., Blakesley, B. A. & Zondervan, R. L. 1994. Scanning electron microscope study of dinospores of *Amyloodinium* cf. *ocellatum*, a pathogenic dinoflagellate parasitic of marine fish, and comments on its relationship to the Peridiniales. *Dis. Aquat. Org.* 20:23-32.

Lee, R. E. 1977. Saprophytic and phagocytic isolates of the colourless heterotrophic dinoflagellate *Gyrodinium lebourae* Herdman. *J. Mar. Biolog. Assoc. U.K*. 57:303-15.

Lemmermann, E. 1900. Beiträge zur Kenntniss der Planktonalgen. X. Diagnosen neuer Schwebalgen. *Ber. Deutsch. Bot. Ges*. 18:306-10.

Lemmermann, E. 1910. *Kryptogamenflora der Mark Brandenburg. Bd. 3. Algen I (Schizophyceen, Flagellaten, Peridineen).* Gebrüder Bornträger, Leipzig, 712 pp.

Lenaers, G., Maroteaux, L., Michot, B. & Herzog, M. 1989. Dinoflagellates in evolution. A molecular phylogenetic analysis of large subunit ribosomal RNA. *J. Mol. Evol.* 29:40-51.

Lindemann, E. 1925. III. Klasse: Dinoflagellatae (Peridineae). In *[Eyferth's] Einfachste Lebensformen des Tier- und Pflanzenreiches*, 5th ed., vol. 1 (ed. W. Schoenichen), pp. 144-95. Berlin: Bermühler.

Litaker, R. W., Steidinger, K. A., Mason, P. L., Landsberg, J. H., Shields, J. D., Reece, K. S., Haas, L. W. et al. 2005. The reclassification of *Pfiesteria shumwayae*: *Pseudopfiesteria*, gen. nov. *J. Phycol.* 41:643-51.

Litaker, R. W., Tester, P. A., Colorni, A., Levy, M. G. & Noga, E. J. 1999. The phylogenetic relationship of *Pfiesteria piscida*, cryptoperidiniopsoid sp. *Amyloodinium ocellatum* and a *Pfiesteria*-like dinoflagellate to other dinoflagellates and apicomplexans. *J. Phycol*. 35:1379-89.

Litaker, R. W., Vandersea, M. W., Kibler, S. R., Madden, V. J., Noga, E. J. & Tester, P. A. 2002. Life cycle of the heterotrophic dinoflagellate *Pfiesteria piscicida* (Dinophyceae). *J. Phycol.* 38:442-63.

Logares, R., Shalchian-Tabrizi, K., Boltovskoy, A. & Rengefors, K. 2007. Extensive dinoflagellate phylogenies indicate infrequent marine-freshwater transitions. *Mol. Phylogenet. Evol.* 45:887-903.

Lom, J. & Lawler, A. R. 1973. An ultrastructural study on the mode of attachment in dinoflagellates invading gills of Cyprinodontidae. *Protistologica* 9:293-309.

Maddison, D. R. & Maddison, W. P. 2003. *MacClade 4.* Sinauer Associates, Inc. Publishers. Sunderland, Massachusetts, U.S.A.

Marshall, H. G., Hargraves, P. E., Burkholder, J. M., Parrow, M. W., Elbrächter, M., Allen, E. H., Knowlton, V. M. et al. 2006. Taxonomy of *Pfiesteria* (Dinophyceae). *Harmful Algae* 5:481-96.

Mason, P. L., Litaker, R. W., Jeong, H. J., Ha, J. H., Reece, K. S., Stokes, N. A., Park, J. Y. et al. 2007. Description of a new genus of *Pfiesteria*-like dinoflagellate, *Luciella* gen. nov. (Dinophyceae), including two new species: *Luciella masanensis* sp. nov. and *Luciella atlantis* sp. nov. *J. Phycol.* 43:799-810.

Murray, S., Jørgensen, M. F., Ho, S.Y.W., Patterson, D.J. & Jermiin, L.S. 2005. Improving the analysis of dinoflagellate phylogeny based on rDNA. *Protist* 156:269–86.

Nylander, J. A. A. 2004. MrModeltest v2. Program distributed by the author. Evolutionary Biology Centre, Uppsala University.

Parrow, M. W. & Burkholder, J. M. 2003a. Estuarine heterotrophic cryptoperidiniopsoids (Dinophyceae): life cycle and culture studies. *J. Phycol*. 39:678-96.

Parrow, M. W. & Burkholder, J. M. 2003b. Reproduction and sexuality in *Pfiesteria shumwayae* (Dinophyceae). *J. Phycol*. 39:697-711.

Parrow, M. W. & Burkholder, J. M. 2004. The sexual cycles of *Pfiesteria piscicida* and cryptoperidiniopsoids (Dinophyceae). *J. Phycol*. 40:664-73.

Parrow, M. W., Elbrächter, M., Krause, M. K., Burkholder, J. M., Deamer, N. J., Htyte, N. & Allen, E. H. 2006. The taxonomy and growth of a *Crypthecodinium* species (Dinophyceae) isolated from a brackish-water fish aquarium. *Afr. J. Mar. Sci*. 28:185-91.

Place, A. R., Saito, K., Deeds, J. R., Robledo, J. A. F. & Vasta, J. R. 2008. A decade of research on *Pfiesteria* spp. and their toxins: unresolved questions and an alternative hypothesis. *Seafood and freshwater toxins: pharmacology, physiology, and detection* 2nd edition, CRC Press.

de Rijk, P., Wuyts, J., van der Peer, Y., Winkelmans, T. & de Wachter, R. 2000. The European large subunit ribosomal RNA database. *Nucleic Acids Res.* 28:117-8.

Ronquist, F. & Huelsenbeck, J. P. 2003. Mr. Bayes 3: Bayesian phylogenetic inference under mixed models. *Bioinformatics* 19:1572-4.

Schnepf, E., Deichgräber, G. & Drebes, G. 1985. Food uptake and the fine structure of the dinophyte *Paulsenella* sp., an ectoparasite of marine diatoms. *Protoplasma* 124:188-204.

Schnepf, E. & Drebes, G. 1986. Chemotaxis and appetence of *Paulsenella* sp. (Dinophyta), an ectoparasite of the marine diatom *Streptotheca thamesis* Shrubsole. *Planta* 167:337-43.

Seaborn, D. W., Tengs, T., Cerbin, C., Kokocinsky, M. & Marshall, H. G. 2006. A group of dinoflagellates similar to *Pfiesteria* as defined by morphology and genetic analysis. *Harmful Algae* 5:1-8.

Senzaki, S. & Horiguchi, T. 1994. A taxonomic survey of freshwater dinoflagellates of Nagano prefecture, Japan. *Jpn. J. Phycol.* 42:29-42.

Spero, H. J. 1982. Phagotrophy in *Gymnodinium fungiforme* (Pyrrhophyta): the peduncle as an organelle of ingestion. *J. Phycol.* 18:356-60.

Spero, H. J. 1985. Chemosensory capabilities in the phagotrophic dinoflagellate *Gymnodinium fungiforme*. *J. Phycol.* 21:181-4.

Spero, H. J. & Morée, M. D. 1981. Phagotrophic feeding and its importance to the life cycle of the holozoic dinoflagellate, *Gymnodinium fungiforme*. *J. Phycol*. 17:43-51.

Steidinger, K. A., Burkholder, J. M., Glasgow, H. B. Jr., Hobbs, C. W., Garrett, J. K., Truby, E. W., Noda, E. J. & Smith, E. A. 1996. *Pfiesteria piscicida* gen. et sp. nov. (Pfiesteriaceae fam. nov), a new toxic dinoflagellate with a complex life cycle and behavior. *J. Phycol*. 32:157-64.

Steidinger, K. A., Landsberg, J. H., Mason, P. L. Vogelbein, W. K., Tester, P. A. & Litaker, R. W. 2006. *Cryptoperidiniopsis brodyi* gen. et sp. nov., (Dinophyceae), a small lightly armored dinoflagellate in the Pfiesteriaceae. *J. Phycol*. 42:951-61.

Swofford, D. L. 2003. PAUP* Phylogenetic analysis using parsimony (*and other methods). Version 4. Sinauer Associates, Sunderland, Massachusetts.

Thompson, R. H. 1951. A new genus and new records of fresh-water Pyrrophyta in the Desmokontae and Dinophyceae. *Lloydia* 13:277-99.

Vogelbein, W. K., Lovko, V. J., Shields, J. D., Reece, K. S., Mason, P. L., Haas, L. W. & Walker, C. C. 2002. *Pfiesteria shumwayae* kills fish by micropredation not exotoxin secretion. *Nature* 418:967-70.

Wedemayer, G. J. & Wilcox, L. W. 1984. The ultrastructure of the freshwater colorless dinoflagellate *Peridiniopsis berolinense* (Lemm.) Bourrelly. *J. Protozool.* 31:444-53.

Weisse, T. & Kirchhoff, B. 1997. Feeding of the heterotrophic freshwater dinoflagellate *Peridiniopsis berolinense* on cryptophytes: analysis by flow cytometry and electronic particle counting. *Aquat. Microb. Ecol*. 12:153-64.

West, G. S. 1907. Report on the freshwater algae, including phytoplankton, of the third Tanganyika expedition conducted by Dr. W. A. Cunnington, 1904-1905. *J. Linn. Soc., Bot.* 38:81-197.

Wołoszyńska, J. 1916. Polskie Peridineae słodkowodne. — Polnische Süßwasser-Peridineen. *Bull. Int. Acad. Sci. Cracovie, Cl. Sci. Math. et Nat., sér. B, Sci. Nat.* 1915:260-85.

SUPPLEMENTARY MATERIAL

The following supplementary material is available for this article:

Movie S1. *Tyrannodinium berolinense* precapture and feeding behavior. Cells exhibiting precapture rotation and attaching to an injured rotifer (0–50 s). Cell attaching to punctured spot on nematode, deploying the feeding tube and repeatedly pulling at it, revealing an apparently empty vesicle in the epicone before any visible uptake of food takes place (50–1’51 s).

Movie S2. *Tyrannodinium berolinense* feeding on punctured nematode. Food uptake in ventral view (0–26 s). Cell feeding on tip of extruded nematode gut, showing feeding tube flexibility (26–1’17 s). Food leaking out of feeding tube and being pulled back in, ventral view (1’17–1’45 s).

CHAPTER 5

ULTRASTRUCTURE AND LARGE SUBUNIT RDNA-BASED PHYLOGENY OF *SPHAERODINIUM CRACOVIENSE*, AN UNUSUAL FRESHWATER DINOFLAGELLATE WITH A NOVEL TYPE OF EYESPOT

Craveiro, S.C., Moestrup, Ø., Daugbjerg, N. & Calado, A.J. 2010. Ultrastructure and Large Subunit rDNA-based phylogeny of *Sphaerodinium cracoviense*, an unusual freshwater dinoflagellate with a novel type of eyespot. *The Journal of Eukaryotic Microbiology* 57 (6)

ABSTRACT

Sphaerodinium cracoviense was collected near Cracow, Poland, and analysed by LM, SEM and serial section TEM. Thecae showed a peridinioid type of plate arrangement with unusual numbers in the anterior intercalary and postcingular plate series: 4 and 6, respectively. The apical pore of *S. cracoviense* differed from the typical arrangement seen in many thecate forms and included a furrow with knob-like protuberances reminiscent of the apical area of some woloszynskioids. The flagellar apparatus included the three microtubular roots that extend to the left of the basal bodies and a striated root connective between the transverse striated root and the longitudinal microtubular root. Both the single-stranded root that associates with the right side of the longitudinal basal body in peridinioids and gonyaulacoids, and the layered connective typical of peridinioids were absent. The eyespot was formed by a layer of vesicle-contained crystal-like units underlain by layers of variably fused globules not bounded by membranes, and represents a novel type. The pusular system included a long canal with a dilated inner portion with radiating tubules. Bayesian and maximum likelihood analyses based on LSU rDNA placed *Sphaerodinium* as a sister taxon to a group of woloszynskioids and relatively far from *Peridinium* and its allies.

Key Words: Bayesian analysis, dinoflagellate phylogeny, electron microscopy, flagellar apparatus, lamellar body, maximum likelihood, peridinioids, pusule, woloszynskioids

INTRODUCTION

The genus *Sphaerodinium* was described by Wołoszyńska (1916, p. 279). In this publication Wołoszyńska described and named three new species and one variety, and noted one further species or variety that she did not name: *Sphaerodinium cracoviense*, *S. limneticum*, *S. polonicum* and var. *tatricum*, and *Sphaerodinium* sp., all collected from several freshwater locations in Poland. The generic description was based on thecal features and included the description of all major thecal plates: in the epitheca, 7 plates regularly arranged around a hexagonal plate (corresponding to plate 3′ in Kofoidian notation) and 7 precingular plates; in the hypotheca, 6 postcingular and 2 antapical plates. All species were

described with an apical pore. The species were distinguished by Wołoszyńska (1916) on the basis of differences in general cell shape, plate ornamentation and in the shape of the sulcus. The type species was not designated in this work and the genus was later typified by Loeblich and Loeblich (1966, p. 56), who selected *Sphaerodinium polonicum* as lectotype. A further species was described by Wołoszyńska from tropical Sumatra, Indonesia, first incompletely (Wołoszyńska 1930, p. 168, as *Sphaerodinium* sp.) and later included by Schiller in his monograph as *S. javanicum* Wołoszyńska (Schiller 1935, p. 87, fig. 72). Another species of *Sphaerodinium, S. fimbriatum* R. H. Thompson, showing the typical tabulation of the genus, was later described by Thompson (1951, p. 296, fig. 63--67) from Kansas, USA. *Sphaerodinium* species have been infrequently reported from several fresh- and brackish-water localities scattered around the world, e.g. Ivory Coast (Couté and Iltis 1984), Burundi (Caljon 1987), Tasmania (Ling et al. 1989), Belize (Carty and Wujek 2003), Austria (Tolotti and Thies 2002) and Hungary (Grigorszky et al. 2003).

Recent works combining external morphology, ultrastructure and DNA-based phylogenies of peridinioids and woloszynskioids have led to changes in our understanding of species phylogenetic relationships, with consequent taxonomic rearrangements (e.g. Calado et al. 2009; Craveiro et al. 2009a; Hansen et al. 2007; Lindberg et al. 2005). However, a complete understanding of the phylogenetic relationships within and between the peridinioids and woloszynskioids has not yet been achieved.

Sphaerodinium is unusual in having a larger number of intercalary plates than is common in peridinioids, and in having 6 (rather than the usual 5) postcingular plates. The relatively high number of thecal plates seems to place *Sphaerodinium* in an intermediate position between the peridinioids and the more thinly thecate woloszynskioids.

The organisms studied in this work were collected in Pieskowa Skała (Ojców National Park) north of Cracow, Poland. The features observed in our specimens match the original description of *S. cracoviense* from near Cracow (Wołoszyńska 1916, p. 281, pl. 14, fig. 28--30).

The present article describes, for the first time, the general fine-structural organization and the flagellar apparatus of a species of *Sphaerodinium* as well as a novel type of eyespot. Thecal morphology is described as seen by SEM. Additionally, *Sphaerodinium* was included in a phylogeny reconstruction with Bayesian inference and maximum likelihood methods, prepared on the basis of partial LSU rDNA sequences. Preliminary results of this work were presented at IPC9 (Craveiro et al. 2009b).

MATERIALS AND METHODS

Biological material. *Sphaerodinium cracoviense* was found in high numbers in the plankton collected from two fishponds in Pieskowa Skała (Ojców National Park), Poland, in August 2007. All the observations and preparations were made with the cells from those samples or from a culture started with cells isolated to SC medium, a soil-water medium (Christensen 1982), maintained at 15 ºC with 16:8 light:dark photoperiod.

Light microscopy. Cells from field samples and from the culture were observed and photographed in a Zeiss Axioskop light microscope with a Zeiss Axiocam HRc digital camera (Carl Zeiss, Oberkochen, Germany).

Scanning electron microscopy. A small portion of the field material (1.6 ml) was fixed with a fixative mixture in a proportion of 2:1 respectively, for 30 minutes. The fixative comprised a 1:3 mixture of saturated $HgCl_2$ and 2% osmium tetroxide. Another portion of field sample was fixed with Lugol's solution overnight. Cells from both fixations were retained on Isopore polycarbonate filters with 8 µm pore size (Millipore Corp., Billerica, MA, USA), washed with distilled water and dehydrated through a graded ethanol series. The cells were then critical-point-dried and the filters glued onto stubs using double-sided adhesive tape. After being sputter-coated with platinum-palladium for 90 s, the stubs were observed in a JEOL JSM-6335F (JEOL Ltd., Tokyo, Japan) scanning electron microscope.

Transmission electron microscopy. Two fixation protocols were followed, both using swimming cells individually picked up from live field samples: (1) cells were transferred to 2% glutaraldehyde in phosphate buffer 0.1 M, pH 7.2, and fixed for one hour at 4 ºC; (2) cells were transferred to a mixture of 1%

glutaraldehyde and 0.5% osmium tetroxide (final concentrations) in phosphate buffer 0.1 M, pH 7.2, and fixed for one hour at 4 ºC. Cells from both fixations (1 and 2) were then rinsed in buffer, included in 1.5% agar blocks and post-fixed in 0.5% osmium tetroxide at 4 ºC overnight. After being rinsed with phosphate buffer and distilled water, the agar blocks with the cells were dehydrated through a graded ethanol series and propylene oxide and embedded in Spurr's resin. The blocks were sectioned with a diamond knife in an EM UC6 ultramicrotome (Leica Microsystems, Wetzlar, Germany). Ribbons of serial sections (70 nm thick) were picked up with slot grids and placed on Formvar film. The sections were stained with uranyl acetate and lead citrate. In total, serial sections of five cells were observed in a Jeol JEM 1010 transmission electron microscope (Jeol Ltd., Tokyo, Japan).

Single-cell PCR. One to three cells of *Sphaerodinium cracoviense* were isolated from culture, washed twice in double distilled water and transferred to 0.2-ml PCR tubes containing a 8-µl droplet of double distilled water. Prior to PCR amplification of nuclear-encoded LSU rDNA tubes containing *Sphaerodinium* cells were heated for 10 min at 94 °C. The PCR cocktail was then added and the temperature profile included denaturing at 94 °C for 3 min, followed by 35 cycles of denaturing at 94 °C for 1 min, annealing at 55 °C for 1 min and extension at 72 °C for 3 min. The PCR temperature profiled ended with an extension step of 10 min. (See Hansen et al. 2000 for details on chemicals and concentrations used). Amplification primers used were D1F and DinoND (for primer sequences see Hansen et al. 2000; Hansen and Daugbjerg 2004). Semi-nested PCR was formed using the primer combination D1F-D3B and D3A-ND1483 and the same temperature profile as outlined above but with only 18 cycles. PCR reactions were electrophorized in an agarose gel containing ethidium bromide for visualization under ultraviolet light. Gels were run at 150V for 15 min. Lanes containing PCR fragments of correct length compared to a molecular marker (viz. PhiX 174 HAE III) were purified applying Nucleofast and following the recommendations of the manufacturer (Macherry Inc., USA). Purified PCR products were aliquoted to reach a final concentration of 500 ng. Before being sent to the sequencing service provided by Macrogen (Korea) they were air-dried. The sequencing primers were

D1R, D2C, D3A, D3B and 28-1483R (for primer sequences see Daugbjerg et al. 2000 and Hansen et al. 2000).

Alignment and phylogenetic analyses. To infer the phylogeny of *Sphaerodinium cracoviense* we added its LSU rDNA sequence to an alignment comprising a total of 58 dinoflagellate species covering a diverse assemblage of thecate and naked taxa. Ciliates (4 species), apicomplexans (5 species) and a single perkinsid comprised the outgroup. In total, 1157 base pairs (including introduced gaps) covering domains D1, D3--D6 (sensu Lenaers et al. 1989) were analysed using Bayesian inference and maximum likelihood (ML). Bayesian inference used MrBayes (ver. 3.1.2, Ronquist and Huelsenbeck 2003) with $2*10^6$ Markov Chain Monte Carlo generations with four parallel chains (1 cold and 3 heated). A tree was sampled every 50^{th} generation and by plotting the log likelihood values as a function of generations the lnL values converged after 20050 generations. Using this as the burn-in provided 39600 trees. All of these were imported into PAUP* (vers. 4b.10, Swofford 2003) to produce a 50% majority rule consensus tree. Branch support values in terms of posterior probabilities were also obtained from the 39600 trees. Bayesian analysis was performed on the freely available Bioportal at www.bioportal.uio.no. For maximum likelihood analyses (ML) we used PhyML (ver. 3, Guindon and Gascuel 2003) with settings according to the results from running our data matrix through Modeltest (ver. 3.7; Posada and Crandall 1998); the best-fit model was TrN+I+G, selected by hierarchical likelihood ratio tests. Parameters for proportion of invariable sites (I=0.2178) and among site rate heterogeneity (alpha=0.6465) were used in PhyML. Support for the topology in ML was obtained by bootstrap analyses with 500 replications. The consensus program from Phylip (ver. 3.68, Felsenstein 2008) was used to draw a 50% majority rule consensus tree.

RESULTS

Observations in light microscopy (LM). Cells of *Sphaerodinium cracoviense* were spherical to oval and slightly compressed dorsiventrally (Fig. 1, 2). Length of cells ranged from 24 to 31 µm, width from 22 to 28 µm and thickness from 24 to 25 µm. The cell surface was underlain by numerous yellowish-brown

chloroplast lobes (thin arrows in Fig. 2). In the sulcal area there was a conspicuous, red, curved eyespot (Fig.1, 2). The theca was generally thin and the plate arrangement was only discernible in empty thecae. Boundaries between cingular plates were difficult to observe and seemed somewhat variable, especially in the distal, right-hand side. The limits of the last two cingular plates are shown for one cell in Fig. 3 (thin arrows).

Stereo-microscope observations revealed a marked positive phototactism, as virtually all cells in the middle of a watch-glass moved along parallel lines toward the light source.

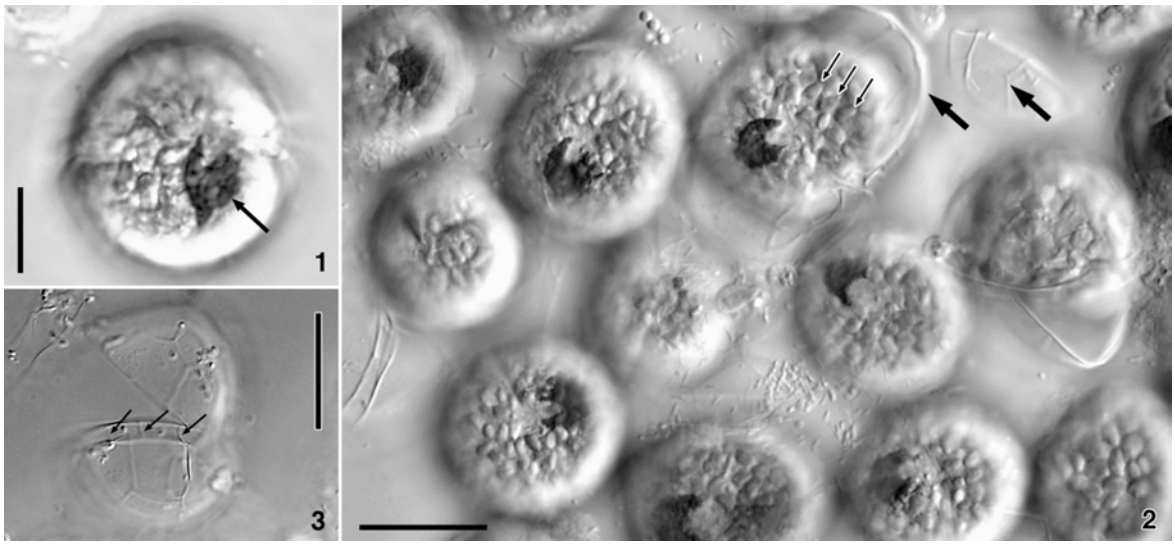

Fig. **1--3.** *Sphaerodinium cracoviense*, LM. Live cells and thecae from field sample. **1.** Ventral view of a cell showing the conspicuous eyespot in the sulcal area. Scale bar = 10 µm. **2.** Several cells showing the eyespot and surface chloroplast lobes (thin arrows). Note detached thecae with visible plate sutures (thick arrows). Scale bar = 20 µm. **3.** Ecdysed theca opened along the upper edge of the cingulum with sulcal plates connecting epi- and hypotheca. Three cingular sutures on the right-hand side of the cingulum are visible (arrows). Scale bar = 20 µm.

Morphology and thecal structure (SEM). Cells were usually spherical with the nearly equatorial cingulum delimiting an epi- and hypotheca of almost equal size (Fig. 4--6). The cingulum descended nearly its own width at the right-ventral side of the cell (Fig. 4, 5). In ventral view the epitheca was slightly twisted to the left with precingular plate 7 partly aligned with the sulcus (Fig. 4, 5). Epithecal tabulation was nearly symmetric with the four apical plates surrounding the apical complex (arrow in Fig. 7).

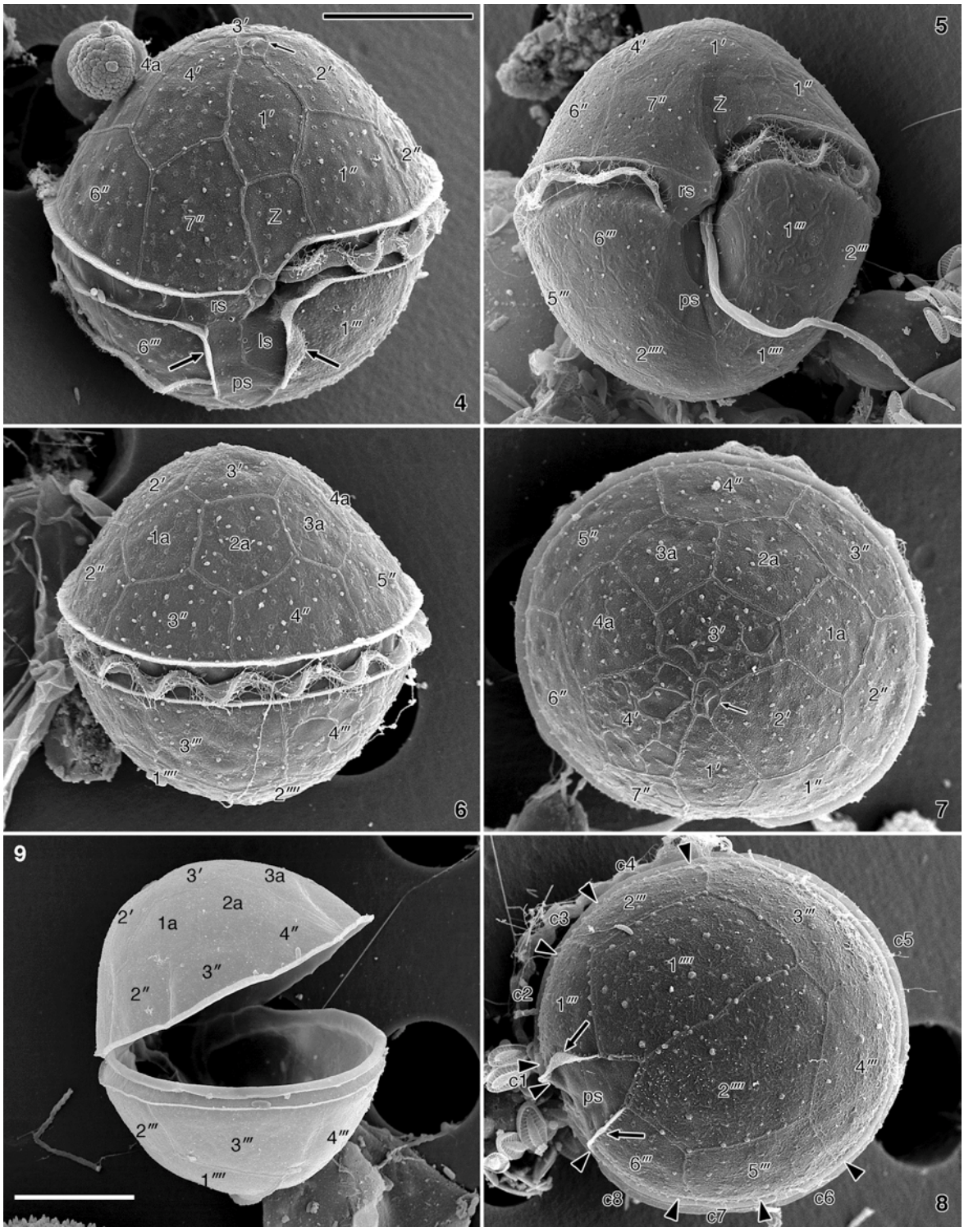

Fig. **4--9.** *Sphaerodinium cracoviense*, SEM. rs, ls, ps, respectively right, left and posterior sulcal plates. The scale bar in Fig. 4 applies to all figures except Fig. 9. Scale bars = 10 µm. **4.** Ventral-anterior view. The apical complex is visible (arrow). The ventral plate contacting the upper edge of the cingulum and plate 1′ is labelled Z. Thick arrows, raised edges of plates 1‴ and 6‴ bordering the sulcus. **5.** Ventral view of a cell with a thin theca, showing a more extensive longitudinal depression on the ventral side. **6.** Dorsal view showing the four anterior intercalary plates. **7.** Apical

view. **8.** Antapical view showing the six postcingular plates and the posterior end of the sulcus indenting the suture between the antapical plates. Arrowheads indicate the approximate position of the maximum number of cingular sutures detected. Thick arrows, raised edges of plates 1‴ and 6‴ bordering the sulcus. **9.** Theca opening along the upper edge of the cingulum with epi- and hipotheca still connected in the sulcal area.

Four dorsally located, similar-sized intercalary plates (1a--4a), together with apical plates 1, 2 and 4, formed a ring around apical plate 3 (Fig. 6, 7). Eight plates contacted the upper edge of the cingulum; seven of these are here labelled precingular. The remaining plate was directed aligned with the elongated plate 1′ and is here labelled Z (Fig. 4, 5). The hypotheca had 6 postcingular and two antapical plates (Fig. 8). Four plates were labelled as sulcal in Fig. 10, 11; this excludes a small plate between the left part of the sulcus and the proximal part of the cingulum, here considered cingular plate 1, and the plate labelled Z (see discussion). The margins of postcingular plates 1 and 6, bordering the sulcus, were raised (Fig. 4, 8, arrows). The posterior sulcal plate (ps) was V-shaped in the posterior side and ended between the two antapical plates (Fig. 4, 11). The anterior sulcal plate (as) was small and round (Fig. 4, 10, 11). The right sulcal plate (rs) was directly aligned with the distal end of the cingulum, whereas the left sulcal (ls) extended from cingulum level to below the middle of the sulcus (Fig. 4, 10, 11).

The number of cingular plates was difficult to ascertain because the sutures were difficult to see even in SEM. Considering as a cingular plate the very short plate in the beginning of the cingulum (c1 in Fig. 10, 12), a maximum of eight cingular plates were counted in several cells. The general positions of cingular plate boundaries, as found in those cells, are marked with arrowheads in Fig. 8. Although in some cells a smaller number of cingular plates was visible, all cells displayed a large plate covering the dorsal side of the cingulum, roughly corresponding to the length of postcingular plates 3 and 4.

On the basis of observations on cells stripped of the outer membranes, the apical complex was apparently composed of three plates: a small, central, elongated plate (labelled 1 in Fig. 13, 14), 1 µm long and 0.3 µm wide, with a furrow along the middle; a larger plate that surrounded almost completely the first

one (marked 2 in Fig. 13, 14) and a medium-sized rectangular plate contacting the ventral edge of the other two plates (marked 3 in Fig. 13, 14). In cells fixed to preserve the outer membranes the limits between these plates was more difficult to see; a row of knob-like protuberances, about 60 nm in diameter, is visible along the length of plate 1 in Fig. 13 (thin arrows).

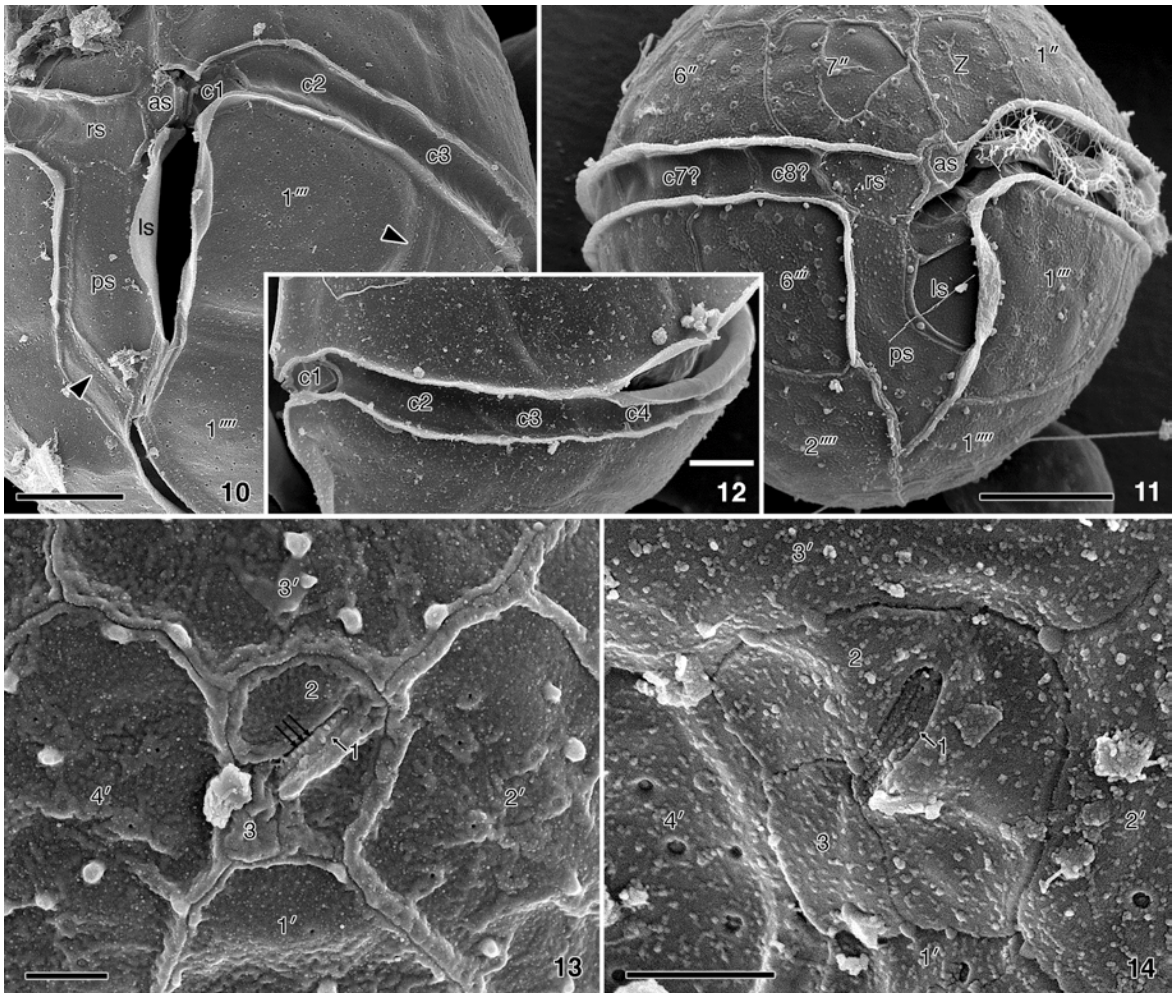

Fig. **10--14.** *Sphaerodinium cracoviense*, SEM. as, rs, ls, ps, respectively anterior, right, left and posterior sulcal plates. **10.** Sulcal region with four visible sulcal plates. The very small plate on the top left corner of the sulcus is labelled cingular plate 1 (c1). Smooth sutures between plates are visible with thin contact lines bearing rows of tiny granules (arrowheads). Scale bar = 5 µm. **11.** Ventral view of an intact sulcal area. Scale bar = 5 µm. **12.** Left side of the cingulum showing the first four cingular plates (not detectable in all cells). Scale bar = 3 µm. **13, 14.** Apical complex in a cell prepared to preserve outer membranes (Fig. 13) and in one stripped of outer membranes (Fig. 14). The three apical complex platelets are labelled 1, 2 and 3. Note a row of small knobs in plate 1 in Fig. 13. Scale bars = 1 µm.

Thecal ornamentation consisted mainly of scattered trichocyst pores and knob-like protuberances that were visible only in thecae that retained the outer membranes (Fig. 4--8, 13). In thecae without outer membranes the plates were somewhat rugose due to tiny and irregular granules covering much of the surface (Fig. 10, 12, 14). Sutures between plates were mostly thin (Fig. 4--8). Somewhat wider sutures not showing any cross-striation are shown in Fig. 10.

The thecae opened along the anterior border of the cingulum, often resulting in empty thecae with the epi- and hypotheca connected only by the sulcal plates (Fig. 9).

General ultrastructure. *G*eneral ultrastructural features of *Sphaerodinium* were typical of dinoflagellates (Fig. 15). The ellipsoid nucleus was located in the dorsal side of the cell at cingulum level (Fig. 15). Figure 16 shows simple nuclear pores in the nuclear envelope. Chloroplast profiles were mainly located at the periphery, connected to inward radiating lobes that did not invade the cytoplasm in the centre of the cell; there were no distinct pyrenoids but thylakoid-free areas were found in some chloroplast lobes (Fig. 15). Relatively large ellipsoid vesicles with diffuse granular contents were common between the chloroplast lobes at the periphery of the cell (Fig. 15). Trichocysts were abundant and bacteria were found in the cytoplasm of all cells (Fig. 15, 42). A few relatively small accumulation bodies were seen, both in the epi- and in the hypocone (Fig. 15, ab). Starch grains were small and more numerous near the antapex (Fig. 15). Electron-opaque microbodies, apparently associated with electron-translucent vesicles, formed a well-developed network in the central cytoplasm, in the ventral region and around the nucleus (Fig. 15, 42, thick arrows).

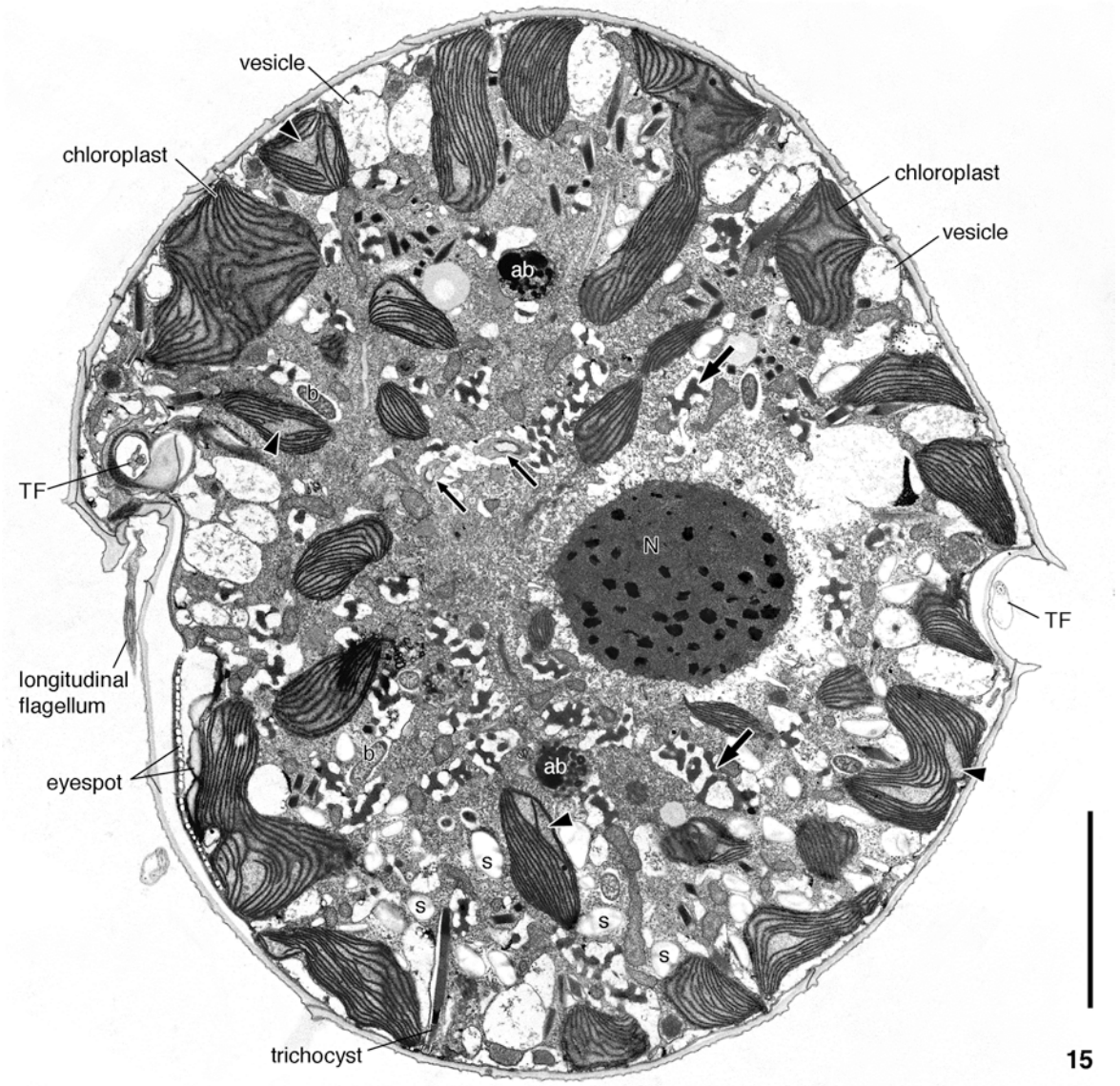

Fig. **15.** *Sphaerodinium cracoviense*, TEM. General ultrastructure. Longitudinal section viewed from the left, showing both longitudinal and transverse flagella (TF), the eyespot beneath the sulcus, chloroplast profiles, the nucleus (N), bacteria (b) in the cytoplasm, starch grains (s) mainly in the hypocone, accumulation bodies (ab) and trichocysts. Thin arrows point to two segments of the pusule canal. Arrowheads mark thylakoid-free areas of choroplasts. Note the number of electron-dense microbodies (thick arrows) distributed mainly in the central part. Scale bar = 5 μm.

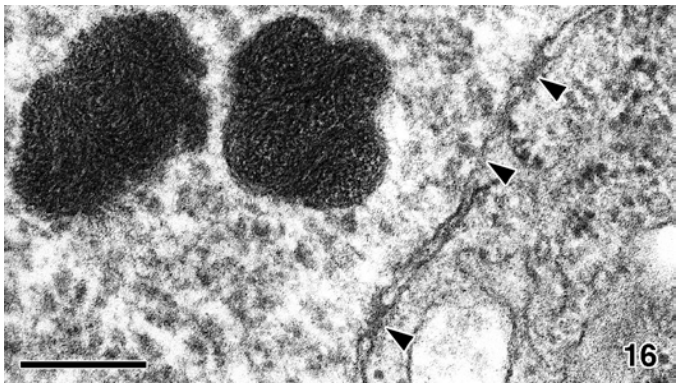

Fig. **16.** *Sphaerodinium cracoviense*, TEM. Detail of the nuclear envelope showing nuclear pores (arrowheads). Scale bar = 200 nm.

Apical complex. The three plates of the apical complex shown in SEM were identifiable in serial longitudinal sections through the cell apex (Fig. 17--20). The cytoplasm projected through the middle of plate 1 (Fig. 17--19), perhaps as a sequence of knob-like protuberances (Fig. 18, 19). In the apical region the cytoplasm showed vesicles with tubular connections to amphiesmal vesicles (Fig. 18, 19, arrowheads).

Flagellar apparatus. A schematic reconstruction of the flagellar apparatus and related structures, as viewed from the left side of the cell, is presented in Fig. 21. The same point of view is shown in Fig. 22--29. Particular features of the flagellar apparatus are shown as viewed from the left-anterior side of the cell in Fig. 30--35. As estimated from serial sections, the angle between the basal bodies was about 90º, except in one cell, for which the angle of insertion of the basal bodies was nearly 140º.

Each flagellum emerged from the cytoplasm into a flagellar canal, which opened to the outside of the cell through a pore encircled by conspicuous fibrous material that was striated in at least some orientations (called transverse striated and longitudinal striated collars — TSC and LSC). The TSC had a striated extension that covered partially the proximal part of a tube extending from the transverse flagellar canal into the cell (Fig. 22--24, 31--33, pusule tube). Both collars were connected by a surface electron-opaque structure here interpreted as a ventral ridge (Fig. 21, double arrow in Fig. 37, 45). The ventral ridge was about 140 nm x 40 nm in cross-section, and extended about 1 µm longitudinally along an

area where the amphiesmal vesicles did not meet, between the posterior side of the TSC and the ventral surface of the LSC (Fig. 21, 37, 45). There were no visible microtubules associated with it.

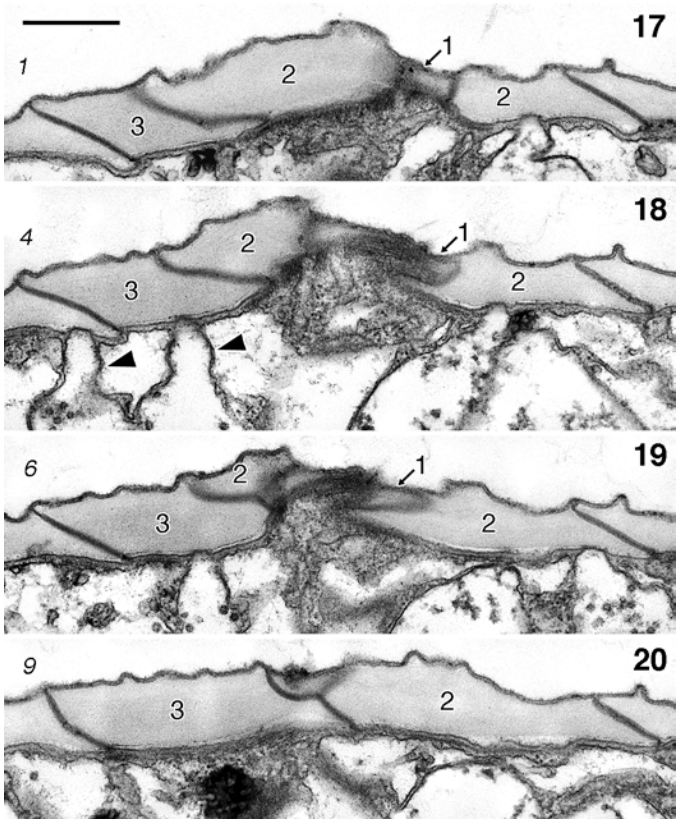

Fig. **17--20.** *Sphaerodinium cracoviense*, TEM. Non-adjacent serial, longitudinal sections through the apical complex, proceeding approximately from left to right. Apical complex platelets are marked 1, 2 and 3, as in Fig. 13 and 14. Slanted numbers refer to the section number. Vesicles with tubular connections to amphiesmal vesicles are marked by arrowheads. Scale bar = 500 nm.

Two single-stranded microtubular roots were associated with the transverse (TB) and a single multistranded one with the longitudinal basal body (LB). The longitudinal microtubular root (LMR, r1 in Moestrup 2000), a multi-stranded microtubular root, associated with the left, anterior end of the LB, passed close to the dorsal side of the LSC and extended along the sulcal area toward the antapex (Fig. 21-29). The number of microtubules of the LMR increased from about 8 at the proximal end to an estimated maximum of 36 (Fig. 21, 36).

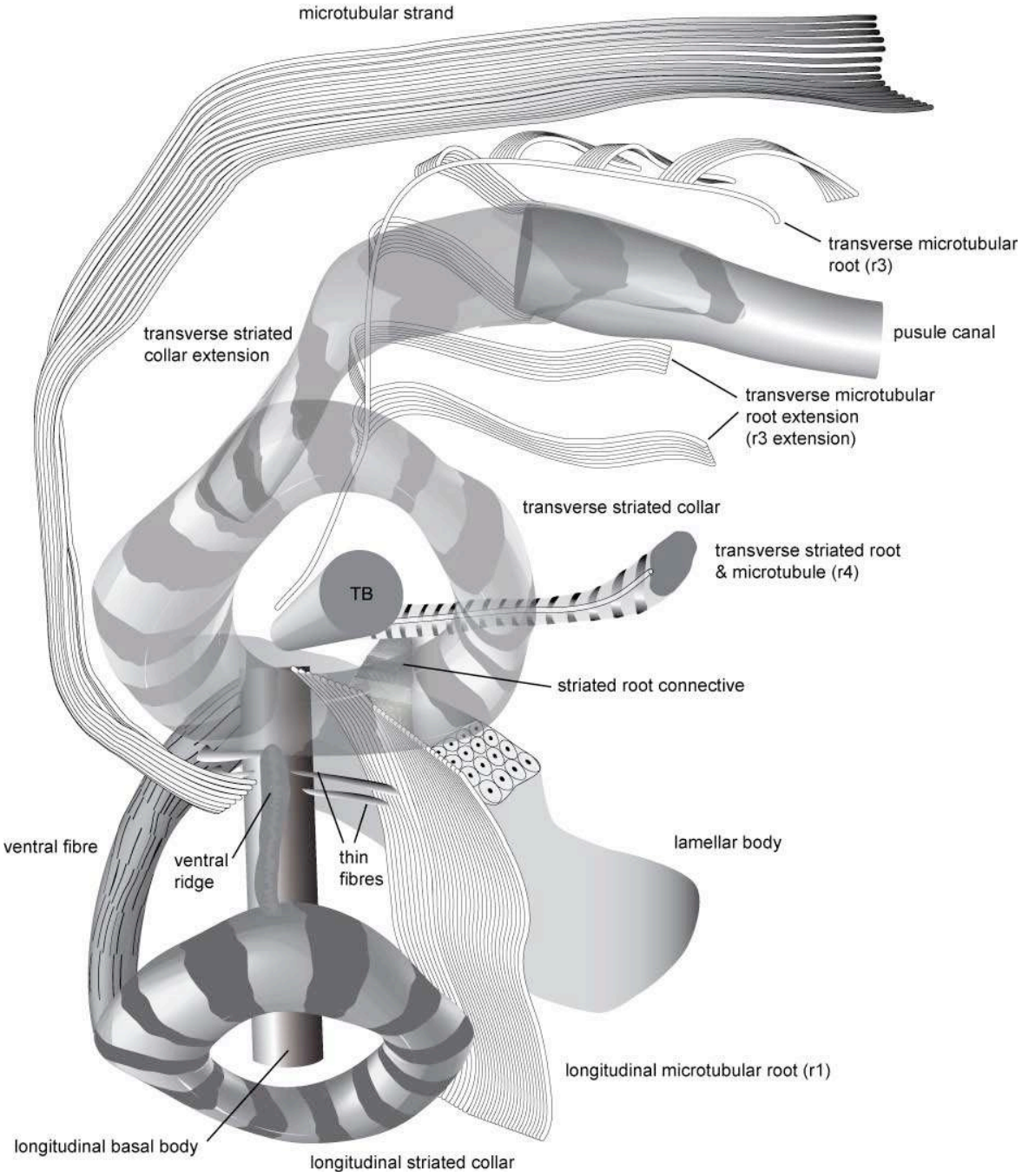

Fig. **21.** Schematic reconstruction of the flagellar base area as seen from the left side of the cell. TB, transverse basal body. The transverse striated collar and its extension are rendered transparent to show underlying structures.

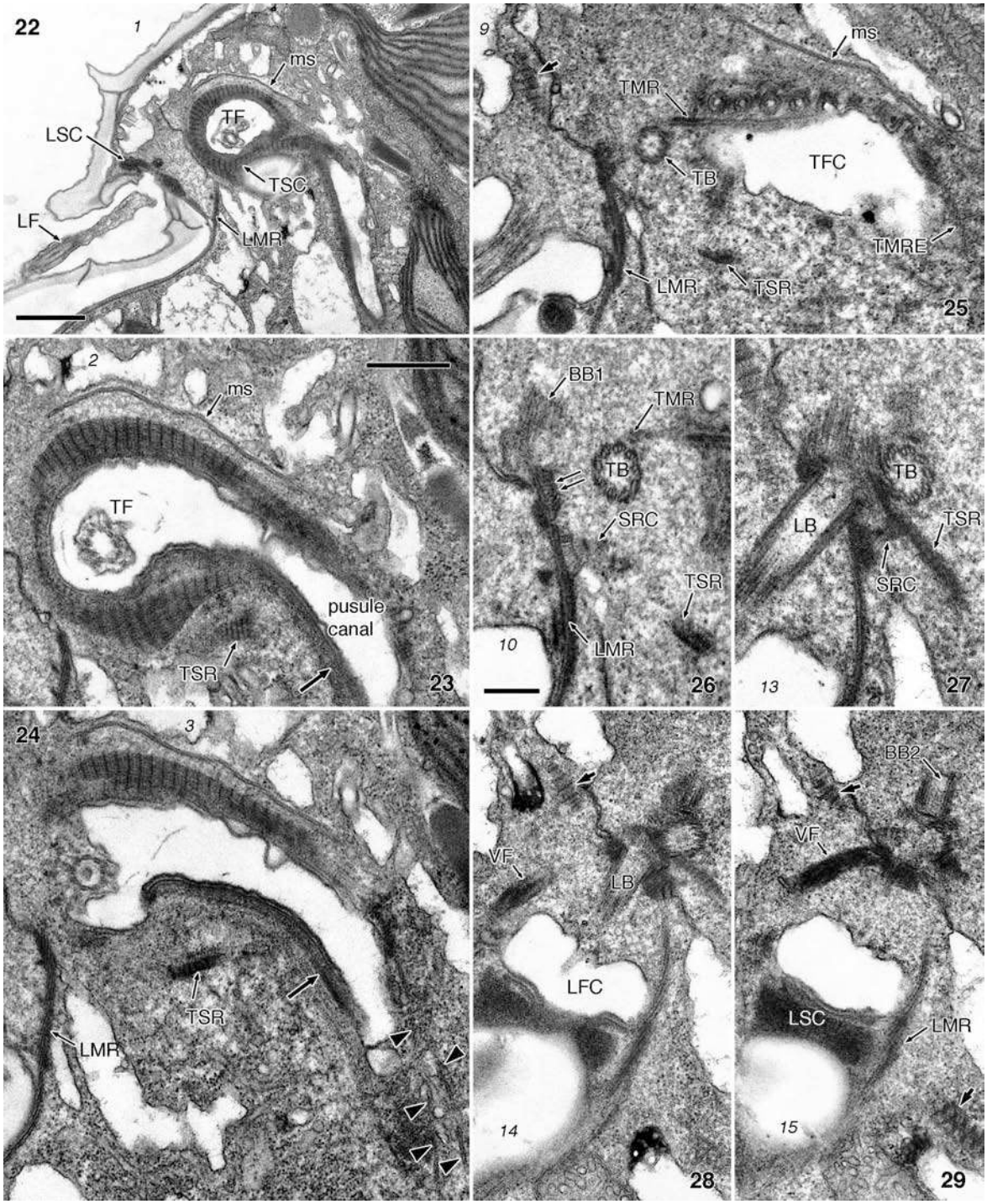

Fig. **22--29.** *Sphaerodinium cracoviense*, TEM. Flagellar apparatus and microtubular strand (ms). Non-adjacent, nearly longitudinal serial sections proceeding from left to right. Slanted numbers refer to the section number. **22--23**. Transverse flagellum (TF) in the transverse flagellar canal (TFC). The transverse striated collar (TSC) is seen as a complete ring from which an extension branches off to the anterior side of the pusule canal. LF, longitudinal flagellum. Scale bar in Fig. 22 = 1 µm. Scale bar in Fig. 23 = 500 nm. **24--27**. The transverse microtubular root (TMR) and the transverse striated root (TSR) approach the transverse basal body (TB). Several rows of the

transverse microtubular root extension (TMRE) are marked with arrowheads in Fig. 24. Note the dark material covering the terminal portion of the pusule canal (arrow in Fig. 24). SRC, striated root connective. The scale bar in Fig. 23 applies to Fig. 24 and 25. Scale in Fig. 26 = 200 nm. Fig. 26 and 27 to the same scale. **28--29.** The ventral fibre (VF) associates with the right side of the longitudinal basal body (LB). Short arrows indicate the lamellar body. LSC, longitudinal striated collar; BB1, BB2, replicated basal bodies. Same scale as Fig. 23.

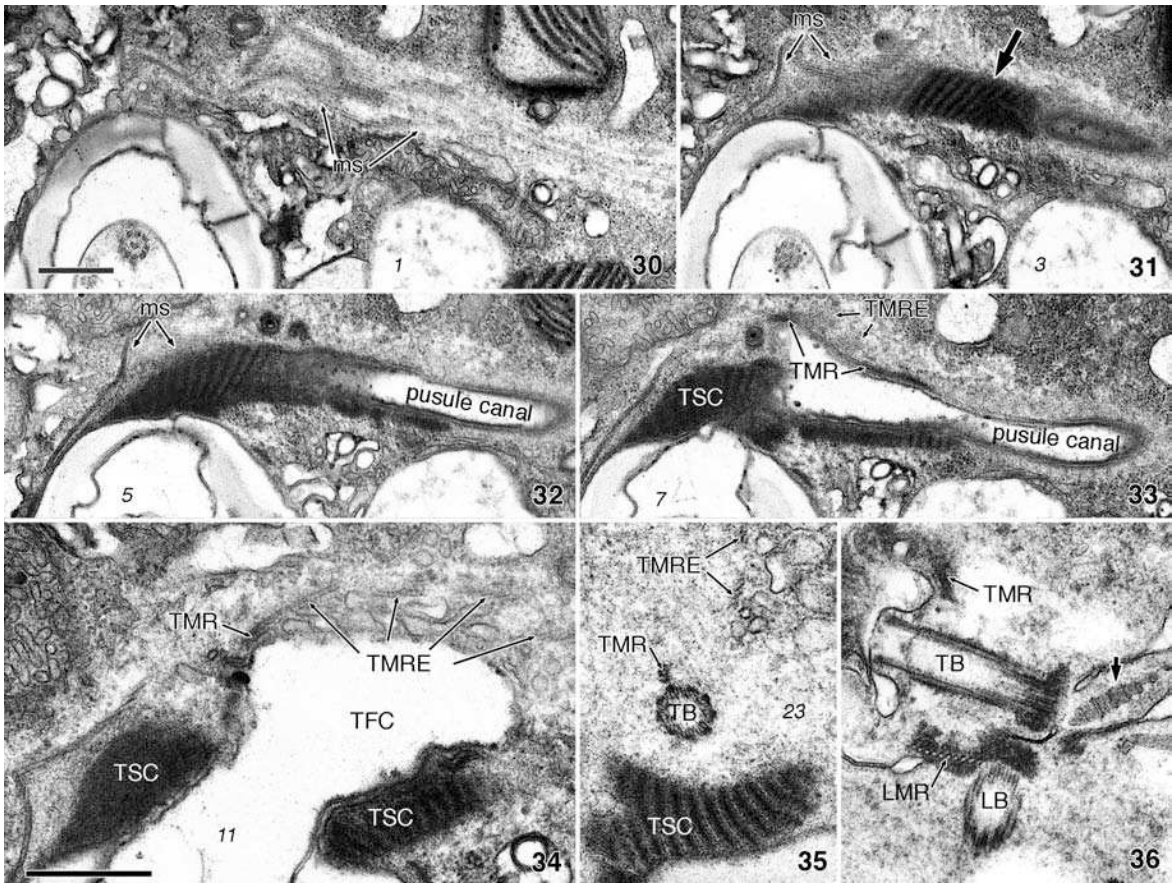

Fig. **30--36.** *Sphaerodinium cracoviense*, TEM. Flagellar apparatus and microtubular strand (ms). Fig. 31--33, same scale as Fig. 30. Fig. 35--36, same scale as Fig. 34. Scale bars = 500 nm. **30--35.** Non-adjacent, nearly longitudinal serial sections proceeding from left to right. Slanted numbers refer to the section number. **30--32.** The ms follows a path roughly parallel to the extension (arrow) of the transverse striated collar (TSC) that runs along the pusule canal. **33--35.** The transverse microtubular root (TMR) nucleates several groups of microtubules (TMRE) and ends adjacent to the anterior-proximal end of the transverse basal body (TB). **36.** Anterior-dorsal view of the basal bodies of another cell, showing the proximal part of the longitudinal microtubular root (LMR). Note the lamellar body (short arrow). LB, longitudinal basal body.

The transverse microtubular root (TMR, r3 in Moestrup 2000) started next to the anterior-proximal end of the TB, ran parallel to it for about 400 nm and then curved toward the apex, passing adjacent to a row of collared pits on the TFC (Fig. 25--27); the TMR then curved toward the dorsal side, running parallel to the pusule canal (Fig. 21, 33, 34). The TMR nucleated 6 or 7 rows of 4 to 8 microtubules each, collectively designated the transverse microtubular root extension (TMRE), in a dorsal direction (Fig. 21, 24, 25, 33--35). The transverse striated root and its associated microtubule (TSR and TSRM, r4 in Moestrup 2000) extended from the posterior side of the TB along the dorsal side of the TSC, close to the ventral cell surface, to the left side of the cell for nearly 1.6 µm (Fig. 21, 23--28).

A striated fibre (striated root connective, SRC) connected the dorsal surface of the LMR to the posterior side of the TSR, close to the point where it attached to the TB (Fig. 21, 25--27). The proximal part of the LMR, next to the connection to the SRC, was covered by electron-opaque material with a layered appearance (Fig. 26, double arrow).

A ventral fibre (VF, so called in the sense of Hansen et al. 2007) was present contacting the right-anterior side of the LB and progressing in a ventral-posterior direction, ending close to the ventral-right side of the TFC (Fig. 21, 28, 29, 37, 38). Two triplets on the ventral-right side of the LB were linked by thin fibres to the VF and two dorsal-left triplets displayed fibrous associations with the ventral side of the LMR (Fig. 21, 37--39); all these fibrous connections were 200 to 380 nm long.

Microtubular strand. A wavy strand of about 15 microtubules (microtubular strand, ms) was found along the anterior surface of the transverse collar extension that covered the pusule canal, curving around the ventral side of the TSC and ending close to its posterior surface (Fig. 21, 22--25, 30--34). Although microtubules of the TMRE were in some places less than 200 nm from the microtubules of the ms, no visible connection was found between this strand and any other structure (Fig. 21, 25, 30--34).

Lamellar body. A structure formed by groups of parallel, tubular membranous components, each about 55 nm wide, was found in the flagellar base area of all cells examined. Transverse sections through this structure showed a

honeycomb pattern with an electron-opaque body in the centre of each tubule (Fig. 21, 37, 38, 40). A less striking, lamellate appearance was found in longitudinal sections of the cell, which were also approximately longitudinal sections of the tubular elements of the lamellar body (Fig. 41, 42). As determined in serial sections, between four and seven independent fragments of lamellar body were found in the cells examined (Fig. 42, 45).

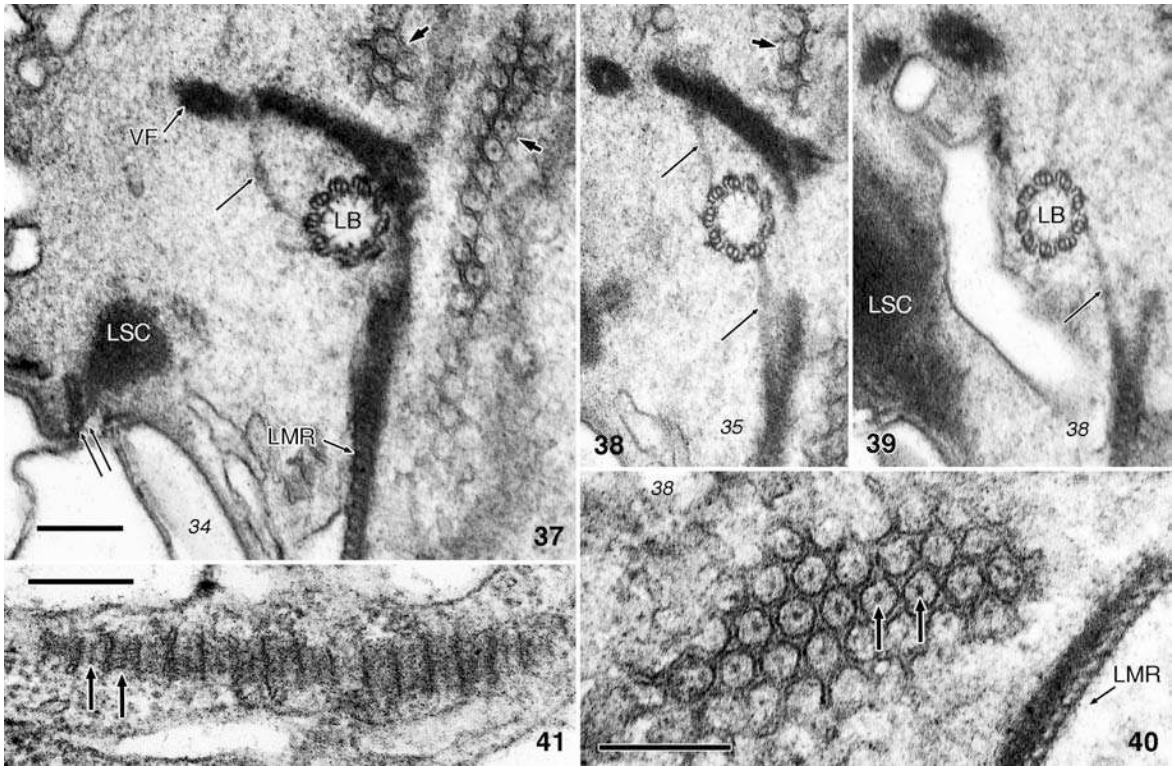

Fig. **37--41.** *Sphaerodinium cracoviense*, TEM. Flagellar apparatus. Same series as in Fig. 30--35 except for Fig. 41. Fig. 37--39 have been tilted to provide a cross-sectional view of the longitudinal basal body (LB). Slanted numbers refer to the section number. **37--39.** Apical view of the LB in cross section, showing the ventral fibre (VF) on the right side and the lamellar body (short arrows). Four connectiing fibres are marked with thin arrows: two between the LB and the VF and two between the LB and the ventral side of the longitudinal microtubular root (LMR). LSC, longitudinal striated collar. **40--41.** Transverse and longitudinal sections (respectively) of the cell showing different aspects of the lamellar body. Arrows point to the electron-opaque central structure. Fig. 38--39, same scale as Fig. 37. Scale bars = 200 nm.

Eyespot. The eyespot occupied a large area, up to 10 µm long, underneath the sulcus (Fig. 19, 42--44). It was made of two types of components, none of

them included in a chloroplast lobe. Ventralmost was a single layer of crystal or brick-like elements, apparently tightly packed inside a flat vesicle located immediately under the LMR or subthecal microtubules (Fig. 44).

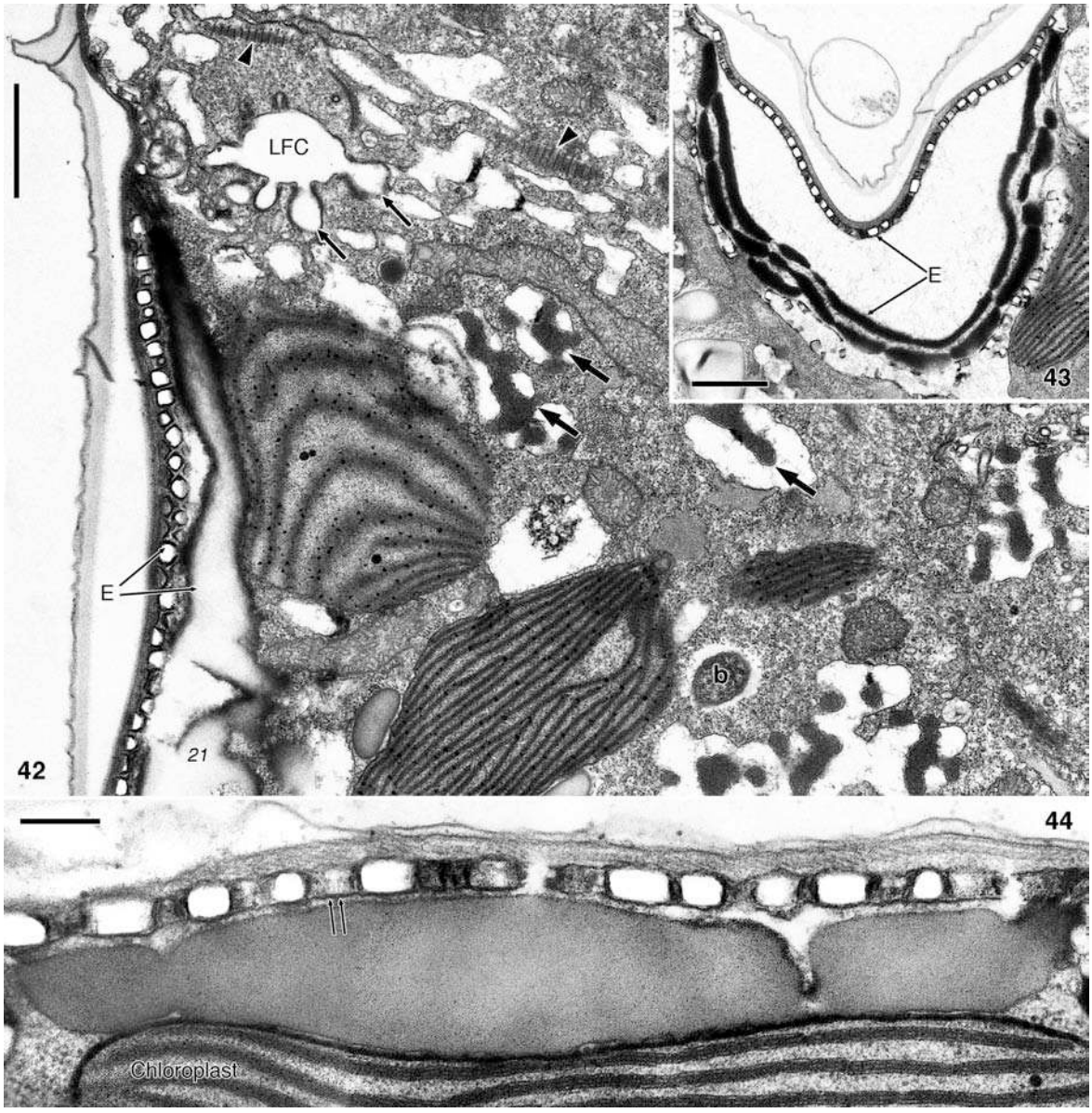

Fig. **42--44.** *Sphaerodinium cracoviense*, TEM. Ventral region, eyespot and pusular vesicles associated with the longitudinal flagellar canal (LFC). **42.** Longitudinal section, seen from the left side of the cell, through the ventral region showing the eyespot (E), and the LFC and attached pusular vesicles (thin arrows). Note the lamellar bodies (arrowheads). Electron-opaque microbodies (thick arrows) and associated vesicles are abundant in the ventral area. b, bacterium. Scale bar = 1 µm. 4**3.** Transverse section through both components of the eyespot. Scale bar = 1 µm**. 44.** Higher magnification of the eyespot. Note the membrane of the vesicle envolving the brick-

like components (double arrow) and the chloroplast lobe adjacent to the oil layer of the eyespot. Scale bar = 200 nm.

The brick-like elements were nearly square, some 130--180 nm wide and 90 nm thick. One to three irregular layers of more or less extensively fused oil globules underlay the brick layer (Fig. 42--44). As measured in transverse sections, individual oil layers, when more than one was present, were about 150 nm thick, with their middle lines approximately 240 nm apart. When only one layer was found, perhaps the result of fusion of several individual layers, thickness was around 450 nm. One chloroplast lobe was adjacent to the innermost oil layer in most of the eyespot area (Fig. 15, 42, 44).

Pusular system. There were two different sets of pusular structures, each one associated with one of the flagellar canals. A tube, here called pusule canal, with a lumen diameter of 250-390 nm opened at the anterior-dorsal side of the TFC (Fig. 21--24, 32, 33). The pusule canal was lined by a single membrane and covered by a layer of micro-fibrillar material (Fig. 48). It extended from the ventral area to the dorsal-right side of the cell for nearly 4 µm (Fig. 19, 22, 45), then curved to the left for 3 µm and ended in a ventral location relative to the nucleus. In its distal end, the pusule canal enlarged into a collecting chamber, also lined by a single membrane, ca. 800 nm long and 500 nm wide. Some 40 pusular tubules, each with a diameter of about 100 nm, radiated from the collecting chamber and coiled into the surrounding area, apparently without ramifications (Fig. 45--47). These tubules were typical pusular elements, wrapped in what appeared to be a single large vesicle. The second set of pusular structures consisted of about 10 spherical to slightly elongated pusular vesicles, each with a constricted connection to the left-posterior side of the LFC (Fig. 42).

Molecular phylogeny. In the phylogenetic inference based on partial LSU rDNA sequences *Sphaerodinium cracoviense* formed a sister taxon to a large assemblage consisting of *Baldinia*, *Borghiella*, *Biecheleriopsis*, *Biecheleria*, *Polarella*, *Protodinium* and *Symbiodinium* (Fig. 49). Hence, *S. cracoviense* takes a basal position among dinoflagellates characterized by possessing eyespots of type B and type E *sensu* Moestrup and Daugbjerg (2007).

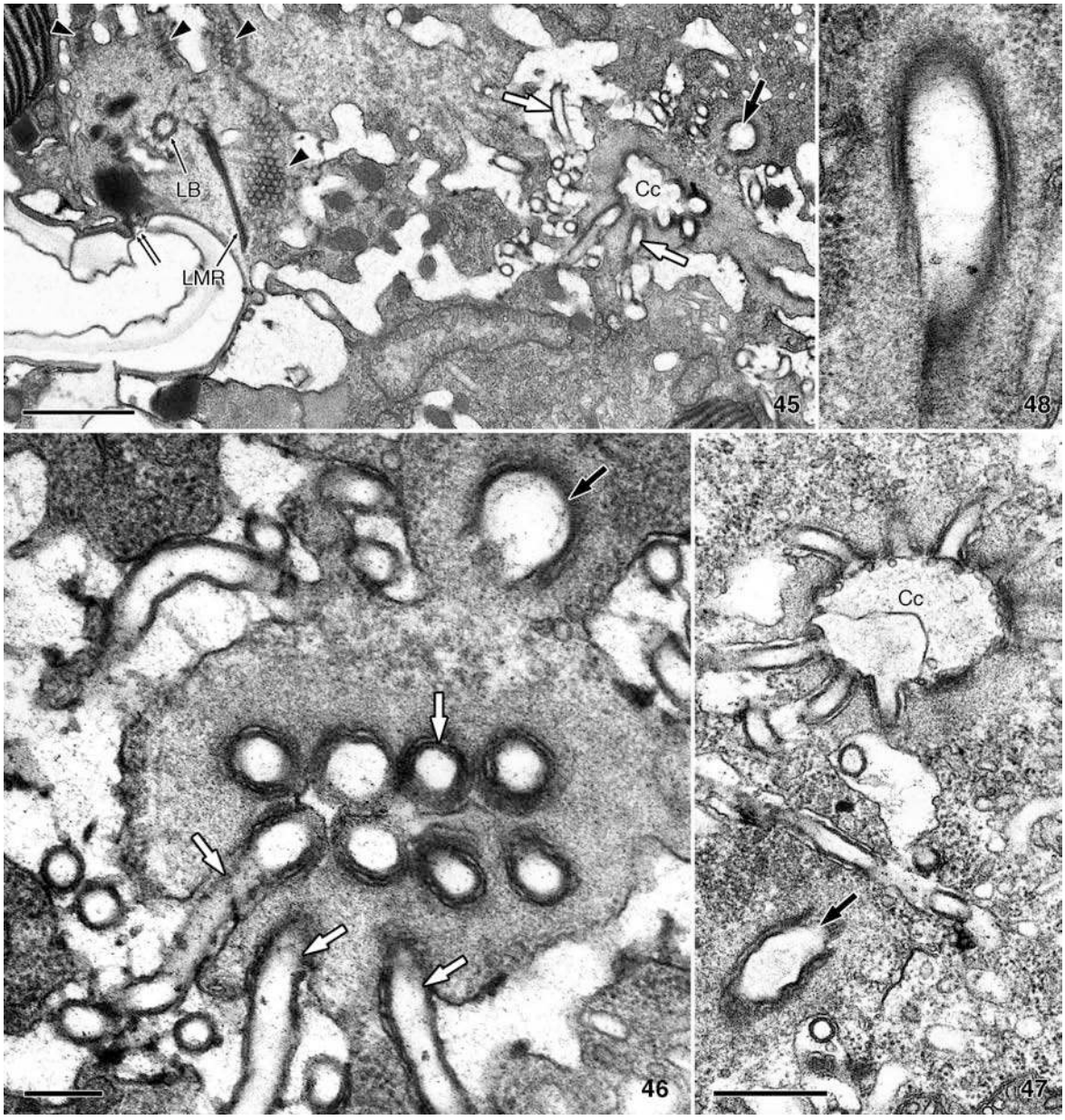

Fig. **45--48.** *Sphaerodinium cracoviense*, TEM. Pusular system. **45--47.** Localization of one of the pusular systems in relation to the basal body area. Some pusular tubules (white arrows) diverge from the collecting chamber (Cc, collecting chamber), which is an enlargement of the pusule canal (black arrow). Note the lamellar bodies (arrowheads) and the area of the ventral ridge (double arrow) in Fig. 45. LB, longitudinal basal body; LMR, longitudinal microtubular root. Scale bar = 1 µm in Fig. 45. Scale bar = 200 nm in Fig. 46. Scale bar = 500 nm in Fig. 47. **48.** Higher magnification of the pusule canal. Same scale as Fig. 46.

This relationship was highly supported by a posterior probability of 1 and a bootstrap value of 87%. The lineage comprising *Sphaerodinium* and its close relatives formed an unresolved relationship with three distinct lineages, the orders

Gonyaulacales and Dinophysales, and the family Tovelliaceae. This assemblage of diverse dinoflagellates was only moderately supported by a posterior probability of 0.78 and not supported by maximum likelihood bootstrap analyses (< 50%). Likewise our phylogenetic analyses of partial LSU rDNA sequences provided no reliable support for the deepest lineages.

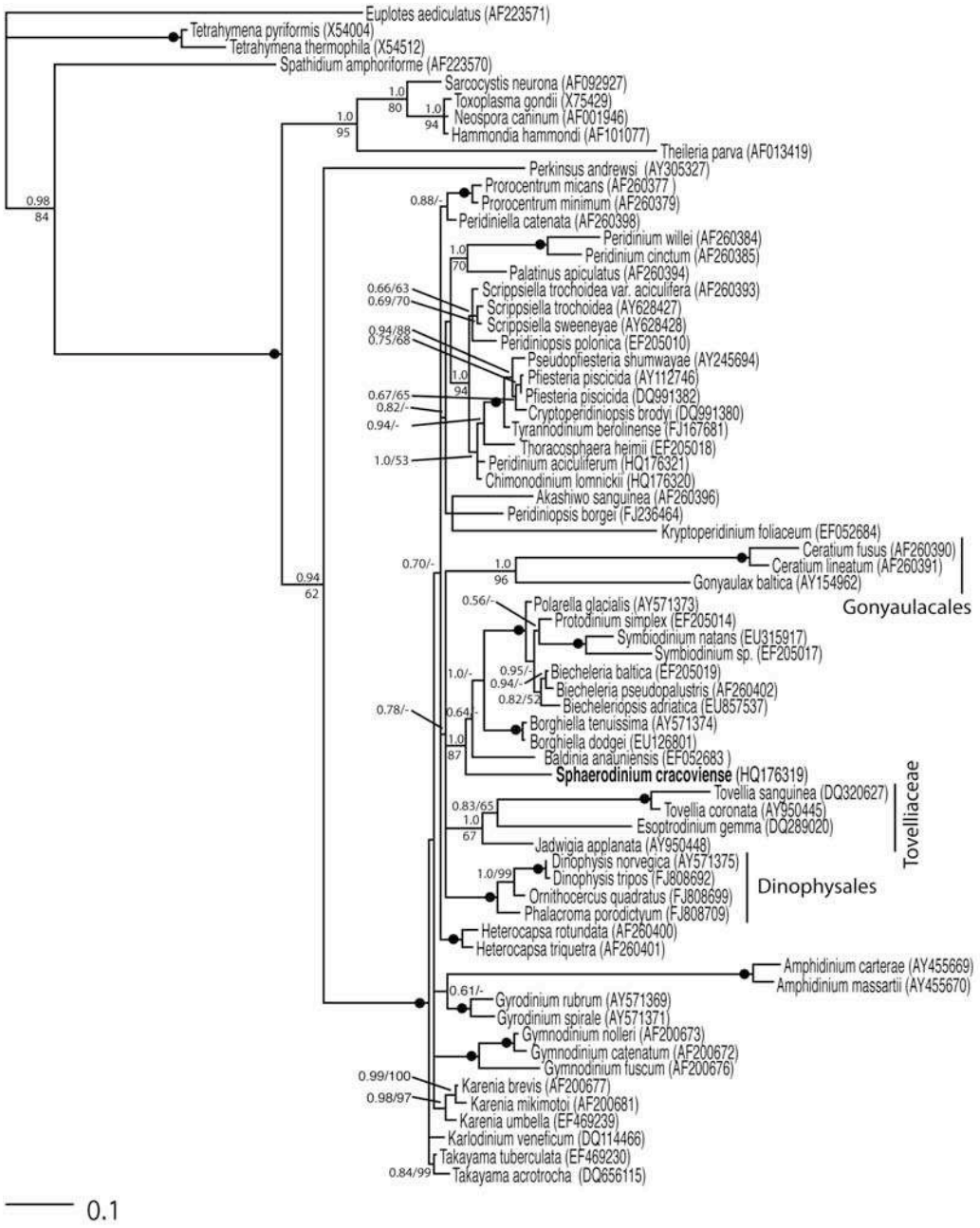

Fig. **49.** Phylogeny of *Sphaerodinium cracoviense* and 57 other dinoflagellate species from Bayesian inference. The data matrix comprised 1157 base pairs of nuclear-encoded LSU rDNA

and the dinoflagellate ingroup was polarized using ciliates, apicomplexans and *Perkinsus*. Branch support values are written to the left of internodes. The first numbers are posterior probabilities from Bayesian inference (≥ 0.5) whereas the last numbers are from maximum likelihood bootstrap analyses with 100 replications (≥ 50%). Maximum branch support (posterior probability = 1 and 100% in maximum likelihood bootstrap) is shown as filled black circles. Branch lengths are proportional to the number of character changes. *Sphaerodinium cracoviense* is bold faced.

DISCUSSION

Morphology and thecal structure. Although morphology and tabulation of the population of *Sphaerodinium* studied herein closely matches *S. cracoviense* as described by Wołoszyńska (1916), differences in the interpretation of particular plates result in different tabulation formulas. As shown here in Fig. 4, the plate labelled Z is longitudinally aligned with the first apical and transversely links precingular plates on the left and right of the sulcus. It may be thought of as one of a complete ring of precingular plates, analogous to what is found in *Heterocapsa* F. Stein, *Fragilidium* A. R. Loeblich, and *Thecadinium* Kofoid et Skogsberg in the interpretations of, e.g. Balech (1988, p. 160), Sournia (1986, p. 95), and Hoppenrath et al. (2005) respectively. In contrast, Wołoszyńska (1916) originally interpreted the plate as part of the sulcus, which she described as penetrating the epitheca. The depressed appearance of plate Z shown in an intact cell with a presumably incompletely developed theca in which cingular and sulcal margins are, for the most part, not raised (Fig. 5), favours Wołoszyńska's interpretation. The analogous plate in several *Heterocapsa* species has also (contrary to Balech 1988) been labelled sulcal anterior (e.g., Hansen 1995; Iwataki 2008; Tamura et al. 2005). However, when observed in well-developed thecae, plate Z was at the same level and had the same appearance as other epithecal plates, and was separated from the depressed sulcus by the raised upper margin of the cingulum (Fig. 4, 11).

Considering plate Z as part of the precingular ring, especially if labelled the first plate because of the alignment with the sulcus, forces the numbering of other precingular plates to change, resulting in an awkward position of plates compared to other thecate species. On the other hand, plates 1′ and Z share the same

orientation and are of similar width, and may be thought of as the result of the division of a single ancestral plate occupying a narrow strip from sulcus to apex.

The set of three small plates surrounded by the four apical plates of *Sphaerodinium* has hitherto been noted by terms equivalent to those used for the apical pore of peridinioids. However, as shown in SEM (Fig. 13, 14), the apical pore of *S. cracoviense* appears quite distinct. The furrow with a row of knobs found in the narrow plate designated 1 in Fig. 13, 14, 17--19 brings to mind the apical furrow of some woloszynskioids, notably *Biecheleria* Moestrup, Lindberg et Daugbjerg and *Biecheleriopsis* Moestrup, Lindberg et Daugbjerg (Moestrup et al. 2009a, b). The general idea of the peridinioid apical complex includes a rectangular, somewhat elongate plate on the ventral side of a round pore plate that completely encircles a smaller platelet (Dodge and Hermes 1981; Toriumi and Dodge 1993). However, in *Tyrannodinium berolinense* (Lemmermann) Calado, Craveiro, Daugbjerg et Moestrup, and perhaps in some other pfiesteriaceans (Litaker et al. 2005), the so-called plate X deeply notches the pore plate to the point of appearing to form an incomplete ring (Calado et al. 2009). The possibility of a pore plate incompletely surrounding the small cover plate, which therefore touches plate X, suggests homology between *Sphaerodinium* plates 1, 2 and 3, and the cover plate, pore plate and canal plate of peridinioids, respectively.

Flagellar base area. Although the overall organization of flagellar bases and roots of *S. cracoviense* is typical for dinoflagellates several aspects are noteworthy. In addition to the three flagellar roots extending toward the cell's left that occur in almost every dinoflagellate, some gonyaulacoids and all peridinioids examined in detail present a single-stranded root (SMR; r2 in Moestrup 2000) that associates obliquely with the right side of the LB (Calado et al. 1999, 2009; Calado and Moestrup 2002; Craveiro et al. 2009a). This root seems to be absent in naked dinoflagellates, but has been reported in the woloszynskioid *Baldinia anauniensis* Gert Hansen et Daugbjerg (Hansen et al. 2007), which approaches *S. cracoviense* in several fine-structural and molecular aspects (see below). The absence of a SMR in *S. cracoviense* is therefore surprising.

The occurrence of microtubules nucleated, either singly or in rows, along the TMR (r3) and extending toward the centre of the cell is a general dinoflagellate

feature (e.g., Calado et al. 1999, 2006; Moestrup et al. 2009b). The orientation of the microtubular extensions of the TMR in *S. cracoviense* is remarkable in that they partially surround and follow the pusule canal near its attachment to the TFC, although whether they play any role in the orientation or functioning of the pusule is unknown.

The fibrous connection between TSR and LMR (SRC) is a common feature of dinoflagellate vegetative cells, except in the peridinioid group, where it is replaced by the so-called layered connective (LC), a possibly homologous structure which links, directly or indirectly, the basal bodies and the proximal ends of the two roots (Calado et al. 1999; Calado and Moestrup 2002; Craveiro et al. 2009a). An exception, insofar as *Heterocapsa* can be considered a true peridinioid, is the observation in *H. pygmaea* A.R. Loeblich, R.J. Schmidt et Sherley of both a LC and a SRC (Bullman and Roberts 1986). The absence of a LC in *S. cracoviense* suggests a relatively distant relationship with the peridinioids.

The prominent ventral fibre (VF) associated with the right side of the LB in *S. cracoviense* is remarkably similar to that described from *Baldinia anauniensis*, not only in general aspect and orientation, but also in its connection to triplets of the LB through thin fibres (Hansen et al. 2007).

Fibrous connectives between triplets of the LB and the LMR, such as documented here for *S. cracoviense*, are common in athecate or thinly thecate dinoflagellates, e.g., *Esoptrodinium gemma* Javornický*, Baldinia anauniensis*, *Symbiodinium natans* Gert Hansen et Daugbjerg (Calado et al. 2006; Hansen et al. 2007; Hansen and Daugbjerg 2009), but not in peridinioids or gonyaulacoids.

Naked or thinly thecate dinoflagellates commonly have a variously prominent, oblique ridge in the area defined by the exit locations of the flagella and, if one is present, the peduncle (Calado et al. 1998; Dodge and Crawford 1968; Lindberg et al. 2005). Fine-structural analysis of these so-called ventral ridges shows a nearly longitudinal area lined by a single membrane and limited on both sides by fibrous material externally attached to amphiesmal vesicles. When a striated collar surrounding the exit point of a peduncle is present it is usually located near the anterior end of the ventral ridge (Calado et al. 1998, 2006). A relatively small ventral ridge was identified in *S. cracoviense* on the basis of its fine

structure and the proximity of its anterior end to the tip of a microtubular strand, here interpreted as homologous to those involved in peduncle extension (see below). Its presence is noteworthy, as ventral ridges are not known to occur in peridinioids.

The membranous body showing a honeycomb pattern in transverse sections of the cell is strikingly similar to that found in *Baldinia anauniensis* (Hansen et al. 2007). It brings to mind the stacked membranous structure found in the flagellar base area of *Kryptoperidinium foliaceum* (F. Stein) Er. Lindemann, a species containing a diatom-derived endosymbiont, and designated 'lamellar body' (Dodge and Crawford 1969a, as *Glenodinium foliaceum* F. Stein). However, a honeycomb pattern is not visible in published material of *K. foliaceum* and was not found during recent re-examination of the lamellar body of this species from different angles (unpublished results). Lamellar bodies were also reported from other species harbouring diatom-derived endosymbionts, viz. *Peridinium quinquecorne* Abé, *Durinskia baltica* (K. M. Levander) Carty et El. R. Cox and *Peridinium penardii* Lemmermann (Horiguchi and Pienaar 1991; Tomas and Cox 1973; Takano et al. 2008). In addition to the lamellar body near the flagellar bases, sets of 'orderly arranged stacked vesicles which appear as dilated smooth endoplasmic reticulum' were described adjacent to the peripherally located storage vacuoles of *Durinskia baltica*; as shown in fig. 42 in Tomas and Cox (1973) these structures resemble the honeycomb pattern found in *S. cracoviense* and *B. anauniensis*. Although the strikingly similar lamellar bodies of *S. cracoviense* and *B. anauniensis* are plausibly homologous, as indicated by the general similarity of the flagellar apparatus and LSU-based phylogeny, there does not seem to be a close relationship between these two species and the diatom-bearing group. The possible role of the lamellar body in phototaxis, mainly through analogy with the stacked membranes of light receptor cells of the retina, was discussed by Dodge and Crawford (1969a) and Hansen et al. (2007).

Microtubular strand, eyespot and pusule. Microtubular strands located in the anterior-ventral area, near the basal bodies, have been found in many dinoflagellates, both heterotrophic and autotrophic, examined in detail.

Cytoplasmic extensions from this ventral area, whatever their function, are typically supported by these microtubular strands, and peduncles demonstrably involved in food uptake are associated with abundant electron-opaque vesicles (Calado et al. 1998, 2006; Hansen and Calado 1999). In *S. cracoviense*, as in *Palatinus apiculatus* Craveiro, Calado, Daugbjerg et Moestrup (Craveiro et al. 2009a), a microtubular strand not associated with electron-opaque vesicles was found in the same location, and with the same orientation, as the ones extending into peduncles, but without reaching the cell surface and thereby suggesting that it is non-functional.

As recently reviewed (Moestrup and Daugbjerg 2007), five different types of eyespot have previously been found in dinoflagellates (excluding the complex ocelloid of the Warnowiaceae; Greuet 1987): type A, characterized by one to several layers of electron-opaque globules inside a chloroplast lobe, as is commonly found in the eyespots of algae; type B, in which a vesicle containing crystal-like units is located in the sulcal area, between the LMR (root 1) and an eyespot type A-like chloroplast lobe; type C, made of electron-opaque lipid globules not bounded by a membrane; type D, in which layers of electron-opaque globules are contained in a vesicle that is not connected to chloroplast lobes; type E, made of several layers of crystal-like units contained in a vesicle. The eyespot of *S. cracoviense* does not fit into any of these types. It is here proposed to represent a new type F, characterized by a single layer of vesicle-contained crystal-like units overlying layers of more or less fused globules not bounded by membranes.

The pusular system of *S. cracoviense* is unusual. Most dinoflagellates have similar pusular types associated with each flagellar canal. In *Prosoaulax lacustris* (F. Stein) Calado et Moestrup a single pusular tube opens either at the transverse or at the longitudinal flagellar canal, leaving the other flagellar canal without associated pusule (Calado et al. 1998, as *Amphidinium lacustre* F. Stein, see Calado and Moestrup 2005). In all cells examined of *S. cracoviense* different pusular types associated with each flagellar canal. The pusular vesicles directly associated with part of the longitudinal flagellar canal resemble those of the pusules of *Amphidinium* sensu stricto, e.g. *A. rhynchocephalum* Anisimova

(Farmer and Roberts 1989), and *Gymnodinium aureolum* (Hulburt) Gert Hansen (Hansen 2001). The pusule canal with an apparently fibrous cover that extends from the transverse flagellar canal of *S. cracoviense* is reminiscent of the one described from *Gymnodinium fuscum* (Ehrenberg) F. Stein (Dodge 1972; Dodge and Crawford 1969b). However, the inner dilated portion of the pusule canal of *G. fuscum* is associated with pusular vesicles instead of tubes. The pusule canal of *S. cracoviense* also bears some similarity with the tube extending from the longitudinal flagellar canal of *B. anauniensis*, which however, appeared lined in its distal part by amphiesmal vesicles and was interpreted as pusular in nature (i.e., with its internal membrane closely appressed to the inner membrane of an enveloping vesicle) (Hansen et al. 2007). Rows of pusular tubes opening to a collecting chamber have been described from *Karlodinium armiger* Bergholtz, Daugbjerg et Moestrup, although two similar pusules were present and the collecting chambers were directly associated with the flagellar canals (Bergholtz et al. 2005).

Phylogenetic affinities. Analysis of nuclear-encoded LSU rDNA provided high support for the position of *Sphaerodinium cracoviense* forming a sister taxon to woloszynskioid dinoflagellates possessing type B and type E eyespots (Fig. 49). A substantial number of morphological features (as well as some missing structures) also seem to favour the somewhat isolated position of *S. cracoviense* between woloszynskioids with thin thecal plates (e.g. *Borghiella* and *Biecheleria*) and the peridinioids. In brief, these are the unique type F eyespot, the pusule system, the apical pore complex, the number of postcingular plates as well as features of the flagellar apparatus. The missing structures are the single-stranded root (r2) and the layered connective characteristic of peridinioids. Thus, the combination of genotypic and phenotypic characters may indicate that *Sphaerodinium* is distinct enough to warrant a new family or perhaps even a new order. However, we refrain from proposing a new family for *Sphaerodinium* before additional species of the genus have been examined in detail by electron microscopy and at the molecular level.

The molecular data also suggest an affinity between *Sphaerodinium* and *Baldinia*. This is reflected in some very detailed morphological features like the

ventral fibre being associated with the right side of the longitudinal basal body and the honeycomb pattern in transverse sections in both species. However, there are also a number of conspicuous differences separating *Sphaerodinium* and *Baldinia* at family level, notably the structure of the eyespot and the fact that *Baldinia* is an unarmoured species.

In conclusion, the arrangement of thecal plates of *S. cracoviense*, which fits the concept of peridinioids as defined by, e.g. Taylor (2004), is contradicted by genotypic and phenotypic features that strongly indicate a closer relationship to several woloszynskioid groups than to *Peridinium* and its splinter genera, and the Pfiesteriaceae.

ACKNOWLEDGMENTS

Thanks to Prof. Konrad Wołowski and Dr Elżbieta Wilk-Woźniak for assistance and hospitality when visiting and collecting near Cracow, Poland, in August 2007. Karin Lindberg participated in the field work and helped with the SEM. SCC was supported by a grant from the financing programme POCI, Portugal (SFRH/BD/16794/2004) and a grant from the European Commission's (FP 6) Integrated Infrastructure Initiative programme SYNTHESYS (DK-TAF) during July-September 2008. ND thanks the Carlsbergfondet for equipment grants.

LITERATURE CITED

Balech, E. 1988. Los dinoflagelados del Atlantico Sudoccidental. *Publ. Espec. Inst. Esp. Oceanogr.,* **1**:1—30.

Bergholtz, T., Daugbjerg, N., Moestrup, Ø. & Fernández-Tejedor, M. 2005. On the identity of *Karlodinium veneficum* and description of *Karlodinium armiger* sp. nov. (Dinophyceae), based on light and electron microscopy, nuclear-encoded LSU rDNA, and pigment composition. *J. Phycol*., **42**:170—193.

Bullman, V. & Roberts, K. R. 1986. Structure of the flagellar apparatus in *Heterocapsa pygmaea* (Pyrrophyta). *Phycologia*, **25**:558—571.

Calado, A. J. & Moestrup, Ø. 2002. Ultrastructural study of the type species of *Peridiniopsis*, *Peridiniopsis borgei* (Dinophyceae), with special reference to the peduncle and flagellar apparatus. *Phycologia*, **41**:567—584.

Calado, A. J. & Moestrup, Ø. 2005. On the freshwater dinoflagellates presently included in the genus *Amphidinium*, with a description of *Prosoaulax* gen. nov. *Phycologia,* **44**:112—119.

Calado, A. J., Craveiro, S. C. & Moestrup, Ø. 1998. Taxonomy and ultrastructure of a freshwater, heterotrophic *Amphidinium* (Dinophyceae) that feeds on unicellular protists. *J. Phycol.*, **34**:536—554.

Calado, A. J., Hansen, G. & Moestrup, Ø. 1999. Architecture of the flagellar apparatus and related structures in the type species of *Peridinium*, *P. cinctum* (Dinophyceae). *Eur. J. Phycol.*, **34**:179—191.

Calado, A. J., Craveiro, S. C., Daugbjerg, N. & Moestrup, Ø. 2006. Ultrastructure and LSU rDNA-based phylogeny of *Esoptrodinium gemma* (Dinophyceae), with notes on feeding behavior and the description of the flagellar base area of a planozygote. *J. Phycol.*, **42**:434—452.

Calado, A. J., Craveiro, S. C., Daugbjerg, N. & Moestrup, Ø. 2009. Description of *Tyrannodinium* gen. nov., a freshwater dinoflagellate closely related to the marine *Pfiesteria*-like species. *J. Phycol.*, **45**:1195—1205.

Caljon, A. G. 1987. Phytoplankton of a recently landlocked brackish-water lagoon of Lake Tanganyika: a systematic account. *Hydrobiologia*, **153**:31—54.

Carty, S. & Wujek, D. E. 2003. A new species of *Peridinium* and new records of dinoflagellates and silica-scaled chrysophytes from Belize. *Caribb. J. Sci.*, **39**:136—139.

Christensen, T. 1982. Alger i naturen og i laboratoriet. 1. ed. Nucleus. p. 1--136. (In Danish).

Couté, A. & Iltis, A. 1984. Mise au point sur la flore péridiniale (Algae, Pyrrhophyta) d'eau douce de Côte d'Ivoire. *Rev. Hydrobiol. Trop.*, **17:**53—64.

Craveiro, S. C., Calado, A. J., Daugbjerg, N. & Moestrup, Ø. 2009a. Ultrastructure and LSU rDNA-based revision of *Peridinium* group palatinum (Dinophyceae) with the description of *Palatinus* gen. nov. *J. Phycol.*, **45**:1175—1194.

Craveiro, S. C., Calado, A. J., Daugbjerg, N. & Moestrup, Ø. 2009b. Fine structure and phylogeny of *Sphaerodinium*, an unusual freshwater dinoflagellate. Abstract. *Phycologia*, **48**:23—24.

Daugbjerg, N., Hansen, G., Larsen, J. & Moestrup, Ø. 2000. Phylogeny of some of the major genera of dinoflagellates based on ultrastructure and partial LSU rDNA sequence data, including the erection of three new genera of unarmoured dinoflagellates. *Phycologia*, **39**:302—317.

Dodge, J. D. 1972. The ultrastructure of the dinoflagellate pusule: a unique osmo-regulatory organelle. *Protoplasma*, **75**:285—302.

Dodge, J. D. & Crawford, R. M. 1968. Fine structure of the dinoflagellate *Amphidinium carteri* Hulbert. *Protistologica,* **4**:231--242 + pls 1—6.

Dodge, J. D. & Crawford, R. M. 1969a. Observations on the fine structure of the eyespot and associated organelles in the dinoflagellate *Glenodinium foliaceum. J. Cell Sci.,* **5**:479—493.

Dodge, J. D. & Crawford, R. M. 1969b. The fine structure of *Gymnodinium fuscum*. *New Phytol.,* **68**:613—618.

Dodge, J. D. & Hermes, H. B. 1981. A scanning electron microscopical sudy of the apical pores of marine dinoflagellates (Dinophyceae). *Phycologia*, **20**:424—430.

Farmer, M. A. & Roberts, K. R. 1989. Comparative analyses of the dinoflagellate flagellar apparatus. III. Freeze substitution of *Amphidinium rhynchocephalum. J. Phycol.,* **25**:280—292.

Felsenstein, J. 2008. Phylogeny Inference Package (PHYLIP). Version 3.68. University of Washington, Seattle.

Greuet, C. 1987. Complex organelles. In: Taylor, F. J. R. (ed.), The biology of dinoflagellates. Blackwell Scientific Publications, Oxford. 117—142.

Grigorszky, I., Borics, G., Padisák, J., Tótmérész, B., Vasas, G., Nagy, S. & Borbély, G. 2003. Factors controlling the occurrence of Dinophyta species in Hungary. *Hydrobiologia*, **506-509**:203—207.

Guindon, S. & Gascuel, O. 2003. A simple, fast, and accurate algorithm to estimate large phylogenies by maximum likelihood. *Syst. Biol*., **52**:696—704.

Hansen, G. 1995. Analysis of the thecal plate pattern in the dinoflagellate *Heterocapsa rotundata* (Lohmann) comb. nov. (=*Katodinium rotundatum* (Lohmann) Loeblich). *Phycologia*, **34**:166—170.

Hansen, G. 2001. Ultrastructure of *Gymnodinium aureolum* (Dinophyceae): toward a further redefinition of *Gymnodinium sensu stricto*. *J. Phycol*., **37**:612—623.

Hansen, G. & Daugbjerg, N. 2004. Ultrastructure of *Gyrodinium spirale*, the type species of *Gyrodinium* (Dinophyceae), including a phylogeny of *G. dominans*, *G. rubrum* and *G. spirale* deduced from partial LSU rDNA sequences. *Protist*, **155**:271—294.

Hansen, G. & Daugbjerg, N. 2009. *Symbiodinium natans* sp. nov.: a “free-living” dinoflagellate from Tenerife (Northeast-Atlantic Ocean). *J. Phycol.*, **45**:251—263.

Hansen, G., Daugbjerg, N. & Henriksen, P. 2000. Comparative study of *Gymnodinium mikimotoi* and *Gymnodinium aureolum*, comb. nov. (=*Gyrodinium aureolum*) based on morphology, pigment composition, and molecular data. *J. Phycol.*, **36**:394—410.

Hansen, G., Daugbjerg, N. & Henriksen, P. 2007. *Baldinia anauniensis* gen. et sp. nov.: a “new” dinoflagellate from Lake Tovel, N. Italy. *Phycologia*, **46**:86—108.

Hansen, P. J. & Calado, A. C. 1999. Phagotrophic mechanisms and prey selection in free-living dinoflagellates. *J. Eukaryot. Microbiol*., **46**:382—389.

Hoppenrath, M., Bolch, C. J. S., Yoshimatsu, S., Saldarriaga, J. F., Schweikert, M., Campbell, C. N., Toriumi, S., Dodge, J. D., Elbrächter, M. & Taylor, F. J. R. 2005. Nomenclatural note on a *Thecadinium* species (Dinophyceae, Gonyaulacales), which was described as new independently three times within two months. *J. Phycol.*, **41**:1284—1286.

Horiguchi, T. & Pienaar, R. N. 1991. Ultrastructure of a marine dinoflagellate, *Peridinium quinquecorne* Abé (Peridiniales) from South Africa with particular reference to its chrysophyte endosymbiont. *Bot. Mar.*, **34**:123—131.

Iwataki, M. 2008. Taxonomy and identification of the armored dinoflagellate genus *Heterocapsa* (Peridiniales, Dinophyceae). *Plankton Benthos Res.*, **3**:135-142.

Lenaers, G., Maroteaux, L., Michot, B. & Herzog, M. 1989. Dinoflagellate in evolution. A molecular phylogenetic analysis of large subunit ribosomal RNA. *J. Mol. Evol.*, **29**:40—51.

Lindberg, K., Moestrup, Ø. & Daugbjerg, N. 2005. Studies on woloszynskioid dinoflagellates I: *Woloszynskia coronata* re-examined using light and electron microscopy and partial LSU rDNA sequences, with description of *Tovellia* gen. nov. and *Jadwigia* gen. nov. (Tovelliaceae fam. nov.). *Phycologia*, **44**:416—440.

Ling, H. U., Croome, R. L. & Tyler, P. A. 1989. Freshwater dinoflagellates of Tasmania, a survey of taxonomy and distribution. *Br. Phycol. J.*, **24**:111—129.

Litaker, R. W., Steidinger, K. A., Mason, P. L., Landsberg, J. H., Shields, J. D., Reece, K. S., Haas, L. W., Vogelbein, W. K., Vandersea, M. W., Kibler, S. R. & Tester, P. A. 2005. The reclassification of *Pfiesteria shumwayae*: *Pseudopfiesteria*, gen. nov. *J. Phycol.*, **41**:643-651.

Loeblich, A. R. Jr. & Loeblich, A. R. III 1966. Index to the genera, subgenera, and sections of the Pyrrhophyta. *Stud. Trop. Oceanogr.*, **3**:i-ix , 1—94.

Moestrup, Ø. 2000. The flagellate cytoskeleton. Introduction of a general terminology for microtubular flagellar roots in protists. In: Leadbeater B. S. C. & Green J. C. (ed.), The flagellates. Unity, diversity and evolution. Taylor & Francis, New York, 69--94. (Systematics Association Special Volume No. 59.)

Moestrup, Ø. & Daugbjerg, N. 2007. On dinoflagellate phylogeny and classification. In: Brodie, J. & Lewis, J. (ed.), Unravelling the algae, the past, present, and future of algal systematics. CRC Press, Boca Raton, 215--230. (Systematics Association Special Volume No. 75.)

Moestrup, Ø., Lindberg, K. & Daugbjerg, N. 2009a. Studies on woloszynskioid dinoflagellates IV. The genus *Biecheleria* gen. nov. *Phycol. Res.*, **57**:203—220.

Moestrup, Ø., Lindberg, K. & Daugbjerg, N. 2009b. Studies on woloszynskioid dinoflagellates V. Ultrastructure of *Biecheleriopsis* gen. nov., with description of *Biecheleriopsis adriatica* sp. nov. *Phycol. Res.*, **57**:221—237.

Posada, D. & Crandall, K. A. 1998. MODELTEST: testing the model of DNA substitution. *Bioinformatics*, **14**:817—818.

Ronquist, F. & Huelsenbeck, J. P. 2003. MRBAYES 3: Bayesian phylogenetic inference under mixed models. *Bioinformatics*, **19**:1572—1574.

Schiller, J. 1935. Dinoflagellatae (Peridineae) in monographischer Behandlung. In: Kolkwitz, R. (ed.), Rabenhorst's Kryptogamenflora von Deutschland, Österreichs und der Schweiz, 2nd ed., vol. 10 (3). Part 2, issue 1. Akademische Verlagsgesellschaft, Leipzig, Germany, 1—160.

Sournia, A. 1986. Atlas du Phytoplankton Marin. Vol. 1. Introduction, Cyanophycées, Dictyochophycées, Dinophycées et Raphidophycées. Éditions du Centre National de la Recherche Scientifique, Paris, 219 p.

Swofford, D. L. 2003. PAUP* Phylogenetic analysis using parsimony (*and other methods), version 4. Sinauer Associates, Sunderland, MA, USA.

Takano, Y., Hansen, G., Fujita, D. & Horiguchi, T. 2008. Serial replacement of diatom endosymbionts in two freshwater dinoflagellates, *Peridiniopsis* spp. (Peridiniales, Dinophyceae). *Phycologia*, **47**:41—53.

Tamura, M., Iwataki, M. & Horiguchi, T. 2005. *Heterocapsa psammophila* sp. nov. (Peridiniales, Dinophyceae), a new sand-dwelling marine dinoflagellate. *Phycol. Res.*, **53**:303—311.

Taylor, F. J. R. 2004. Illumination or confusion? Dinoflagellate molecular phylogenetic data viewed from a primarily morphological standpoint. *Phycol. Res.*, **52**:308—324.

Thompson, R. H. 1951. A new genus and new records of freshwater Pyrrophyta in the Desmokontae and Dinophyceae. *Lloydia*, **13**:277—299.

Tolotti, M. & Thies, H. 2002. Phytoplankton community and limnochemistry of Piburger See (Tyrol, Austria) 28 years after lake restoration. *J. Limnol*., **61**:77—88.

Tomas, R. N. & Cox, E. R. 1973. Observations on the symbiosis of *Peridinium balticum* and its intracellular alga. I. Ultrastructure. *J. Phycol*., **9**:304—323.

Toriumi, S. & Dodge, J. D. 1993. Thecal apex structure in the Peridiniaceae (Dinophyceae). *Eur. J. Phycol.*, **28**:39-45.

Wołoszyńska, J. 1916. Polnische Süßwasser-Peridineen. *Bull. Int. Acad. Sci. Cracovie, Cl. Sci. Math., Sér. B: Sci. Nat.*, **1915**:260--285, pl. 10—14.

Wołoszyńska, J. 1930. Beitrag zur Kenntnis des Phytoplanktons tropischer Seen. *Arch. Hydrobiol. i Ryb.* **5**:159—169.

CHAPTER 6

CLOSING REMARKS

CLOSING REMARKS

Previous studies of the detailed fine-structural organization of the flagellar apparatus of peridinioids are few. Only the type species of the freshwater genera *Peridinium* and *Peridiniopsis*, and the marine *Heterocapsa pygmaea* have been subject to observations detailed enough to enable the description and three-dimensional reconstruction of the flagellar apparatus (Bullman and Roberts 1986, Calado et al. 1999, Calado and Moestrup 2002). In the present work two species until recently included in the genus *Peridinium*, *P. palatinum* and *P. lomnickii*; one heterotrophic species previously included in the genus *Peridiniopsis*, *P. berolinensis*; and the unusual *Sphaerodinium cracoviense* were analysed ultrastructurally, and partial LSU rDNA sequences of these species were included in DNA-based phylogenetic hypotheses (Chapters 2, 3, 4 and 5, respectively). Three-dimensional reconstitutions of the flagellar apparatus of the two former *Peridinium* species and of *S. cracoviense* were prepared. Taxonomical changes involving three new genera were proposed for the two *Peridinium* and the *Peridiniopsis* species (Chapter 2, 3 and 4).

The general characteristics of tabulation and ultrastructure of the taxa studied in this thesis, together with the type species of both *Peridinium* and *Peridiniopsis,* and of *Heterocapsa pygmaea* are summarized in Table 1.

The genus *Palatinus* was described to include the *Peridinium* species without apical pore and with two intercalary and six cingular plates. This decision was based on ultrastructural observations, general morphology and molecular phylogeny (Chapter 2, Craveiro et al. 2009). One characteristic of this genus is the almost smooth or finely to coarsely granulate plate surface, which is quite different from the areolate ornamentation seen in the group of *Peridinium* species lacking an apical pore and with five cingular plates, which includes the type species, *P. cinctum*. Internally, *Palatinus apiculatus* (= *Peridinium palatinum*), the type species of the new genus, has chloroplast lobes radiating from a conspicuous, central, branching pyrenoid penetrated by cytoplasmic channels, and a microtubular strand homologous to peduncle-related microtubules (MSP homologous) of other dinoflagellates, whereas none of these features is present in *Peridinium cinctum*.

Table 1. General comparison of morphology and fine structure of the species examined in this thesis, plus *Heterocapsa pygmaea* and the type species of *Peridinium* and *Peridiniopsis*. +, present; –, not present; ?, no information, uncertain.

Features	*Peridinium cinctum* (1)	*Palatinus apiculatus* (2)	*Chimonodinium lomnickii* (3)	*Scrippsiella trochoidea* (4)	*Peridiniopsis borgei* (5)	*Tyrannodinium berolinense* (6)	*Heterocapsa pygmaea* (7)	*Sphaerodinium cracoviense* (8)
Tabulation	4′, 3a, 7″, 5c, 5s, 5‴, 2⁗	4′, 2a, 7″, 6c, 5s, 5‴, 2⁗	4′, 3a, 7″, 6c, 5s, 5‴, 2⁗	4′, 3a, 7″, 6c, 6s, 5‴, 2⁗	3′, 1a, 6″, 6c, 5s, 5‴, 2⁗	4′, 0a, 6″, 6c, 6s, 5‴, 2⁗	5′, 3a, 7″, 5-7c, 5s (?7s), 5‴, 2⁗	4′, 4a, 7″, Z, 6-8c, 4s, 6‴, 2⁗
Apical pore	–	–	Po, cp, x	Po, cp, x	Po, cp, x	Po, cp, x	Po, cp	3 plates, apical furrow
Chloroplast	numerous peripheral lobes	lobes radiating from central pyrenoid	numerous peripheral lobes	few peripheral lobes	lobes radiating from dorsal pyrenoid	–	few peripheral lobes	numerous peripheral lobes
Pyrenoid	absent, only thylakoid-free areas	one central, branching, penetrated by cytoplasmic tubes	absent, only thylakoid-free areas	several, stalked, with tubular structures derived from thylakoids, with starch sheath	one large, dorsal, with starch sheath	–	few, with starch sheath	absent, only thylakoid-free areas
Eyespot type[a]	A	A	A	A	B	–	?	F[b]
BBs angle (°)	65	80-85	85-90	90	90	90-100	20	90(140)
LC	+	+	+	+	+	+	+	–
SRC	–	–	–	–	–	–	+	+
SMR, r2	+	+	+	+	+	+	?	–

[a] Moestrup and Daugbjerg (2007).
[b] New type described in this work, Chapter 5.

Features	*Peridinium cinctum* (1)	*Palatinus apiculatus* (2)	*Chimonodinium lomnickii* (3)	*Scrippsiella trochoidea* (4)	*Peridiniopsis borgei* (5)	*Tyrannodinium berolinense* (6)	*Heterocapsa pygmaea* (7)	*Sphaerodinium cracoviense* (8)
TMRE	several strands	one strand	one strand, association with fibre short	one strand	one strand, association with fibre long	one strand	?	several strands
LB-LMRc	–	–	–	–	–	–	–	+
TB-LMRc	–	+	+	+	+	+	–	–
MB	–	–	+	–	–	+	?	–
MSP	–	–	–	–	+	–	?	–
MSP homologue[c]	–	+	–	–	–	–	?	+
Peduncle	–	–	+	–	+	+	?	–
Pusule	pusular elements opening at large vesicles connected to the FCs	two pusular tubes opening at TFC + one pusular tube opening at LFC	one pusular tube opening at each FC	flattened, ramified pusular vesicles	pusular elements opening at large vesicles connected to the FCs	pusular elements opening at large vesicles connected to the FCs	?	pusule canal opening at TFC, in distal end with collecting chamber with pusular tubes + pusular vesicles opening at the LFC

Abbreviations: BBs, basal bodies; LC, layered connective; SRC, striated root connective; SMR, single-stranted microtubular root; TMRE, transverse microtubular root extension; LB-LMRc, connective between LB and LMR; TB-LMRc, connective between TB and LMR; MB, microtubular basket; MSP, microtubular strand of the peduncle; TFC and LFC, transverse and longitudinal flagellar canals; FC(s), flagellar canal(s); Po, pore plate; cp, cover plate; x, canal plate.

References: **1** Calado et al. (1999); **2** Craveiro et al. (2009) (this thesis, Chapter 2); **3** this thesis, Chapter 3; **4** this thesis, Chapter 3, Janofske (2000); **5** Calado and Moestrup (2002); **6** Wedemayer and Wilcox (1984), Calado and Moestrup (1997), Calado et al. (2009) (this thesis, Chapter 4); **7** Bullman and Roberts (1986), Iwataki (2008); **8** this thesis, Chapter 5.

[c] Not associated with electron-opaque vesicles and not shown to extend into a peduncle.

The well-defined pusular tubes in *Palatinus apiculatus* are also quite different from the pusular structures found in *Peridinium cinctum* and the type species of *Peridiniopsis*, *P. borgei*. In the flagellar apparatus of *Palatinus apiculatus*, two well-defined fibers, connecting the transverse basal body (TB) with the dorsal side of the longitudinal microtubular root (LMR), are similar to connectives found in *Peridiniopsis borgei*; such connectives were not seen in *Peridinium cinctum*. The LSU rDNA-based phylogeny is compatible with the separation of this genus (although with moderate statistical support). The new genus *Palatinus* includes *Palatinus apiculatus* as the type species, *Palatinus apiculatus* var. *laevis* (= *Peridinium palatinum* f. *laeve*) *and P. pseudolaevis* (= *Peridinium pseudolaeve*), i.e., all the members of *Peridinium* group palatinum sensu Popovský and Pfiester (1990) and previous monographers.

Chimonodinium gen. ined. is a new genus proposed to accomodate *Peridinium lomnickii* (Chapter 3). This species has an apical pore, and three intercalary and six cingular plates (Table 1). The same tabulation is present in *Scrippsiella*, a marine genus producing calcareous cysts, hence the interest of looking at the ultrastructural features of *Scrippsiella trochoidea.* This species has been considered identical to the type species of *Scrippsiella, S. sweeneyae*, by some authors (Fine and Loeblich 1976, Janofske 2000) and its fine-structural characters are here taken as representative of *Scrippsiella*. *Chimonodinium lomnickii* comb. ined. has a particular combination of internal features different from other photosynthetic peridinioids with an apical pore, e.g., *S. trochoidea* and *Peridiniopsis borgei*. In *C. lomnickii* comb. ined. the chloroplast lobes are near the surface, are not connected in the central cytoplasm and show no distinct pyrenoids; the pusular system is formed by two pusular tubes, at least near the connection point to each of the flagellar canals (FCs); a microtubular basket (MB) with four or five rows of microtubules supports a small extruded peduncle and extends internally for over 12 µm (Chapter 3). In contrast, in *S. trochoidea* neither a MB nor a microtubular strand of the peduncle (MSP) were found; there are two or three conspicuous pyrenoids and the pusule is composed of several flattened, ramified vesicles (Chapter 3). In *Peridiniopsis borgei* a MSP is present instead of a MB, the pyrenoid is dorsal with radiating chloroplast lobes and the pusular system

is composed of several pusular elements opening at large vesicles connected to the FCs (Calado and Moestrup 2002). The calcareous cyst of *S. trochoidea* is quite characteristic, with a calcareous outer wall furnished by generally triangular spines with irregular bases and pointed or blunt tips, whereas in *C. lomnickii* comb. ined. cysts are not calcareous, have a smooth wall, and are roughly the same shape as the motile cell (Chapter 3). The LSU rDNA-based phylogeny shows *C. lomnickii* comb. ined. as a sister group to a clade grouping *Thoracosphaera* with *Pfiesteria* and related taxa (e.g., *Tyrannodinium berolinense*). All together they are included in a larger clade with *Scrippsiella* species and *Peridinium aciculiferum* (Chapter 3).

The genus *Tyrannodinium* was proposed to include the very common freshwater dinoflagellate that feeds on other protists and injured metazoans, known previously as *Peridiniopsis berolinensis* (Chapter 4, Calado et al. 2009). This organism uptakes food using a feeding tube (a kind of peduncle) that is supported by a MB, in a similar way to the marine and estuarine pfiesteriaceans (Jeong et al. 2007, Volgelbein et al. 2002). It has been documented for some pfiesteriaceans that there is an attraction to their prey by chemotaxis (Spero 1985, Calado and Moestrup 1997, Volgelbein et al. 2002). This feature, the feeding mode and a distinct plate covering the proximal part of the sulcus, usually called the peduncle cover plate, seem to form a combination characteristic for this group of organisms (Chapter 4, Calado et al. 2009). *Tyrannodinium berolinense* differs from the other members of the group in plate tabulation and in having a freshwater habitat (Chapter 4). The phylogenetic tree based on LSU rDNA sequences strongly supports the inclusion of *Tyrannodinium berolinense* in the Pfiesteriaceae.

Sphaerodinium cracoviense has more anterior intercalary and postcingular plates, 4 and 6 respectively, than the common peridinioid (Table 1). Although three plates were visible in the apical complex of *S. cracoviense*, they were not arranged as in the apical pore system of peridinioids; a groove in one of the plates was reminiscent of the apical structures of some woloszynskioids (Chapter 5). The prominent eyespot found in *S. cracoviense* was shown by TEM to be extraplastidial and of a type not described previously (designated type F in Chapter 5), made by the combination of two components, each known from some

eyespot types found in woloszynskioids, but not previously found together: a layer of vesicle-contained crystal-like units underlain by one to few layers of more or less fused oil globules not bounded by a membrane. A membranous structure (lamellar body) showing a honeycomb arrangement in cross-section was present in the mid-ventral area, near the flagellar roots. The recently described dinoflagellate genus *Baldinia* contains a similar structure (Hansen et al. 2007). Details of the flagellar roots, like the presence of a striated root connective (SRC) instead of a layered connective (LC), the presence of a ventral fibre (VF), and the associated pusular system link *Sphaerodinium* to the woloszynskioids in general and to *Baldinia* in particular (Chapter 5). A phylogenetic analysis based on LSU rDNA positions *S. cracoviense* as a close relative of a group of woloszynskioids, including the Suessiaceae and the Borghiellaceae, and not as a close relative of peridinioids (Chapter 5).

This thesis adds to the number of detailed ultrastructural descriptions of peridinioids available, allowing for a more clear view of the ultrastructural characteristics typical of peridinioids as a whole and of groups that can be recognized within the peridinioids (Table 1). The clarification of the phylogenetic affinities of *Sphaerodinium cracoviense*, which is apparently similar to the peridinioids but has some distinctive features that place it closer to the woloszynskioids, is important to clarify the boundaries of peridinioid features (Table 1). The particular tabulation of *Sphaerodinium*, with six post-cingular plates, is different from that found in peridinioids, which, except for casual or irregular variations, have only five post-cingular plates. The presence of a complete series of epithecal plates (eight) contacting the upper edge of the cingulum in *Sphaerodinium* is also peculiar and not found in peridinioids except for *Heterocapsa* (Iwataki 2008). However, recent phylogenetic studies have repeatedly shown relatively remote affinities between *Heterocapsa* species and several peridinioids (Gottschling et al. 2005, Logares et al. 2007, Zhang et al. 2007), suggesting that the taxonomic position of *Heterocapsa* needs to be reevaluated.

The flagellar apparatuses of *Palatinus*, *Chimonodinium* gen. ined. and *Tyrannodinium* showed all the regular features of peridinioids: the single

microtubule (SMR) that associates with the right-hand side of the longitudinal basal body (LB), of general occurrence also in gonyaulacoids; the layered connective (LC), only found in peridinioids, that presumably takes up the function of the striated connective (SRC) found in other dinoflagellate groups between LMR and the transverse striated root (TSR). A fibrous connective between the TB and the LMR (TB-LMRc) was not found in *Sphaerodinium cracoviense* but was present in all peridinioids examined here although it was not seen in *Peridinium cinctum*. On the other hand, fibrous connectives between the LB and the LMR (LB-LMRc) are present in *Sphaerodinium cracoviense* and in most woloszynskioids (see Table 1 in Chapter 1), but not in peridinioids.

The LSU-rDNA based phylogenetic tree in Chapter 5 (Fig. 49) contains all taxa studied in this work and shows the peridinioids without apical pore (*Peridinium cinctum*, *P. willei* and *Palatinus apiculatus*) as a sister group to a cluster of peridinioids with an apical pore complex that includes *Scrippsiella* spp., *Peridiniopsis polonica*, the pfiesteriaceans, *Thoracosphaera heimii* (a mainly coccoid, calcareous, marine dinoflagellate, for which peridinioid morphological features have yet to be demonstrated), *Chimonodinium lomnickii* comb. ined. and *Peridinium aciculiferum*. In this clade of peridinioids with an apical pore there are two sister groups: the *Scrippsiella* and *Peridiniopsis polonica* on one side and *C. lomnickii* comb. ined., *Peridinium aciculiferum, Thoracosphaera heimii* and pfiesteriaceans on the other. The closer affinity between *C. lomnickii* comb. ined. and the pfiesteriacenas than to the *Scrippsiella* is supported by the presence of two particular features: the microtubular basket and the connection through extra-cytoplasmic fibres between the edge of one sulcal plate and the middle of another (Chapter 3 and 4). There is no information available about the ultrastructure of *Thoracosphaera* but its position in the phylogenetic tree is consistent with published results (Gottschling et al. 2005). In relation to *P. aciculiferum*, a MB was not found in preliminary ultrastructural observations; the species position in the molecular tree is not well supported and more information is needed to correctly assign *P. aciculiferum* to a genus — it is clearly not a close relative of *Peridinium* sensu stricto. *Peridiniopsis borgei* appears together with *Akashiwo sanguinea* and

Kryptoperidinium foliaceum in a position not easily explained, as a sister group to all the peridinioids, in a branch without any statistical support.

Peridinium willei forms a well supported group with *P. cinctum* (Fig. 49, Chapter 5), with which it shares the tabulation formula (although not the asymmetry) and the typical ornamentation of the plates by areolate ridges. The ultrastructural features of *Peridinium willei* are, however, unknown. *Palatinus apiculatus* forms a sister group to both these taxa (Fig. 49, Chapter 5), perhaps consistent with the absence of an apical pore and of a true MSP.

From the above, it is obvious that the internal structure of dinoflagellates is notoriously diverse and the distribution of particular features is notoriously complicated. Peridinioid groups can be defined by combinations of features compatible with molecular phylogenetic hypotheses, but it is in general not readily apparent how a particular state of a character can stand as a synapomorphy for a particular genus. Part of this difficulty may lie on the paucity of comparison points and on the possible inadequacy of some of the existing ones; the available ultrastructural studies do not provide the same level of detail, leaving sometimes features unaccounted for or misinterpreted. It is especially important to look beyond the words used to describe or designate structures and attempt to evaluate what is essentially similar, or different, between character states in different species. An example of a feature in need of a revised classification is the pusule. Adequate descriptions of pusule morphology, especially in large cells, are difficult and time consuming, and are often left incomplete, causing incertainty when trying to characterize pusular types.

A look at the *Peridinium* groups in Popovský and Pfiester (1990) will show a number of species in need of taxonomic reevaluation. This includes all the species with an apical pore complex, which are unlikely to be close relatives of *P. cinctum*. However, as the study of *Chimonodinium* gen. ined. shows, they are not necessarily close relatives of one another. Examination of key species, not only of *Peridinium* sensu lato but also of *Peridiniopsis* sensu lato, is required to reach a stable, phylogenetic taxonomy of the freshwater peridinioids.

Character variation among closely related species is largely unknwon, mostly because the lenghty, detailed examination of cells without the prospect of

advancing our understanding of their relationships is hardly inspiring. However, until we discover how much the individual fine-structural characters vary from one species to a close relative, our understanding of the stability and, therefore, value as proxies of phylogenetic relationship, of each character state will be uncomfortably limited. Examples of species of freshwater peridinioids that would rank as candidates for this type of analysis are *Palatinus pseudolaevis* (to compare with *P. apiculatus*) and *Peridinium willei*, or *P. gatunense* (to compare with *P. cinctum*).

REFERENCES

Bullman, V. & Roberts, K. R. 1986. Structure of the flagellar apparatus in *Heterocapsa pygmaea* (Pyrrophyta). *Phycologia* 25:558–71.

Calado, A. J., Craveiro, S. C., Daugbjerg, N. & Moestrup, Ø. 2009. Description of *Tyrannodinium* gen. nov., a freshwater dinoflagellate closely related to the marine *Pfiesteria*-like species. *J. Phycol.* 45:1195–205.

Calado, A. J., Hansen, G. & Moestrup, Ø. 1999. Architecture of the flagellar apparatus and related structures in the type species of *Peridinium*, *P. cinctum* (Dinophyceae). *Eur. J. Phycol.* 34:179–91.

Calado, A. J. & Moestrup, Ø. 1997. Feeding in *Peridiniopsis berolinensis* (Dinophyceae): new observations on tube feeding by an omnivorous, heterotrophic dinoflagellate. *Phycologia* 36:47–59.

Calado, A. J. & Moestrup, Ø. 2002. Ultrastructural study of the type species of *Peridiniopsis*, *Peridiniopsis borgei* (Dinophyceae), with special reference to the peduncle and flagellar apparatus. *Phycologia* 41:567–84.

Craveiro, S. C., Calado, A. J., Daugbjerg, N. & Moestrup, Ø. 2009. Ultrastructure and LSU rDNA-based revision of *Peridinium* group palatinum (Dinophyceae) with the description of *Palatinus* gen. nov. *J. Phycol.* 45:1175–94.

Fine, K. E. & Loeblich, A. R. III. 1976. Similarity of the dinoflagellates *Peridinium trochoideum*, *P. faeroense* and *Scrippsiella sweeneyae* as determined by chromosome numbers, cell division studies and scanning electron microscopy. *Proc. Biol. Soc. Wash*. 89: 275–88.

Gottschling, M., Keupp, H., Plötner, J., Knop, R., Willems, H., & Kirsch, M. 2005. Phylogeny of calcareous dinoflagellates as inferred from ITS and ribosomal sequence data. *Mol. Phylogenet. Evol.* **36**:444–55.

Hansen, G., Daugbjerg, N. & Henriksen, P. 2007. *Baldinia anauniensis* gen. et sp. nov.: a "new" dinoflagellate from Lake Tovel, N. Italy. *Phycologia* 46:86–108.

Iwataki, M. 2008. Taxonomy and identification of the armored dinoflagellate genus *Heterocapsa* (Peridiniales, Dinophyceae). *Plankton Benthos Res.* 3:135–42.

Janofske, D. 2000. *Scrippsiella trochoidea* and *Scrippsiella regalis*, nov. comb. (Peridiniales, Dinophyceae): a comparison. *J. Phycol*. 36:178–89.

Jeong, H. J., Ha, J. H., Yoo, Y. D., Park, J. Y., Kim, J. H., Kang, N. S., Kim, T. H., Kim, H. S., & Yih, W. H. 2007. Feeding by the *Pfiesteria*-like heterotrophic dinoflagellate *Luciella masanensis*. *J. Eukaryot. Microbiol.* 54:231–41.

Logares, R., Shalchian-Tabrizi, K., Boltovskoy, A. & Rengefors, K. 2007. Extensive dinoflagellate phylogenies indicate infrequent marine-freshwater transitions. *Mol. Phylogenet. Evol.* 45:887–903.

Popovský J. & Pfiester L. A. 1990. Dinophyceae (Dinoflagellida). *In* Ettl, H., Gerloff, J., Heynig, H. & Mollenhauer D. [Eds.] *Süsswasserflora von Mitteleuropa*, vol. 6. G. Fisher, Jena. 272 pp.

Spero, H. J. 1985. Chemosensory capabilities in the phagotrophic dinoflagellate *Gymnodinium fungiforme*. *J. Phycol.* 21:181-4.

Vogelbein, W. K., Lovko, V. J., Shields, J. D., Reece, K. S., Mason, P. L., Haas, L. W. & Walker, C. C. 2002. *Pfiesteria shumwayae* kills fish by micropredation not exotoxin secretion. *Nature* 418:967–70.

Wedemayer, G. J. & Wilcox, L. W. 1984. The ultrastructure of the freshwater colorless dinoflagellate *Peridiniopsis berolinense* (Lemm.) Bourrelly. *J. Protozool.* 31:444–53.

Zhang, H., Bhattacharya, D. & Lin, S. 2007. A three-gene dinoflagellate phylogeny suggests monophyly of Prorocentrales and a basal position for *Amphidinium* and *Heterocapsa*. *J. Mol. Evol*. 65:463–74.